AN ELECTROPHYSIOLOGICAL STUDY OF CHROMATIC PROCESSING IN THE HUMAN VISUAL SYSTEM

Using visual evoked potentials and electroretinograms to study cortical and retinal contributions to human trichromatic vision

Naveen Kumar CHALLA

Submitted for the degree of

Doctor of Philosophy

Bradford School of Optometry and Vision Science

University of Bradford

2011

ABSTRACT

AN ELECTROPHYSIOLOGICAL STUDY OF CHROMATIC PROCESSING IN THE HUMAN VISUAL SYSTEM

NAVEEN KUMAR CHALLA

Key words: Colour vision, electrophysiology, visual evoked potentials, electroretinograms.

The work in this thesis is concerned with examining the retinal and cortical contributions to human trichromatic colour vision. Chromatic processing at the cortex level was examined using visual evoked potentials (VEPs). These responses were elicited by chromatic spot stimuli, which were manipulated in order to selectively activate the chromatic processing system. Chromatic processing at the retinal level was examined using the electroretinograms (ERGs) for which cone isolating stimuli were used to assess the nature of L and M cone inputs to cone-opponent mechanisms.

The results from the VEP experiments suggest VEP morphology is dependent upon 1) chromatic and or luminance contrast content of the stimulus, 2) stimulus size, and 3) extent to which the chromatic stimulus activates either the L/M or S/(L+M) opponent mechanism. The experiments indicate that chromatic stimulation is indexed by large N1 component and small offset responses. Optimal stimulus size for chromatic isolation is 2-4 ° along L/M axes and 6° along S/(L+M) axis.

From the ERG experiments, It has been shown that the low (12Hz) and high (30Hz) temporal frequency flickering stimuli can isolate the chromatic and luminance processing mechanisms in the retina. For low temporal frequency ERGs, the L:M ratio was close to unity and L/M phase difference was close to 180°. For high temporal frequency ERGs, the L:M ratio was more than unity and L/M phase difference was close to 90°. In addition to this, the variation in L:M ratio across the retinal eccentricity was also examined. These results suggest, for the chromatic processing, L:M ratio is close to unity independent of retinal eccentricity and individuals. For the luminance processing, L:M ratio is more than unity and depends upon the region of the retina being stimulated. These findings indicate the maintenance of cone selective input for the chromatic processing across the human retina.

ACKNOWLDEGEMENTS

Primarily I owe my deepest gratitude to Dr. Declan McKeefry for his invaluable support and guidance over the past four years. This thesis would not have been possible without his stimulation and continuous moral support. The contagious enthusiasm that he has towards the research has been motivational factor all through my tenure as a PhD student.

It is my pleasure to thank Dr. Jan Kremers (University of Erlangen, Germany), Dr. Neil Parry (Manchester Royal Eye Hospital), Dr. Ian Murray and Dr.Thanasis (University of Manchester) for their support during my visit to learn the electrophysiological techniques at Manchester Royal Eye Hospital. I am grateful to the subjects those who participated in this study and spend their time in the dark room. Their willingness and interest to be a part of my thesis is a great pleasure and highly appreciative.

It is my pleasure to thank Dr. Marina Bloj and Professor Bill Douthwaite for their useful comments during MPhil transfer manuscript. I would like to thank all my friends for their time, interest and valuable comments. I would also like to thank all my colleagues and friends in the department for creating a homely environment at work place.

I am indebted to my entire family for their endless love and support during all my pursuits. Their constant encouragement has helped me to achieve this milestone of my career.

Table of contents

CHAPTER-1 ANATOMY AND PHYSIOLOGY OF COLOUR PROCESSING IN THE PRIMATE VISUAL SYSTEM.

1.1 INTRODUCTION

Colour vision confers on an organism the ability to differentiate between objects based on differences in the wavelength of light they emit, reflect or transmit. Colour vision facilitates object perception, recognition and has an important role in scene segmentation and visual memory (Gegenfurtner and Kiper, 2003). Colour is one of the most important components of visual information and is carried by distinct processing pathways from the retina to cortex; the anatomy and physiology of which will be the major focus of attention in this review chapter.

1.2 ANATOMY OF COLOUR AND LUMINANCE PATHWAYS

1.2.1 Retina

Microscopic examination of the retina reveals a regular laminar structure in most vertebrate retinae. Retina consists of ten layers which are illustrated in figure 1.1. Ten layers of the retina are:

1) Retinal pigment epithelium(RPE)
2) Photoreceptor layer
3) External limiting membrane
4) Outer nuclear layer
5) Outer plexiform layer (OPL)

6) Inner nuclear layer
7) Inner plexiform layer (IPL)
8) Ganglion cell layer
9) Nerve fibre layer
10) Inner limiting membrane

Three of the ten layers of the retina form the cell bodies of neural and glial cells:

1) The Outer nuclear layer (ONL): cell bodies of the photoreceptors
2) The Inner nuclear layer (INL): cell bodies of horizontal, bipolar, amacrine and Müller cells
3) Ganglion cell layer

These three layers are inter-connected by two layers known as outer and inner plexiform layers. Inner and outer limiting membranes are formed by the inner and outer segment of the rods and cones, and end processes of Müller cells. Nerve fibre layer (NFL) is made up of ganglion cell axons.

The anatomy and physiology of neural elements of the retina will be described in the following sections.

Photoreceptors

Visual processing begins in the photoreceptor layer of the primate retina with the excitation of one or more photo-receptors. Photoreceptors are divided into two main groups known as rods and cones. There are about 120 million rods which are active in scotopic conditions, and about 7 million cones that responsive in photopic conditions (see figure 1.2). Cones are mainly concentrated in central retina within 10 degrees around the fovea. Rods are

absent at foveal region but gradually appears outside the fovea and increase in numbers with maximum density at about 20 degrees, after which there is a decrease in their density.

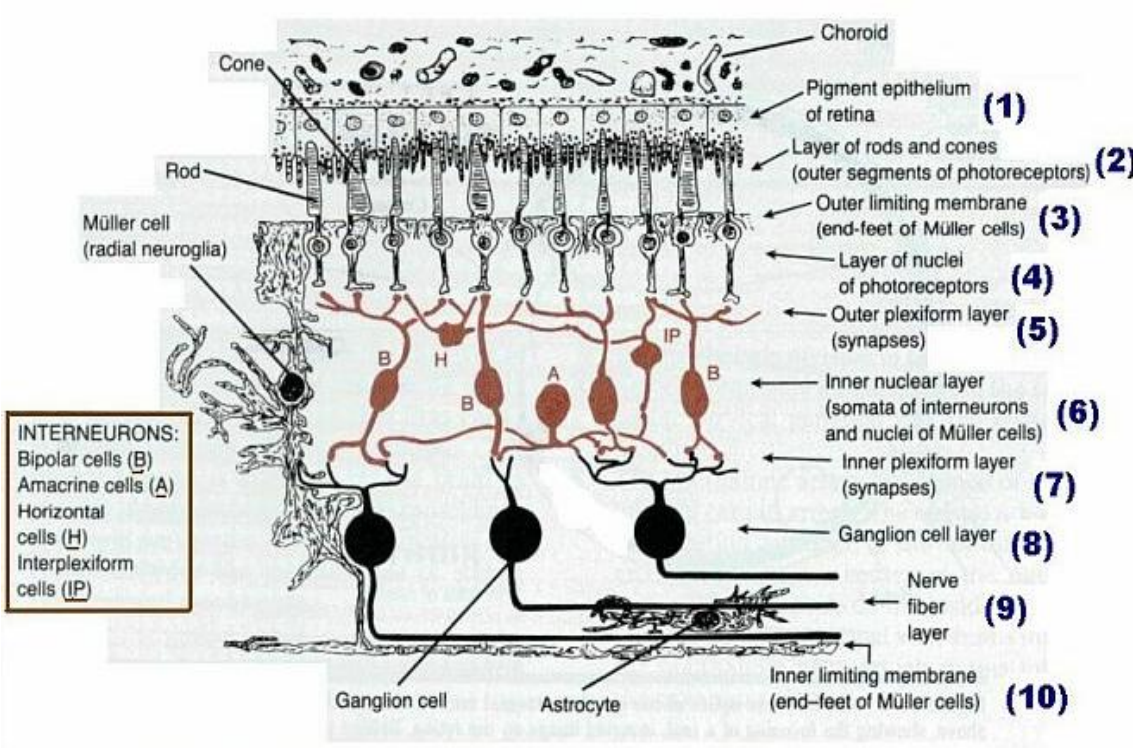

Figure 1.1 Schematic representation of organisation of the retina. Ten layers of the retina were listed on right hand side of the figure. Inter neurons are represented in colour. Source: http://instruct.uwo.ca/anatomy/530/retina.jpg.

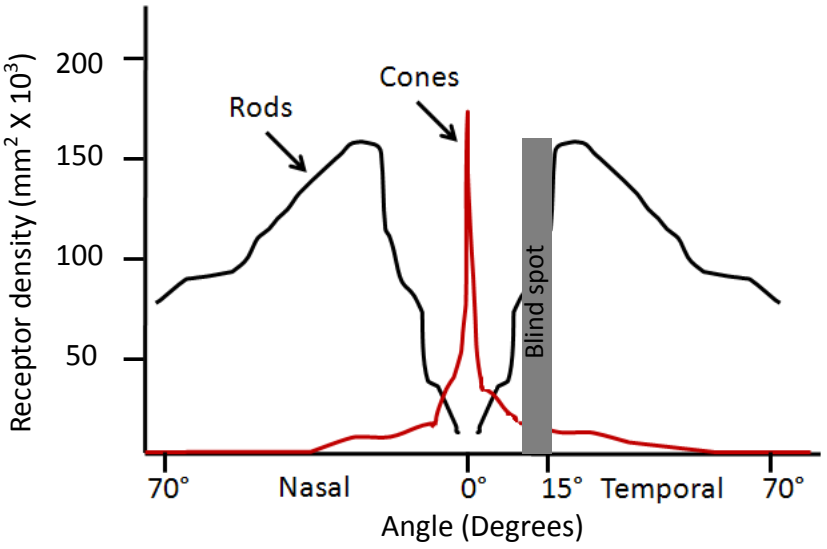

Figure 1.2 Photoreceptor density and distribution across the retina.

Cones are divided into long (L), medium (M) and short (S) wavelength sensitive types based on their spectral wavelength absorption. In primates, the peak sensitivity of L cones is at a wavelength of around 560nm, M cones around 530nm and S cones around 420 nm (Schnapf et al., 1987; Baylor et al., 1987). Maximum rod spectral sensitivity is around 500nm. The spectral sensitivity curves for three types of cones and rods are as shown in figure 1.3.

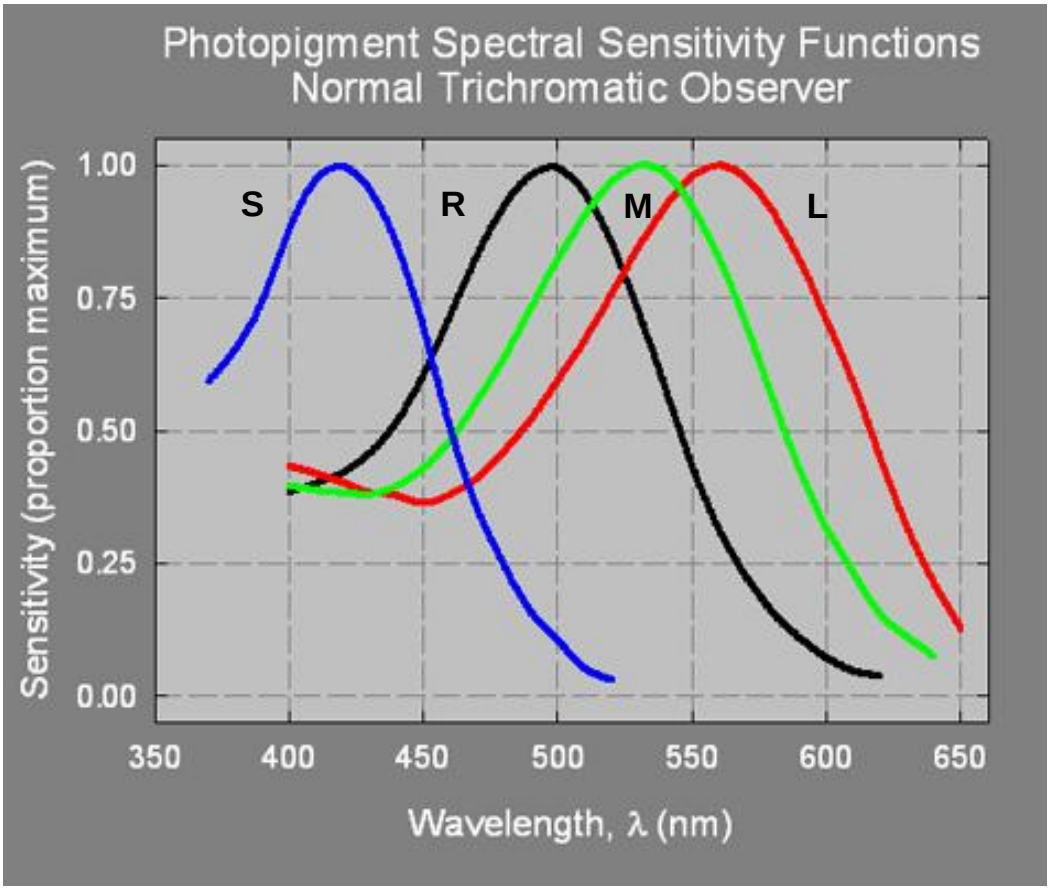

Figure 1.3 The spectral sensitivity curves of three types of cone photoreceptors and rod receptors in human. Note that the relative absorption is on a normalized scale. Rod spectral sensitivity is shown by the black curve. S, M and L cone photoreceptor sensitivities are shown in blue, green and red colour curves, respectively.

Source:http://www.psych.ndsu.nodak.edu/mccourt/Psy460/Color%20Vision/Photopigment%20spectral%20sensitivity%20-%20normal.JPG

The L and M cones constitute about 90-95% of the cone population and are densely packed at the foveola and gradually decrease with increasing retinal eccentricity. By comparison, S cones make up about 5-10% of the cone population (Calkins, 2001) and are most densely packed just outside the foveola at 2 degrees eccentricity. S cones are absent at the central fovea (Curcio et al., 1991). Studies have revealed that there is considerable variation among individuals in the relative proportion and distribution of L and M cones (Roorda and Williams,1999; Brainard et al., 2000) (See figure1.4). This observation implies that evolutionary process ignored the relative proportion and distribution of L and M cones in human retina. Roorda and Williams (1999) believe that this is because of two reasons. Firstly, red-green colour vision is a relatively new trait of vision in old-world primates (Nathans et al., 1986; Mollon, 1989). Secondly, statistics of natural scenes make high contrast, high spatial frequency signals rare events, optical blurring in the eye reduces potential for aliasing, and smart post-receptoral processing based on prior information about natural visual scenes may also tend to make M and L cone topography unimportant for visual performance (Packer and Williams, 2003).

Martin et al (2000) studied the arrangement of S cones in different species and found that their arrangement is random in most primates. However, few species have shown a regular hexagonal mosaic pattern of S cones. They have also shown that two species can have similar S cone density despite the differences in the local order of S cone array. From their observations, they concluded that at there are no two modes of mosaic organization. Implication of their results is that the regular hexagonal mosaic arrangement of S cones may not improve the quality of spatial processing in S cone pathways.

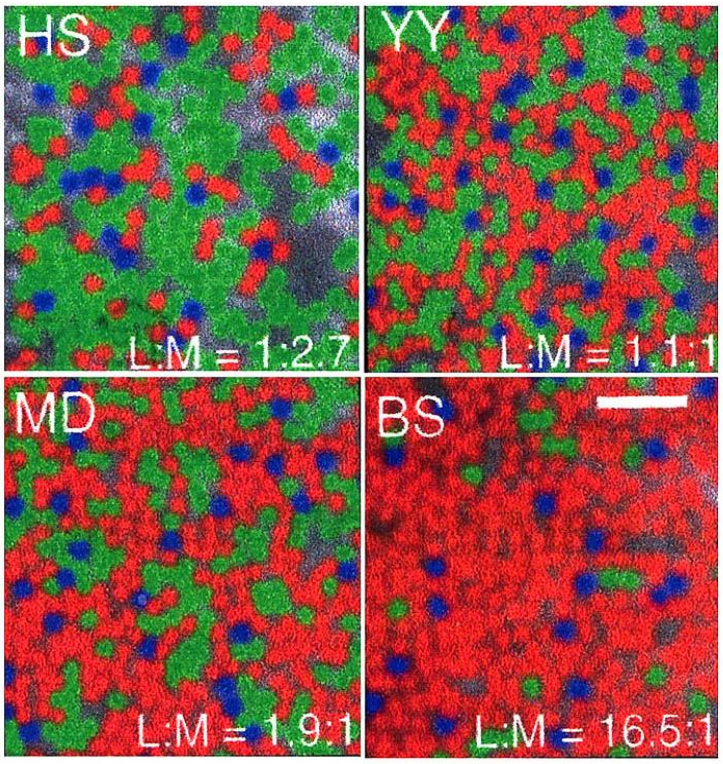

Figure 1.4 A view of the distribution of L-, M- and S- cones in the central retina obtained in four observers using adaptive optics. L cones are shown in red, M cones in green and S cones in blue. The relative difference in L and M cone numbers for each individual is listed in the figure.

Source: http://webvision.med.utah.edu/imageswv/GourasFig%2021.jpg.

Horizontal cells

Horizontal cells are lateral inter neurons in the outer retina with their dendritic processes inter connected with the axon terminals of the photoreceptors. These cells provide a negative feed-back signal to photoreceptors. They play an important role in the generation of receptive field surrounds of the bipolar cells and ganglion cells either via a feed-back pathway and/or by a direct feed forward to the bipolar dendrites (Dacey, 1999).

It has been observed that there are three different types of horizontal cells in the human retina (see figure 1.5), which synapse with all three types of cones (Kolb et al., 1994; Ahnelt and Kolb, 1994). Horizontal cells are not colour selective, but they are differentiated based on the relative inputs they receive from three cone classes.

A) **B)**

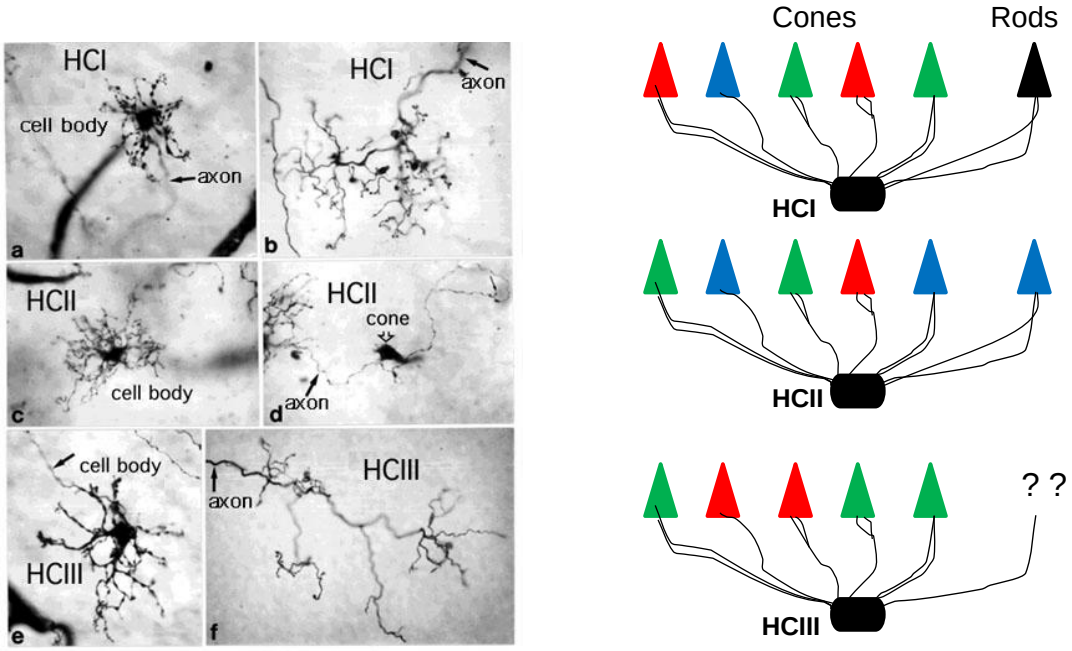

Figure 1.5 A) Light micrograph showing the cell body and axon type of three types of horizontal cells in human retina. B) Spectral connections of the three horizontal cell types of the primate retina. HCIII cells may or may not connect with S- cones.

Source: http://webvision.med.utah.edu/imageswv/LM3HChu.jpeg.

The first type of horizontal cell (HCI) makes substantial contacts with L and M cones and a small number of contacts with S cones. HCI cells have smaller receptive field with small dendritic diameters (Packer and Dacey, 2002). These cells hyperpolarize to light across the spectrum and show a spectral sensitivity similar to that of the photopic luminosity function (Vλ), which is strongly dominated by L and M cone input.

The second type of cell (HCII) connects with the S cones but also makes some contacts with L and M cones. The HCII cells, due to their selectivity for S cones, are involved in the blue-yellow (S-(L+M)) opponent pathway.

The third type of cell (HCIII) is selective for L and M cones and has no contacts with S cones. The role of HCIII cells in visual function, either in luminance processing or red green colour-opponency, is uncertain (Kolb et al., 1994).

Bipolar cells

Bipolar cells receive direct input from the photoreceptors and indirect input from the horizontal cells. Distinct cone bipolar cell types and one rod bipolar cell type have been identified in the primate retina (Boycott and Wassle, 1991; Kolb et al., 1992; Mariani, 1985) (See figure 1.6). Four main types of bipolar cells have been identified:

1) Diffuse bipolar cells
2) Midget bipolar cells
3) S-cone bipolar cells.
4) Rod-bipolar cells

Diffuse cone bipolar cells non-selectively contact multiple cones but can be divided into seven distinct populations on the basis of discrete levels of axonal stratification in the inner plexiform layer (Boycott and Wassle, 1991 , Grunert et al., 1994). Diffuse cells are thought to play a major role in processing luminance information (Boycott and Wassle, 1991; Wassle and Boycott, 1991).

Midget bipolar cells form two distinct populations that largely contact single cones: firstly, the flat midget bipolar (FMB) cells that make non-invaginating or basal contacts with cone pedicle and terminate in the outer portion of inner

plexiform layer. Secondly, the ‘Invaginating midget bipolar’ cells which extend their dendritic tips into the cone pedicle and terminate in the inner portion of inner plexiform layer. Midget bipolar cells are mainly involved in L-M cone opponent pathway and have connections with midget ganglion cells (see review by Dacey and Packer (2003)).

The ‘S cone bipolar’ cell type selectively contacts S cones (Mariani, 1984; Kouyama and Marshak, 1992). S cone bipolar cells receive excitatory and inhibitory S cone signals. Excitatory S cone signals are transmitted to S-ON bi-stratified ganglion cells and inhibitory signals are mediated via OFF midget ganglion cells via OFF midget bipolar cells (Dacey and Lee, 1994).

Rod bipolar cells form the major part of the bipolar cell population since the rods are more numerous than cones in the retina. The cell bodies of the rod bipolar cells are located in the middle and higher regions of the inner nuclear layer. Dendrites of rod bipolar cell enter the OPL and connect to the stacked rod spherules which are situated between cone pedicles. In the central retina, dendrites of the rod bipolar cells are small and can make contact with 10-15 rods. On the other hand, in the peripheral retina, dendrites are larger in size and make contact with 25-30 rods.

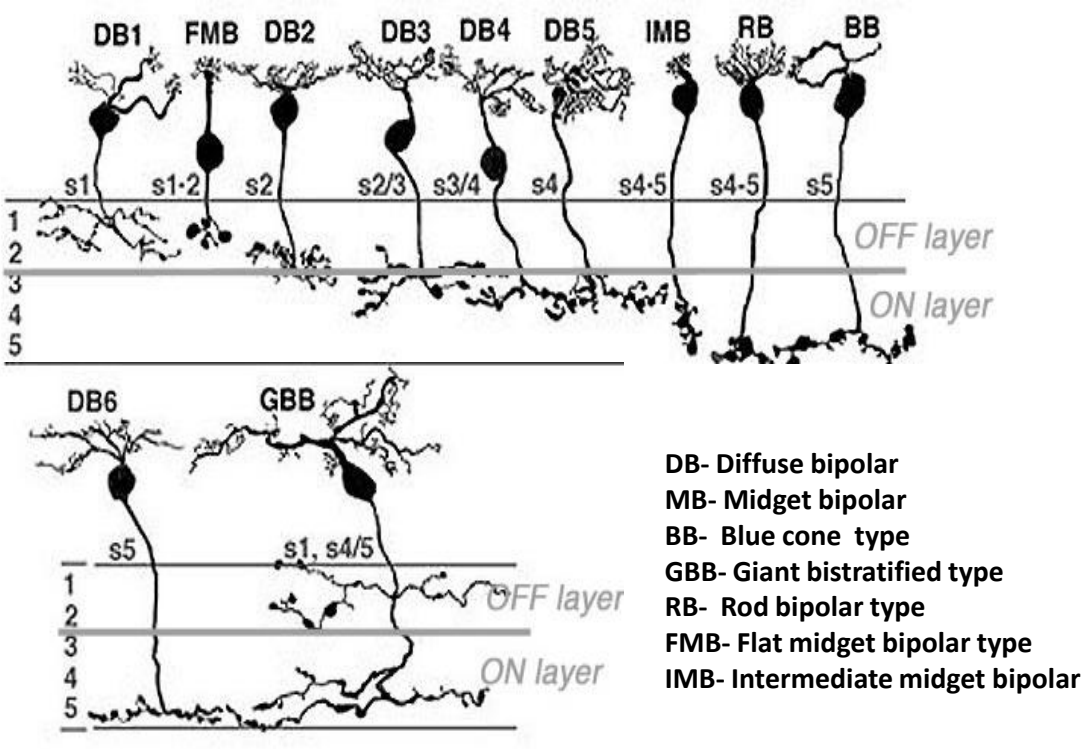

Figure 1.6 Summary of the distinct types of bipolar cells in the human retina (Boycott and Wassle, 1991).

All these type of bipolar cells exhibit centre-surround receptive field arrangements with on and off response regions (Dacey et al., 2000).

Amacrine cells

Amacrine cells are so named because they are nerve cells beleived to lack axons. Though these cells do not have true axons, their processes into the IPL functionally act like true axons. The cell nuclei of amacrine cells are found in the INL. About twenty two different morphological subtypes of amacrine cells are seen in the primate retina. They are classified in terms of: a) the width of their dendritic field connections b) the layer(s) in which they are located and c) their neurotransmitter type.

Amacrine cells (see figure 1.7) are broadly classified into narrow-field (30-150 μm), small field (150-300 μm), medium field (300-500 μm) and large field (>500

μm) cells, based on the measurement of their dendritic field diameter (Kolb et al., 1981).

Many varieties of amacrine cell are restricted to a single stratum, while others are bi or tri-stratified. When amacrine cell processes pass through all the five strata of the IPL from distal to proximal or vice versa, they are called diffuse cells. Superimposed upon Cajal's five strata subdivision of the IPL, is a sub laminar division of the IPL. The first two strata, 1-2, are known as sub lamina ***a*** of the IPL while strata 3-5 are known as sub lamina ***b*** (Famiglietti and Kolb, 1976). Sub lamina ***a*** contains bipolar axons and ganglion cell connections that lead to OFF-center ganglion cell receptive field (RF) formation, while sub lamina ***b*** contains bipolar to ganglion cell connections resulting in ON-centre ganglion cell RFs (Nelson et al., 1978).

Many of the roles of amacrine cells remain unclear; however there is some evidence that they might play a role in lateral inhibition (Wassle and Boycott, 1991). Stafford and Dacey (1997) studied two types of amacrine cells, A1 and A2. Both these types receive additive input from both L and M cones to both ON and OFF components of the receptive field, and do not seem to respond to S cone stimuli. These cells have spectral sensitivity similar to that of photopic luminosity function and are excluded from transmitting inhibitory cone signals to bipolar or ganglion cells. Bistratified A2 types are involved in transmission of rod signal (Wassle et al., 1989).

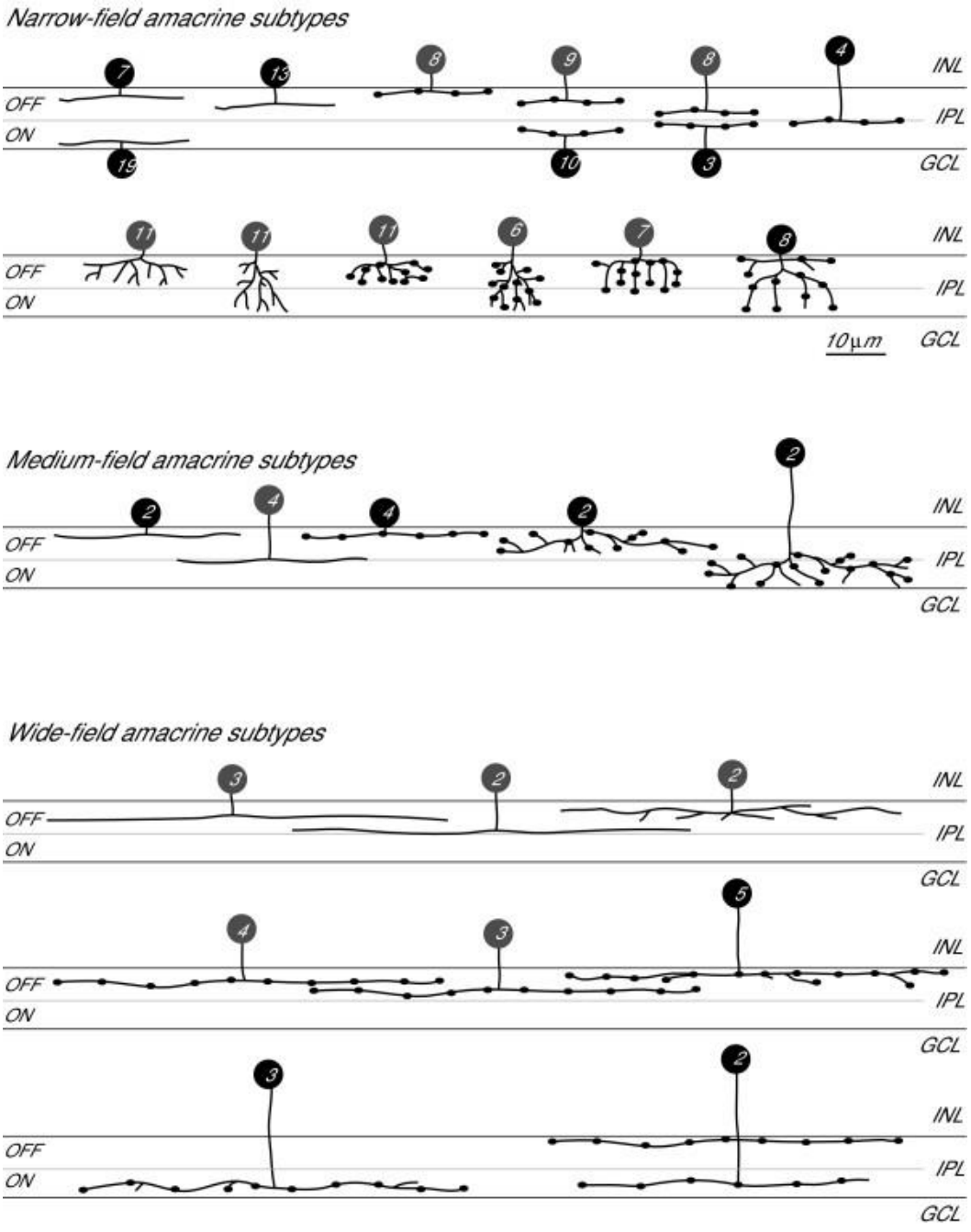

Figure 1.7 Schematic representation of small, medium, and large field amacrine cell types based on their stratification (Polayak, 1941) in Zebra fish retina. The subtypes shown in grey suggest that their somas were randomly distributed throughout the inner nuclear layer. GCL- Ganglion cell layer; INL-Inner nuclear layer; IPL- Inner plexiform layer. (Adapted from Jusuf and Harris, 2009).

Ganglion cells

Ganglion cells receive visual input from the photoreceptors via the bipolar, amacrine and horizontal cells. There are about 1.2 to 1.5 million ganglion cells in the human retina and each ganglion cell receives input from a single photoreceptor in the macular region, with increasing retinal eccentricity this number increases and in the extreme periphery each ganglion cell can receive information from hundreds of photoreceptors (Watanabe and Rodieck, 1989; Dacey, 1993; Croner and Kaplan, 1995). There are about twenty types of ganglion cells but they are divided into three major categories based on their axon projection and function. These are;

1) Midget ganglion cells

2) Parasol ganglion cells

3) Bistratified ganglion cells

The three types of ganglion cells mentioned above have axons which project to lateral geniculate nucleus (LGN) (see figure 1.8). Midget ganglion cells project to the dorsal layers of LGN and forms the parvo cellular (P) pathway. Parasol ganglion cells project to the ventral layers of the LGN and forms the magno cellular (M) pathway. Small bistratified ganglion cells project to the interlaminar zone of the LGN, this forms konio cellular (K) pathway.

Midget retinal ganglion cells are so named because of the small size of their dendritic trees and cell bodies. They receive inputs from relatively few rods and cones. They have a slow conduction velocity. These cells have linear luminance contrast gain functions and respond well to changes in colour (Gouras, 1969; Purpura et al., 1990).

Four sub types of midget ganglion cells were identified based on the basis of their receptive field structure. All these four types of cells have a receptive field centre, that is either excited or inhibited by L or M cones and a surround which displays antagonistic properties (see figure 1.9). These cells project to P layers of the lateral geniculate nucleus. About 80% of retinal ganglion cells are midget cells (Perry et al., 1984). In the foveal region, midget bipolar cells receive input from a single cone and transmit their input to midget ganglion cells (Kolb and Dekorver, 1991; Calkins et al., 1994). This is known as the private line arrangement.

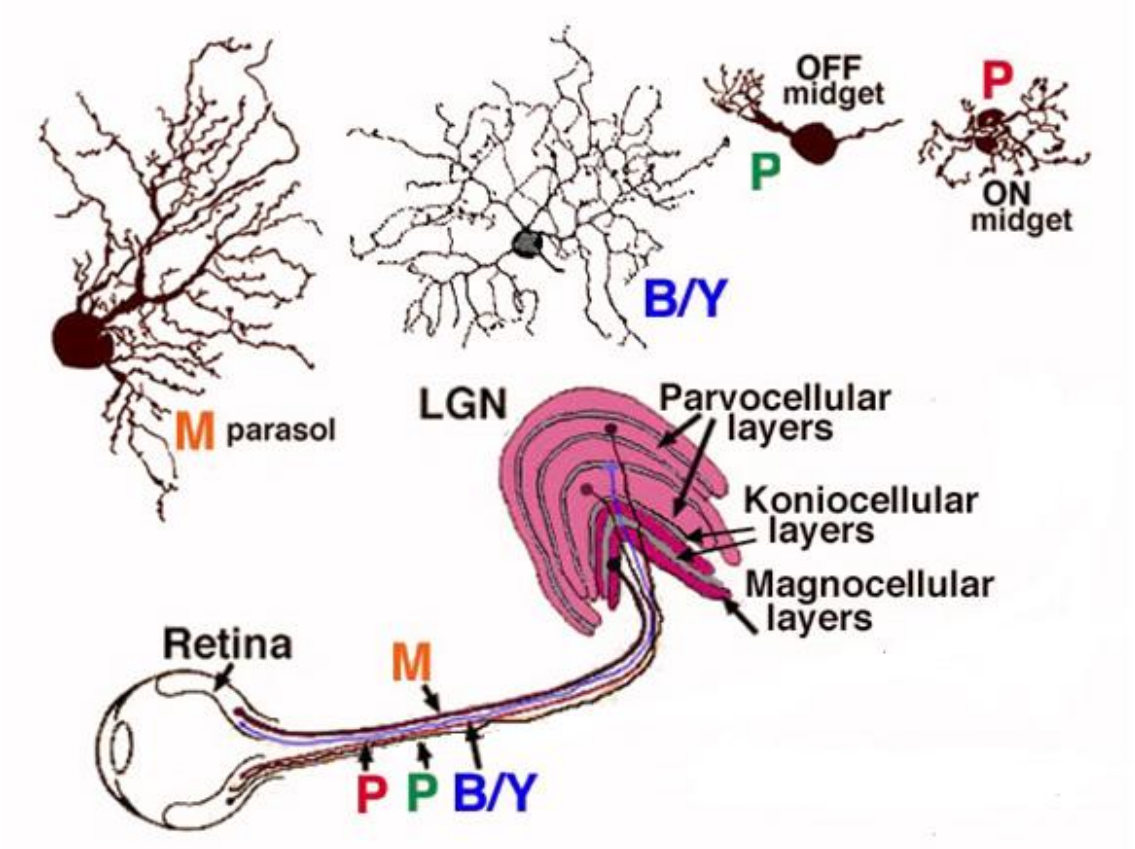

Figure 1.8 Three distinct types of ganglion cells and their projections to the LGN. These projections form the basis for M-, P- and K- cellular pathways. Picture re drawn from Shapley and Perry (1986). P- P-cellular pathway, M-magnocellular pathway, B/Y- Konio cellular pathway.

Source: http://webvision.umh.es/webvision/imageswv/hugcproj.jpeg

Parasol retinal ganglion cells are so named because of their large size dendritic trees and cell bodies. These cells receive visual inputs from a relatively large number of rods and cones. They have a fast conduction velocity and can respond to low-contrast stimuli, but are not very sensitive to changes in colour. These cells have saturating luminance contrast gain functions (Gouras, 1969; Purpura et al., 1990).

Parasol ganglion cells have much larger receptive fields with center-surround organization and project to the M layers of the lateral geniculate nucleus. About 10% of retinal ganglion cells are parasol cells (Perry et al., 1984).

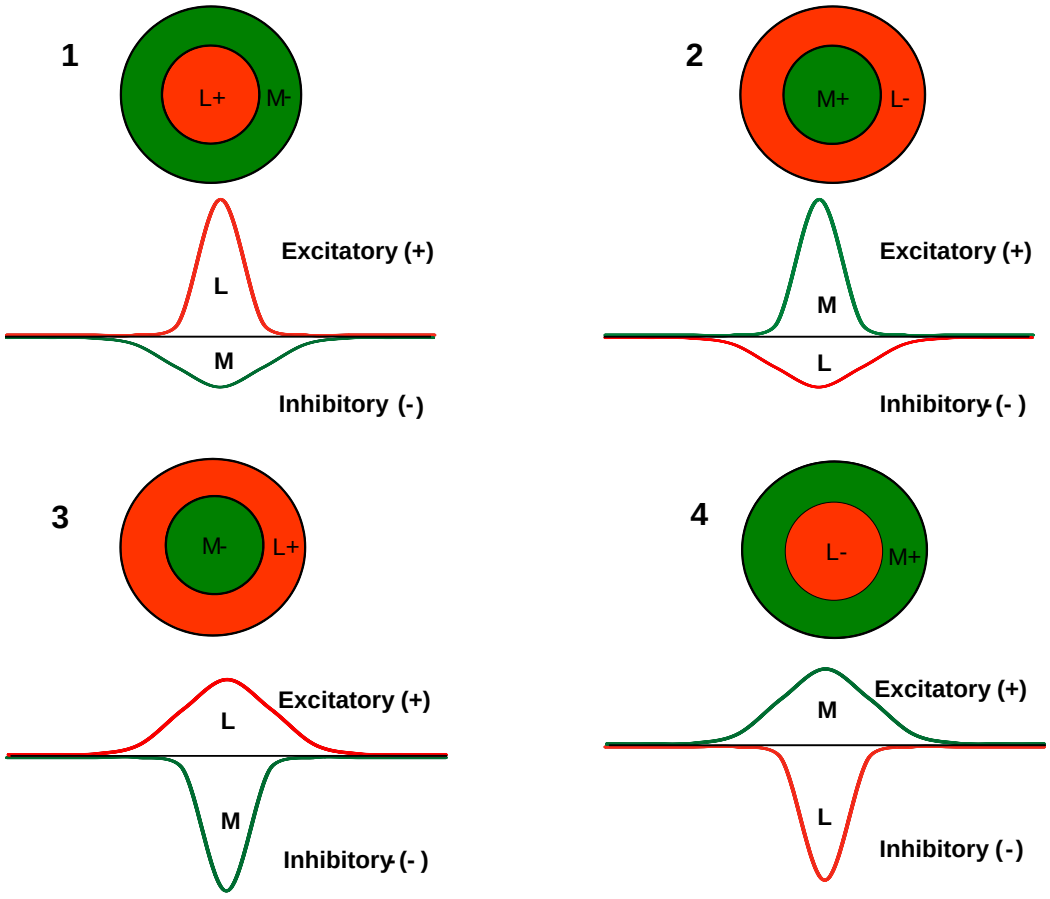

Figure 1.9 Different receptive field types of midget ganglion cells in the retina.

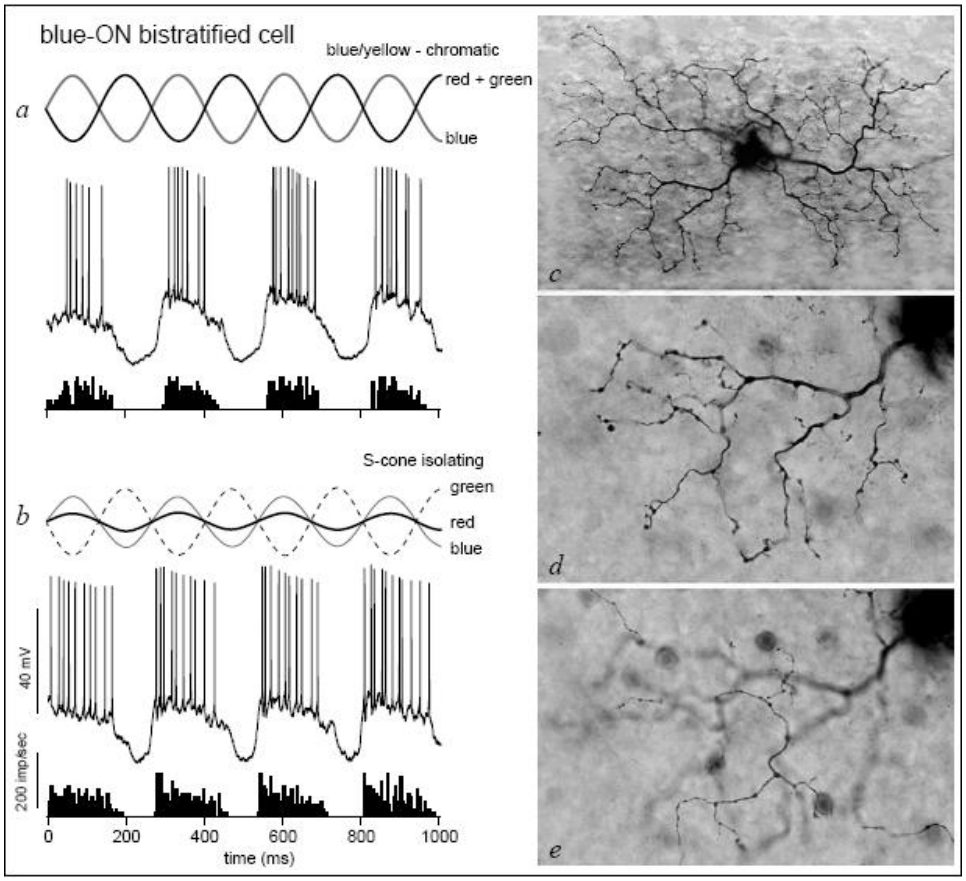

Figure 1.10 an example of a bi-stratified ganglion cell in the monkey retina. a) S-on response to a blue-yellow chromatic stimulus. *Top:* the stimulus waveform (output form a blue light is modulated in counter phase to isoluminant red-green *middle:* Intracellular voltage response shows a blue-on depolarization and spike discharge. *Bottom:* spike histogram. b) S-cone mediated on response. *Top:* amplitude and phase of red, green and blue lights are adjusted such that L and M cones are silenced and S cones only modulated. *Middle:* voltage response of a cell which shows strong depolarization and spike discharge with S-cone modulation. *Bottom:* post stimulus histogram as in a. c) Dendritic morphology of bistratified ganglion cell whose light response is shown in a. d) higher magnification of portion of dendritic tree that shows inner tier of dendrites. e) Same field as shown in d but the focus is changed to the sparsely branched outer dendritic tier (After Dacey, 1994).

Bi-stratified retinal ganglion cells project to the K layers of the lateral geniculate nucleus (LGN). About 10% of retinal ganglion cells are bi-stratified cells and they receive inputs from fewer rods and cones than parasol ganglion cells. They

have a moderate spatial resolution and conduction velocity that falls between that exhibited by M and P cells and can respond to moderate levels of luminance contrast (Dacey and Lee, 1994).These cells have very large receptive fields that only have centres with no surrounds and are always ON to the S cone signals and OFF to both the L and M cone signals (See figure 1.10).

1.2.2 Post receptoral chromatic and achromatic pathways

Hering in the late 1800's proposed a theory known as *Opponent Process Theory*, which attempted to explain how we perceive the colour of an object. However, Hering's theory failed to describe sufficiently all aspects of colour vision e.g. chromatic after images and the perceptual absence of certain colours. According to this proposal, we perceive colour and luminance using three independent antagonistic channels; red-green, blue-yellow, and black-white. This theory has been supported by electrophysiological recordings from the LGN, indicating the presence of three distinct channels (Derrington et al., 1984). These three channels compare the relative activation between the three cone types (see figure 1.11):

1) Red-green pathway compares the L and M cones
2) The blue-yellow pathway compares the S cones with the L and M cones
3) Luminance pathway combines the signal from L and M cones.

Various groups have investigated the circuitry of opponent and non-opponent pathways in the retina. Summary of their investigations can be simplified as follows:

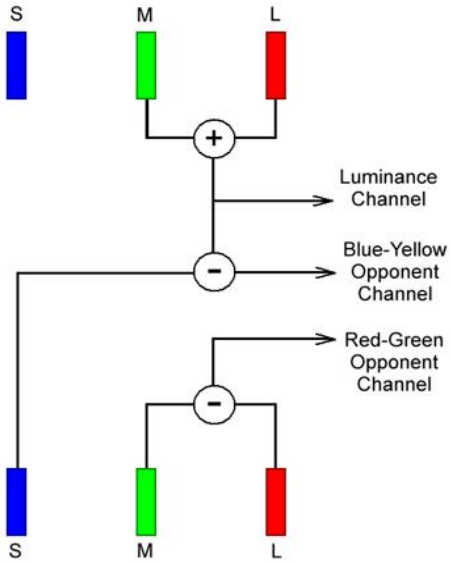

Figure 1.11 The opponent colour process. The red-green pathway is formed from comparison of the L and M cone signal; the blue-yellow pathway from comparison of the S-cone signal with the L and M cone product; luminance pathway from the sum of the L and M cone signal.

Source:http://www.psych.ndsu.nodak.edu/mccourt/Psy460/Color%20Vision/Color%20Vision_files/image006.jpg

The L-M opponent (Red-Green) pathway in retina

The receptive field centre of a midget ganglion cell receives excitatory input from either an L or M cone via on-center midget bipolar cell. The receptive field surround of the same ganglion cell receives inhibitory input from the opposing cone type to that of centre via off-center midget bipolar cells. An example of L-M opponent pathway in central retina is described in figure 1.12.

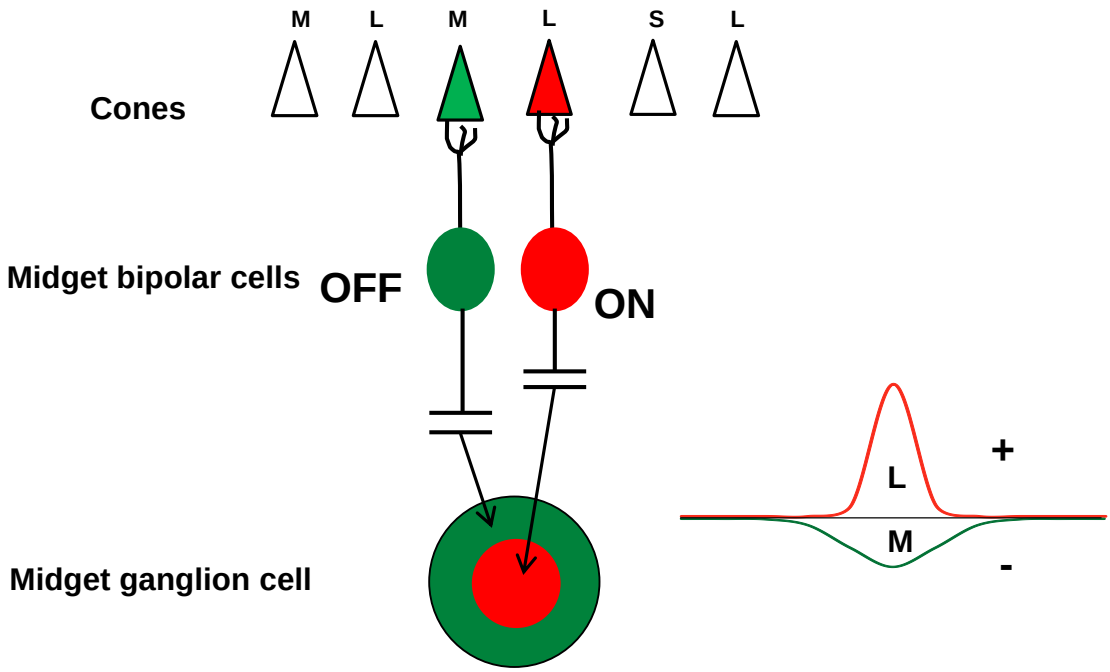

Figure 1.12 Simple diagrammatic representations of L-M opponent pathway in the retina. L and M cones make contact with both on- center and off-center bipolar cells. Only one example for each is drawn in figure for the clarity.

The S/(L+M) (Blue-Yellow) pathway in retina

Small bi-stratified ganglion cells difference the S cone signal with summed signals from the M and L cones i.e. +S-(L+M). The inner layer of dendrites receives input from the ON S-cone bipolar, and the outer layer receives input from OFF bipolar with L- and M- cone input, providing opponency (Lee, 2004) (See figure 1.13). One study has suggested that S cones provide input to an OFF- midget bipolar cell and presumably OFF-midget ganglion cells (Klug et al., 2003). However, the existence of S-OFF bipolar cells has proved to be controversial (Lee et al., 2005). Solomon and his associates (Tailby et al., 2006; Solomon and Lennie, 2005) have re-examined the cone inputs to the receptive fields of macaque lateral geniculate nucleus neurons and found OFF- S cone input to these neurons. According to them, S-OFF cells receive the input from

both M cones and S cones with the same sign, and opposed to the input from L cones (Solomon and Lennie, 2007).

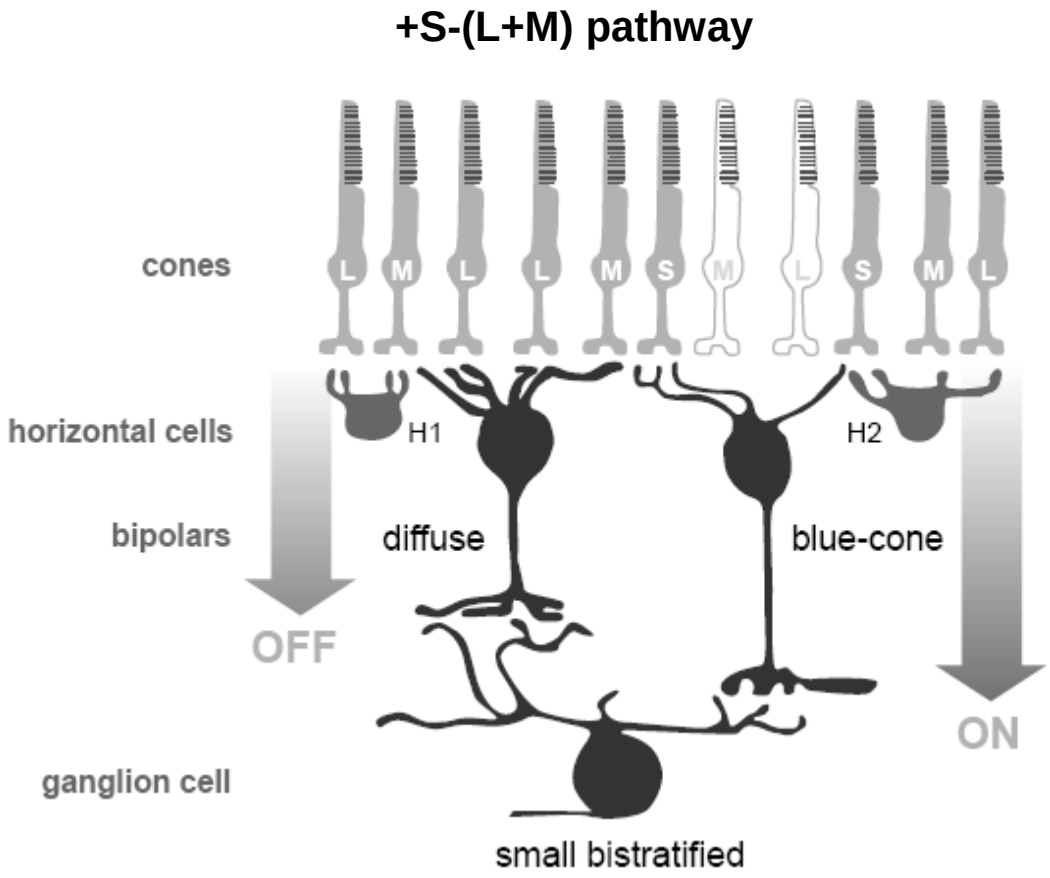

Figure 1.13 Simple diagrammatic representations of +S-(L+M) opponent pathway in the retina. Picture adapted from Dacey (2000b).

The L+M, non-opponent (Luminance) pathway in retina

L+M pathway is mediated by parasol ganglion cells. These cells receive an excitatory input from diffuse bipolar cells, which contact both L and M cones (figure 1.14) and therefore no colour opponency is observed. However, spatial opponency is still maintained.

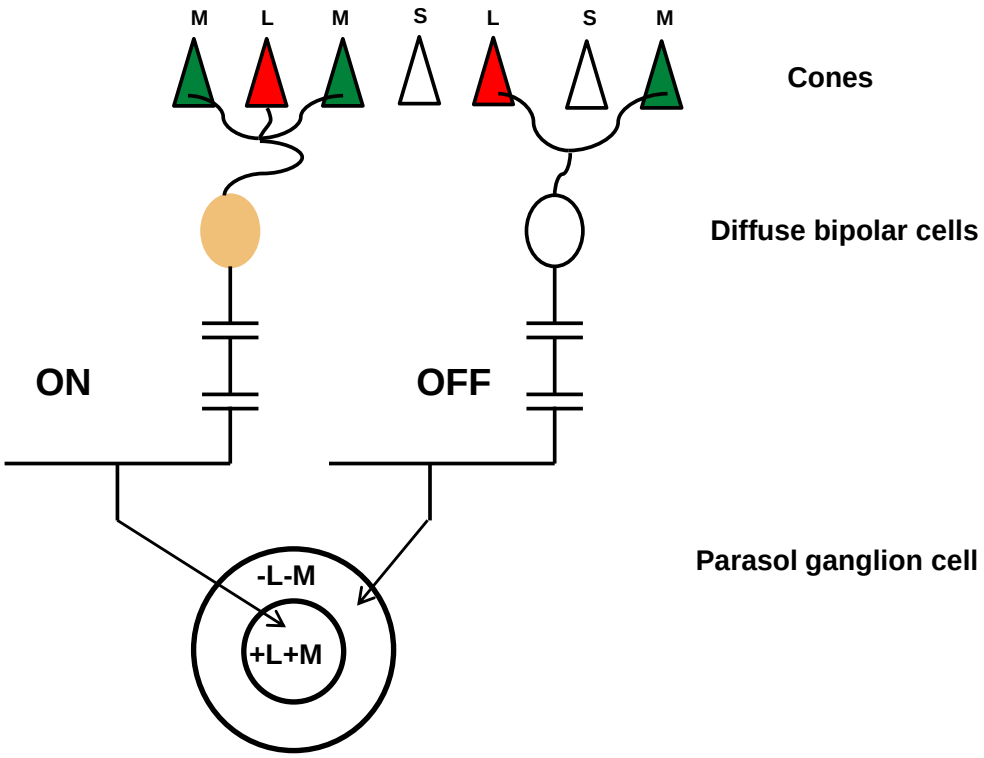

Figure 1.14 Simple diagrammatic representations of non-opponent pathway in the retina.

1.2.3 The Lateral geniculate nucleus (LGN)

Chromatic and luminance information is carried from the retina to the LGN via the axons of different ganglion cell types. In primates, the LGN is divided into six main layers separated by cell-sparse interlaminar or K cellular zones (Casagrande, 1994). The two most ventral layers (layers 1 and 2) receive input primarily from parasol retinal ganglion cells (Leventhal et al., 1981; Perry et al., 1984) and contain M cells; the four dorsal layers (layers 3-6) receive input from midget ganglion cells (Leventhal et al., 1981; Perry et al., 1984; Rodieck and Watanabe, 1993) and contain P cells. The interlaminar zone receives input from small bi-stratified ganglion cells and contains K cells (See fig1.15).

Studies conducted on rhesus monkeys have shown that M cells have relatively large receptive fields with high contrast sensitivity. They show phasic responses

to maintained contrast and show little sign of cone opponency. P cells on the other hand, have small receptive fields; respond tonically to high contrast achromatic and low contrast chromatic stimuli. P-LGN cells posess red-green (L/M), centre-surround colour opponency with on-centre cells dominating the dorsal P layers with the majority off-centre cells lying in the ventral layers (Wiesel and Hubel, 1966; Dreher et al., 1976; Demonasterio and Gouras, 1975). Recent studies on marmoset LGN have demonstrated that the majority of K cells have a centre-surround receptive field organization and carry information from the S-ON pathway (White et al., 1998; White et al., 2001).

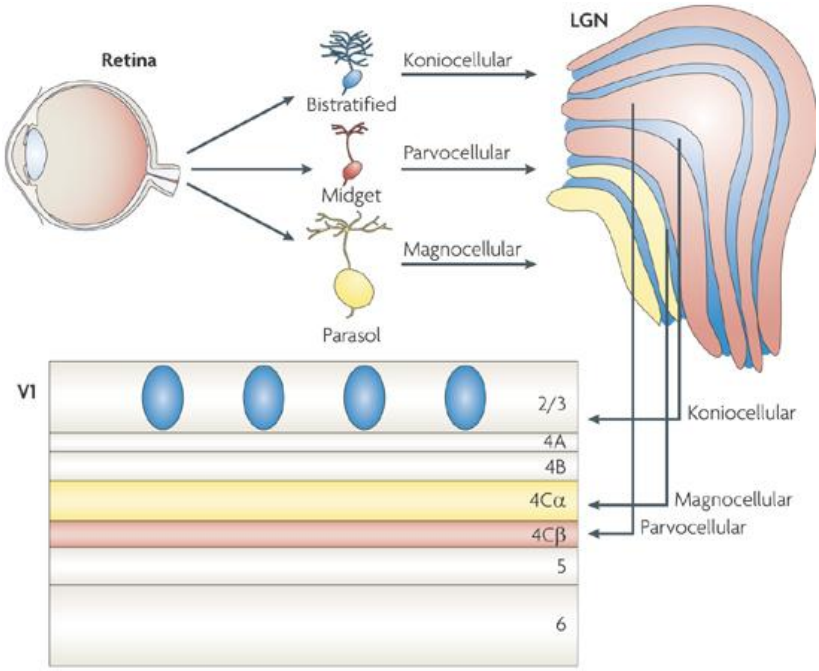

Figure 1.15 Midget, parasol and bi-stratified ganglion cells and their projections to LGN and further areas of primary visual cortex (V1), which forms the basis for the P, M and K pathways. Picture adapted from Jonathan et al., 2009.

M cells respond to higher temporal and lower spatial frequencies, whereas P cells show a preference for high spatial frequencies and lower temporal frequencies (Hicks et al., 1983; Derrington et al., 1984; Derrington, 1984). P cells respond well to luminance contrasts below 10%, whereas M cells often

respond to stimuli with contrasts as low as 2% (Shapley et al., 1981; Purpura et al., 1988; Sclar et al., 1990). M cells display transient responses with fast conduction velocities, whereas P cells have tonic responses with medium conduction velocities.

The feature that distinguishes K cells from M and P cells is that K cells have low peak firing rates (60 impulses/second) and low levels of spontaneous activity (White et al., 2001). Response characteristics of three types of cells are summarized in table1.1.

Response characteristic/ type of cell	**M cells**	**P cells**	**K cells**
Colour opponency	Not present	Present	Present
Contrast sensitivity	High	Low	Low
Spatial frequency	Low	High	Low
Temporal frequency	High	Low	High
Size	Large	Medium	Small
Response	Fast, transient	Slower, sustained	Slowest

Table 1.1 Summary of the properties of P, M and K cells. Source: (Wiesel and Hubel, 1966; Dreher et al., 1976; Demonasterio and Gouras, 1975; Derrington et al., 1984; Derrington, 1984; Hicks et al., 1983; Purpura et al., 1988; Sclar et al., 1990; Shapley et al., 1981).

In terms of receptive field (RF) structure, the lateral geniculate nucleus has various types of colour opponent cells. The four dorsal layers (P layers) of the macaque LGN contain three varieties of neurons; 1) colour opponent center-surround (Type-I), 2) colour opponent center only (Type II), and 3) non-opponent, broad band type (Type III) (Hubel and Wiesel, 1968; Kruger, 1977; Schiller and Malpeli, 1978; Tsumoto et al., 1978; Creutzfeldt et al., 1979). Two types of cells have been observed in two ventral layers (similar to type III and type IV) of the rhesus monkey LGN.

Type I cells (see figure 1.16) make-up 65% of the cell population in the dorsal layer cells. With diffuse light stimuli, they show opponent colour responses, giving on-responses to one set of wavelengths and off-responses to other set of wavelengths and no response at intermediate wavelengths. Five sub varieties of type I cells are seen in order of frequency: 1. red-on center and green-off surround, 2. red-off center and green-on surround, 3. green-on center and red-off surround, 4. green-off center and red-on surround, and 5. blue-on center and green-off surround (Hubel and Wiesel, 1966).

Type-II cells (see figure 1.17) constitute a minority of dorsal layer cells. These cells have no center surround receptive field arrangement but show colour opponent responses over all regions of the field. They behave as though they receive opponent inputs from two sets of cones with identical distributions over the retina.

Cells in ventral layers are of two types: III and IV. Type-III cells (see figure 1.18) have concentrically arranged on-center or off-center receptive fields, the center and surround having identical spectral sensitivities. Type IV cells have

concentrically arranged on-centre fields with large off surrounds and a spectral sensitivity displaced towards red with respect to the centre.

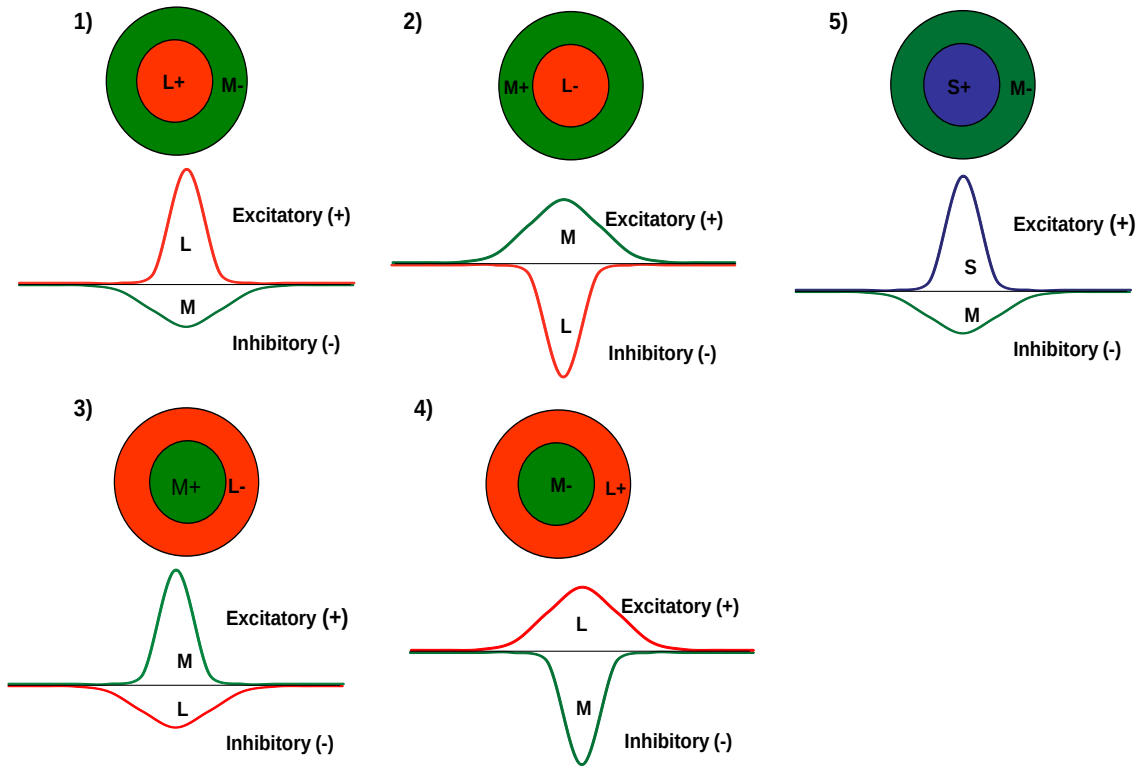

Figure 1.16 Receptive field types of Type–I cells in LGN. Center and surround organisation with opponent cone input. Picture is drawn on the basis of Hubel & Wiesel (1966) findings.

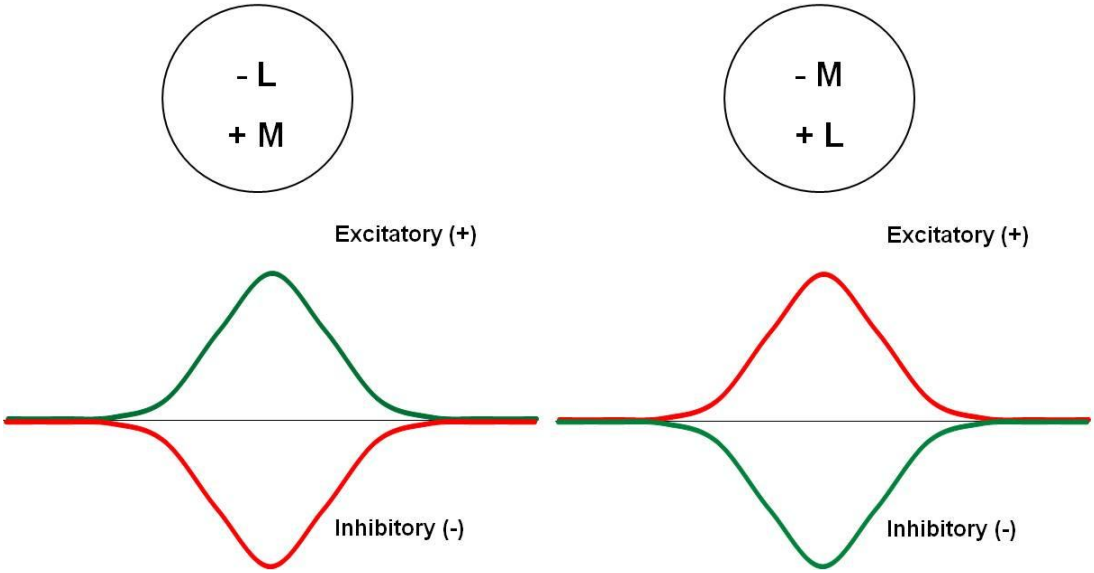

Figure 1.17 Receptive field types of type-II cells in LGN.

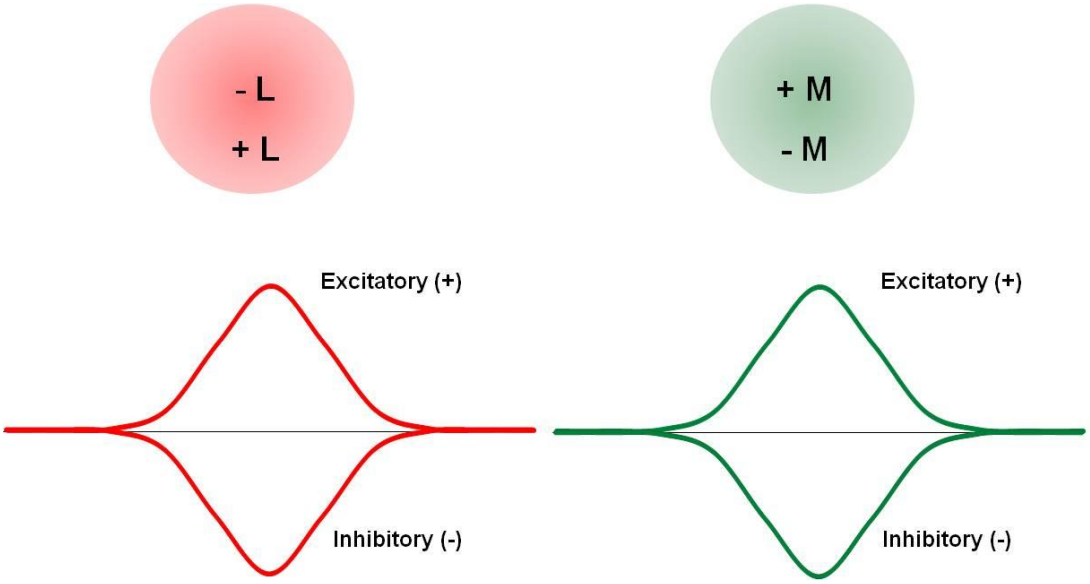

Figure 1.18 Receptive field types of type-III cells in LGN.

1.2.4 The Primary visual cortex (V1)

The segregation of M-, P- and K- pathways is largely preserved in the primary visual cortex (see fig.1.19). P pathway neurons project predominantly to layer 4Cβ of V1 and then on to Cyto-chrome oxidase layers 2 and 3[1] (Hubel and Wiesel, 1972; Lund, 1973; Fitzpatrick et al., 1985), which contain blob and inter-blob regions. M pathway neurons project to layer 4B via the layer 4Cα of V1 (Hubel and Wiesel, 1972; Lund, 1973; Blasdel et al., 1985) and K pathway neurons project into layers of 2, 3 and 4A of V1 (Livingstone and Hubel, 1987; Casagrande, 1994; Chatterjee and Callaway, 2003).

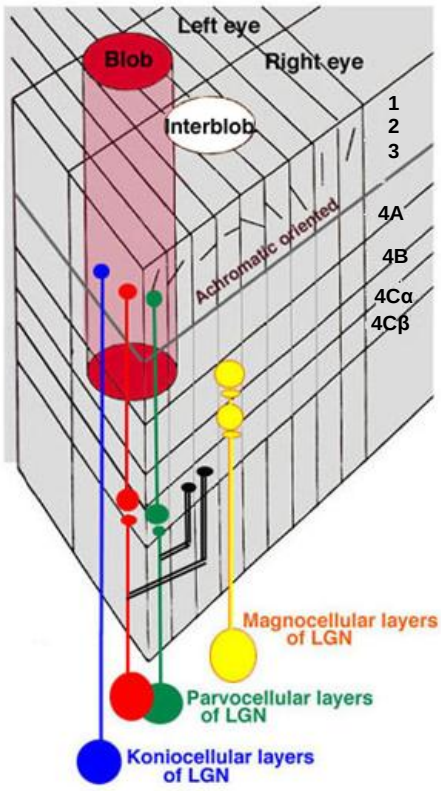

Figure 1.19 M-, P- and K-cellular layers of LGN inputs to the various layers of the primary visual cortex. Source: http://webvision.med.utah.edu/Color.html

[1] Cyto-chrome oxidase is mitochondrial enzyme that is present in every living cell except in hair and bone. Wong Riley (1979) was the first person to make observations using Cyto-chrome Oxidase. Different concentration of Cyto-chrome Oxidase can be used to study the different regions of the brain. Livingstone and Hubel (1984b) have exploited this technique and made number of observations. They termed these high concentrated cyto-chrome oxidase areas in the cortex as blobs. Cytox blobs are set of functional domains in upper cortical layers that contain high Cyto-chrome Oxidase activity (see Murphy et al., 1995).

Layer 4Cβ contains colour-opponent center-surround cells (Type-I) and broadband cells (Livingstone and Hubel, 1988). Cytox blobs in layers 2 and 3 contain one third centre only single opponent colour cells (Type II) and the other two thirds are double-opponent cells (Tootell et al., 1988). Double opponent cells are first observed in striate layer 4Cβ, and not seen in the retina or in the LGN (Livingstone and Hubel, 1984a; Tootell et al., 1988). Double opponent cells have centre surround receptive fields, show colour-opponency when either centre or surround is stimulated (Michael, 1985; Shapley and Hawken, 2002). The centre of the double opponent cell resembles the receptive field of colour-opponent cell, receiving two opponent sets of cone inputs where as the surround has opponent colour inputs, opposite in sign to the inputs feeding the centre (see figure1.20). An example of such type of cell is one whose field centre is +L-M and surround is –L+M. These cells respond poorly to uniform fields of any colour but respond well to purely chromatic edges (Solomon and Lennie, 2007).

Early studies of the primary visual cortex adopted stringent criteria to define luminance cells and colour coded cells (Hubel and Wiesel, 1968). According to this criterion, cells that respond to luminance are called luminance cells and those which respond exclusively to chromatic stimuli are called colour cells. Colour cells make up only 10% of the cells according to this definition. However, in recent years this definition has changed. Cells that add L- and M- cone inputs are called luminance cells, and the cells that subtract L-, M-, or S-cone inputs are called colour cells (see Gegenfurtner, 2003 for review). Using the new criteria for defining cells, it is estimated that about 50% of cells are colour selective in the early visual areas of macaques with little differences between V1, V2,V3 and V4 (Dow and Gouras, 1973; Kiper et al., 1997; Shipp and Zeki,

2002; Gouras, 1974; Johnson et al., 2001). L/M opponent cells form 3/4 of colour opponent population and the S/ (L+M) opponent cells forms 1/4 of this population in the cytox blob colour cells (Ts'o and Gilbert, 1988).

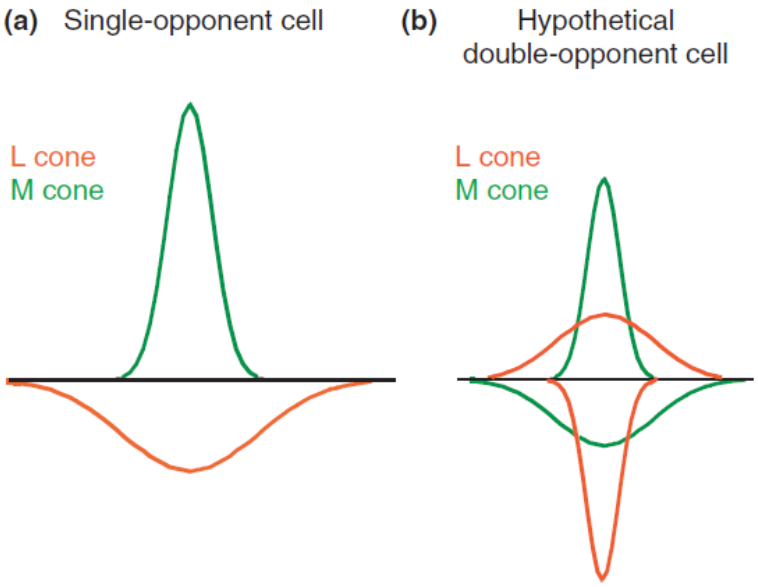

Figure 1.20 Receptive field models of single (a) and double (b) opponent cells in primary visual cortex. a) single-opponent L-M sensitive neurons receive input from L and M cones of equal strength but are of opposite sign. These cells were seen both in V1 and LGN. b) Hypothetical double-opponent neurons that receive both excitation and inhibition from each single cone input (Shapley and Hawken, 2002).

Recent optical imaging studies (Xiao et al., 2007; Conway and Tsao, 2006) have shown that primate V1 contains neurons that respond preferentially to various hues such as red, green, blue, yellow etc. Different hues activate different patches of the supra granular layers (layers 2 and 3) of the parafoveal V1 and they overlap partially (see figure 1.21). The hue order is well preserved within each peak cluster, but the clusters have various geometrical shapes.

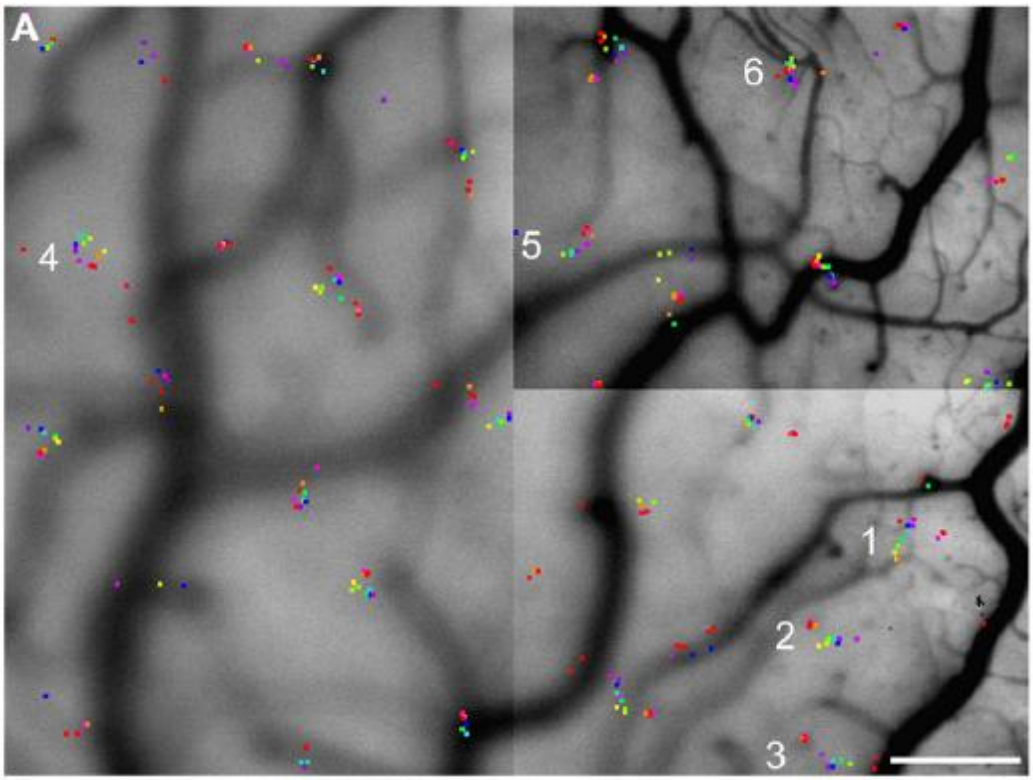

Figure 1.21 Clusters of hue specific activated patches in primary visual cortex (V1). All these patches marked on an anatomical image of cortical surface. Picture adapted from Xiao et al (2006).

The spatial and chromatic properties of magno, parvo and konio cellular layers are well preserved in the primary visual cortex. Layers 4Cα and 4B in the macaque have been found to be sensitive to variations in luminance and insensitive to colour, on the other hand, layer 4Cβ and blob regions of superficial layers 2 and 3 are very sensitive to colour information (Tootell et al., 1988). The lack of colour sensitivity in layers 4B and 4Cα may be as a result of their input and output targets. Layer 4Cα receives major input from M layers of the LGN, in which colour sensitivity is weak (Blasdel and Lund, 1983; Livingstone and Hubel, 1984a). Layer 4B derives a major input from layer 4Cα, and in turn neurons in layer 4B project to area MT, where color sensitivity has

been reported to be absent and neurons are responsive to motion (Zeki, 1978b).

A study by Chatterjee and Callaway (2003) studied cone-opponent properties of afferent axon terminals in the macaque V1 and demonstrated that there are specific regions for L/M and S/(L+M) on-off pathways (see figure 1.22). These pathways are described as:

1) L-M opponent signals project to layer 4Cβ.
2) L+M (achromatic, non-opponent) signals project to layer 4Cα
3) S-ON signals project to layer 4A and blob regions of 2 and 3
4) S-OFF signals project to layer 4A.

1.2.5 The Second visual area (V2)

Cytochrome-oxidase histochemistry of area V2 has revealed a pattern of parallel stripes running at right angles to the V1 border (Horton, 1984), separated into repeating cycles of regions. These regions are named as thick, thin and inter-stripe regions (Tootell et al., 1983). Livingstone and Hubel (1984a, 1987) speculated that regions with comparable levels of cytochrome oxidase might be connected together.

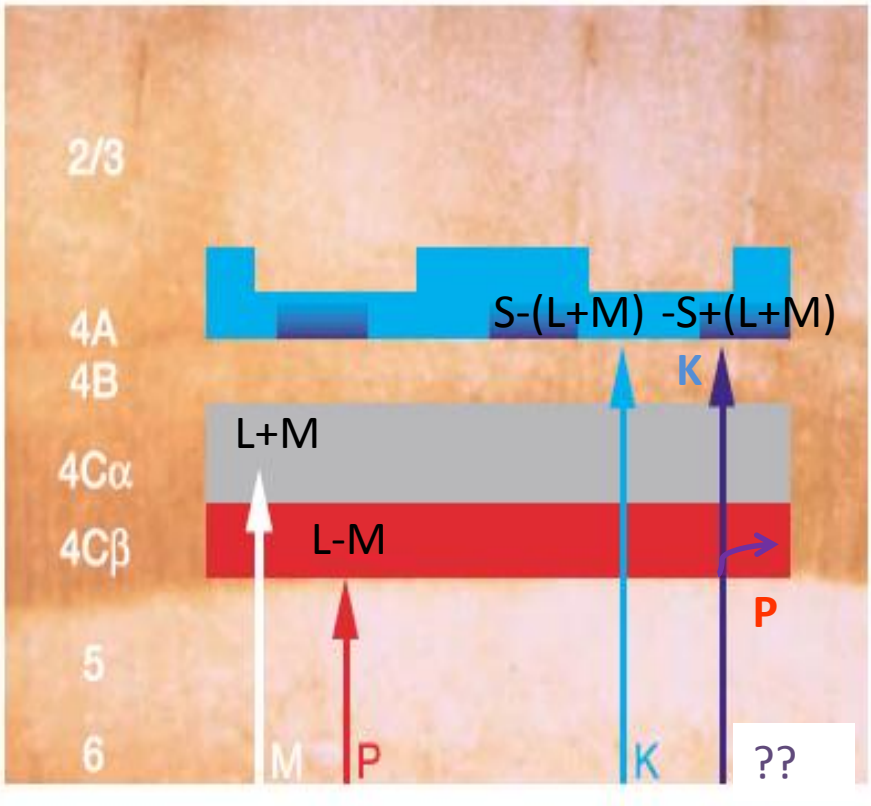

Figure 1.22 Hypothetical relationships between physiology of colour inputs and anatomical projections in V1. L-M and L+M afferents to layer 4C probably arise from M and P contributions to 4Cα and 4Cβ respectively. S-ON inputs to 4A and 2/3 are probably K cellular. S-OFF afferents can be konio cellular, but there is also a P projection to 4A, raising the probability that a separate S-OFF parvo substream bypasses its usual target of 4Cβ project solely to 4A (Adapted from Chatterjee and Callaway, 2003). Red region shows the P cellular input, grey region suggest magno cellular input and finally blue region suggest K cellular input.

Cytochrome oxidase (CO) Blobs in layers 2 and 3 of V1 project to the thin stripes of V2, inter-blob regions of V1 projects to inter-stripe regions of V2 (Livingstone and Hubel, 1983) and layer 4B projects into thick stripes of V2 (Livingstone and Hubel, 1987). In turn the thick stripes of V2 project to cortical area (V5/MT), whilst the thin & inter-stripe regions project to cortical area V4 (DeYoe and Van Essen, 1985; Shipp and Zeki, 1985) (See figure 1.23).

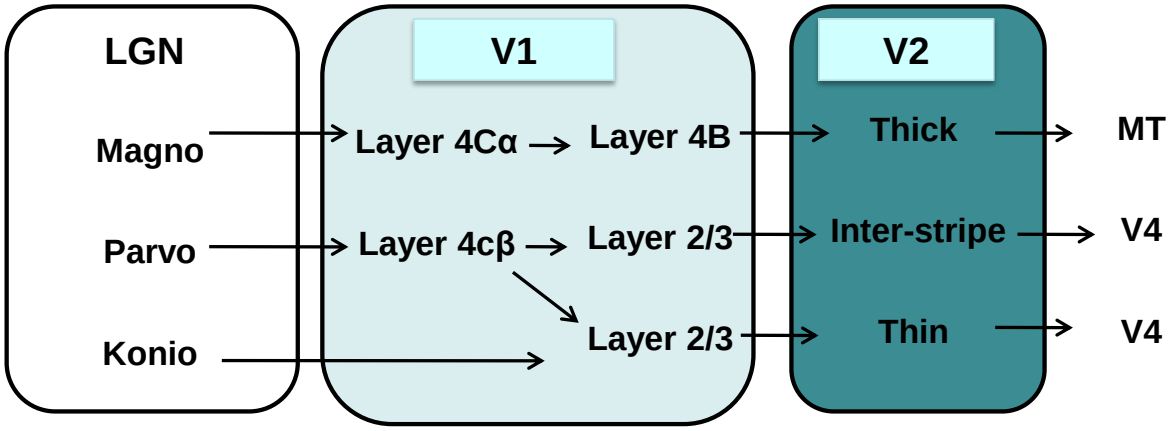

Figure 1.23 Projections of M-, P- and K-cellular neurons from LGN to further areas of visual cortex. We can also note the type of visual information processed in different layers of V2. Adapted from (Sincich and Horton, 2005).

Recent studies (Xiao et al., 2003; Conway, 2003) on macaque V2 have suggested that colour selective neurons in V2 are organized into maps (see figure 1.24) in which the colour of the stimulus is represented by the location of the peak response to the stimulus and the colour selective bands occupy 60% of the area of the thin stripes. Recently discovered hue maps in V1 and V2 are likely to play an important role in hue perception in primates.

1.2.6 Processing of colour and other visual attributes in V1 and V2

One of the important questions that remain unanswered about the cortical processing of chromatic information is whether colour is processed independently of other visual attributes such as form, motion or depth or whether these computations are carried out at the same time within the same group of neurons. Even though studies have shown the anatomical segregation,

it is still unclear whether it reflects a segregation of visual function at the same time.

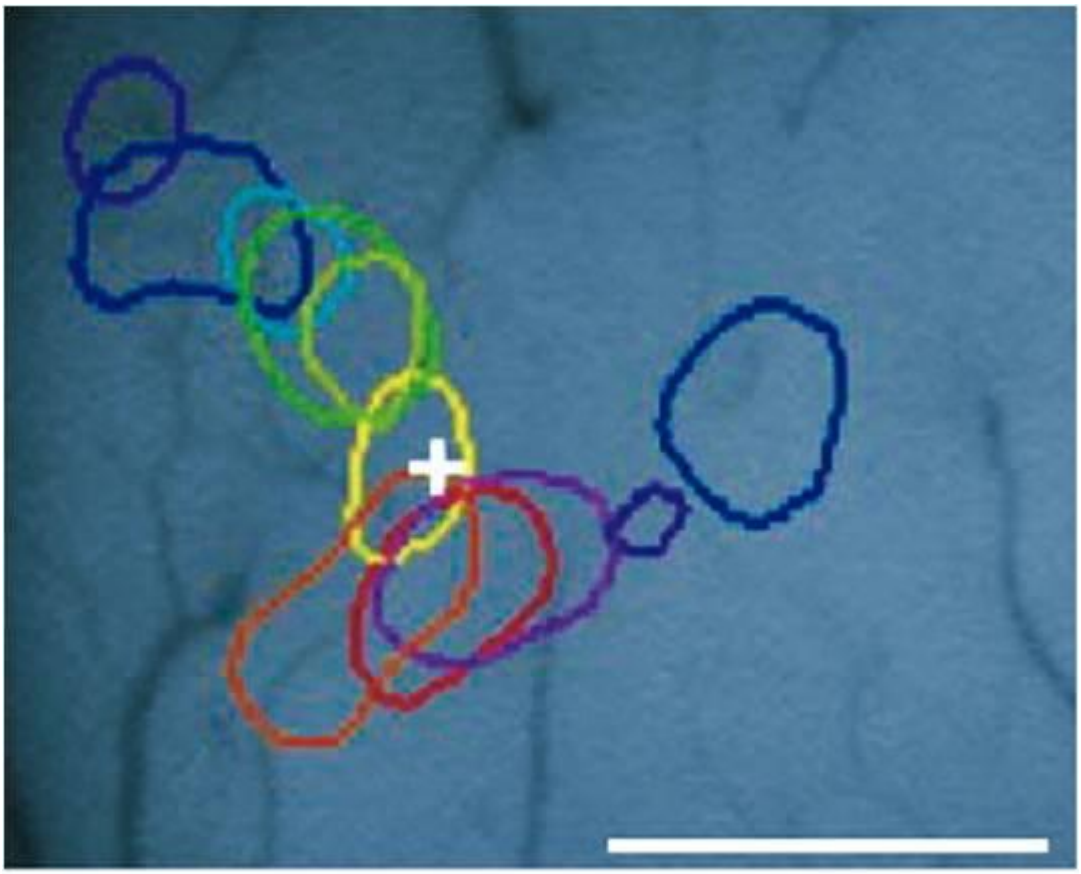

Figure 1.24 Colour specific bands in the second visual area (V2). Regions corresponding to the peak hue activity to different coloured stimuli are outlined on the surface picture of the brain (note the darkly-imaged blood vessels). Scale bar is 0.5 mm. Picture adapted from Conway (2003).

According to the segregation hypothesis (Zeki, 1978a; Livingstone and Hubel, 1984b; DeYoe and Van Essen, 1985; Livingstone and Hubel, 1988; Shipp and Zeki, 2002), the processing of various visual attributes occurring between retino-geniculate pathway and extrastriate cortex remains independent. Large group of anatomical studies have provided ample support to the notion that segregated pathways exist throughout most of the cortex. Mitochondrial staining of the visual cortex has revealed two separate regions in V1 and V2 areas: cytochrome oxidase CO-rich and CO-poor regions (Zeki, 1978a; Livingstone

and Hubel, 1984b; DeYoe and Van Essen, 1985; Livingstone and Hubel, 1988; Shipp and Zeki, 2002). Cells in CO-rich regions of layers 2/3 in V1 were found to have large number of unoriented, colour selective cells. In area V2, the same cells have been reported in the thin CO-bands (also known as thin stripe regions). So the anatomical organisation revealed by CO staining gives rise to functional pathway where colour information is being processed in V1 and V2 by unoriented colour cells located in the CO-rich blobs and the thin bands respectively.

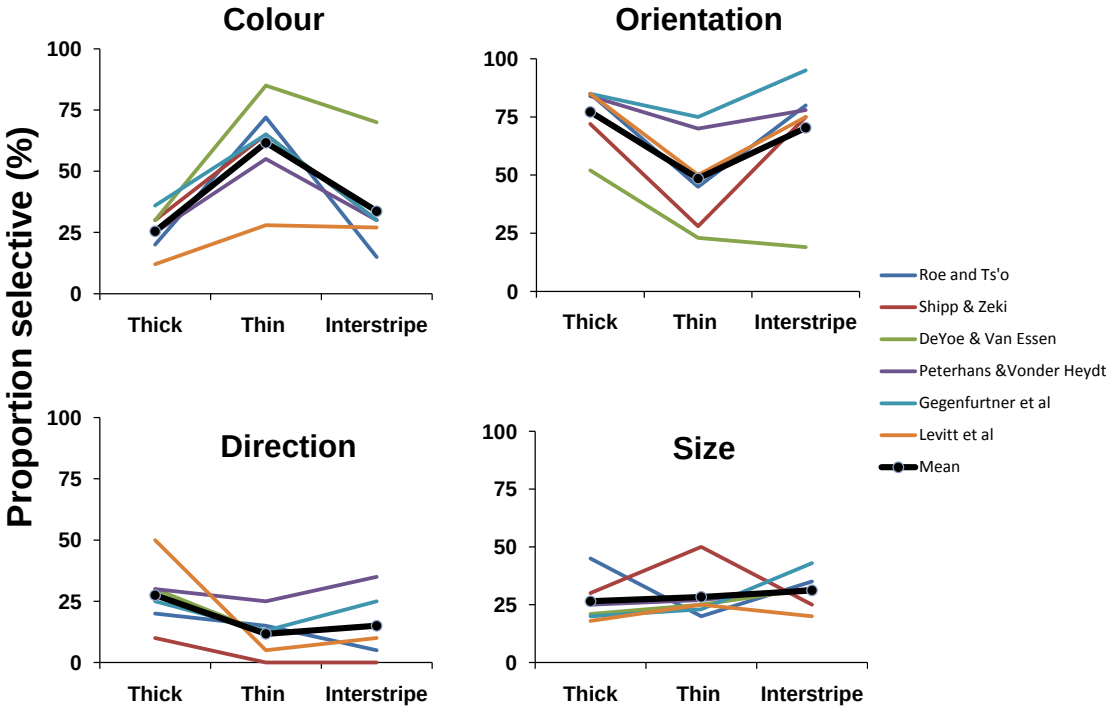

Figure 1.25 Segregation and integration in V2. Plots show the proportion of cells selective for each attribute. The thick black lines represent the mean across all six studies. Re drawn from Gegenfurtner(2003).

There have been many studies that investigated the degree of segregation in the cortex. The pool data from six studies that have investigated the proportion of neurons in V2, which are selective for colour, orientation, direction, and size,

are as shown in figure 1.25 (Gegenfurtner, 2003b). Data suggest that there is partial segregation of these attributes in three regions of V2. If there would have been no segregation then the mean data would have been a flat line. If there would have been a complete segregation then we would expect each attribute would have been processed by single CO-compartment; colour in thin stripes, direction and motion in thick stripes and orientation and size in the inter-stripe regions. If there was no segregation at all, the four black lines would be flat, with the same amount of selectivity across the all regions. However, the results from these studies indicate that neither of the two extreme views (either complete segregation or no segregation at all) is correct. Instead there seems to be a gradual degree of the segregation between the different stripe components, which could be either functional characteristics or due to different techniques used in different laboratories.

1.2.7 The Third visual area (V3)

V3 receives direct input from V2 and layer 4B of V1. In turn it sends its projections to both the middle temporal area V5 and area V4. Neurons in macaque area V3 respond to motion and have direction selectivity and showing a preference for lower spatial and higher temporal frequencies than V2 neurons (Gegenfurtner et al., 1997). Studies also show that colour selective cells are as numerous as they are in V2 and appeared to be involved in the integration of colour and motion processing. This contradicts previous suggestions by other studies, that cells in V3 are insensitive to colour (Baizer, 1982; Van Essen and Zeki, 1978). However, recent studies on the macaque visual cortex using fMRI

showed that there is a limited response from V3 to chromatic stimuli (Conway and Tsao, 2006).

1.2.8 The Temporal Cortex (V4)

Monkey V4

According to Zeki (1990) the monkey temporal cortex is subdivided into at least two parts named the posterior part (V4) and the anterior part (V4A). The Posterior part (V4) receives input from the thin and pale stripes region of V2 and the anteiror part (V4A) receives input from the posterior part of V4 (DeYoe and Van Essen, 1985; Shipp and Zeki, 1985) (see Fig1.26).

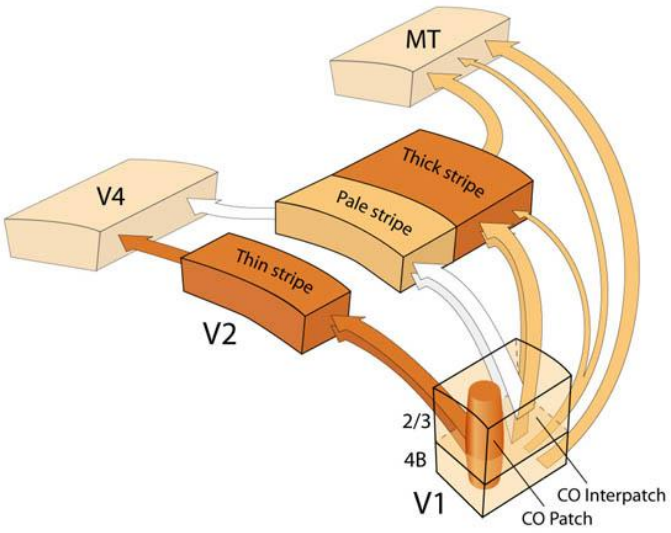

Figure 1.26 Summary of the general separation of visual information from V1toV4. (Adapted from Sincich and Horton, 2002).

V4 predominantly consists of two compartments in which one compartment has wavelength selective cells and the other compartment has orientation selective cells. Orientation selective cells within V4 display some kind of wavelength selective function, like cells in V1 and V2 (Desimone and Schein, 1987; Zeki,

1973; Zeki, 1977) and these cells receive input from inter-stripes region of V2. The compartment which has wavelength selective cells receives input from the thin stripes of V2 (Zeki and Shipp, 1989). Since most of the cells in the inter-stripes are not wavelength selective, it follows that wavelength selectivity is conferred on the orientation selective cells of V4 either by a convergence of inputs from the thin and inter-stripe regions of V2 or by intrinsic connections within V4 itself (Zeki, 1990).

Human V4

V4 is located in fusiform gyrus (see figure 1.20) and has a representation of both superior and inferior fields (McKeefry and Zeki, 1997). V4 is subdivided into two parts named as V4 and V4α. These are posterior and anterior parts of V4 and known together as V4 complex. These two are linked together anatomically and act cooperatively (Zeki and Bartels, 1999). Early studies have observed that human V4 is rich in chromatic sensitive cells (Essen and Zeki, 1978 , Zeki, 1983). Purely ventral lesion can damage human V4 and result in achromatopsia[2] (Wade et al., 2008). A recent fMRI study has shown that extra striate cortex responses to the chromatic stimuli are mainly confined to the ventral surface of the occipital lobe. This response decreases significantly in more anterior regions (Wade et al., 2008).

Area V4 does not seem to have the feature of colour opponency, rather, the main feature is colour constancy (Wildberger, 1985; Schein and Desimone, 1990; Walsh et al., 1993; Bartels and Zeki, 2000), a mechanism that allows colours to be recognized under a variety of lighting conditions, and also alternate colour based visual processing (Schein and Desimone, 1990);

[2] Achromatopsia is complete colour blindness.

However, recent studies proposed that V4 is not solely responsible for colour constancy rather it is gradually computed through a series of visual areas and finalised in V4 (Gegenfurtner and Kiper, 2003).

Studies have established that area V4, both in humans and monkeys, is not only responsible for colour vision, but is the main centre for spatial vision (Gegenfurtner, 2003a). It also plays an important role in coordinating vision, attention and cognition (Chelazzi et al., 2001). Lesions in V4 can affect the visual functions such as discrimination of colour, shape (Walsh et al., 1992) and texture (Merigan, 2000) etc.

From the past three decades, controversy exists about the colour selective region (V4) in the visual cortex of a human and macaque (see figure 1.27). Some studies support that there is homology exist between area V4 of human and macaque (Lueck et al., 1989; McKeefry and Zeki, 1997; Bartels and Zeki, 2000) and some contradict this (Hadjikhani et al., 1998; Van Essen et al., 2001; Tootell and Hadjikhani, 2001). Irrespective of these contradictions, the topography of macaque visual cortex is frequently used as a model for that in human visual cortex (Tootell and Hadjikhani, 2001).

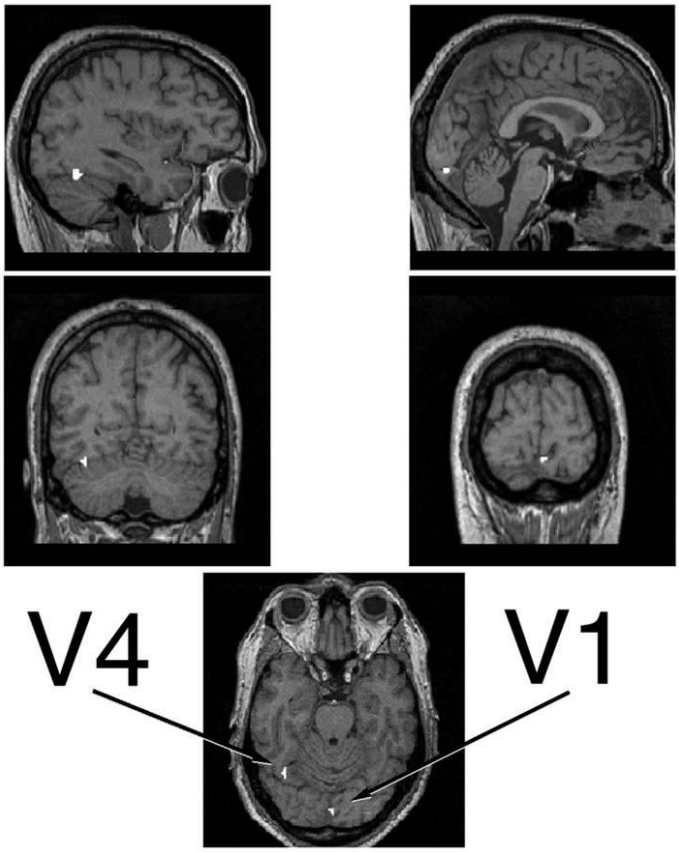

Figure 1.27 Structural and functional MRI data from a human colour normal subject showing activation in the calcarine fissure (V1) on the left and in the fusiform gyrus (V4) on the right. Picture taken from Zeki et al, 1999.

Zeki's (1973) original proposal that, colour is processed selectively in V4, has been questioned by various groups. Some have suggested that the colour is processed in discrete regions anteriorly, in or near TEO (Hadjikhani et al., 1998; Tootell and Hadjikhani, 2001; Tootell et al., 2004; Van Essen et al., 2001) and others have suggested that colour is processed in further anterior areas to TEO (Komatsu et al., 1992; Buckley et al., 1997). Recently Tootell et al (2004) have shown that the limited colour selective activity in V4 was segregated into discrete, relatively large columns, in both dorsal and ventral V4 regions, which have misled researchers to suppose that V4 was a selective colour processing area. They also showed that colour biased activity took the form of patches or

isolated columns in the cortex, outside the colour-biased regions the cortex appear to have a more balanced sensitivity to luminance and colour.

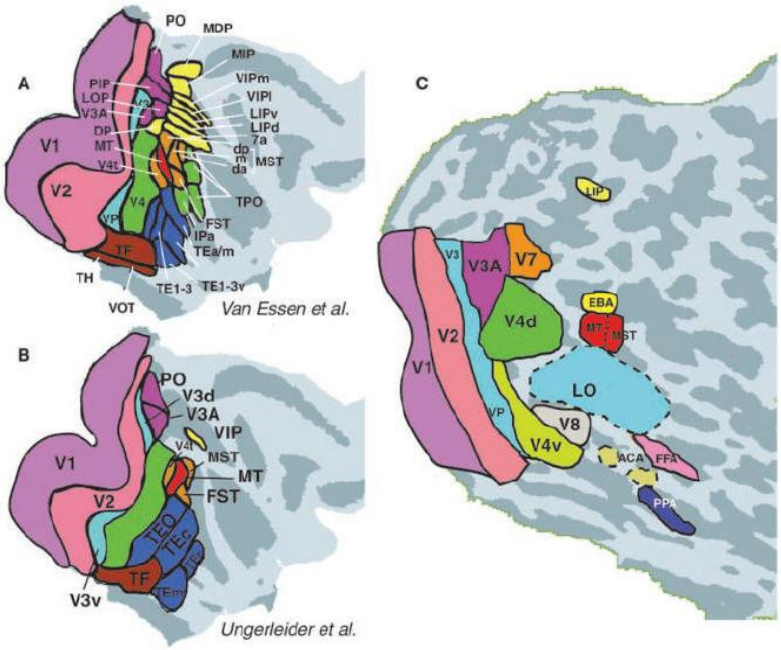

Figure 1.28.Summarizes the retinotopic organisation in the cortex. Note that visual processing areas are shown in colours. Left side plots a, b shows the visual processing areas in macaque cortex. Right side plot shows the visual processing areas in human cortex.. We can also see the topographical differences in V4 area of monkey to that of human. Picture adapted from Van Essen et al, 2001.

Source: http://psychology.uwo.ca/fmri4newbies/RetinotopicandEarlyVisualAreas.html

1.2.9 Beyond V4

Regardless of the apparent complexity of colour processing in V4 and the anterior V4 areas mentioned, further processing takes place beyond V4 (see figure 1.28). V4 and the areas of anterior V4 project to a number of areas in the temporal cortex including the infero-temporal visual cortex, where a large proportion of neurons have been found to respond to complex stimuli, and

individual neurons of this group were found to possibly be selective to shape, colour, and texture (Desimone et al., 1984).

Initially, Zeki (1978) described the region encompassing V4 and PITd (Posterior blank of the superior temporal sulcus) as a single complex but he intimated that these regions could be distinguished as distinct areas. Retinotopic mapping revealed that PITd is distinct from regions V4 (Gattass et al., 1988; Pigarev et al., 2002; Stepniewska et al., 2005) and TEO (Zeki, 1996; Stepniewska et al., 2005); although the boundaries between these areas are tentative.

A recent study (Conway and Tsao, 2006) in the macaque cortex, claims that the PITd could be a strongly colour biased area, responsible for the integration of all chromatic signals and possibly the colour centre in the macaque, serving similar functions to that of the human colour centre. This statement is strongly supported by Conway and Tsao (2006). According to their study, very large lesions encompassing the PITd result in impaired colour vision whereas large regions of the IT cortex that do not include PITd fall short of achromatopsia. However, the claims made by Conway and Tsao (2006) require further investigation of targeted single-unit recordings, perhaps guided by fMRI.

1.2.10 Higher order visual processing pathways

The visual system can be commonly classified into two processing streams known as ventral and dorsal stream (Figure 1.29). The Dorsal stream represents the processing of spatial location and motion information, whilst ventral stream has been recognised as processing object shape, colour and texture (Ungerleider and Mishkin, 1982).

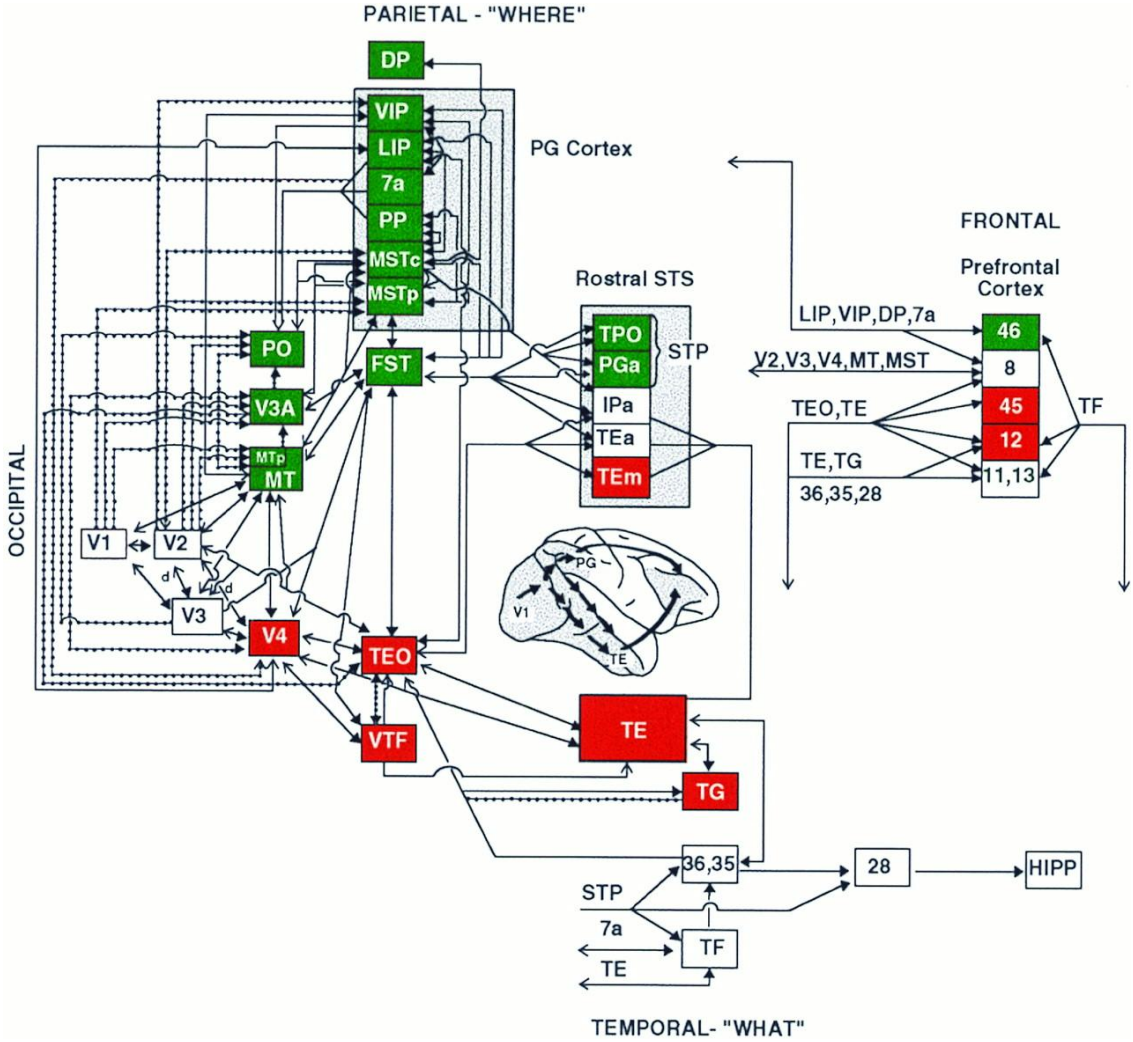

Figure 1.29 Summary of the dorsal (shown in red) and ventral (shown in green) streams in the cortex.

Source: http://www.pnas.org/content/95/3/883/F1.small.gif

These dorsal and ventral streams are believed to be supplied by either M type or P type cells. These streams originate in sub regions of V1 and remain largely distinct in V2. Beyond V2 they separate out ventrally towards temporal cortex, connecting with V4 and then on to higher cortical areas, and dorsally to the parietal cortex, connecting with V5/MT and then on to higher cortical regions of parietal cortex (Merigan and Maunsell, 1993). M and P pathways deemed to supply these streams clearly respect their segregation up to V1. Beyond this point, the pathway of inter-connections between visual areas begins to

resemble more to a network of activity rather than hierarchical pathway. Certainly, there is an ample potential for signal intermixing following the first synapse in V1 (Sincich and Horton, 2005). The anatomical basis of the dorsal and ventral segregation is intrinsically arguable as the segregation of the M and P pathways supplying them. The extent of such interactions is substantiated from the observation that deficits in form identification, after deactivation of V4, are diminished when attended stimuli move. In addition to this, removal of magnocellular layers from LGN has little effect on motion perception. These interactions do not necessarily mean that parallel processing does not take place, indeed such processes are likely to provide efficient stimulus perception, but such processing may not be purely M versus P basis (Born, 2001).

An alternative view of dorsal and ventral systems hypothesizes that the segregation of image processing depends upon ‘output requirements’ as opposed to ‘input distinctions’ (Goodale and Milner, 1992). Milner and Goodale suggested that visual actions are guided by unconscious online processing, separate from those that underlie conscious visual perception and recognition. The dorsal and ventral streams, ending in the posterior parietal and inferotemporal cortex respectively, form the substrates for these two systems. It is believed that fast processing, unconscious ‘action’ system is necessary to co-ordinate motion and undertake body-object interactions. Conscious visual perception is undertaken within the ‘perception’ pathway which plans decision based upon ‘insight, hindsight and foresight’ (Milner and Goodale, 1995). This model suggests that the dorsal stream initiates unconscious visual guidance actions, focusing attention on a particular object, whilst the ventral stream then undertakes slower processing of its attributes.

CHAPTER - 2 ELECTROPHYSIOLOGICAL STUDIES OF PRIMATE COLOUR VISION

One of the aims of the thesis was to study the cortical contribution to the chromatic processing in human trichromatic vision. In order to investigate the cortical contributions, we elicited visual evoked potentials (VEPs) using chromatic spots. We have also investigated the effects of luminance contrast and chromatic contrast on VEPs. Before proceeding to the experiments, we have summarized the introduction of VEPs, source of the VEPs, the morphological changes to various stimuli and also the clinical application of VEPs in this chapter.

2.1 INTRODUCTION TO VISUAL EVOKED POTENTIALS

Visual evoked potentials (VEPs) are recordings of electrical activity generated within the brain in response to visual stimulation by a flash of light or a change of pattern. VEPs are the subset of more general brain electrical activity that is recorded in the form of electroencephalogram (EEG). VEP recordings are derived from the difference between potentials recorded from an active and reference electrodes which are placed at different locations on the scalp. Placement of the electrodes will help improve signal noise ratio as the reference electrode is placed over an area relatively unresponsive to visual stimuli and will therefore only record general brain activity. Active electrodes record both general activity and visual potentials specific to a stimulus. VEPs tend to be recorded from locations found in relation to the physical markers such as the inion and nasion. However, it is important to

keep in mind that magnetic resonance imaging (MRI) studies have shown variability in the boundaries of visual areas (Sereno et al., 1995; De Yoe et al., 1996) so that the area of the cortex underlying a particular spot on the scalp may not be exactly same for each subject.

Visual evoked potentials are used to measure the responses from the human brain. The potentials generated in the cortex must pass through the layers of tissue and bone that lie between the active cells and the recording electrode (i.e. cerebral spinal fluid, dura, skull, skin), and this process is called volume conduction. The evoked activity recorded at the scalp will therefore be attenuated by volume conduction.

Early studies (Dawson, 1951, 1954) have shown that small amplitude visual evoked potentials (1-20μV) are submerged in the larger amplitude brain activity (60-100μV). By averaging multiple responses, we can reduce general brain activity (noise) and record VEP responses. The improvement in the signal noise ratio is directly proportional to the square root of number of sweeps.

2.2 ORIGIN AND COMPONENTS OF VEP

The sources of the EEG are believed to be the post synaptic potentials (PSPs) that are generated between thalamo cortical axons and pyramidal cells (see review of Holliday (2003)). PSPs can be excitatory (EPSP), or inhibitory (IPSP). EPSP are depolarisations that occur in the postsynaptic membrane caused by the flow of positively charged ions into the

postsynaptic cell. This in turn results in the extracellular space becoming more negative.

Excitatory PSPs are created in quick succession at the post synaptic membrane and are summed together. Once excitatory PSPs reach the voltage threshold of a cell, an action potential is generated. These action potentials are not apparent while recording the cortical activity from the surface or from the scalp, the synchronised activity of multiple synapses produces instead a smooth wave form. There is no fixed relationship between the action potentials generated by single cells and the slow waves recorded on the surface of the cortex. Furthermore, differences in amplitude and waveform have been reported for slow waves recorded from the cortex and the scalp (Kulikowski and VidyaSagar, 1987; Regan, 1972). It is believed that glial cells also play a part in the generation of surface waves (Regan, 1972).

VEP morphology changes according to the type of stimulus used. Earlier studies used flash stimuli (Ciganek, 1961; Dustman and Beck, 1969; Vaughan and Gross, 1969), but this has been overtaken by use of the pattern onset/offset or pattern reversal stimulation. The reason for this is that the flash VEP waveform varies markedly from subject to subject, making it difficult to identify the components of VEP with certainty (Ciganek, 1961; Spekreijse et al., 1977). The most commonly used stimulus for clinical recording is the pattern reversal stimulation (Odom et al., 2004; Odom et al., 2010). The morphology of the VEP for a pattern reversal stimulus is as shown in figure 2.2 (Lower trace). It has three major components.

1) An initial negativity observed at about 75-80ms known as the N75 component.
2) A large positive component at 100-115ms known as the P100 component.
3) A second negative component N135 which usually occurs between 125-140ms.

The latencies of P100 vary marginally among individuals (Odom et al., 2004; Odom et al., 2010). Recording conditions across laboratory conditions also vary, so it is important to have a normative data for the interpretation of VEPs.

Pattern reversal VEPs can only be obtained in subjects who have good fixation. This type of VEP cannot be used in neonates or people who cannot fixate because of the media opacities such as cataract. Under these circumstances VEPs can be recorded using a flash that can be generated by stroboscope or a ganzfield. Such VEPs are termed as flash VEPs. Flash VEPs (Figure 2.1, upper trace) help to get rudimentary information such as whether visual information is reaching the brain or not, however, integrity of the visual system cannot be determined. The morphology of flash VEP varies largely among individuals (Ciganek, 1961; Dustman and Beck, 1969). It is very important to compare the morphology of flash VEP between the two eyes and also repeatability to interpret the flash VEP results.

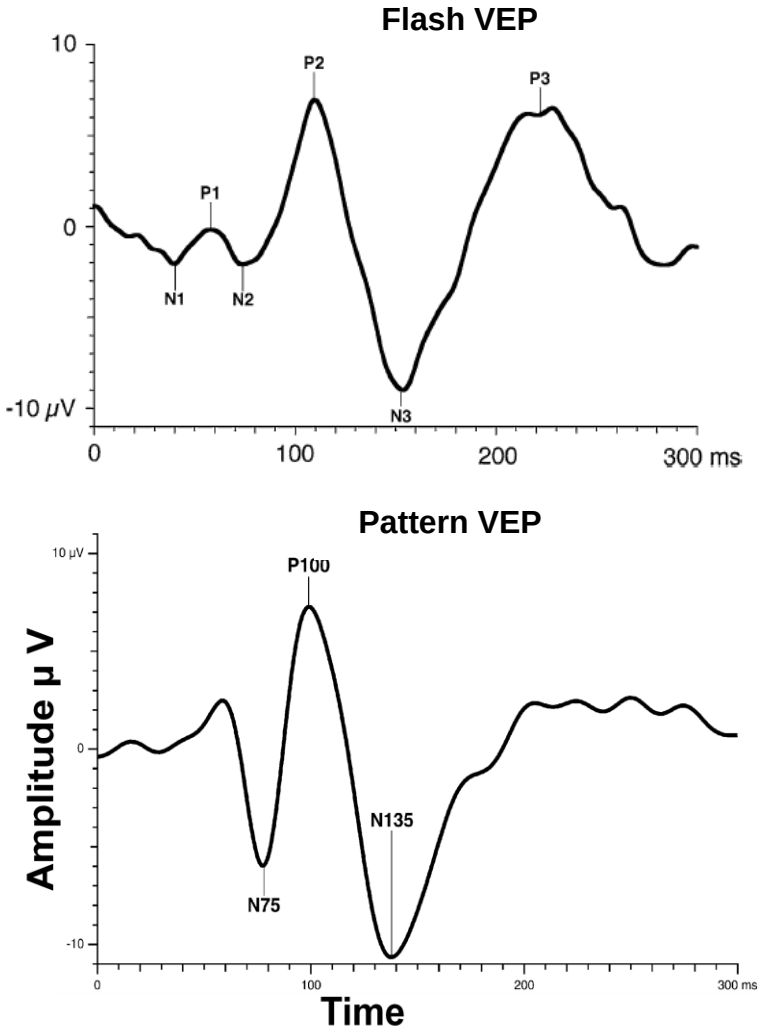

Figure 2.1 Morphology of VEP to flash stimulus (upper trace) and pattern reversal checker board (lower trace). See the major components are tick marked. (Picture taken and modified from Odom et al, 2010).

2.3 CHROMATIC AND ACHROMATIC VEPs

2.3.1 Physiology of chromatic and achromatic responses

As discussed in chapter 1, visual information in primates is processed by three anatomically distinct retino- geniculate striate pathways called the P-, M- and K-cellular pathways (Livingstone and Hubel, 1984a). P and M pathways have

distinct properties in terms of their response to stimulus. M pathway responds better to luminance contrast (Valberg and Lee, 1992; Kaplan, 1990), whereas P pathway responds better to chromatic contrast (Schiller et al., 1990). Connections between M-, P- and K- inputs of the neurons in the primary visual cortex suggest that there is interaction between the colour system and other distinct sub-modalities such as form, texture and motion (Lund et al., 1995; Maunsell et al., 1990).

When appropriate stimulus parameters are applied (McKeefry et al., 1996; Baseler and Sutter, 1997) to cells of the M pathway, they appear to prefer luminance modulated stimuli of low spatial and high temporal frequency, while the cells of P pathway are more sensitive to chromatic contrast to luminance modulated stimuli of high spatial frequency and low temporal frequency (Schiller et al., 1990; Anderson et al., 1996). Separation of M and P pathways is only possible at lower stimulus contrast. At lower contrast, M pathway cells respond better to luminance modulated grating stimuli and P pathway cells respond better to chromatic grating stimuli (Kulikowski, 1989; Kulikowski, 1991a). On the other hand K cells have low peak firing rates (60 impulses/second) and low levels of spontaneous activity (White et al., 2001).

Selective activation of colour mechanisms has typically depended upon the use of isoluminant chromatic patterns. Kulikowski et al (1991a) have suggested that such stimuli help to isolate the chromatic responses from achromatic responses. Psychophysically, isoluminance is determined using heterochromatic flicker photometry (HFP). The basis for HFP is when a chromatic stimulus is presented at high temporal frequency (≥15Hz) and its relative luminance is altered, the flicker is minimal at isoluminance (see methods section for a more detailed explanation).

However, isoluminant grating stimuli are still prone to the effects of transverse and longitudinal chromatic aberration. Apart from chromatic aberration, responses to +S-(L+M) stimuli are also subject to the effect of macular pigmentation, which varies in density and distribution in different subjects (Moreland, 1984; Ruddock, 1963). Moreover, recent studies have shown that macular pigment optical density and distribution can be measured by steady state VEPs to blue-green stimuli (Robson and Parry, 2008; Robson et al., 2006)

Zrenner (1983) claimed that large stimulus fields introduce variations in isoluminance with eccentricity. However, Kulikowski (1991a) using low contrast stimuli showed that responses are similar to small or large fields suggesting that the contrast plays a more important role than field size for selective stimulation of M and P mechanisms.

Recently Ribeiro and Branco (2010) used gabor stimuli of varing sizes and varying contrasts to examine the effects of contrast and area summation in VEPs. Their results showed that for L-M cone opponent channel, the effect of stimulus size is significantly smaller and not modulated by stimulus contrast. On the other hand, S- cone opponent and achromatic channels are significantly affected by size and contrast of the stimulus. They suggest that L-M cone-opponent channel is more specialized for central vision and the S- cone opponent and achromatic channels, are better adapted to peripheral and spatial vision.

2.3.2 Chromatic VEPs by pattern stimuli

Early attempts were made to isolate the chromatic responses from achromatic responses using red-green checkerboard isoluminant chromatic patterns. These

stimuli elicited VEPs similar to those elicited by luminance modulated checkerboards (Regan and Spekreijse, 1974 , Regan and Beverley, 1973). Furthermore, studies on humans and monkeys, using isoluminant chromatic gratings of low spatial frequency with on-off presentations, generated colour VEPs that were different from achromatic VEPs (Carden et al., 1985; Previc, 1986b; Murray et al., 1986; Berninger et al., 1989; Rabin et al., 1994).

Parry et al (1988) suggested that colour specific VEPs can be best obtained at low spatial frequencies of about 2 cycles/ degree. They also suggested that gratings of spatial frequency >7 cycles /degree would not be suitable to elicit the chromatic responses because stimuli with higher spatial frequency are prone to chromatic aberrations. Kulikowski et al (1997) has shown that VEPs elicited by the blue-yellow grating stimuli, whose spatial frequency is more than 6 cycles / degree, are prone to chromatic aberration and macular pigmentation,.

Kulikowski and Parry (1987) showed that gratings produce much better differentiation between chromatic and achromatic VEPs than equivalent checkerboards. In their study, low spatial frequency achromatic and chromatic gratings using pattern reversal presentation elicited similar responses dominated by positive going peaks. Responses elicited by pattern onset are different for achromatic and chromatic components. The achromatic stimuli were dominated by positive going peak and with a negative going peak at a similar latency for the chromatic stimuli. Studies by Berninger et al (1989) and Rabin et al (1994) also strongly support the Kulikowski and Parry findings, that pattern-onset presentation is better than pattern reversal for recording consistent, robust, isoluminant chromatic responses.

The differences between the pattern reversal and the pattern onset waveform for chromatic and achromatic gratings are illustrated as in figure 2.2. Clear differences can be noted between negative going chromatic onset VEP from all other waveforms, i.e. chromatic offset and reversal as well as achromatic onset-offset and reversal VEPs.

Recently Souza et al (2008) studied the effect of stimulation mode on transient VEPs amplitude as a function of contrast for chromatic and chromatic gratings. Their results strongly suggest that, at higher contrasts, the M pathway is the main candidate for pattern reversal and pattern onset-offset VEPs. On the other hand, P and K pathways either in combination or in isolation may be responsible for VEPs obtained with isoluminant chromatic gratings at both onset-offset and reversal mode.

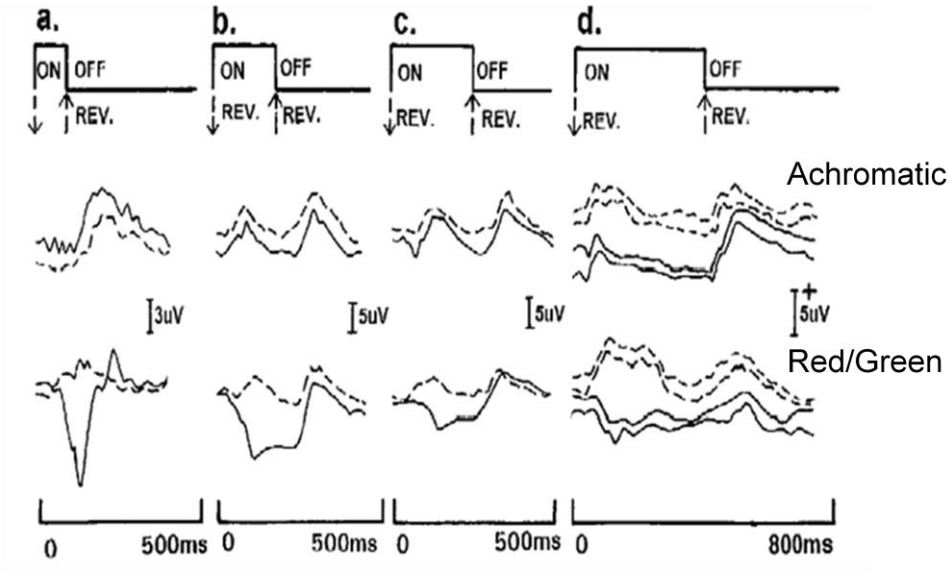

Figure 2.2 The VEP generated by the pattern reversal (dotted lines) and pattern onset (solid lines) of achromatic gratings (top waveforms) and isoluminant R/G gratings. Different onset/reversal duration: (a) 100ms, (b) 200ms, (c) 260ms and (d) 400ms. Other stimulus parameters: spatial frequency 1 c/deg (a-c) and 1.5 c/deg (d); contrast change 0.22 (b, c) and 0.28 (a, d); lower mean luminance of 40cd/m2 (b, c). Stimulus size 30 degrees in diameter. Adapted from Kulikowski et al (2002).

Different components of colour specific VEPs have been identified by various stimulation methods. Kulikowski et al (1989) used chromatic and achromatic onset/offset gratings of low spatial frequency, and showed that a significant negative response is evoked by chromatic red/green stimuli at a peak latency of 130-140ms whilst an opposing positive component is observed at the same latency by achromatic stimuli. These authors also reported that apart from isoluminance, colour or dominant wavelength does not influence the shape of VEP waveform. To support the idea that the negativity recorded in response to red/green stimuli in colour normals is specific to colour contrast and isoluminant stimuli, (i.e. colour dependent signal) these authors used similar stimuli with colour anomalous subjects and showed that no response occurs at isoluminance. Berninger et al (1989), using pattern isoluminant chromatic stimuli in on-off mode, also found that peak negativity occurs at 130ms in trichromats, whilst the negativity was absent at this latency in colour anomalous subjects.

Low contrast isoluminant chromatic gratings were used by Kulikowski et al (1997) to elicit the colour specific sustained activity. They observed differences for red/green and blue/yellow VEPs at contrasts higher than 0.1 (see figure 2.3). Red /green VEPs showed two negative components in onset responses with peaks at 120ms and 250ms respectively, whereas blue/yellow VEP exhibited only one negative peak around 250ms. When contrast was increased colour selectivity was lost, showing two positive peaks for both blue/yellow and red/green at contrast of 0.5. This finding strongly suggests that high contrast isoluminant gratings are generated by transient mechanisms. Adding to this, Girard and Morrone (1995) showed maximum amplitudes for pure luminance contrast and minimum amplitudes for intermediate luminance ratios (between

0.3 and 0.7) of red and green colours. Their observations also include a secondary peak at isoluminance (0.5), producing a W shape function and latency difference exists between chromatic and achromatic VEPs, with latter leading by 35ms.

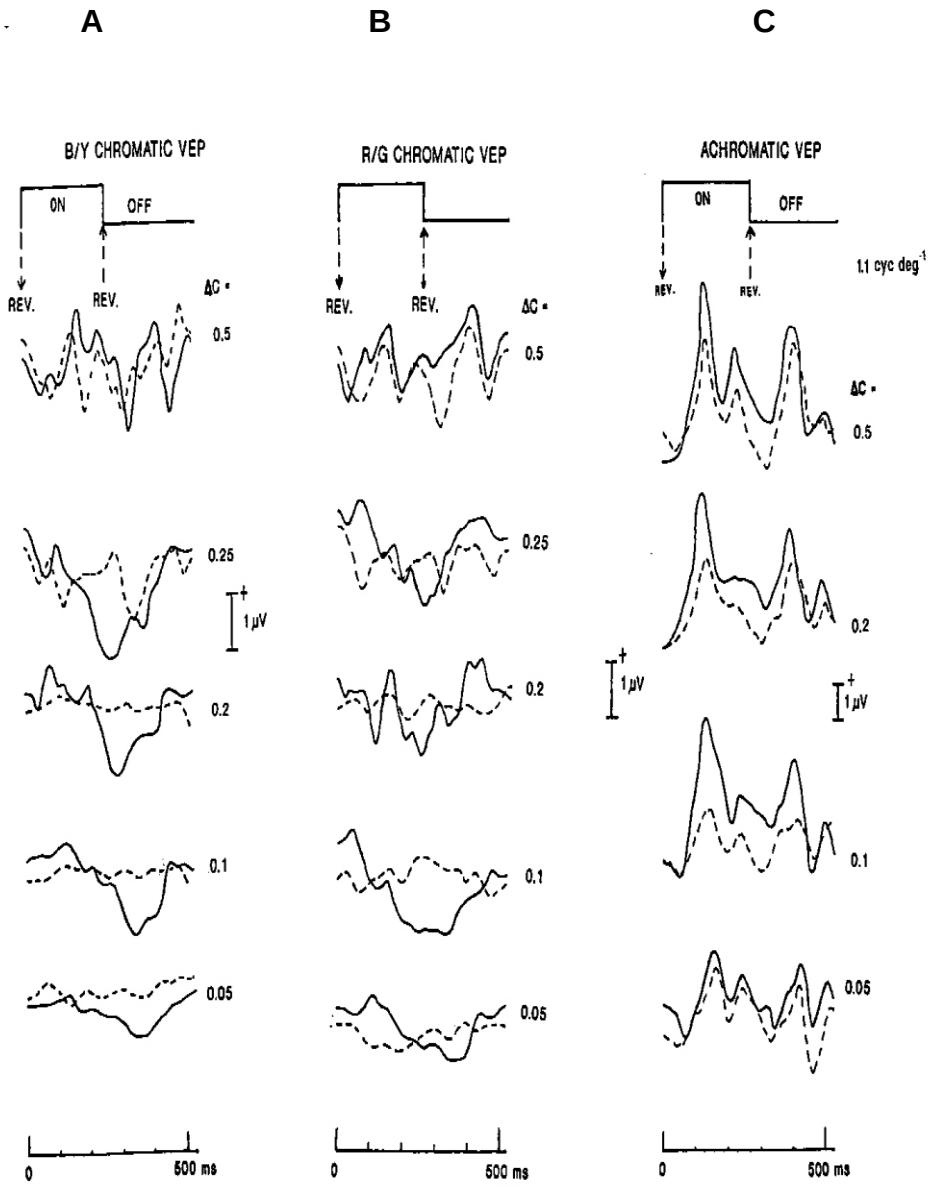

Figure 2.3 Visual evoked potentials elicited by blue-yellow (A), red/green (B), and achromatic (C) sinusoidal gratings as function of contrast change (ΔC from 0.05 to 0.5); the gratings are presented in pattern on-off (solid lines) and reversal (dashed lines) modes. There is a VEP waveform change with increasing contrast. Mean luminance 25 cd / m^2. In all cases spatial frequency was 1.1 cycles / degree and the grating contained 4 spatial cycles. Adapted from Kulikowski et al (1997).

The onset-offset VEPs were recorded with stimuli of low spatial frequency sinusoidal gratings in which chromatic modulation was defined in three dimensional colour space. The nature of the VEP responses were characterised along number of spatial, temporal and chromatic stimulus directions (Crognale et al., 1993; Rabin et al., 1994). These studies have shown that both isoluminant L-M and S cone modulation gratings elicit robust VEPs in terms of amplitudes. However, the VEPs elicited by the modulation of L and M cones have shorter latencies (25-30ms) than that resulted from modulation of S cones. In addition to this, VEP response was always dominated by a chromatic component, when used with a mixture of chromatic and achromatic contrast. These results have also shown that the VEP latencies were increased with increase in spatial frequency correlating with psychophysically measured chromatic contrast sensitivity functions (Kelly, 1974, 1983).

VEP frequency analysis using different stimulation methods such as pattern reversal and pattern onset-offset was studied by McKeefry et al (1996). In their study they noticed that pattern reversal stimulus response is at the second harmonic and the magnitude of the second harmonic component is maximum for isoluminant achromatic stimuli and minimum for chromatic stimuli. On the other hand, the pattern on-off VEP showed different responses for chromatic and achromatic stimuli. Chromatic onset VEPs are dominated by the fundamental component and the achromatic onset VEP contain predominantly second harmonic components in addition to the fundamental.

The effect of stimulus size on chromatic pattern onset-offset VEPs was studied by Korth and Nguyen (1997). In their study, two stimuli of different wavelengths were used. The results showed dominant negative polarity VEPs obtained by a 460nm pattern stimulus which saturates in amplitude with a stimulus size of 7

degrees. Dominant positive polarity VEPs were obtained using a 550nm stimulus with amplitudes continuously increasing up to 32 degrees. The peak time of the negative component decreased with increasing stimulus size whilst the peak time of positive component remained constant.

2.3.3 Localization of chromatic VEPs in the brain

A different approach was taken by Givre et al (1995) to find a cortical source for the colour specific component of the VEP in primates, for which they used laminar profiles, current source density analysis and multiunit activity methods to analyse the responses to full field chromatic and achromatic flashes. Their results (see figure 2.4) showed that the colour flashes enhanced trans-membrane current flow in layers 4C and also in supra-granular layers (layers 2 and 3 of V1) whilst there is no change in activity of current flow in the M-layers. They also found that variation in wavelength affects the colour response amplitude. For example in their study there was a larger response amplitude for red compared to other wavelengths (approximately 140-350% more).

Topographical VEP studies of colour responses have indicated a cortical route through V1 to V4. Paulus (1997) attributed the VEP responses obtained with homogenous colour stimuli (for example chromatic spots) to the primary visual cortex, while activity evoked by colour Mondrian patterns was identified in areas V1, V2, V3 and V4. Using dipole source analysis, Buchner et al (1994) observed three areas displaying colour activity, which they suggest to be relate to areas V1, V2 and V4. Alison et al (1993) recorded VEPs from electrodes placed subdurally on the cortical surface and reported that colour responses were mainly from the posterior fusiform gyrus, lateral lingual gyrus and also

areas of the dorso-lateral surface cortex. There is evidence to suggest that the primary posterior fusiform gyrus is involved in colour perception and dorso-lateral surface cortex may be involved in selective attention to colour. It was also noted that latencies were shorter in the medial lingual gyrus, posterior fusiform gyrus and inferior temporal gyrus leading the authors to conclude that wavelength selective processing begins in the medial lingual gyrus and progresses through other areas.

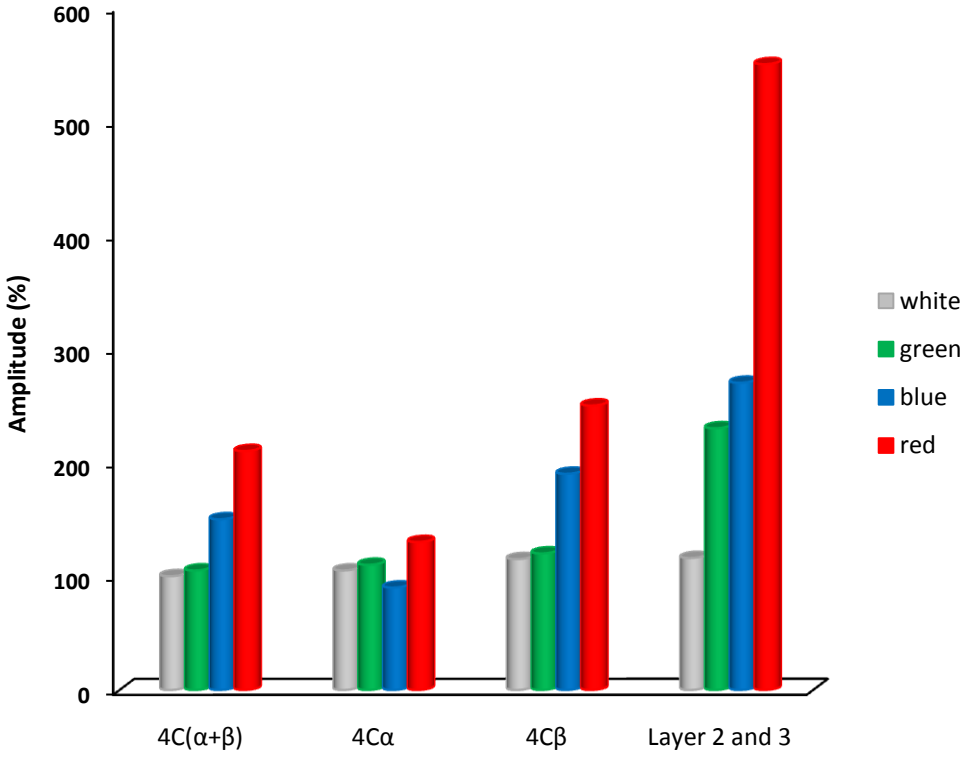

Figure 2.4 Colour effects in the striate cortex. The mean peak amplitude of current sinks in layer 4C (combined α+β), layer 4Cα, layer 4Cβ, and supra granular laminae for each each colour of full field flash is plotted as percentage of response to white intensity matched signal. Boxes on legend indicate significant colour effects (Picture reproduced from the data of Givre et al., 1995).

2.3.4 Development of VEP

Crognale (2002) used VEPs to investigate the development and maturation of chromatic and achromatic visual pathways in human. According to his study, chromatic VEPs continually change from birth to puberty though they are robust and reproducible. Rapid, complex and dramatic changes in chromatic onset VEPs are seen until the age of one year. In contrast, low spatial frequency achromatic reversal responses are stabilised at the age of 3 months. Responses generated by S cone stimuli become stable one month after development of L-M cone opponent responses. Throughout the remainder of lifespan after puberty, the amplitude of the major negative component of the chromatic onset VEP decreases slowly and latency slowly increases.

2.3.5 Chromatic VEPs elicited by spot versus pattern stimuli

VEPs to homogeneous colour stimulation differ from those elicited by pattern stimulation, particularly in the early response components (Paulus, 1997). In addition to this, studies have also shown that the VEPs elicited by pattern stimuli differ in many aspects from those obtained with homogeneous light stimuli (Sperkreijse et al., 1977). Pattern VEPs may contain many components which relate to the luminance changes occurring in the stimulus rather than to spatial contrast as such. For instance, CII (P120) is the clearest component which one can associate with the changes in spatial contrast, especially around sharp contours. If this is the case then the VEPs elicited by isoluminant chromatic gratings elicit different VEPs to those of isoluminant chromatic homogenous stimuli. In order to get a pure colour response, it is necessary to use homogeneous colour stimuli. Additionally for onset VEPs, the colour

stimulus should be exchanged with an achromatic stimulus of same mean luminance to avoid contamination with luminance onset stimuli (Paulus, 1997). To get unadulterated colour evoked responses, few studies have used hmogeneous equibright colour stimuli (Paulus et al., 1984; Paulus et al., 1986; Valberg and Rudvin, 1997). The authors of these studies argue that isoluminant chromatic spot stimuli offer more selective activation of chromatic mechanisms since they are more able to stimulate cells that are colour opponent, but not spatially opponent. They also claim that these stimuli have fewer edges and are less susceptible to chromatic aberrations. Studies of chromatic VEPs using isoluminant spot stimuli showed the presence of a colour specific component (N87), with largest amplitudes towards a red colour (Paulus et al., 1984; Paulus et al., 1986). The N87 component is suggested as a response of the geniculate afferents in the dendritic arborisation of cells in layer 4C of the striate cortex rather than the next stage of colour processing (Paulus, 1984). This colour specific negative component (N87) obtained with spot stimuli occur much earlier than negativity (120-140ms) generated by equiluminant grating stimuli. A study on single-neuron responses of V1 also favours the idea that, grating and spot stimuli involve different neural populations for chromatic processing (Johnson et al., 2001). According to Johnson et al, colour-luminance cells in primary visual cortex are responsible for chromatic processing. Those are different from the cells that give preferential response to colour, as they show evidence of chromatic opponency, often demonstrate a high degree of orientation selectivity, and have spatial tuning to both colour and luminance. Colour-luminance neurons may respond to cues for form, like boundaries or features, and they may use chromatic and/or luminance signals as necessary to define the form cue. They may also provide inputs for colour contrast induction because they

are spatially selective responding at colour boundaries, but not to the interior of coloured regions.

2.4 CLINICAL APPLICATION OF CHROMATIC VEPs

Chromatic VEPs have a clinical application in assessment of congenital and acquired colour vision deficiencies. Crognale et al (1993) showed that chromatic VEPs can be used as sensitive indicator for different colour vision deficiencies. In their study, chromatic VEP responses were obtained along the L, M, L-M and S cone axes from colour normal subjects and but were selectively diminished in congenital colour deficient subjects. Differences in waveform were clearly appreciated as shown in figure 2.5. For a tritanopic individual, only the waveform along S cone axis differed substantially from those colour normal observers. The waveforms for the protanope are normal along the S axis but are nearly absent along the L axis. In addition, the waveforms for modulation along the L-M and M axes exhibit normal amplitude but have long latencies. The shaded boxes indicate chromatic waveforms judged to have much longer latencies and/or much smaller amplitudes than those of colour normal observer's waveforms.

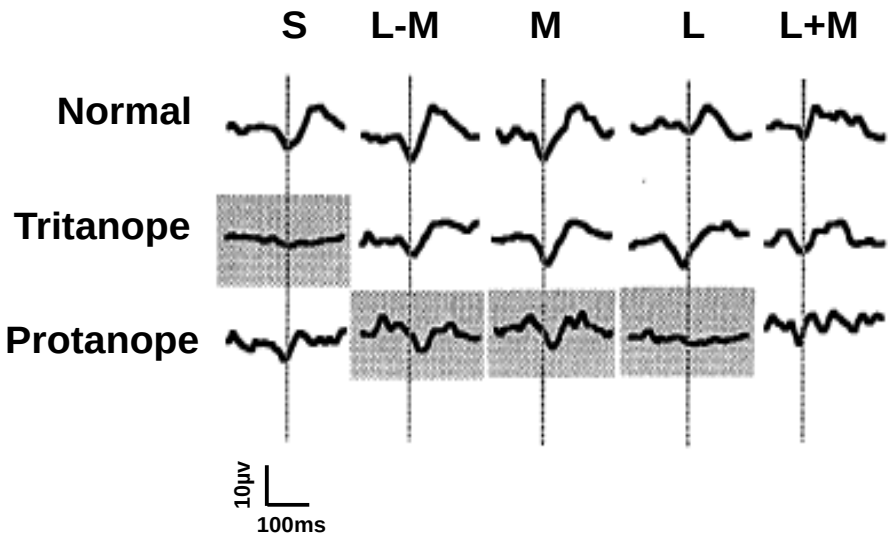

Figure 2.5 Waveforms obtained from severely colour-defective observers by use of modulation along five axes in colour space. Waveforms from a normal observer are shown in the top row for comparison. The vertical lines indicate the latency of the normal waveforms. Waveforms that appear to have much longer latencies and/or much smaller amplitudes than those of normal observer are shaded. Adapted from Crognale et al (1993).

Figure 2.6 illustrates latency differences between colour normal and colour deficient observers as a function of direction of colour space within the isoluminant plane. The data shown illustrate the difference in latency between the the N1 component of the VEP for colour-defective and average normal for each direction, i.e. points near the innermost ring indicate latencies close to those for normal observers. The grey rings indicate a latency difference of 20ms. The polar plot at the top of figure 2.6 shows the responses obtained from protanomalous individual and protanope. The relative response latencies for these subjects are greatest near the L-M axis and are near normal along the S axis. The protonomalous observer showed the increased latency along the L-M axis, demonstrating that the spatio-chromatic VEP is sensitive to mild colour deficiencies and the magnitude of dyschromatopsia is reflected in the VEP

response. The polar plot at the bottom figure 2.6 shows the latency difference of responses obtained from a tritanopic individual. The greatest latency increase occurs near the S axis.

Crognale et al (1993) also demonstrated a deficit in S-cone pathway in patients with diabetes (figure 2.7) and unilateral central serous retinopathy (CSR) (figure 2.9). Their results showed that latencies along the S-cone isolating axis modulation in diabetic patients are consistently greater than those of normal observers, whereas the latencies of the L-M axis remains close to those of normal observers (see figure 2.8). This is suggestive of an early S-cone functional deficit of the S-cone pathway in diabetic patients. In the unilateral CSR patient (figure 2.8), the unaffected eye shows near normal latencies at all contrasts along both L-M and S-cone axes. The response latency for the affected eye show a near normal response along the L-M axis, but for modulations along S-cone axis the response latencies are much longer.

Suttle and Harding (1999) demonstrated that, at isoluminance, the offset response is minimal or absent in colour normal observers. When the stimulus shifts from the isoluminance point, the offset response begins to appear and becomes more apparent with increasing the luminance contrast. In their study, a protanomalous observer showed minimal response to chromatic contrast, and the response to pattern offset was demonstrated to increase with luminance differences. This was also seen in the responses from colour normal observers. These results show that morphological changes to pattern offset responses in addition to the pattern onset responses can be effectively used in colour-normal and colour-defective observers, as part of the signature of the transient response to chromatic stimuli at isoluminance.

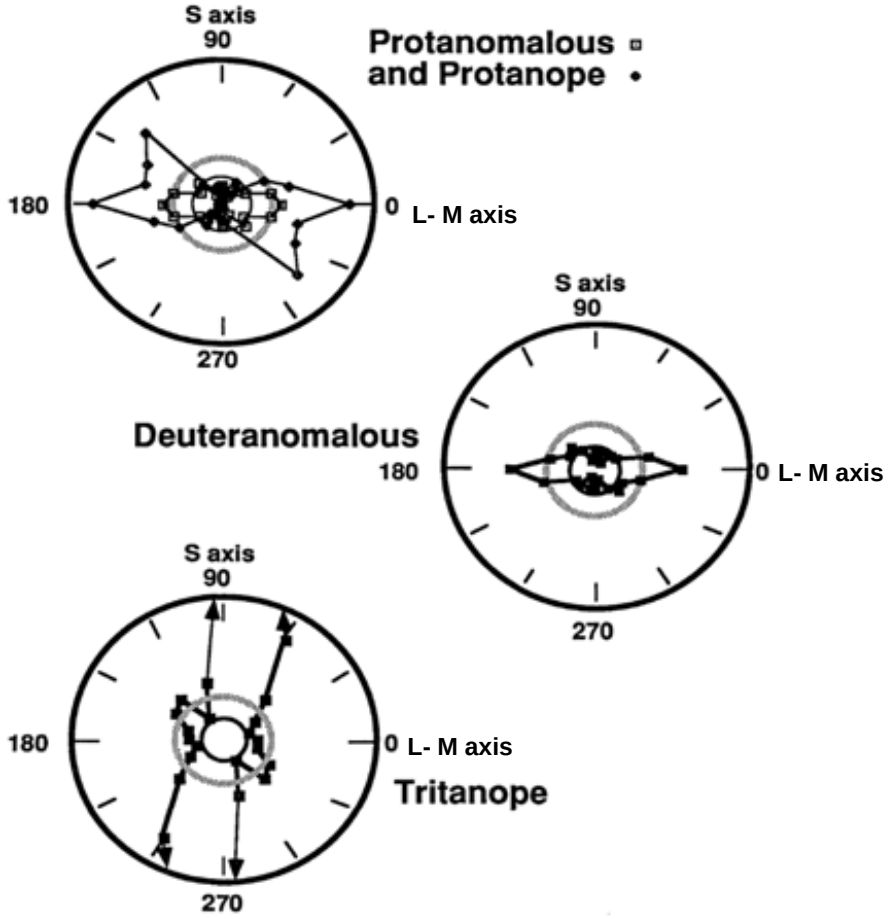

Figure 2.6 Polar plots of the latency differences obtained by use of modulation within the isoluminant plane in congenital colour-defective observers. The latencies are plotted relative to normal observers for each direction in colour space (inner most ring, zero difference; grey ring 20-ms slower). Adapted from Crognale et al (1993).

Recent work has shown that red-green and blue-yellow chromatic VEPs have greater importance for conditions like multiple sclerosis (Sartucci et al., 2001) and Parkinson disease (Sartucci and Porciatti, 2006). These studies suggest that VEPs to red-green and blue-yellow isoluminant gratings are equally involved in multiple sclerosis. In Parkinson's disease VEPs to Blue-yellow

gratings have longer latencies suggesting the vulnerability of S-(L+M) pathway in early stage of disease.

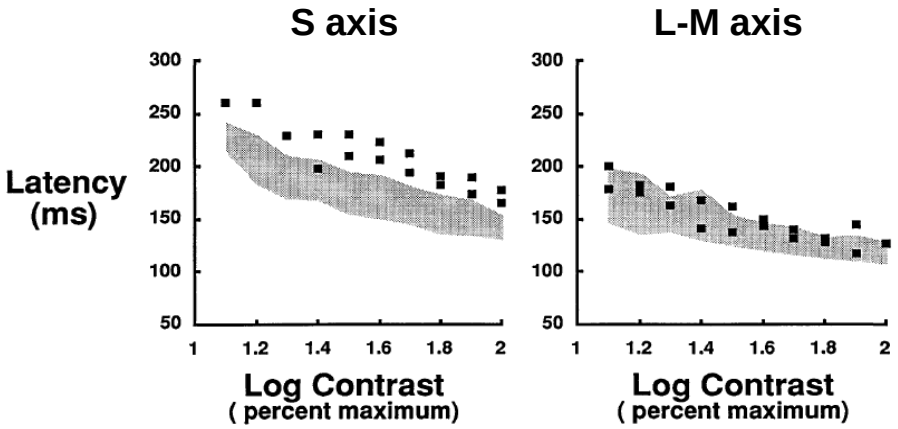

Figure 2.7 Latencies of the VEP obtained from two diabetic subjects (squares) for modulations along the S and L-M axis. Grey shaded areas represent the latencies of that of normal. Taken from Crognale et al (1993).

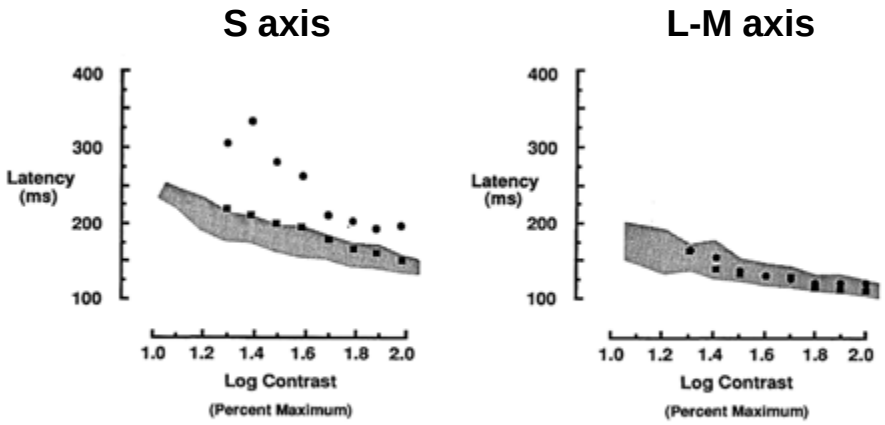

Figure 2.8 Latencies of the VEPs obtained from a subject with central serous retinopathy (Affected eye, circles; unaffected eye, squares) for the modulations along S and L-M axes. Shaded areas represent the latencies of that of normal. Adapted from Crognale et al (1993).

2.5 INTRODUCTION TO THE ELECTRORETINOGRAMS

One of the goals of the thesis is to study the retinal contributions to the chromatic processing in human trichromatic vision. In order to investigate the retinal contributions, we elicited flicker elctroretinograms (ERGs) using silent substitution stimuli. Before proceeding to the experiments, we have summarized the history of the ERGs, source of the components of the ERGs, methods of eliciting the various photoreceptor responses to the ERGs and the also the clinical application of flicker ERGs. In addition to this we have also summarized the recent investigations that evaluated the post-receptoral mechanisms and also L:M raios in the retina using flicker ERGs.

The Electroretinogram (ERG) is a mass electrical response produced by the retina in response to light stimulation. It can be measured non-invasively and provides an objective technique that reflects the physiological and structural integrity of the retina. The ERG was first discovered by Holmgren (1865) in Sweden but it appears that Dewar and McKendrick (1873) working independently in Scotland also demonstrated that retinal potentials change with the variation of light. Gotch (1903) was the first to create the visible record of the ERG response and was able to report that there is an initial negativity in ERG response. Later, Einthoven and Jolly (1908) described all of the classic components of ERG that are known today. The forms of ERG responses in different species are shown in figure 2.9. The responses shown were recorded in dark adapted states when bright light stimuli were applied. ERG responses in different species clearly show differences in amplitude and morphology. At least part of this variability is due to the differences in density of rods and cones of retina in different species. The other factors that account for variability in

ERG response are stimulus duration, stimulus intensity and method of recording. In spite of all these differences, the ERG responses of turtle, bullfrog, rabbit and human consist of common features such as negative a-wave followed by positive b-wave.

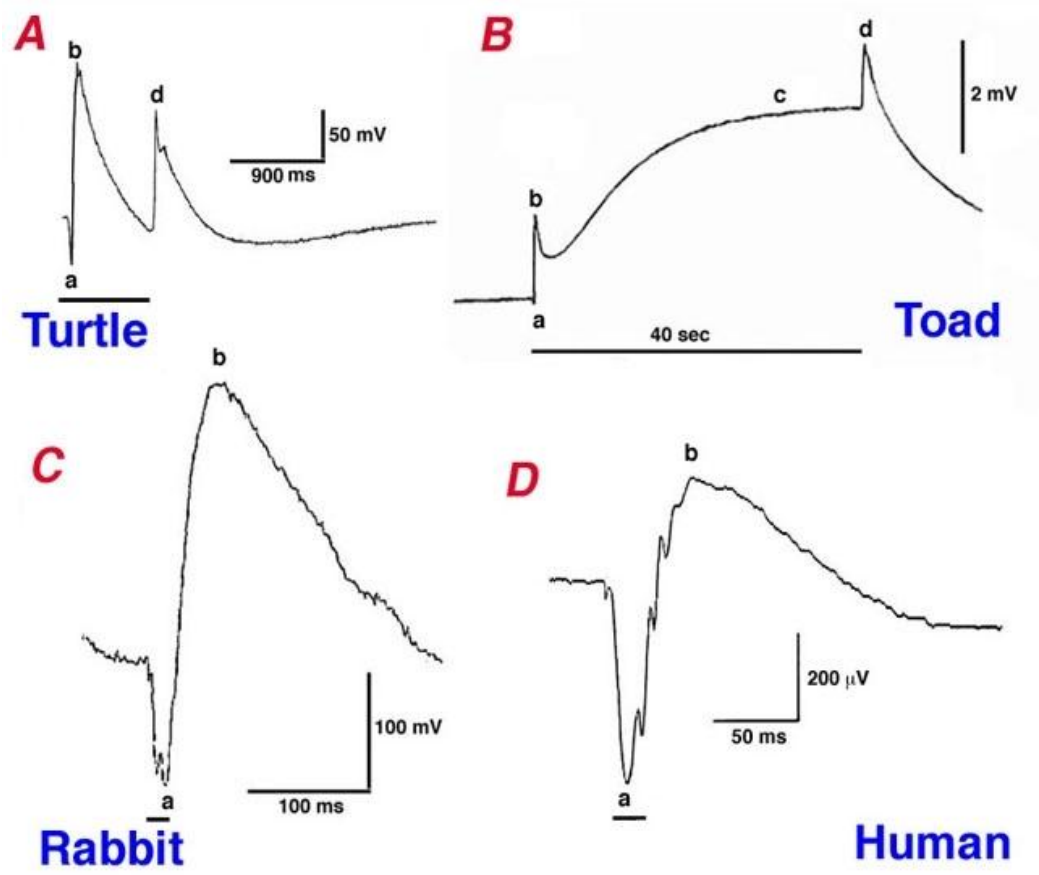

Figure 2.9 Scotopic ERGS: A) ERG from turtle retina elicited by a 900ms light stimulus in order to separate a, b and d-wave components. B) The ERG of a bullfrog elicited by a long light stimulus (40sec) in order to show the c-wave in addition to the a , b and d-waves (Oakley, 1977). C) The ERG response of a rabbit to a flash of a white light (100ms). Note that the c and d-wave have disappeared D) The ERG response to a brief flash from a human as typically recorded in the clinic. Note the fast oscillations on the ascending limb of b-wave. Scales denoted separately for each ERG response. Vertical scale represents the amplitude in micro volts (μV) and horizontal scale represents the time in milliseconds (ms).

Source:

http://www.ncbi.nlm.nih.gov/books/NBK11554/figure/ch35erg.F1/?report=objectonly

A detailed component analysis of the cat ERG was published by Ragnar Granit (1933). He used corneal electrodes to record ERGs from anesthetized cats and observed the gradual abolition of different components as anaesthesia was deepened. Granit named these components as P-I, P-II and P-III respectively. These three components are as shown in figure 2.10. The P-I component is a slow positive wave at the cornea. The P-II component is also a corneal positive wave which rises relatively fast to peak amplitude and recovers to intermediate amplitude when the light stimulus is on. The P-III component is a negative wave that develops quicker than P-I and P-II and remains negative till the stimulus is switched off. This component is more resistant to the level of anaesthesia.

The resultant form of the ERG depends on the summation of these three components which vary in magnitude and polarity before and after the stimulus onset. From Granit's analysis, we may conclude that the negative a-wave is the leading edge of the negative P-III component; the positive b-wave is formed by the summation of P-II and P-III component and slow going c-wave reflects the summation of P-I and P-III. The cellular origin of the ERG components can be understood by physiological and pharmacological approaches. The former approach is based upon the hypothesis that the ERG components are generated in specific retinal layers and as a result when these are passed by the intra-retinal microelectrode, the polarity of the specific ERG waves will reverse. This process is known as current source density analysis and helps in finding the anatomical location of the different ERG components within the retina. Later, the pharmacological approach utilises the application of agonists and antagonists of cellular mechanisms and then studying their effects on the ERG components.

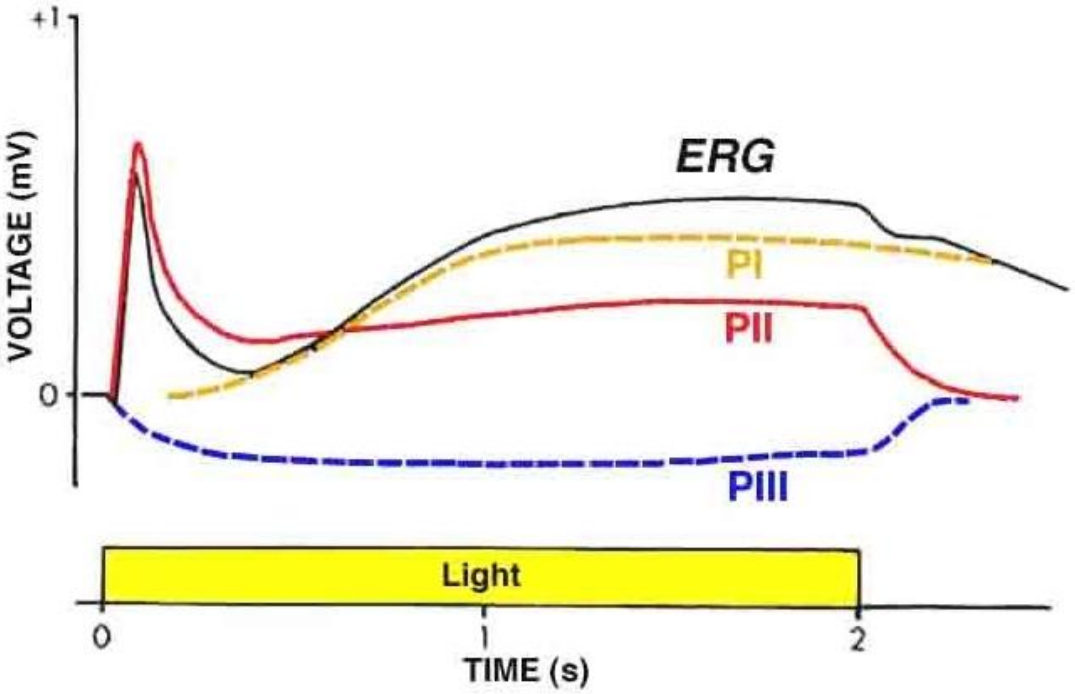

Figure 2.10 The ERG response elicited from a cat with 2 sec light stimulus. The anaesthesia was deepened slowly to isolate P-I (dotted yellow line), P-II (red line) and P-III (dotted blue) components (Granit, 1933). Solid black line represents the ERG response to the same light stimulus.

Source: http://webvision.med.utah.edu/ERG.html

2.6 MAJOR COMPONENTS OF ERG

2.6.1 The a-wave

The a-wave is the negative wave that appears at the beginning of the ERG and equivalent to the leading part of P-III component. It has been shown that P-III component can be divided into fast and slow P-III components (Murakami and Kaneko, 1966; Sillman et al., 1969). Studies have shown that the origin of the fast P-III component is in the photoreceptor layer (Tomita, 1950; Brown and

Murakami, 1964b; Brown and Murakami, 1964a; Brown and Wiesel, 1961a; Brown and Wiesel, 1961b).

The a-wave can be separated by flooding a retinal preparation, which is separated from its eyecup (i.e., it has no RPE attached to it), with sodium aspirate that blocks synaptic transmission between the photoreceptors and second order neurons. Subsequent investigation of this preparation showed that that the a-wave is a complex waveform that is made up of three subcomponents:

1) The early receptor potential (ERP)
2) The Late Receptor Potential
3) The Slow P-III Component

The ERP can be only seen in ERG when very bright stimuli are used. This component represents the photochemical process in the outer segment of the receptors when their pigment absorbs light energy.

The recordings from within retina at different depths and different regions showed that the late RP also originates in the photoreceptor layer (Witkovsky et al., 1975). This component has fast onset and this onset forms leading edge of the a-wave.

Current source density analysis reveals that the slow P-III component source is in the inner segment of the photoreceptor. This component arises from currents created by the decrease in concentration of potassium ions around the inner segment in response to light, which flows into the Müller cells in more proximal retinal layers. The slow P-III component, as its name suggests, develops slowly integrating the effect of prolonged light stimulation over time.

2.6.2 The b-wave

The b-wave of ERG has been a focus of interest for many research groups since it is the major component of the human ERG. Early work has shown that b-wave originates in more proximal layers of the retina to that of a-wave. The b-wave is completely abolished in the aspirated retina (where there is complete block of the synaptic transmission from photoreceptors to the cells post synaptic to the photoreceptors) indicating that the origin of the b-wave is post synaptic to the photoreceptors. Based on current source density analysis of the b-wave, the origin of the b-wave was thought to be in Müller cells (Faber, 1969). The main aim of the Faber study was to find the current sink and source of the b-wave. The results of this study have shown that the current sink was in the outer plexiform layer and the main source was in the inner nuclear layer. The other evidence that supported the Müller cell as the source of b-wave come from the work by Miller and Dowling (Miller and Dowling, 1970). They sought to identify the source of b-wave by recording the ERG responses intra-cellularly and matched the responses to the b-wave morphology and latency. The results showed that intracellular ERG recordings from Müller cells exhibited slow, depolarising potentials with a similar latency and waveform to that of b-wave.

Pharmacological studies that used specific agonists and antagonists to glutamate receptors have shown that by exposing the vertebrate retina to 2-amino-4-phosphonobutyric acid (APB), a specific agonist of glutamate metabotropic receptors, eliminates the ERG b-wave (Gurevich and Slaughter, 1993) as shown in figure 2.11B. Since APB-sensitive metabotropic glutamate receptors are only present in ON-centre bipolar cells (Slaughter and Miller, 1981), this finding clearly indicates that the bipolar cells play a major role in the generation of the b-wave.

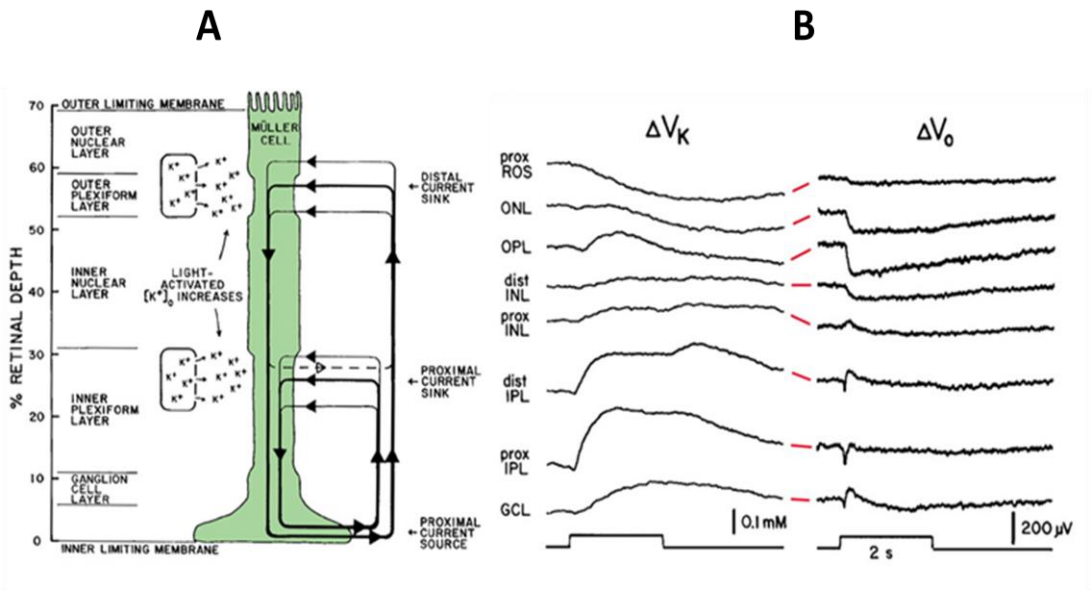

Figure 2.11 A) The pathways of extracellular currents, which have been suggested to underlie the generation of the ERG b-wave. The two sinks (OPL and IPL) reflect the increase in extracellular potassium ions due to light-induced electrical activity. The vitreous serves as a large current source due to high potassium conductance of the end-feet of the Müller cells (Newman, 1989). B) The Müller cell hypothesis of the ERG b-wave. Depth profile of light induced changes in the extracellular concentration of potassium ions (_V_K) and of local field potential (_V_0) (Karwoski et al., 1985).

Source : http http://webvision.med.utah.edu/ERG.html

Relatively recent studies on primates by Sieving et al (1994) proposed that the b-wave of photopic ERG is mainly generated by ON-centre bipolar cells and opposed by OFF-centre bipolar cells. Other studies that used sink/source analysis (Karwoski and Xu, 1999) and pharmacological dissection of the ERG (Green and Kapousta-Bruneau, 1999) suggest that the ON-centre bipolar cells are the generators of the b-wave without Müller cells.

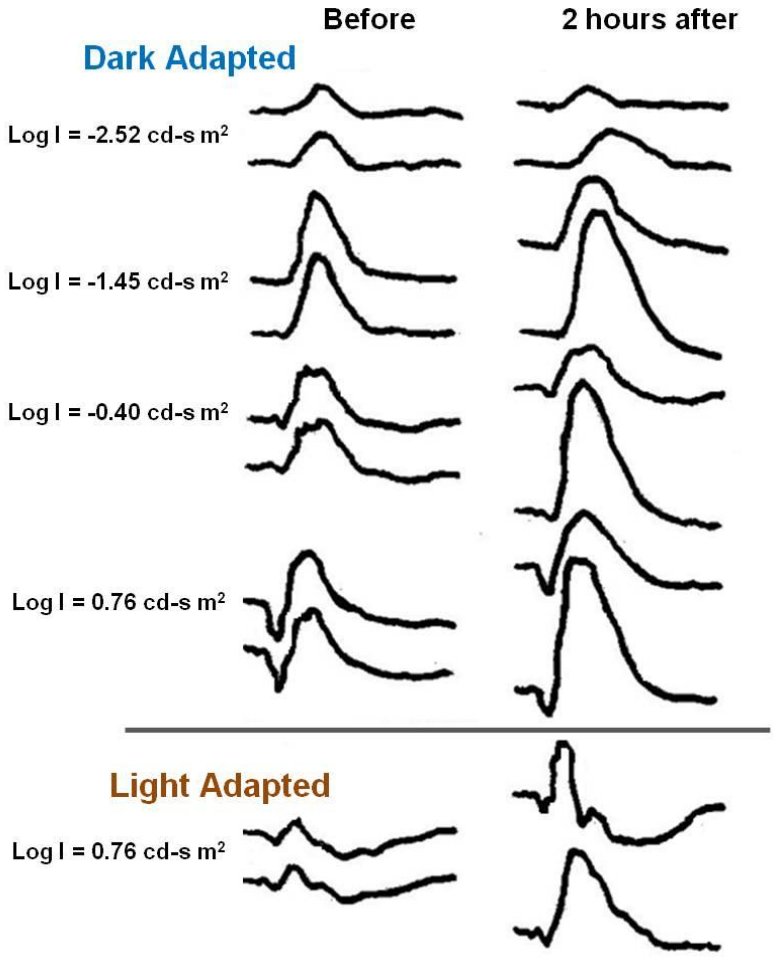

Figure 2.12 Effects of barium ions on the ERG responses of the rabbit. Saline solution containing barium chloride was injected into vitreous of right eye and saline into vitreous of the left eye (lower and upper traces respectively). The ERG responses before were shown on left traces. ERG responses after 2 hours of injection were shown on right traces. Note that the b-wave responses were augmented in the right eye (Lei and Perlman, 1999).

Source: http://webvision.med.utah.edu/ERG.html

The generation of the b-wave is thought to be from Müller cells. In order to find this, Lei and Pearlman (1999) recorded ERG responses from rabbit both eyes. The right eye vitreous was injected with the barium ions and left eye vitreous was injected with saline solution. Since barium ions block the potassium permeability of Müller cells (Newman, 1989 , Reichelt and Pannicke, 1993 , Linn

et al., 1998), they are expected to abolish the ERG b-wave in left eye. However, their assumption proved to be wrong. The b-wave remained persistent even after injection and in certain conditions the b-wave increase in amplitude (see figure 2.12). This observation opposes the Müller cell hypothesis for the b-wave generation and supports ON-center bipolar cell hypothesis.

Recent studies (Dong and Hare, 2000) have investigated the inner retinal contributions to the b-wave of the ERG using tetrodotoxin (TTX). This pharmacological agent was used to block action potentials in third-order retinal neurons (amacrine and ganglion cells), and specific antagonists to GABA and glycine receptors. From this study, it was concluded that amacrine and ganglion cells contributed to the amplitude and kinetics of the ERG b-wave.

2.6.3 The c-wave

The c-wave corresponds to the P-I component of Granit, and is known to have its current source in the retinal pigment epithelium. Noell (1954) was the first person to note that the c-wave disappears from the ERG after selective poisoning of the RPE by sodium iodate. The intracellular recordings from the retinal pigment epithelium (Steinberg et al., 1970) showed that the potential changes that were recorded from these cells in response the light stimuli are similar to the morphology and temporal properties of the ERG c-wave. In addition to this, when the retina was separated from the pigment epithelium, the ERG responses showed an a- and b-wave, but not c-wave. Figure 2.13 represents the recording of a, b and c-waves in the ERG from the eyecup (upper trace). Once the retina is separated from RPE and sclera, the ERG response shows ‘a’ and b-wave only (middle trace).

Though the c-wave originates from the RPE, it is dependent upon the integrity of the photoreceptor layer. This is because the absorption of light in the photoreceptors stimulates the events that lead to the reduction in extracellular concentration of potassium ions. So the ERG c-wave is useful to study the functional integrity of the photoreceptors and RPE cells and also the interactions between them.

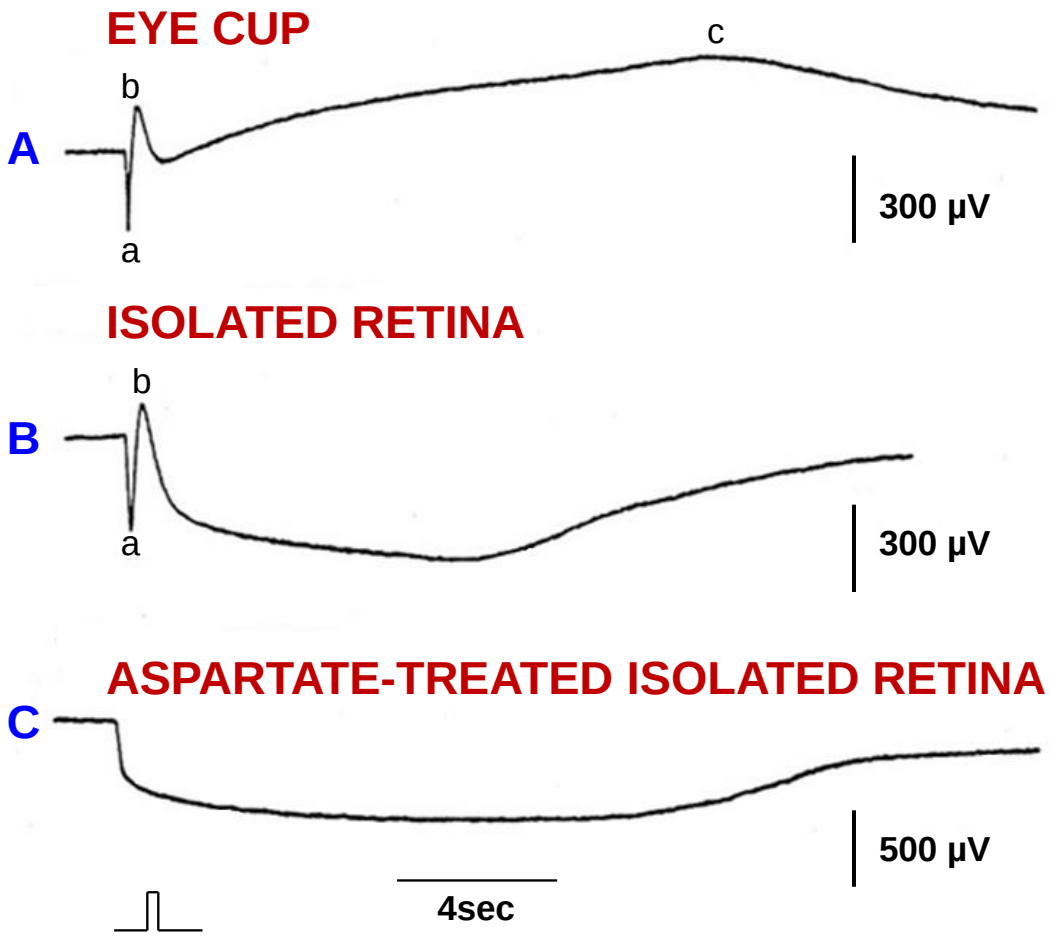

Figure 2.13 ERG recording from the skate. Upper trace shows the recording from the whole eye cup. Middle trace shows the response after separation of the retina from the pigment epithelium. Lower trace shows the response after exposing the retina to aspartic acid. Vertical scale represents the amplitude in micro-volts and horizontal scale represents the time in seconds (adapted and modified from Pepperberg et al (1978)).

Source: http://webvision.med.utah.edu/ERG.html

2.6.4 The d-wave

The final major component of the ERG is the d-wave or off response, which is observed mostly in cone-dominated retinas. The d-wave can be obtained only if we can separate ON and OFF phases of the ERG responses in time by applying prolonged light stimuli (>100ms). The current source density analysis of d-wave shows that the source of d-wave is in OFF-center bipolar cells (Xu and Karwoski, 1994; Xu and Karwoski, 1995). Pharmacological agents were used to block the glutamate metabotropic receptors of ON bipolar cells and AMP/KA type receptors of OFF bipolar cells in primates (Sieving et al., 1994) and amphibians' retina (Stockton and Slaughter, 1989; Szikra and Witkovsky, 2001). These studies have shown that the d-wave mainly depends on synaptic transmission between photoreceptors and OFF-centre bipolar cells.

2.7 MINOR ERG COMPONENTS

In addition to the major components observed in the ERG response, there are also a number of minor components revealed during the course of research of ERG components. Two of these components are:

1) The early receptor potential (ERP)

2) The oscillatory potentials

2.7.1 The early receptor potential (ERP)

It is part of a-wave complex seen at the beginning of the ERG response. This component was first noted in monkey eye (Brown and Murakami, 1964b). Later it was also noted in rat (Cone, 1964) and human eyes (Yonemura and Kawasaki, 1967). The ERP is the electrical response seen instantly after a stimulus is presented and has a two phase pattern as shown in figure 2.14. In humans, the duration of the ERP is 1.5 ms and is followed by a-wave. The origin of the ERP is in photoreceptors (Brown et al., 1965; Murakami and Pak, 1970) and its amplitude depends on two factors: 1) the density of visual pigment in the outer segment of photoreceptor and, 2) the stimulus intensity. The ERP is recorded to calculate the amount of rhodopsin in patients suffering from the photoreceptor diseases like retinitis pigmentosa (Berson and Goldstein, 1970).

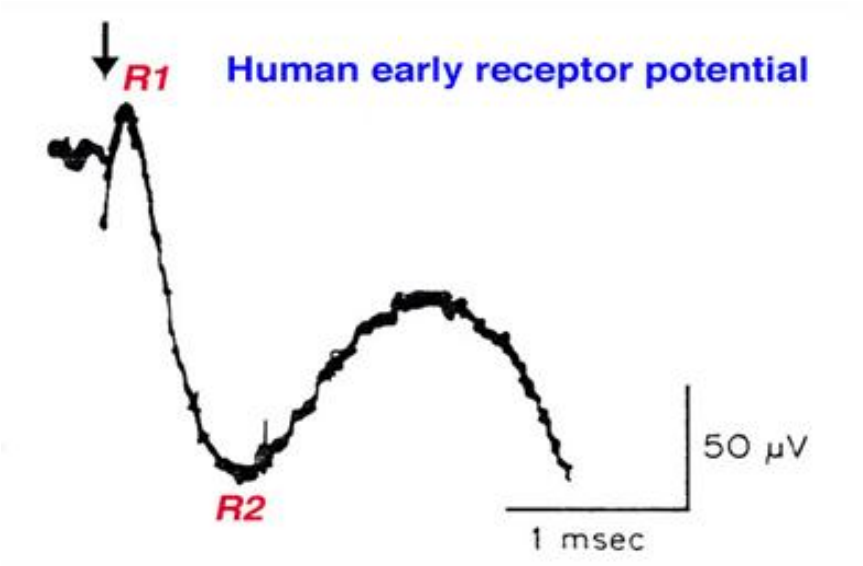

Figure 2.14 The early receptor potential (ERP) of the human eye elicited using a very bright light flash (right arrow). Two components were identified as R1 (positive) and R2 (negative) components (Yonemura and Kawasaki, 1967). Horizontal scale represents the time in milliseconds and vertical scale represents the amplitude in micro-volts.

Source:

http://www.ncbi.nlm.nih.gov/books/NBK11554/figure/ch35erg.F10/?report=objectonly

2.7.2 The oscillatory potentials (OP)

A group of high frequency oscillations often observed on the ascending limb of the b-wave are known as oscillatory potentials (see figure 2.15). The OP was first noted in 1937 (Granit and Munsterhjelm) and has gained clinical importance when it is observed in humans by Cobb and Morton (1954). OP can be easily elicited in light adapted retina using high intensity light flashes of shorter duration (15-40 ms). OP can be better resolved by applying the digital filters and increasing the amplification. The power spectrum can be derived using Fast Fourier Transform (FFT) to measure the amplitude and frequency of OP quantitatively. Since the amplitude and light intensity of OP are different from that of b-wave, it is believed that the source of origin for OP is in inner plexiform layer (Ogden, 1973; Wachtmeister and Dowling, 1978). The exact retinal layer of origin of OP is not known.

Intra-retinal recordings and pharmacological studies have shown that these are the reflections of extracellular currents generated from the negative feedback pathways between amacrine cells and bipolar cells (Wachtmeister and Dowling, 1978; Yonemura and Kawasaki, 1979; Heynen et al., 1985). OP has their clinical importance in finding ischemic retinal areas in conditions like central retinal artery occlusion (Speros and Price, 1981).

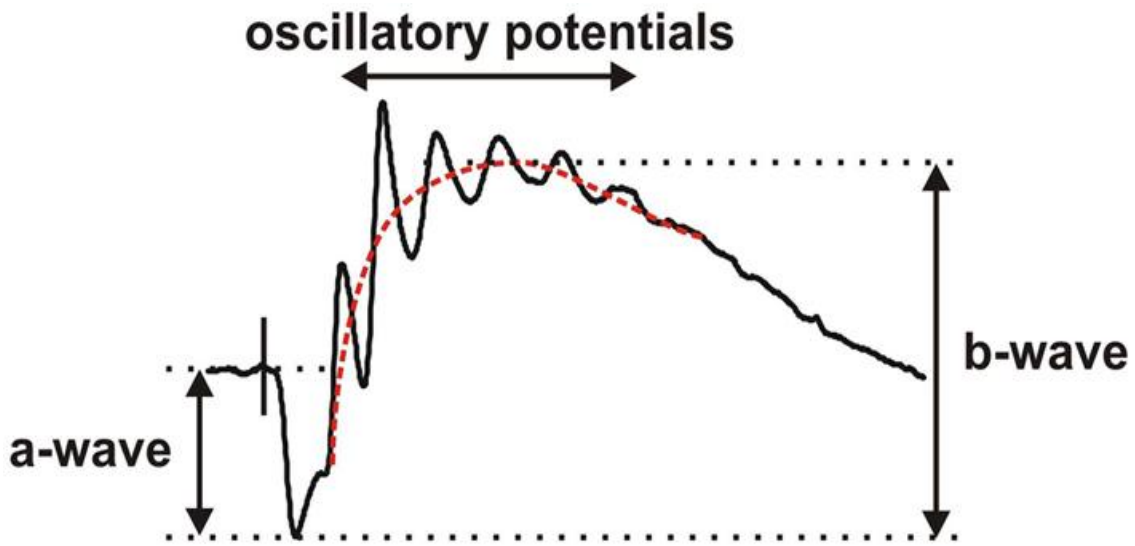

Figure 2.15 Diagram showing oscillatory potentials (OP) from the flash ERG elicited in a mouse. As in the human ERG responses, the b-wave immediately follows the a-wave. In mice, the b-wave is not seen clearly because of large osciilatory potentials. Therefore, the b-wave is marked with red dotted curve which runs through the midpoints of all oscillatory potentials. Midpoints are defined as an average of adjacent minimum and maximum of oscillations.

Source: http://www.bioscience.org/2009/v14/af/3409/figures.htm

2.8 THE ERG AND DUPLICITY THEORY OF VISION

The main idea of the duplicity theory of vision is that there are two visual mechanisms that operate at different levels of illumination. The origin of the idea takes its root from the anatomy of the retina which has two types of photoreceptors called rods and cones. These two types of photoreceptors are found in most animals. The rod dominated retina is seen in nocturnal animals and cone dominated retina are found in diurnal animals. However, it is not

possible to separate vertebrate retinas into two simple categories because most of them show combination of two types of retinal activity which enable them to operate over a wider range of illumination. Most animals have the ability to change from one to other type of visual mechanism and these changes can be revealed in the ERG recordings.

Granit was the first to observe the differences in ERG recordings of nocturnal and diurnal animals. He named the responses as E-type and I-type respectively. He also found that I-type responses from mixed retinas, which contain both rods and cones, after dark adaptation were very similar to E-type responses. Adrian (1945) went a step further by showing that the change in wavelength of the ERG, temporal frequency of stimulus and adaptation of the eye can elicit and isolate the responses of rod and cone vision. He soon realised that the responses need to be referred as scotopic (rod) and photopic (cone) responses rather than direct recordings of photoreceptor activity.

2.9 SCOTOPIC AND PHOTOPIC ERG RESPONSES

There are a number of ways we can separate the scotopic and photopic responses in human retina.

1) Spectral sensitivity of ERG
2) State of adaptation
3) Temporal frequency of the stimulus

2.9.1 Spectral sensitivity of ERG

Scotopic and photopic responses in the ERG can be isolated using different coloured stimuli. Figure 2.16 represents the human spectral sensitivity of the rods and cones across visible spectrum, rods are more sensitive across the whole spectrum but the relative cone sensitivity increases at longer wavelengths. Rod peak sensitivity reaches a maximum in the blue-green region of the visible spectrum at about 500nm, and the cone peak spectral sensitivity depends on the summation of the long (red) and medium (green) and short (blue) wavelength sensitive cones. Usually, this net summation is in the orange region of the visible spectrum around 560nm. Cone responses can be isolated in light adapted eye with stimuli of longer wavelengths, whereas the rod responses are isolated in dark adapted eye with stimuli of shorter wavelengths. Figure 2.17 shows the responses from the eye to deep red, orange red and blue stimulus. The orange-red stimulus produced responses that are mixture of both scotopic and photopic components.

Recordings from light and dark adapted eyes to stimuli of different wavelengths are shown in figure 2.18. In the light adapted eye, rod responses are saturated and photopic responses are maximal to long wavelength stimuli. On the other hand, in dark adapted eye the responses are maximal to short wavelength stimuli.

More quantitative analysis of the ERG sensitivty to different wavelengths of light can be performed by plotting a spectral sensitivity curve. Armington (1976) has shown that such curves can be obtained using criterion response method. The curves obtained using this method was useful to correlate the ERG responses

to perceptual visual phenomena such as absorption of light in the visual pigment.

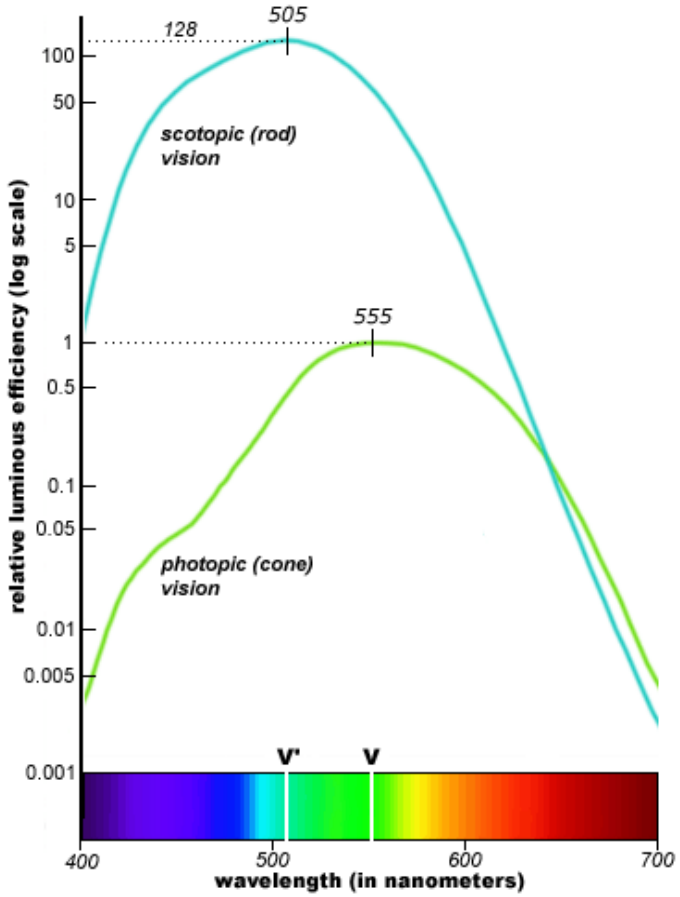

Figure 2.16 CIE 1951 scotopic luminous efficiency (blue line) and CIE 1964 wide field (10°) photopic luminous efficiency (green line), relative to peak photopic sensitivity on log vertical scale; relative peak sensitivities V (photopic) and V1 (scotopic). Horizontal colour bar represents the visible spectrum. Picture adapted from Kaiser & Boynton (1996).

In the dark adapted state, the peak spectral sensitivity of the retina corresponds to green range of colour and light adapted state is shifted towards yellow range of colour. This colour shift, also known as Purkinje shift (Himstedt and Nagel, 1901) is caused by a change in response from photoreceptors, i.e. from rods to cones. The ERG recorded based on this shift would help to record the response from the rods and cones.

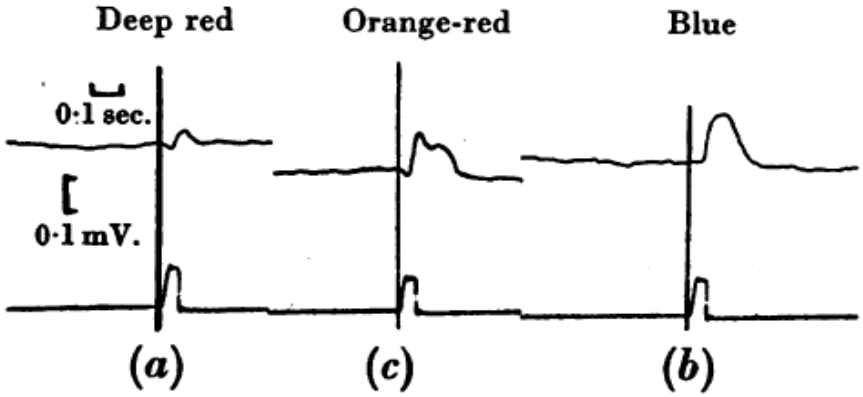

Figure 2.17 Human ERG responses showing the dual character of the response (Adrian, 1945). Brief di-phasic response with red light (a), longer monophasic response with blue (b), and composite response with orange-red (c).

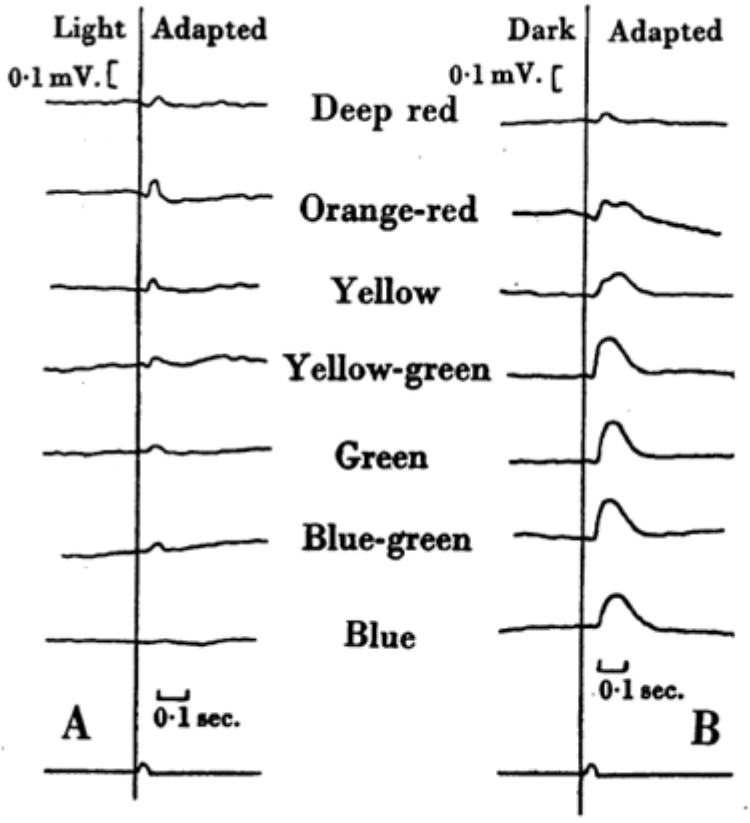

Figure 2.18 Responses to various wavelengths in light adapted eye (A) and dark adapted eye (B), slower component is only present in B. The light source has same intensity throughout, but the brightness of screen varies with the colour filter in use (Adrian, 1945).

2.9.2 State of adaptation

The two types of photoreceptors, rods and cones, vary widely in terms of the luminance range of their responses. The rod system is very sensitive to the low light levels in dark adapted state and least responsive to step inputs of light increments (Field et al., 2005; Baylor et al., 1979). In contrast, the cone system is not as sensitive as rod system but has an ability to respond to bright lights and allows visual system to adapt to background illumination over range of intensities. The ERGs generated by rods and cones are easily distinguished by recording at different adaptation conditions.

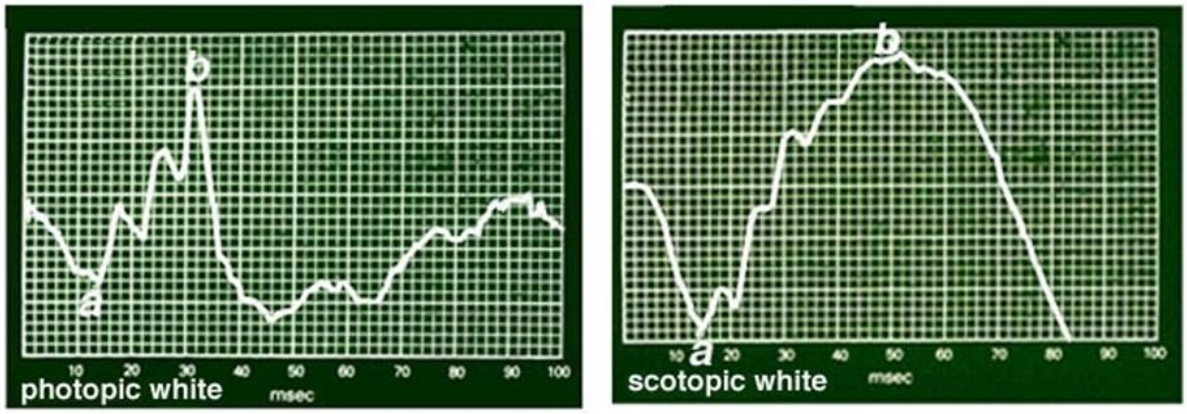

Figure 2.19 Typical clinical recordings of photopic (Left) and scotopic (Right) conditions with white flash of light. Difference in temporal properties of rods (scotopic) and cones (photopic) can be clearly shown. Scotopic response has rod-cone type, but the contribution of the cones is very small. Verical scale is mV per square (R) mV per square (L)

By modulating the state of adaptation (figure 2.19), we can separate the two systems. To a given light stimulus, background illuminations saturate the rod activity and mainly reflect the ERG of a cone system. The left hand side of the figure2.19 shows the ERG that has small amplitude but time to peak is very fast (at about 30-32ms). In contrast, right hand side shows the ERG response

elicited by the same stimulus configurations as in the left one but recorded after 30 minutes of dark adaptation. The ERG has a considerably larger b-wave amplitude with a longer latency (time to peak is about 50-55ms).

2.9.3 Temporal frequency responses of the ERG

The third method of separating the photopic and scotopic components of the ERG is by the use of flickering stimuli. This method is based on the fact that there is a difference in the temporal properties of the scotopic and photopic visual systems. As the temporal frequency is changed, the ERG waveform is also changed (Dodt, 1951; Bornschein and Schubert, 1953). At low temporal frequencies (≤ 10Hz), the ERG develops completely with different components (similar to classical ERG shape) showing scotopic and photopic components, at higher temporal frequencies (≥ 19Hz) these components start fusing together and look like a single waveform. Standard clinical flicker ERGs are recorded to 30Hz scotopic flicker and are cone driven (Marmer et al.,1999).

One common psychophysical method to investigate the performance of visual system to temporally modulating stimuli is in terms of what is known as Critical Flicker Fusion Frequency (CFF). In ERG terms, it refers to the temporal frequency at which the ERG is just too small to be distinguishable against background noise. When CFF is plotted against retinal illuminance of the stimulus across the visible spectrum (see figure 2.20), it gives two limbed function in which one limb covers the lower frequency and describes the performance of scotopic visual system and the other limb covers the higher frequency range and describes the performance of the photopic visual system.

The single flash response time for the cones is different from the rods. The cone mediated flash ERG has implicit time of 27-33ms (ISCEV standard), whereas

the standard rod mediated ERG has an implicit time in the range of 78-95ms (Birch and Anderson, 1992; Jacobi et al., 1993). Rod driven ERGs have larger phase delays than the cone driven ERGs to modulating stimuli. Furthermore, ERGs produced by the rods show lower flicker fusion frequency than those produced by cones (Abraham and Alpern, 1984; Kremers and Scholl, 2001).

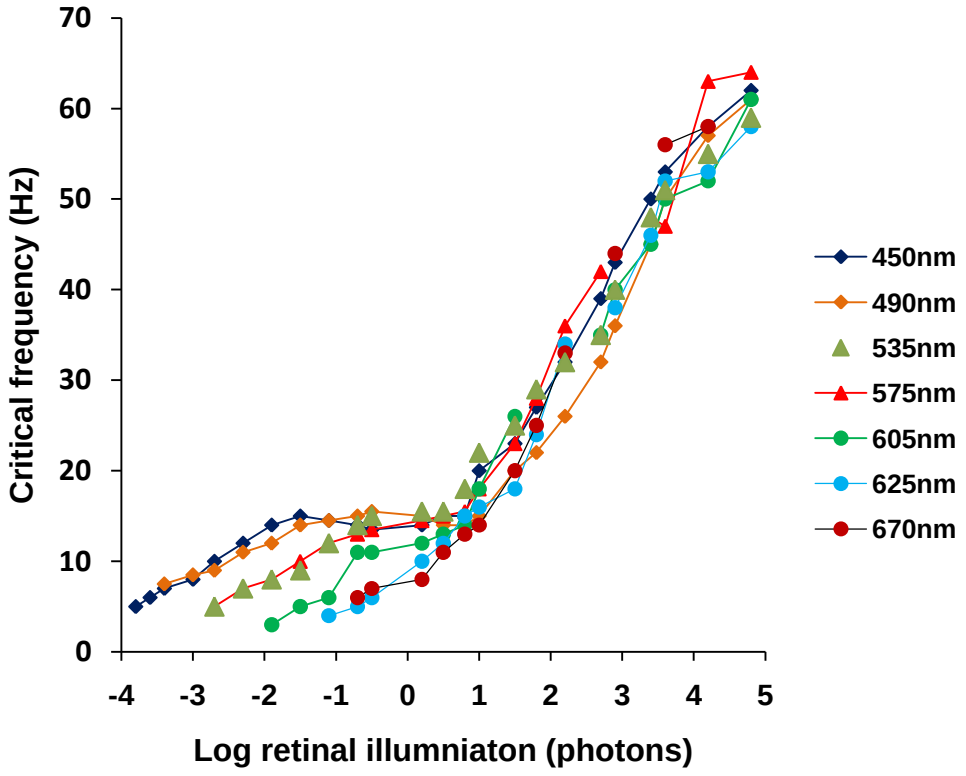

Figure 2.20 CFF over range of retinal illuminance for different monochromatic lights of different wavelengths (corresponding wavelengths were shown in box). 19 degree test fields were used for the data. Re drawn from Hecht and Shlaer's data (values are of approximation) from Hart Jr, W.M., (1987) 'The Temporal Responsiveness of Vision'.

2.10 ISOLATION OF CONE DRIVEN ERGs

ERGs recorded under high illumination, isolate the cone responses from rods. However, it is difficult to say which cone class contributes to the ERG response. Due to differences in the physiological properties of the L, M and S cone classes, their contribution to the final ERG response varies. The post-receptoral pathways of each cone class also vary, so it is important to know how each cone contributes to the final ERG response.

Cone driven ERG responses can be isolated using two methods:

1) Chromatic adaptation
2) Silent substitution

2.10.1 Chromatic adaptation

The signals from the three cone classes have their inputs to different post-receptoral pathways at the bipolar cell level. The L and M cones contact with midget bipolar cells and the outputs of L and M cones also connect with diffuse bipolar cells. The former is a part of colour processing whilst the later contributes luminance processing (Dacey and Lee, 1994; Lee et al., 1989). The L and M cone driven signals are distributed and processed depending upon which post-receptoral pathway they enter. Exactly how the outputs of these different cone types are combined to produce the ERG signal is still under investigation. The best way to answer this question is to isolate the responses of different cone classes by using a stimulus that elicits a response from only a single cone type.

Anatomically, S-cones are different from L and M cone classes. Molecular genetics (Nathans et al., 1986) has revealed that there were only two cone classes in ancestral mammals; one absorbed short wavelength light and the other absorbed middle and long wavelength light. The division of L and M cones was occurred after the split between new and old world primates, some 30 to 40 million years ago (Dayhoff, 1972). The S-cones are different from L and M cones in terms of their anatomical, biological and biochemical characteristics. Furthermore, S-cone driven signals make use of distinct post-receptoral pathways. For instance, S cones contact with blue cone bipolar cells, which in turn contact with bistratified ganglion cells (Martin, 1998 , Kremers et al., 1999) (see section 1.2.2).

One method of obtaining cone isolated ERG responses is to record responses from monochromats. This works well for S-cone monochromats, since they can be identified clinically (Gouras and MacKay, 1990). It is not certain whether the lack of L and M cones have any influence on S cones and their post-receptoral processes or whether the S-cone driven ERG measured in these subjects are similar to these recorded from normal (Kremers, 2003).

In colour normal subjects, the isolation of cone driven responses can be obtained on the basis of the difference in spectral sensitivities of different cone types (Zrenner and Gouras, 1979; Stockman et al., 1993a; Stockman et al., 1993b). Chromatic adaptation is one of the methods that can be used to separate the signals driven by different cone types. This method relies upon selective desensitization in the different cone classes using coloured backgrounds. By selectively adapting a single cone class to specific coloured background, its sensitivity to a stimulus can be reduced and the remaining cones responses are favoured (Kremers, 2003). By doing this, the spectral

sensitivity of the non adapting cones can be studied. For example, L cone activity can be suppressed using 650nm background (Drasdo et al., 2001).

Chromatic adaptation has been successfully used in many psychophysical studies. Chromatic backgrounds have been used to adapt one or more cone types in order to isolate the responses from remaining cones (Wald, 1964; Eisner and Macleod, 1981; Stockman et al., 1993a; Stockman et al., 1993b). Using this technique, S cone isolation would be easier to achieve because S cone spectral sensitivity is quite different from that of L and M cones. S cone driven ERGs can be isolated using a chromatic background such as long wavelength background that desensitizes L and M cones. For example, Sawusch et al (1987) used 571nm narrowband adaptation field of 7000 trolands to improve S cone isolation. Other psychophysical studies have also successfully used chromatic backgrounds to suppress the specific cone activity and isolate the S-cone activity (Sawusch et al., 1987; Jacobs et al., 1996; Drasdo et al., 2001).

Zrenner and Gouras (1979) have recorded S-cone ERGs using a 441nm wavelength stimulus on steady yellow background in anesthetised cats (see figure 2.21). The ERG driven by S cones has a different morphology from that originating from L and M cones. The S-cone ERG (441nm stimulus) consists of a b-wave (peak latency = 45 to 60ms), followed by a slow negative response; a small a-wave was seen preceding to the b-wave; the slow negative response was noted at the stimulus offset but there is no positive d-wave seen at any intensity level. L cone isolating stimuli (583nm) on the other hand elicited a larger a-wave preceded to quicker b-wave and at the stimulus offset a prominent d-wave appeared following slow negative response. M cone isolating stimuli (511nm) generated ERGs with shorter latency b and d-waves with

amplitudes smaller than that produced by L cone isolating stimuli. In addition to this, a large negative response was observed at both onset and offset of the stimulus. These differences give the opportunity to determine whether the isolation is satisfactory or not.

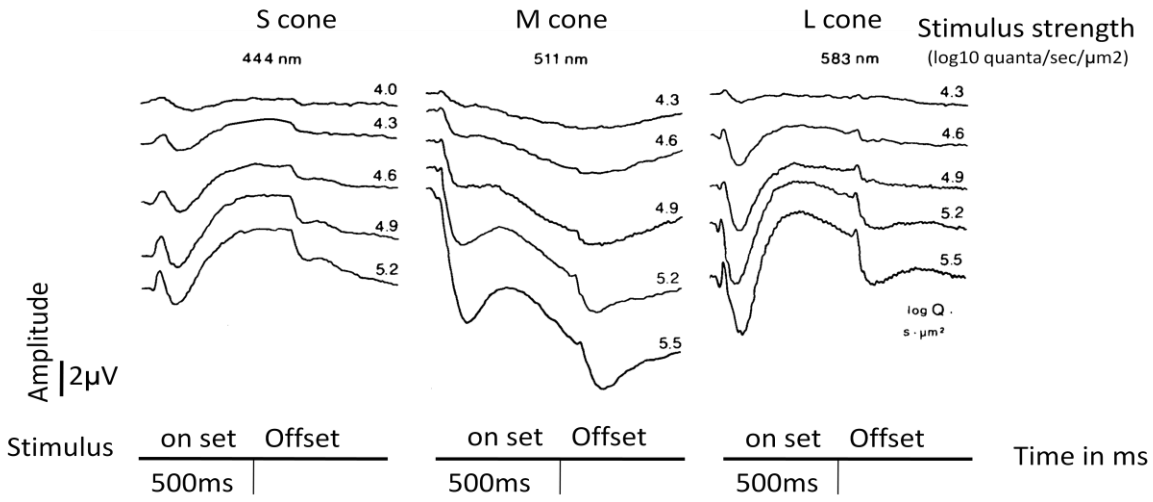

Figure 2.21 Represents the difference between L, M and S cone driven ERGs. 444nm (left traces), 511nm (middle traces), 583 nm (right traces) represents S-cone, M-cone and L-cone stimulating monochromatic flashes respectively. The stimulus strength is shown beside each record (log $_{10}$ quanta/sec/µm^2. Stimulus duration is 500ms. Picture adapted and modified from Zrenner and Gouras (1979). Amplitude scale is shown at the left bottom corner.

The spectral absorption of the L and the M cones overlap with each other. This makes the isolation of these two cone responses difficult. Adaptation of L cones will unavoidably adapt the M cones as well. The difference in sensitivity between L and M cones is relatively small, so that the response to monochromatic stimuli might still originate the response in the cone that meant to be desensitized. The other major problem is that the appearance of L and M

cone driven flicker ERGs are similar to each other (Eisner and Macleod, 1981) so that the effectiveness of the response isolation cannot be determined easily.

As well as failing to selectively isolate L and M cones, chromatic adaptation has an additional drawback as it induces non-linearities in the response characteristics of visual system at higher contrasts (Eisner and Macleod, 198; Webster and Wilson, 2000). Chromatic adaptation often adjusts partially to the mean colour of the stimulus, and thus leaves a residual bias in the colour appearance of the field (Webster and Wilson, 2000).

A study designed to investigate the cone contributions to the intra-retinal ERG by chromatic adaptation showed that the adaptation of cones is a complex process involving compression of the response, bleaching of photo pigments and adaptation of the cells. There is also a possibility of additional post-receptoral adaptation, for instance, in horizontal cells and retinal ganglion cells, which could affect the ERG (Valeton and van Norren, 1983).

Since there are a number of limitations with the chromatic adaptation method with regards to isolation of three cone classes, silent substitution may constitute a better method of isolation.

2.10.2 Silent substitution

The silent substitution paradigm was first introduced by Donner and Rushton (1959) but was extensively used in the field of electrophysiology by Estevez and Spekreijise (1982). Under the same states of adaptation, the isolation and comparison of cone driven signals can be studied more reliably. In order to understand the interaction between the cones, it is important to know the

response characteristics of each cone type and its signal strength. Recent studies (Kremers et al., 2003) have demonstrated that these objectives can be easily achieved under the similar states of adaptation, i.e., isolation of cone responses without changing their sensitivities.

The silent substitution method, also called spectral compensation (Estevez and Spekreijse, 1982) can be used to isolate cone responses in electrophysiological and psychophysical experiments. The silent substitution technique is based on the “Principle of Univariance”. The Principle of Univariance states that the excitation of a photoreceptor caused by the photo isomerisation process is invariant and does not rely upon the energetic content and wavelength of the absorbed photon. However, the probability that a photon is absorbed by the photoreceptor depends upon its wavelength which is described in terms of its absorption spectrum.

Although the stimulus may vary in intensity and in wavelength, the response of a cone can only vary in one dimension; the extent of its excitation. Once a photon is absorbed by the photoreceptor, all information about that photon is lost. Although the wavelength can vary, the probability of a given photon being absorbed by a photoreceptor depends upon the spectral sensitivity of the photo pigment that the cone contains. The Principle of Univariance means only by comparing the outputs of the individual cones in the visual system, we are able to discriminate wavelength.

The significance of this principle is that a stimulus of particular wavelength can be replaced with stimulus of different wavelength, without producing the change in the excitation strength of a photoreceptor. In order to do this, the intensity of two stimuli should be chosen such that the absorption quanta remain the same.

Figure 2.22 represents the two photo pigments (say L and M) with peak spectral sensitivity of 600nm and 550nm, respectively. The probability that a photon of certain wavelength will be absorbed by a photoreceptor depends upon the pigment's absorption spectra. The number of photons and the probability of one photon reaching the photoreceptor are directly proportional to the number of isomerizations. For example, photoreceptor L is excited equally by a stimulus, which modulates between two monochromatic lights of wavelength $\lambda 1$ and $\lambda 2$; whereas the photoreceptor M is excited differently by this modulation. The number of photo-isomerizations elicited in photoreceptor L by these two monochromatic lights is equal (7). However, the number of isomerizations elicited in photoreceptor M is different (at about 1 for $\lambda 1$ and about 12 for $\lambda 2$). This means that this modulation is silent for photoreceptor L (i.e., there is no net response from photoreceptor L), whereas the response in photoreceptor M is large. The Principle of Univariance cannot only be used to find the silent substitution condition but can also be used to measure the number of photo-isomerizations for non-silent substitution conditions (Kremers, 2003).

The specific stimulus strength for each cone photoreceptor can be calculated in terms of its cone contrast (Estevez and Spekreijse, 1982). It is important for us to understand that these measurements are at the level of photoreceptor, not at the output of the photoreceptor. The output of the photoreceptor depends not only from the contribution of the photoreceptor itself, but also the signals contributing from its feedback pathways (Kremers, 2003).

The number of photoreceptor types that can be kept silent for a specific condition depends on the number of independent light sources used for the stimulus. For example, in a CRT monitor if we use three phosphors, then we can control three photoreceptors at a time. Recent studies have used four

LEDs, which has given the opportunity to selectively stimulate all four photoreceptor types (rods and three cones) independently (Shapiro et al., 1996; Shapiro, 2002; Murray et al., 2008).

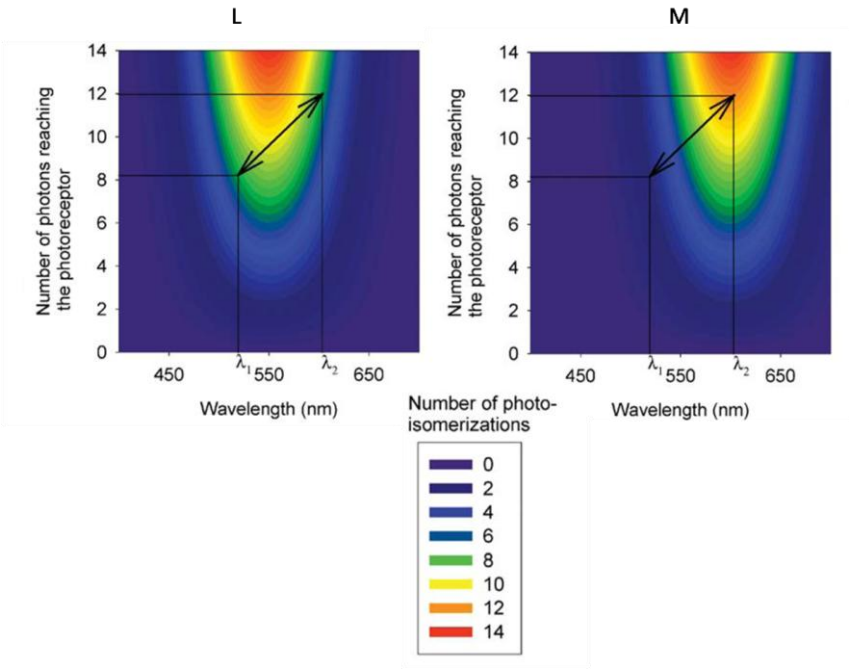

Figure 2.22 Two hypothetical photo pigments L (left plot) and M (right plot) and their modulation for two different wavelengths λ1 and λ2 (shown by arrow). The number of photo-isomerizations is not changed for photo pigments L for this modulation. In contrast, the number of photo-isomerizations in pigment M modulates between 12 and 1. This would result in a photoreceptor contrast of 84.6% (calculated based on equation 2). The colour topography scale is shown in the bottom of the figure (Redrawn from Kremers, 2003).

In theory, any required stimulus strength combination can be obtained in all photoreceptors, but practically the combinations are limited by two factors:

1) The lowest luminance of a light source is 0cd/m^2. It means that the output of a light source cannot be negative.

2) Maximal output of light source has a fixed value which cannot be exceeded.

The concept of stimulus strength quantification was first used by Spekreijse et al (1977) to record Visual Evoked Potentials (VEPs). Using this technique, they studied the response of a single cone type and also the interactions between the signals derived from two or more cone types. This is possible because unlike the adaptation paradigm, the time averaged luminance and chromaticity is identical at all stimulus conditions, since the state of adaptation remains same and mode of operation of the retina is not altered by nonlinearities that are induced by adaptation. As a result, the responses elicited by the different stimuli can be compared.

L and M cone driven ERGs at identical states of adaptation have been measured in various studies (Usui et al., 1998; Kremers et al., 1999). They measured responses in terms of cone excitation strength. The cone excitation of each cone type is obtained by multiplying the emission spectra of phosphors with psychophysically determined cone fundamentals (Stockman et al., 1993a, 1993b) and integrating over a range of wavelength. For example, L cone excitation by red phosphor ($E_{L,R}$) was measured using the equation 2.1 (Kremers et al., 1999):

$$E_{L,R}(t) = F_R . L_R(t) . \int_{380}^{780} IR(\lambda) . A_L(\lambda) . d\lambda \quad \text{---------- (2.1)}$$

Where; L_R = luminance of the red phosphor

$E_{L,R}$ = L cone excitation by the red phosphor

t = changes as function of time

$I_R(\lambda)$ = emission spectrum of red phosphor at unit luminance,

$A_L(\lambda)$ = L cone fundamental,

F_R= conversion factor for red phosphor relating the photometric measurements to the cone fundamentals.

The total excitation of L cones is the sum of the excitations caused by each phosphor.

The modulation of cone excitation can be calculated in terms of Michelson's cone contrast which is given by the equation 2.2:

$$CC = \frac{E_{max} - E_{min}}{E_{max} + E_{min}} \quad \text{----------} \quad (2.2)$$

Where; E_{max} = Maximal excitation and E_{min} = Minimal excitation.

2.11 INTERACTION BETWEEN ERGs DRIVEN BY DIFFERENT PHOTORECEPTORS

As stated earlier, under mesopic conditions both rods and cones operate to fulfil the visual requirements of vertebrates. Physiological studies have shown that under mesopic conditions both rod and cone signals interact with each other at the level of retinal ganglion cell responses in macaque (Gouras and Link, 1966) and in cats (Rodieck and Rushton, 1976; Enroth-Cugell et al., 1977). Psychophysical and electrophysiological investigations have shown that colour perception in part depends upon opponent interaction between L and M cones (see review of Kremers, 2003). In order to study such interactions, a linear model is required that can summate the responses from two or more cones. One such model is the vector addition model.

2.11.1 Vector addition model

Mathematically speaking, a vector has an amplitude and phase and two vectors can be added using parallelogram method as seen in figure 2.23. Let us consider two vectors A and B with their coordinates X_1, Y_1 and X_2, Y_2 respectively. The addition of A and B is a resultant vector C and its coordinates would be $X_1 + X_2$, and $Y_1 + Y_2$ respectively. The phase of the resultant vector is calculated using the equation 2.3.

$$\theta = \tan^{-1}(Y_2+Y_1/X_2+X_1) \text{ ---------- } (2.3)$$

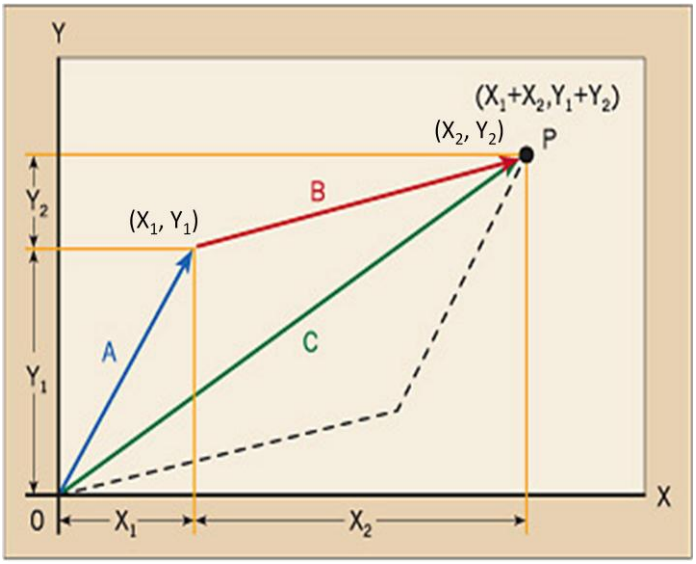

Figure 2.23 Figure represents the addition of two vectors A (blue line; co-ordinates are X_1, Y_1) and vector B (red line; co-ordinates are X_2, Y_2) using a parallelogram method. Resultant vector is C (green line), which is the diagonal of the parallelogram. The co-ordinates for resultant vector at point P ($X_1 + X_2$, $Y_1 + Y_2$).

In ERG terms, this model mainly allocates separate signals that have specific response delays, representing the temporal processing of the signals in each of the pathways (Kremers, 2003). The purpose of the model is to study the interactions between two pathway responses that are elicited by the same

temporal frequency but differ in their phase. The responses in pathways are sinusoidal and can be expressed as vectors. The interaction between two pathways is the sum of the two vectors which is also represented as a vector. Figure 2.24 represents two sinusoidal responses of two different pathways with their amplitudes A1 and A2 and phases P1 and P2 respectively to a given sinusoidal stimulus. The combined response is again sinusoidal at same temporal frequency with amplitude $A_{1 \text{ and } 2}$ and phase $P_{1\text{and } 2.}$

2.11.2 Application of vector addition model in ERG work

This model has been successfully applied to the study the rod and cone input to ganglion cells and LGN neurons in primates. The interactions studied have included the signals carried by chromatic and luminance mechanisms (Smith et al., 1992; Lee et al., 1993) and also signals from rods and cones (Lee, 1996; Weiss et al., 1998). The association of receptive field centre and surround of ganglion and LGN cells have also been studied by the vector addition model (Enroth-Cugell et al., 1983; Frishman et al., 1987; Lee et al., 1998). Furthermore, the vector addition model was extensively used to study the interaction between fast and slow rod signals (Stockman et al., 1991; Stockman et al., 1995) and also to study the interaction between L and M cones (Kremers and Meierkord, 1999).

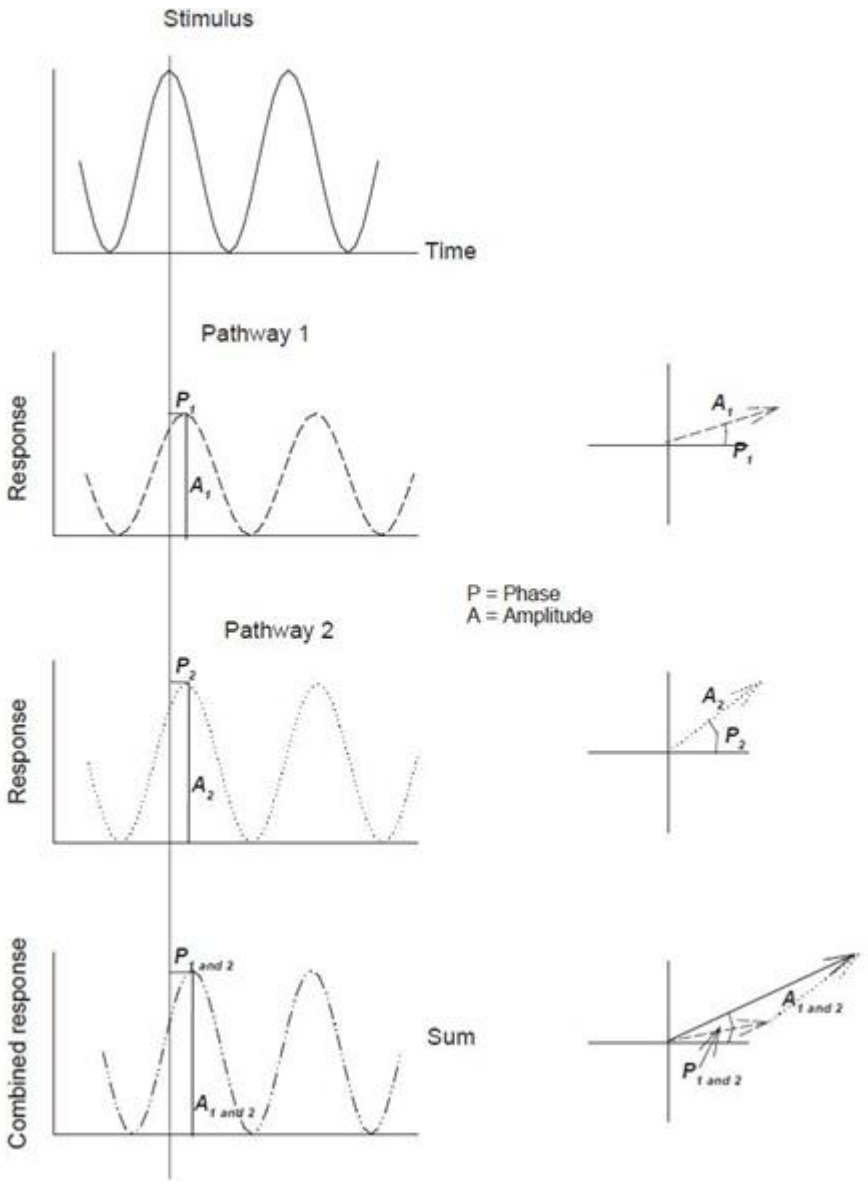

Figure 2.24 Visualisation of the concept of vector addition. Top trace represents the sinusoidal stimulus with specific temporal frequency. A sinusoidal shaped response in pathway 1 can be described by its amplitude A_1 and phase P_1. Phase is given relative to the sinusoidal stimulus. The corresponding response is described by a vector with length A_1 and angle P_1 with positive abscissa. In pathway 2, the response amplitude is A_2 and phase is P_2 at same temporal frequency. The response in pathway 2 is also described by a vector with its length A_2 and angle P_2 with positive abscissa. The combined response is also sinusoidal at the same temporal frequency and has amplitude $A_1$and$_2$ and phase $P_1$and$_2$. The vector describing the combined response equals the addition of the two vectors describing the separate responses (Kremers, 2003).

Kremers et al (2003) used the vector addition model to fit the elliptical threshold contours (see figure 2.25) to study the interaction between L and M cones. The elliptical contours are drawn from the threshold data points obtained at various L and M cone modulation contrasts. These contours estimate the sensitivity and the absolute phase difference between L and M cone driven signals. Moreover, the form and the orientation of the ellipses guide the L and M cone driven ERG responses. The size of the ellipse and overall sensitivity are inversely proportional to each other, i.e. if the ellipse size is large which means the threshold ERG amplitudes are also large indicating a low sensitivity. According to them, the orientation of the ellipse is determined by the ratio between the sensitivity of L and M cone stimulation. For example, if ellipse is tilted towards the M cone axis, it means that the sensitivity of L cone driven response is higher than that of M cones. In their study, most of the trichromats showed higher sensitivities of L cone driven responses than M cones.

According to the vector addition model, if the phase difference between L and M cone driven ERG is less than 90° then the L and M cone interact in additive manner and the major ellipse axis would be in quadrant 2 and 4 (see figure 2.26A). On the other hand, if the phase difference is more than 90^0, which means the interactions would be subtractive and the major axis would be in quadrants 1 and 3 (See figure 2.26B). When the phase difference is 180°, then the length of the major axis would be infinitely long and in quadrants 1 and 3.

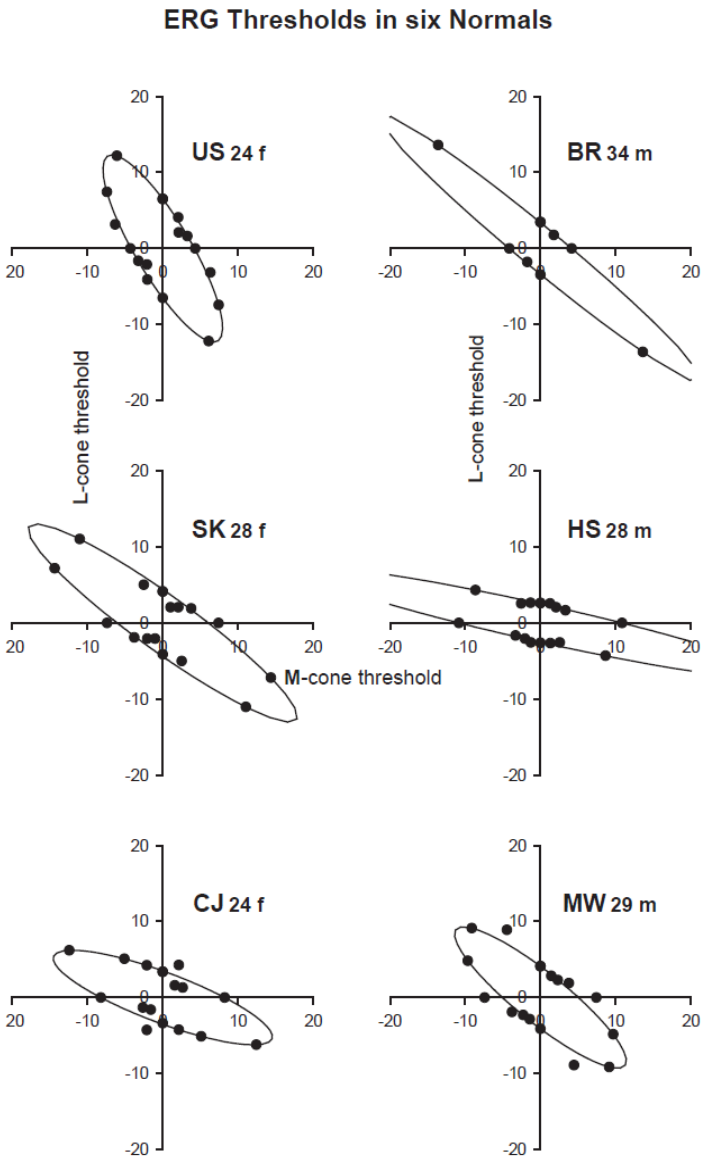

Figure 2.25 ERG thresholds of six normal trichromat observers. Ellipses are best fits of the vector addition model data. Most subjects show high sensitivity to L-cone modulation (i.e., ellipses are tilted towards M-cone axis) (Scholl and Kremers, 2000).

A

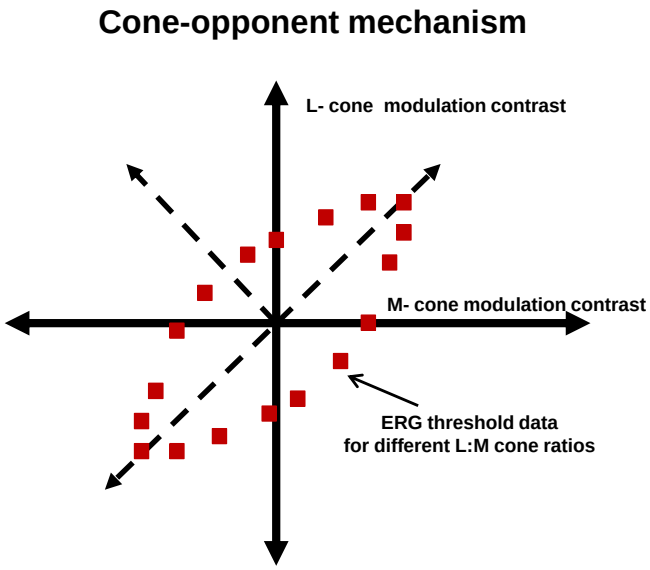

B

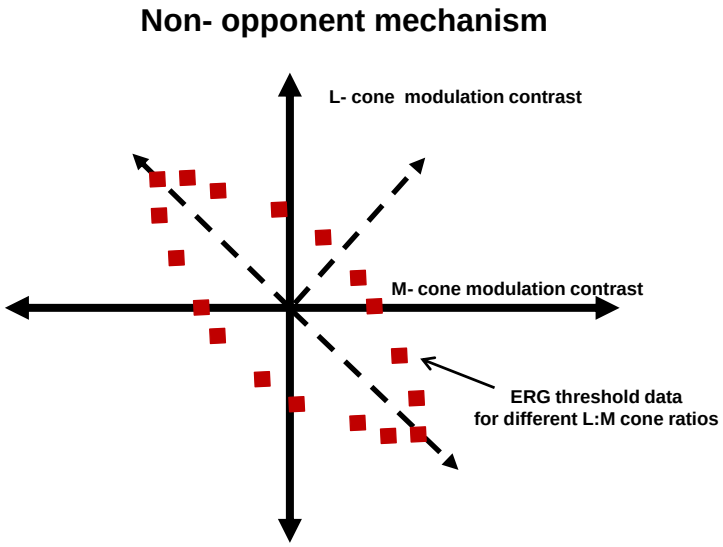

Figure 2.26 A hypothetical example of ERG thresholds (shown in brown squares). Ellipses are best fits of the vector addition model. Ellipse is tilted towards quadrant 1 and 3 means the sensitivity is higher along quadrant 2 and 4 which means L and M cones interact in opponent manner. B) Ellipse is tilted towards quadrant 2 and 4 means the sensitivity is higher along quadrant 1 and 3 which means L and M cones interact in additive manner.

2.12 USE OF ERGs TO ASSESS THE CONE FUNCTION IN NORMAL AND COLOUR DEFICIENT SUBJECTS

One approach to measure the cone function is to record the ERGs from monochromats. Since S-cone monochromats can be identified clinically (Gouras and MacKay, 1990), we can measure the S-cone responses. (S-cone specific ERG characteristics were clearly explained in chromatic adaptation technique). The task of measuring L and M cone function is difficult in comparison to S cones because of their overlap of spectral sensitivity. One way of doing this is measuring the ERG responses in protanopes and deuteranopes, but in these patients the L or M cone specific responses are interfered with by rod and S-cones. Flicker ERGs using silent substitution in dichromats gives the opportunity to control the rod and S cone interference. High luminance stimuli would control the interference of rods and silent substitution would control the interference of S cones.

The approach of silent substitution was successfully used to measure the L and M cone driven ERGs in both normal and colour deficient subjects (Kremers et al., 1999; Kremers, 2003). The results from these studies showed that all ERG responses obtained were sinusoidal and mainly dominated by first harmonic component. Trichromats had larger responses for L cone isolating stimuli than M cone isolating stimuli (see figure 2.27). The data of X-chromosome linked dichromats suggest that missing cone type is replaced by the remaining cone type. It means in protanope the missing L cones are replaced by the M cones and in deuteranopes the missing M cones are replaced by L cones.

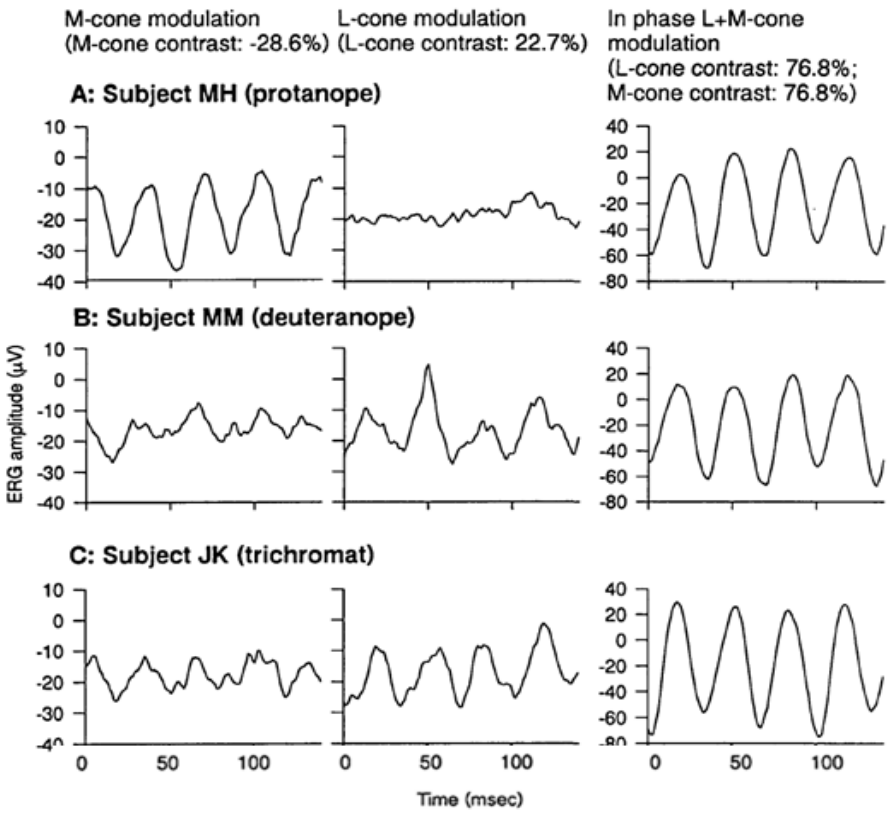

Figure 2.27 ERG tracings of a protanope (First row), a deuteranope (Second row) and a trichromat (Third row) to M cone modulation (First column; silent substitution for L and S cones; M cone contrast: -28.6%) L cone modulation (Second column; silent substitution for S and M cones; L cone contrast: 22.7%) and in phase modulation of L and M cones (Third column; silent substitution for S cones; L and M cone contrast: 76.8%). The ERG responses are averages of 12 runs. Picture is adapted from (Kremers et al., 1999).

2.13 APPLICATION OF CONE SELECTIVE ERGs IN PATIENTS WITH RETINAL DISORDERS

The cone isolation technique can be useful to detect changes caused by each retinal disorder that produce some characteristic changes in comparison to the normal ERG. The particular changes that occurred in a course of disease would provide some useful information regarding the patho-physiology of the disease. Kremers et al (2003) used cone isolating ERGs to study the patients with retinal

disorders such as Retinitis Pigmentosa, Stargardts macular dystrophy, Cone and cone rod dystrophy, and Macular dystrophy etc. The Vector addition model has been successfully used to study the interactions between L and M cone driven ERGs in all these disorders. The vector addition model simplifies the characteristic changes of the disease by number of parameters.

1. The overall sensitivity of the retina.
2. The sensitivity of the L and M cone driven ERGs
3. The phases of the L and M cone driven signals and
4. The phase difference between L and M cone driven ERGs.

Retinitis Pigmentosa (RP)

RP is a group of inherited progressive retinal diseases in which the abnormalities of the photoreceptors that lead to a progressive loss in vision. The standard ERG shows an abnormal scotopic response (Gouras and Carr, 1964) with reduced amplitude and latency for 30Hz white flicker stimulation (Berson, 1993; Berson and Kanters, 1970; Massof et al., 1986; Swanson et al., 1993). Kremers (2003) measured cone isolating ERGs in 26 patients with RP. He showed that in comparison to the normal group the amplitudes of L and M cone driven ERGs are decreased. This finding suggests that there is a decrease in sensitivity of L and M cones. However, the L/M ratios remain stable. The M cone driven responses are phase advanced and L cone driven responses are phase delayed in comparison to the normals. He also noted that, normals show an increase in phase with increase in cone contrast where as some RP patients showed decrease in phase with increasing cone contrast. From the data recorded from RP patients he suggests that there is a large individual variation

in phase difference. In general, RP causes many changes in the L and M cone driven ERGs.

Cone and cone-rod dystrophy

In cone and cone-rod dystrophies one might expect that the photopic ERG is more strongly affected than the scotopic ERG (Krill et al., 1973; Ripps et al., 1987). Studies have shown that different cone types are affected, resulting in S cone dystrophy (Bresnick et al., 1989; Van Schooneveld et al., 1991) or L cone dystrophy (Kellner et al., 1995; Reichel et al., 1989). Kremers measured L and M cone driven ERGs in fifteen patients with cone and cone rod dystrophies. He observed that the sensitivity and amplitudes of L and M cone driven ERGs were substantially reduced in comparison to normals. In most patients he noted that both L and M cones were affected. He also observed selective L cone loss in one and selective M cone loss in other patient. L/M ratios in most of the patients were in normal range indicating that L and M cones were equally affected.

The brief summary L and M driven ERG results, in patients with different retinal disorders are described in table 2.1.

Disease	Overall sensitivity	Amplitude of Cone driven ERG		Phase of cone driven ERG		Phase Difference	Phase change with increasing contrast	
		L cones	M cones	L cones	M cones		L cones	M cones
RP	Reduced	Reduced	Reduced	Delayed	Advanced	Increased	Delay or advance	Delay or advance
Sector RP	Reduced	Reduced	Reduced	Slightly delayed	Slightly delayed	Normal?	Advance	Advance
Stargardts's	Normal but variable	Normal	Normal	Slightly delayed	Advanced	Increased	Advance	?
Best	Increased	Increased	Normal	Normal	Advanced	Increased	Advance	Advance
Cone dystrophy	Reduced	Reduced	Reduced	Delayed	Advanced	Increased	Advance	Delay or advance
Cone-rod dystrophy	Reduced	Reduced	Reduced	Delayed	Advanced	Increased	Advance	Delay or advance

Table 2.1 Summary of the changes in several parameters that are estimated from cone selective ERGs, caused by different retinal disorders (Re-produced from Kremers (2003)).

CHAPTER-3 GENERAL METHODS

We have investigated the cortical and retinal contributions of colour processing in trichromatic humans using VEPs and ERGs respectively. This chapter summarizes the general methodology used for recording the VEP and ERG responses.

3.1 VEP STIMULI

3.1.2 Stimulus structure

The stimuli consist of homogenous circular discs of a varying diameter that were centered on the fovea (see fig. 3.1). The mean luminance of the disc was 25cd/m^2 and was presented on a grey background of the same mean luminance. The circular stimulus could be made to undergo equiluminant hue modulation over time which involved presenting a target with a specific hue for 500ms, then replacing it for the same period with a neutral grey stimulus (CIE 1931 chromaticity co-ordinates: x = 0.310, y = 0.316) of the same mean luminance. Thus the stimulus had the appearance of a circular patch, the hue of which was modulated in an onset-offset fashion with a square wave temporal profile. Subjects were instructed to view the black cross, positioned in the centre of the stimulus to maintain steady fixation and all stimuli were viewed binocularly at 114cm in the darkened room (Krauskopf et al., 1982). These stimuli were modulated along sixteen chromatic axes of MBDKL colour space (detail description in section 3.2) as shown in table 3.1.

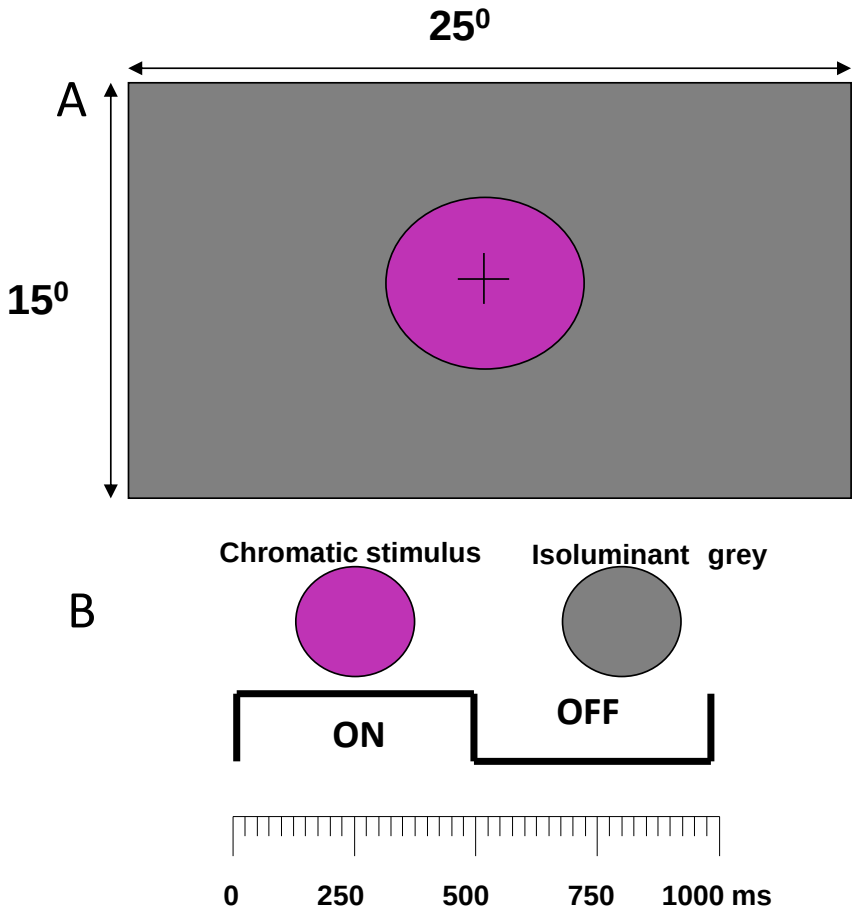

Figure 3.1 The spatial A) and temporal B) configurations of the stimuli used to elicit spot VEPs.

3.1.1 Stimulus Generation

The VEP stimuli were generated by a VSG2/3 graphics card (version5, Cambridge research systems) and presented on a sony 21" FD Trinitron CRT monitor with refresh rate of 120 HZ. Stimuli were modulated by change in luminance contrast or colour contrast. Luminance contrast was measured by the Weber contrast, which is calculated using the equation 3.1:

$$C = \frac{L_s - L_b}{L_b} \quad \text{---------- (3.1)}$$

Where, L_s = Luminance of the stimulus, L_b = Luminance of the background

If the stimuli are isoluminant (i.e. the luminance of the background is equivalent to the luminance of the stimulus) then we measured the chromatic contrast.

Chromatic contrast measurement depends upon the stimulus configuration i.e. spot stimuli or grating stimuli. Since the stimuli are the spots and have different spectral composition to that of background as shown in figure 3.2, the model of transformation between cone excitation and cone contrast co-ordinates is given by equation 3.2:

$$(C_L\ C_M\ C_S)^T = \left[\frac{\Delta P_L}{P_{LO}}\ \frac{\Delta P_M}{P_{MO}}\ \frac{\Delta P_S}{P_{SO}}\right] \text{----------} \quad (3.2)$$

Where; $(C_L\ C_M\ C_T)^T$ is a vector of conventional contrast seen by each cone class and $(\Delta P_L\ \Delta P_M\ \Delta P_{S)}{}^T$ is the vector difference between the cone excitation co-ordinates of the area to be assessed and $(P_{LO}\ P_{MO}\ P_{SO})^T$ is the cone-excitation area of the background $(P_L\ P_M\ P_S)^T$.

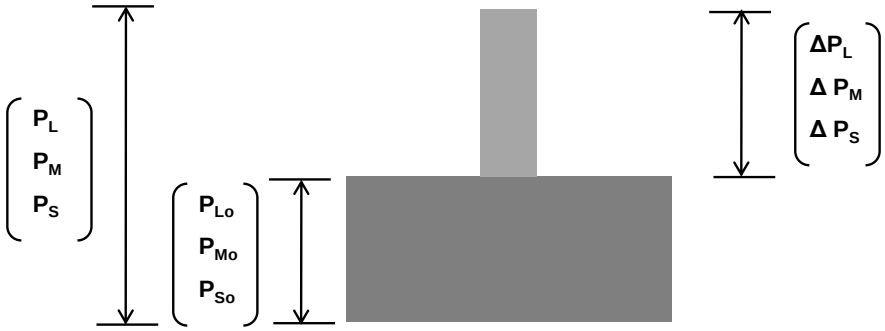

Figure 3.2 Description of cone contrast for a stimulus that is presented in a uniform background. Stimulus may be a decrement or increment to that of background. Background spectral composition may not be the same as that of the stimulus which may result in increment in one cone type and decrement for another. The cone excitation co-ordinates for the stimulus and background together are given by $(\Delta P_L\, \Delta P_M\, \Delta P_{S)}{}^T$. This is obtained by accounting the vector difference between the cone excitations for the background $(P_{LO}\, P_{MO}\, P_{SO})^T$ and the stimulus $(P_L\ P_M\, P_S)^T$. Adapted from (Brainard, 1996).

Chromatic axis	Chromaticity coordinates			Cone contrasts	
	x co-ordinates	y co-ordinates	L cone	M cone	S cone
0	0.3819	0.2826	0.085566	-0.16386	-0.00106
28	0.3464	0.2458	0.075533	-0.14465	0.390358
53	0.3151	0.229	0.051557	-0.09873	0.664989
73	0.2913	0.225	0.025034	-0.04794	0.796314
90	0.2724	0.228	9.3E-05	-0.00018	0.833568
110	0.2521	0.2392	-0.02923	0.055985	0.783141
130	0.2349	0.2595	-0.055	0.105318	0.638441
155	0.2205	0.2998	-0.07754	0.148497	0.351513
180	0.2197	0.3584	-0.08559	0.163899	-0.00124
208	0.2459	0.4402	-0.07566	0.144882	-0.39258
233	0.2992	0.5043	-0.05158	0.098783	-0.66747
255	0.3528	0.5238	-0.02509	0.048041	-0.79895
270	0.3926	0.5092	-6.5E-05	0.000124	-0.83558
290	0.4204	0.4627	0.029099	-0.05572	-0.78569
310	0.4257	0.4033	0.054966	-0.10526	-0.64014
335	0.4099	0.3355	0.076901	-0.14727	-0.35859
background	0.31	0.316			

Table 3.1 CIE chromaticity coordinates and L, M and S cone contrast values for sixteen chromatic axes.

3.1.3 Isoluminance

Heterochromatic flicker photometry (HFP) was conducted for all the chromatic test axes in order to determine the isoluminance for each subject. The stimulus of particular homogeneous disc (see figure 3.1) that was centered on the fovea and the mean luminance of the circular disc was 25cd/m^2 which is same as that of background. Subjects were directed to fix at the centre of the stimulus and the disc was set to flicker at 15 Hz. Adjusting the luminance ratio[3] of the colour and neutral grey phases of the stimulus enabled variation of the luminance contrast content of the stimulus (see figure 3.3). For a luminance ratio =1.0 (see figure 3.3A) the stimulus effectively was a luminance increment, for a luminance ratio = 0 it was a luminance decrement. When the luminance ratio approached 0.5 (see Fig.3.3C) the stimuli consisted of equiluminant changes in hue.

The exact value of the equiluminant point was determined by a minimum flicker criterion. Subjects were first shown the progression from flicker to minimum and back to flicker as the isoluminance ratio was altered to pass through the point of isoluminance. The procedure was then repeated twice with the subject for each colour axes and also for each size of the disc, indicating the luminance ratio at which minimum flicker was perceived.

[3] Luminance ratio is the ratio of the luminance of the stimulus divided by the sum of the luminance of the stimulus and the luminance of background. For example luminance of the background and stimulus is 25cd/m^2 then the luminance ratio = 25/25+25=1/2 =0.5

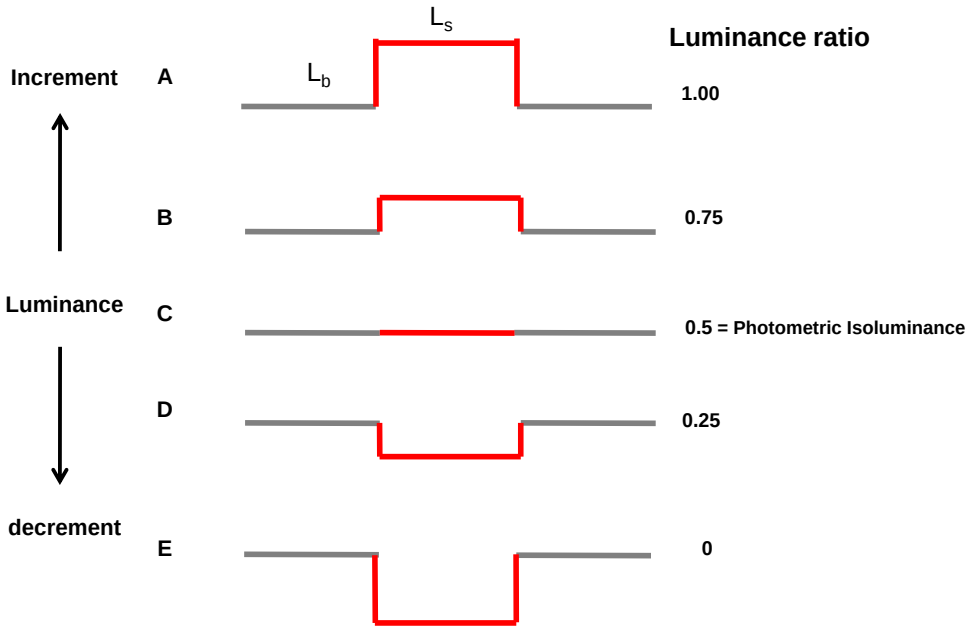

Figure 3.3 Luminance profiles of isoluminant (C) and non-isoluminant (A, B, D, and E) square wave stimuli. The numerical values represent the luminance ratio. Grey line (Lb) represents the background luminance and red lines (Ls) represent stimulus. At photometric isoluminance (0.5), luminance of the background is same as that of the stimulus.

3.2 COLOUR SPACE

Visual processing begins with the excitation of three cones. Since cone excitations are directly proportional to their quantal absorption rates, it is possible to understand the subsequent visual mechanisms that process the combination of cone signals. Luckily there is an agreement on currently available estimation of cone spectral sensitivities (Brainard, 1996). Similarly, we can justify the application of cone excitations to build up the colour space that clearly corresponds to the responses of subsequent visual processing. Two designs about the nature of retinal processing are widely applied in this context. Firstly, the cone excitations are usually expressed as contrast signals, so that

the information of further processing is relative rather than absolute. Secondly, the signals from the three types of cones are specified into three post-receptoral mechanisms; one is additive and other two are colour-opponent. Colour spaces that are based on first design are known as contrast spaces and those based on second one known as opponent modulation space.

An example of widely used opponent modulation space is MBDKL colour space. It was first introduced by Derrington, Kraukopf and Lennie (1984) based on ideas suggested by MacLeod and Boynton (1979). Figure 3.4 shows MBDKL colour space and illustrates how chromaticity varies with the angle of projection in the isoluminant plane (azimuth,ϕ), with illuminant C (x 0.310, y 0.316) at the centre of the diagram. Luminance varies with the angle of elevation from the isoluminant plane (elevation,θ) within the isoluminant plane, saturation increases horizontally from the centre to the edge of the isoluminant plane. Along the 0-180 axis S-cone excitation is nulled allowing the stimulation of the L and M cones only, and likewise, along the 90-270 axes L and M cone excitation is nulled resulting in stimulation of S cones only. The L/M cone axis, S/ (L+M) cone axis and luminance axis are perpendicular to each other in the colour space and these three axes are known as cardinal axes. Thus the stimuli were designed to stimulate the post-receptoral mechanisms. It should be noted, however, that the colours perceived along the red-green and blue-yellow cardinal chromatic axes do not correspond to red, green, blue and yellow colour categories especially in the case of the S/ (L+M) axis, which corresponds to a tritanopic confusion line rather than a red-green equilibrium line (DeValois et al., 1997).

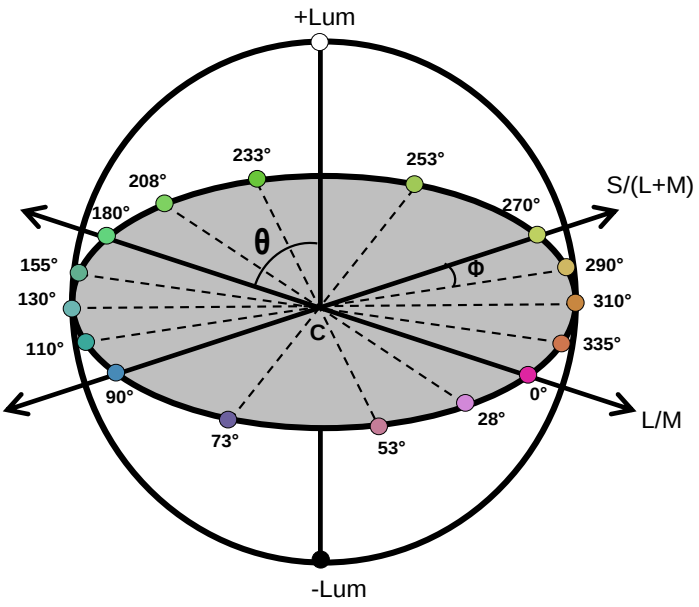

Figure 3.4 MBDKL colour space.

Stimuli were modulated along the sixteen chromatic axes (see figure 3.4), where the relative amounts of L, M and S cone excitations is varied. The relative amount of L, M and S cone excitations in terms of cone contrast were summarized in figure 3.5.

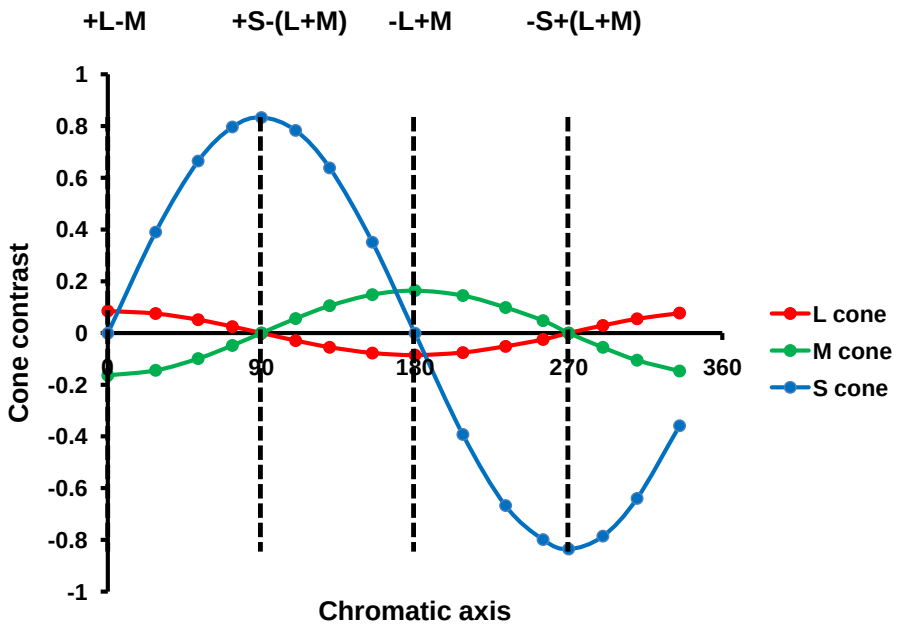

Figure 3.5 Relative cone contrasts of L, M and S cone contrasts of stimuli that were modulated along sixteen chromatic axes.

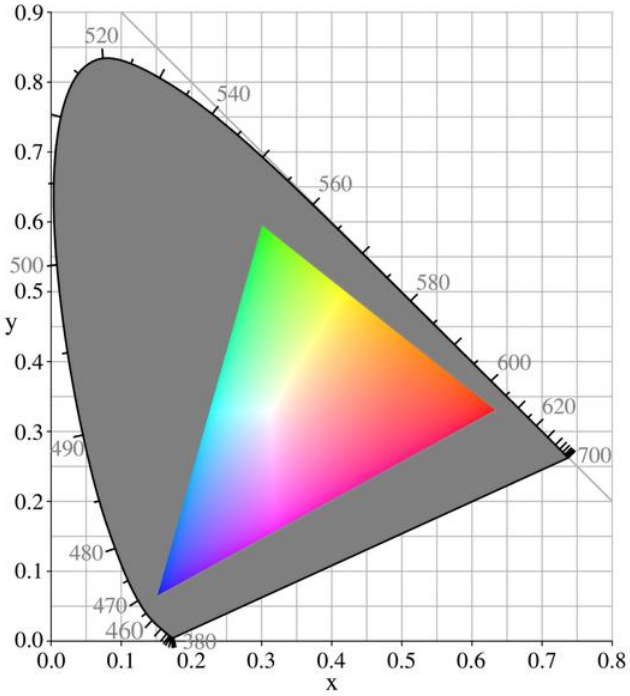

Figure 3.6 CIE chromaticity diagram showing the gamut of colours available on the average CRT monitor. Source: http://www.answers.com/topic/gamut-1.

The range of colours used in the experiments, lie within the gamut of colours attainable with the specific CRT phosphors as shown in the adapted version of the CIE chromaticity diagram in figure 3.6. The dome shape forms the spectrum locus and represents the boundary of physically realizable colour, and the triangle represents the range of colours achievable on the CRT monitor, with the corners of the triangle marking the co-ordinates of the red (0.622, 0.342), green (0.276, 0.610), and the blue (0.148, 0.068) phosphors. The CIE co-ordinates for each chromatic axis tested are shown in table 3.1.

3.3 CALIBRATION

Luminance is the term given to the amount of light per unit area emitted from a source of reflective surface and is measured in candelas per meter square

(cd/m^2). Radiometry is the measurement of the electro-magnetic energy and spectroradiometry specifies how radiance varies with wavelength. Photometry is the measurement of electromagnetic radiation that can be detected by human eye. The range of electromagnetic radiation that is detected by human eye is between 360-830nm. Stimulus luminance calibration was performed using PR-650 Spectrascan Spectra Colorimeter (Photo Research Inc., Chatsworth, Calif.). The diffraction grating in this spectroradiometer divides the emitted light into its constituent wavebands and measures the radiation of each wavelength with a suitable detector. Calibration of the stimulus luminance is necessary because the relationship between voltage and luminance is not linear. This process of calibration is known as gamma correction. CRTs use the function shown in equation 3.3 (Robson, 1999). The relationship between voltage and luminance for the three phosphors colours takes the form shown in figure 37.

$$\text{Luminance} = k\,(V-V_0)^{\gamma} \quad \text{----------} \qquad (3.3)$$

Where V = applied voltage, V_0 = brightness level, γ= 2.5, k = constant

Colour calibration was performed using a ColourCal (Cambridge Research Systems Ltd, Rochester, UK) and by doing this, the spectral distribution of the screen colour is measured. From this information the tri-stimulus values and the chromaticity coordinates can be calculated in turn.

The colour calibration was done as described by Parry et al (2006). The procedure consists of calibrating the monitor using ColourCal probe which was it-self calibrated against SpectrascanSpecta- Colorimeter.

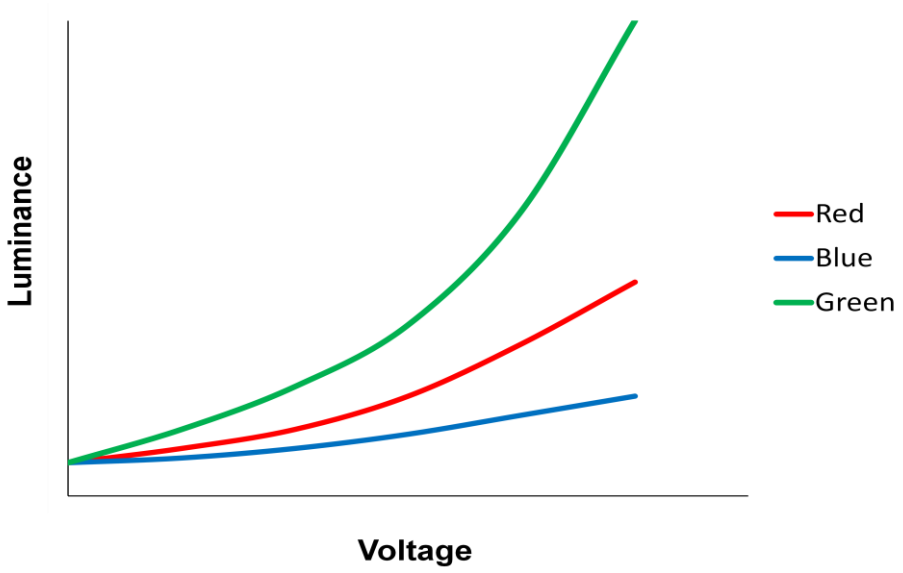

Figure 3.7 Relationship between luminance and voltage for RGB phosphors in CRT.

Correction factors (Cr, Cg, and Cb) were incorporated in the OptiCal software that compensate for inherent errors in sensitivity that the instrument has for red, green and blue CRT phosphors. These errors mean that following gamma correction input x, y and Y CIE (1931) values do not match to output measured by the PR-650 Spectrascan Spectra Colorimeter from the CRT. Product of correction factor and measured luminance gives corrected luminance. Once the initial gamma functions derived Cr, Cg and Cb were set to unity. The software then asked to display a CIE (1931) x, y, and Y stimulus of (0.31, 0.316, 12.5), and its actual chromaticity was measured with PR 650. The voltages of R, G and B guns were noted, and then the stimulus was then adjusted in x, y and Y directions until it was correct according to the PR650 Spectrascan spectra Colorimeter. Each original R, G, and B gun voltage was divided by the adjusted value, which gave new correction factors that were then employed in the final calibration. This method gives very high reliability within the range of stimuli used in this experiment, while still permitting rapid calibration. The computer

monitor was calibrated before the experiments commenced and was rechecked in regular intervals throughout the series of experiments.

3.4 VEP ACQUISITION

3.4.1 Recording equipment:

A CED 1401 ‘micro’ signal averager and accompanying signal software (Cambridge Electronic Design, Cambridge, United Kingdom) were used to average the VEPs. The arrangement of the recording equipment is as shown in figure 3.8, in which the evoked activity recorded by each active electrode is fed through separate channels into the amplifier and then into the signal averager. The stimulus is generated on a separate monitor using custom built software. Stimulus onset recording is triggered by transistor-transistor logic (TTL) pulse generated by the onset of stimulus signal from the visual stimulus graphics (VSG) graphics card that is connected to the computer. The signals are collected in a computer itself in which individual waveforms and waveform average can be monitored using the signal software. A 1902 amplifier (Cambridge Electronic Design , Cambridge, UK) band width was 0.5-30Hz. Sampling rate was 250Hz over 1sec. The low pass filter was set well below 1/5 of the digitisation rate (167 samples per second) and the sampling rate was over eight times the highest frequency of interest in-order to avoid temporal aliasing. The amplifiers were electrically isolated from the patient. Automatic artefact rejection was used on signals exceeding 90% of the analogue digital range (e.g. signals from blinks or eye movements) with amplifiers returning to the baseline following artifactual signals. Minimum of 128 sweeps were

averaged. Overly long recording times were avoided and recording sessions were limited to two hours.

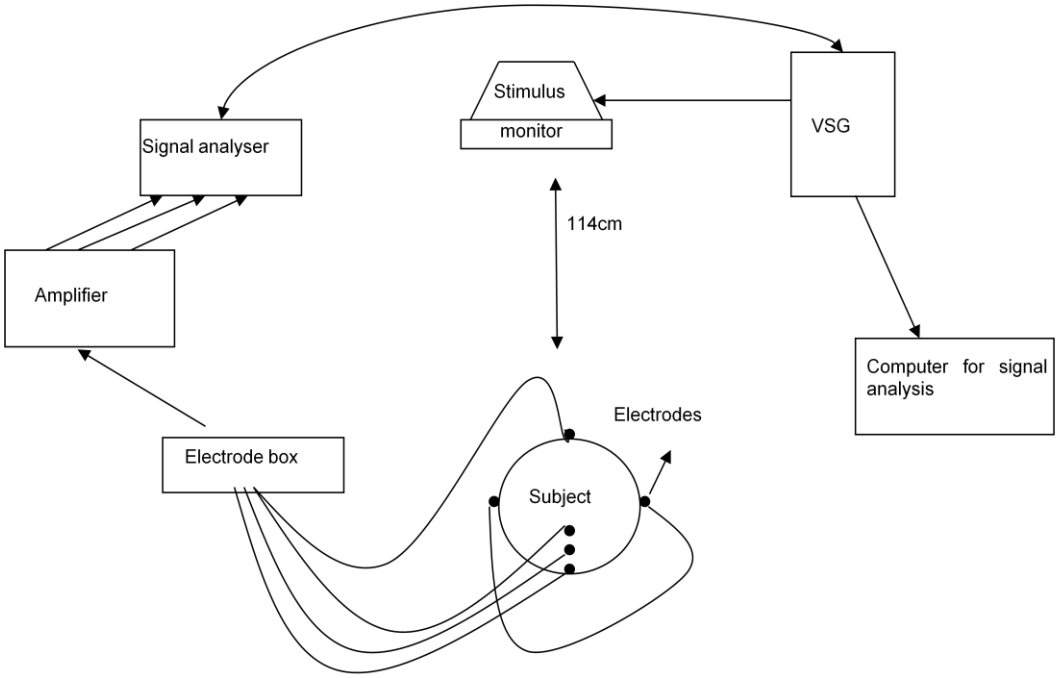

Figure 3.8 VEP recording equipment.

3.4.2 Electrode placement

Silver-silver chloride electrodes, 6mm in diameter, were attached to the scalp and ears with Ten20 conductive paste and injected with electrode gel. Before attachment of the electrodes the skin was prepared by cleaning with Omniprep exfoliating fluid and iso-prop to reduce the resistance between the electrodes and the skin. Electrode impedances were maintained below 8kΩ. VEPs were recorded from three active electrodes, placed on;

1. The mid-occipital (Oz) (located above the inion by 10% of the distance between the nasion and the inion).

2. Mid-parietal (Pz) site (located above the inion by 20% of the distance between the nasion and the inion).

3. Half way between Oz and Pz (POz) (located above the inion by 30% of the distance between the nasion and the inion).

The distribution of electrode locations was based on the 10/20 system (Jasper, 1957) set out as shown in Figure 3.9. The ground electrode was placed on the forehead and reference electrodes were linked to the ears.

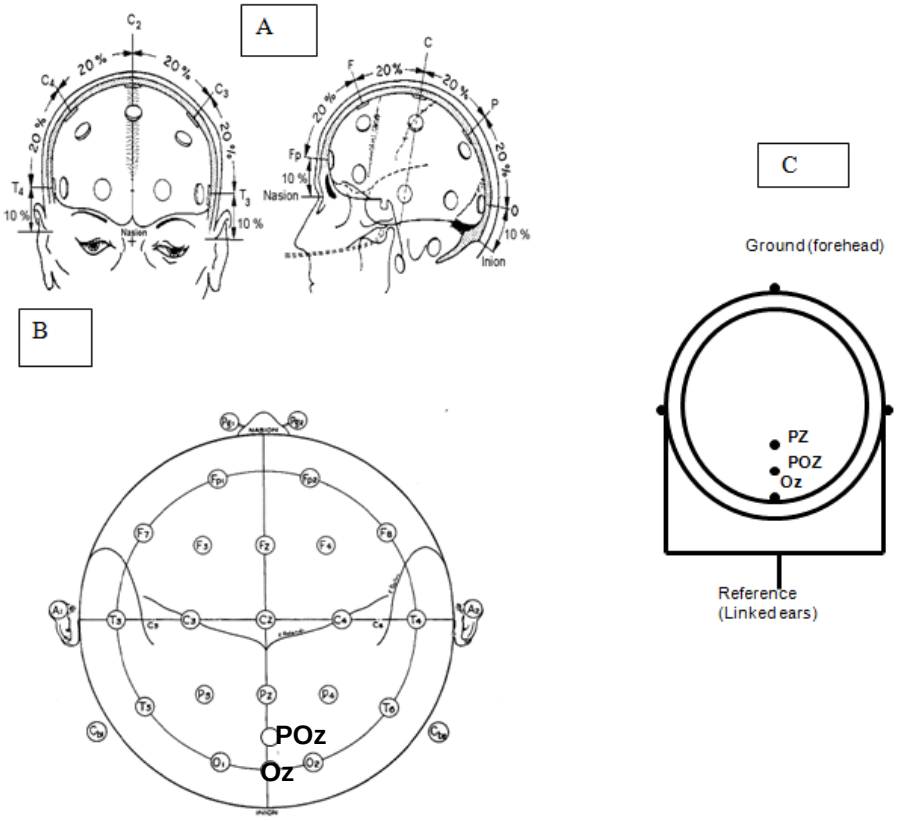

Figure 3.9 (A) and (B) showing 10-20 electrode arrangement. Picture adapted from Jasper (1957). C) The electrode array used in VEP recording.

Source: http://www.egi.com/summer.school/electrode.pos.PL.pdf

3.4.3 VEP components and analysis.

The VEP elicited by an isoluminat chromatic spot stimulus is illustrated by figure 2.6. The VEP waveform consists of five components which are as follows;

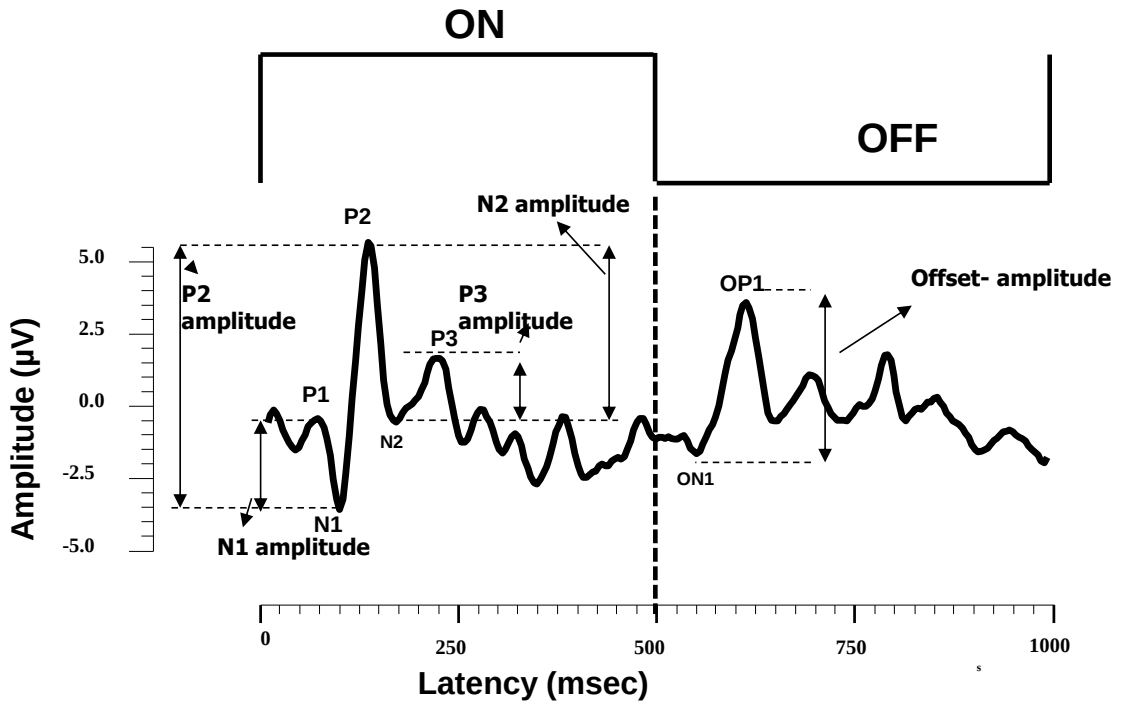

Figure 3.10 an example of the VEP waveform elicited by an isoluminant chromatic spot stimulus. The stimulus is presented in on-off mode. All components amplitudes were measured from the wave peak or trough to the proceeding trough or peak.

1. First early positive component (P1) with a latency to peak between 55-80 ms.

2. First early negative component (N1) with latency at about 90-105ms.

3. The large second positive component (P2) with a latency to peak between 145- 170ms.

4. The second negative component (N2) with a latency to peak between 180-225ms.

5. The third positive component (P3) that has latency at about 245-275ms.

6. Offset response arise at about 60-140ms.

All the VEP signals were analysed using Signal application software (Cambridge Electronic Design, UK).

ERG METHODS

3.5 ERG STIMULI

3.5.1 Stimulus configuration

We used different stimulus configurations for the ERG recordings in two different experiments. In chapter 7, stimuli consist of a circular homogeneous disc that is centred on the fovea (see figure 3.11). The stimulus configuration, varied for the two experiments, was described in detail in each experimental chapter. Stimulus was presented on a uniform grey background with mean luminance of 66 candelas/meter^2. Fixation cross was placed in the middle of the disc.

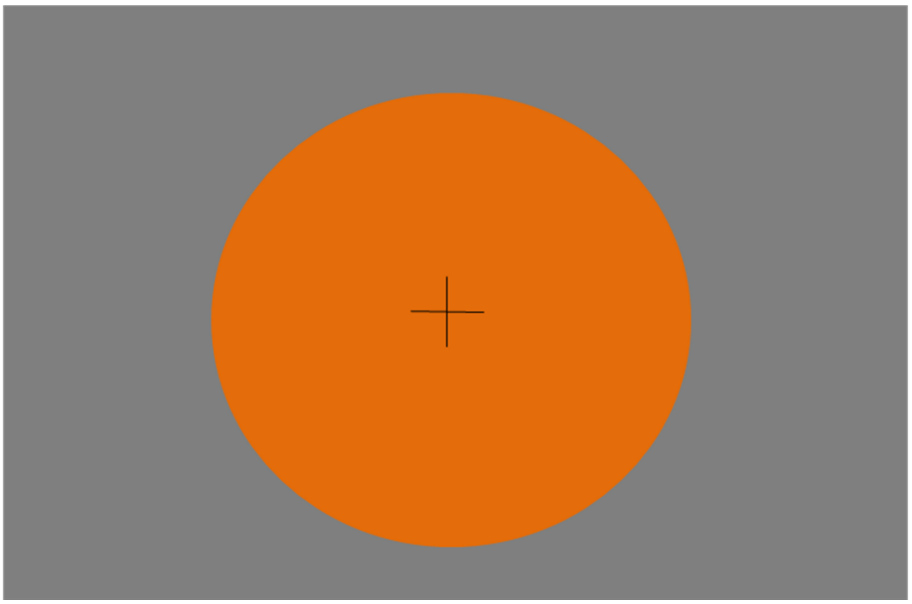

Figure 3.11 Stimulus configuration used to record the ERGs. Note that the background luminance is 66cd/m^2 silent substitution stimulus is flickered at various temporal frequencies to record the ERG responses. Stimulus was subtending 70° at 10cm distance.

In Chapter 8, stimulus configurations could be grouped into two main types: (1) Circular stimuli of different angular substance which increased in 10° steps from 10° up to 70° in diameter, and (2) annular stimuli with a 70° outer diameter but gradually ablated from the centre in 10° steps (see figure 3.12). These stimuli were presented in a single sequence of 15 steps which included blank trials at the beginning and the end. Modulation depth and phase were chosen in such a way that either L- or M-cones were stimulated and cone contrasts were equalized for each stimulus condition at 20%.

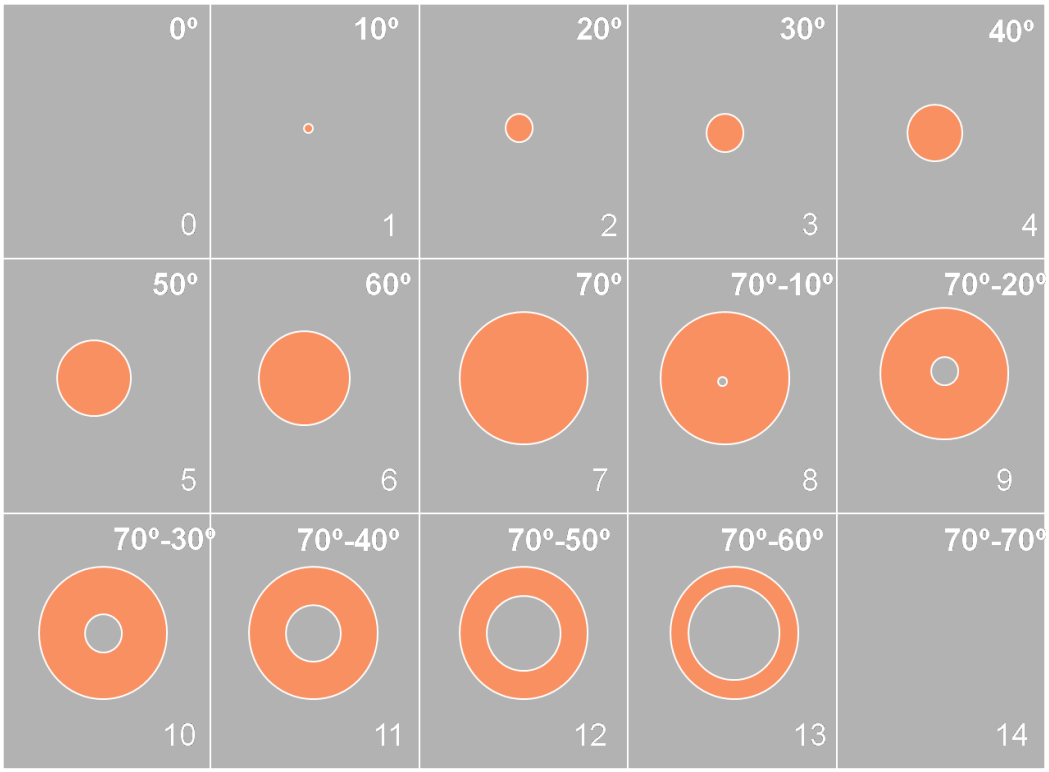

Figure 3.12 A representation of 15 different spatial configurations used for the L- and M-cone isolating stimuli that were used to elicit ERGs. Condition 1-7 comprise of circular stimuli of different angular subtense which increase in 10° steps to 70° in diameter. Conditions 8-13 are annular stimuli with 70° outer diameters the centres of which are gradually ablated in 10° steps. Condition 0 and 14 contain no stimuli. The background was uniform grey with luminance of 66cd/m^2.

3.5.2 Silent substitution

Silent substitution method was used to derive different stimulus conditions which isolated the responses of one or more photoreceptors. The stimuli comprised temporal exchanges between two colours, the chromaticities and luminance of which were chosen so that some photoreceptor types did not respond to the exchange and are therefore 'silenced' (see: Estevez & Spekreijse, 1974; 1982; Kremers, 2003). All stimuli were presented on a Sony GDM500 CRT monitor (refresh rate = 120Hz) (Sony Corporation, Tokyo, Japan) controlled by a VSG 2/4 graphics card. The time and space averaged luminance of the monitor was 66cd/m2. Spectral characteristics of the CRT phosphors were calibrated using a PR650 spectrascan spectroradiometer and presented as shown in figure 3.13.

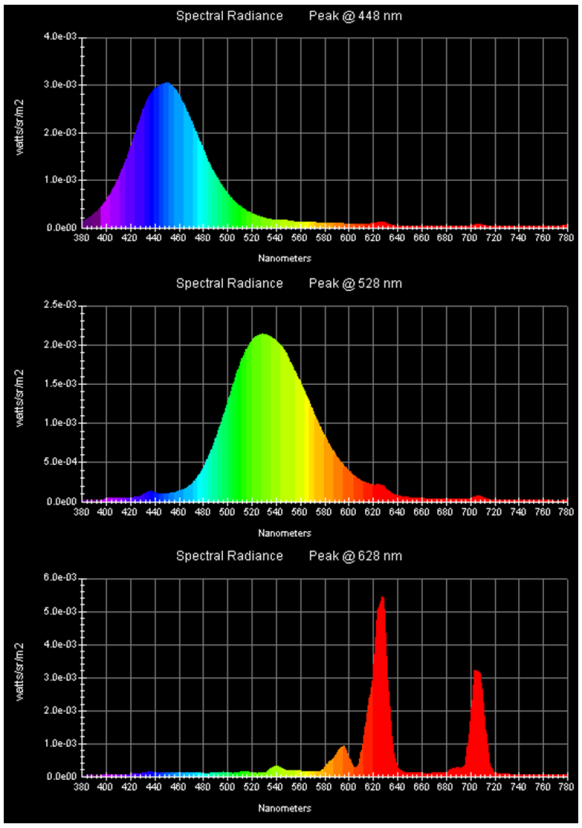

Figure 3.13 Spectral characteristics of blue, green and red phosphor calculated from PR 650 Spectrascan spectra radiometer.

The stimuli that were employed for ERG recordings actually constituted *double* silent substitutions. To isolate the M cone responses, L cones along with rods were silenced and to isolate the L-cone responses, M cones along with rods were silenced. In order to obtain silent substitution stimuli for L- and M-cones, their excitations were obtained by multiplying emission spectra of phosphors with psychophysically calculated cone fundamentals (Stockman et al., 1993a) and integrating over a range of wavelengths. For example, L cone excitation by red phosphor ($E_{L,R}$) is measured using the following equation 3.4:

$$E_{L,R}(t) = F_R . L_R(t) . \int_{380}^{780} IR(\lambda) . A_L(\lambda) . d\lambda \quad \text{----------} \quad (3.4)$$

Where, L_R = is the luminance red phosphor, $E_{L,R}$ = L cone excitation by red phosphor, $I_R(\lambda)$ = emission spectrum of red phosphor at unit luminance, $A_L(\lambda)$ = L cone fundamental, F_R= conversion factor for red phosphor relating the photometric measurements to the cone fundamentals. The total excitation of L cones is the sum of the excitations caused by each phosphor. The modulation of cone excitation can be calculated in terms of Michelson's cone contrast which is given by the equation 3.5:

$$CC = \frac{E_{max} - E_{min}}{E_{max} + E_{min}} \quad \text{----------} \quad (3.5)$$

Where, E_{max} = Maximal excitation, E_{min} = Minimal excitation. In all conditions the rod responses were kept silent.

The mean quantal catches and corresponding retinal illumination for various wavelengths that were used as pairs to achieve the silent substitution were summarised in table 3.2

Wavelength	420nm	535nm	566nm	500nm
Quantal catches	13180.99	21472.79	27239.77	21839.22
Retinal illumination in Trolands	2192.85	3003.60	3632.43	3285.17

Table 3.2 summarizes the average quantal catches and retinal illumination for wavelengths of light used to achieve the silent substitution.

Modulation depth and phase were chosen in such a way that either L- or M-cones were stimulated and cone contrasts were equalized for each stimulus condition at 20%. The rods were not stimulated in any of these conditions. The L and M cone isolating stimuli were presented at various flickering rates.

In order to obtain substitutions that also silenced rod photoreceptors we used the scotopic spectral sensitivity function V'(λ) (Wyszecki and Stiles, 1982) to compute wavelength pairings that elicited no modulation of rod excitation. Preference was given to silencing the rods rather than the S-cones as there is little change in S-cone flicker sensitivity to the stimuli that modulate L and M cones (Cao et al., 2006).

3.6 VALIDATION OF ISOLATION OF L AND M CONE RESPONSES

The isolation of L and M cone stimuli were validated for all the conditions in additional control experiments on two dichromats (one protanope and one deuteranope). From the figure 3.14, it can be observed that protanope has very small L cone amplitudes for L cone isolating stimuli and in contrast, deuteranope has very small M cone amplitudes for M cone isolating condition. This data suggests that isolating conditions revealed minimal cross contamination that may have resulted from any errors in calculations or calibrations of cone isolating stimuli. If there is any contamination of the responses, we would expect the response from M cones for L cone isolating conditions in a protanope and response from L cones for M cone isolating stimulus for a deuteranope. However, this was not the case.

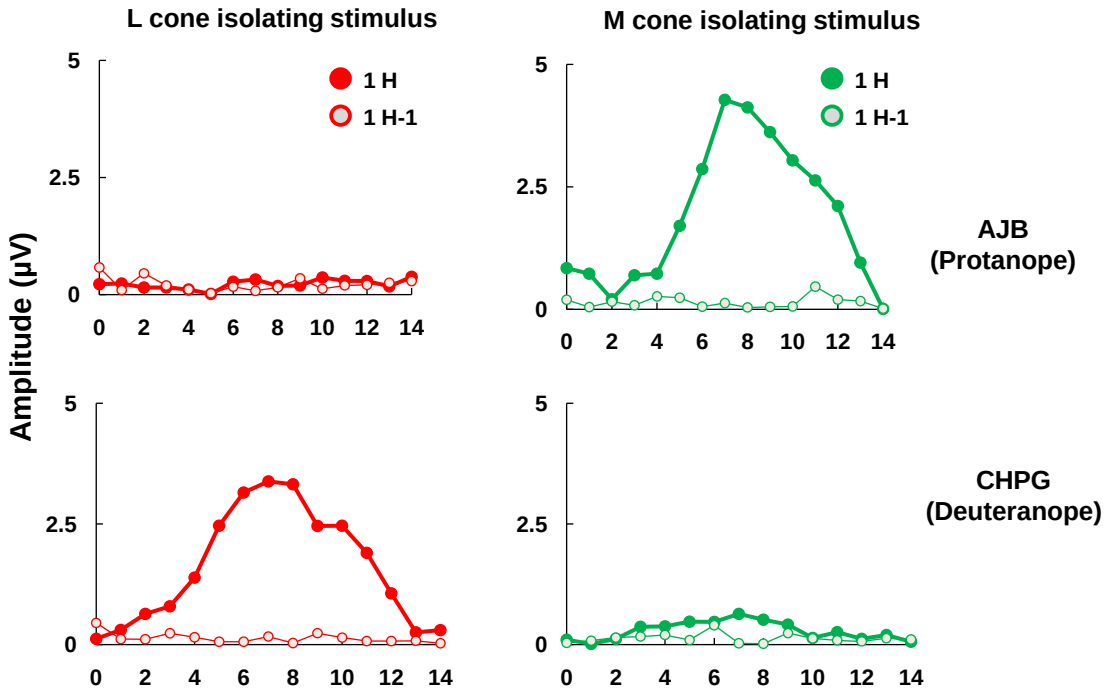

Figure 3.14 L and M cone ERG magnitudes in a protanope (see the first row plots) and deuteranope (see the second row plots) as function of retinal regions stimulated at 30Hz. Filled circles represent the first harmonic (1H) responses and open circles represent the measure of noise (1H-1). It is obvious from the figure that protanope has poor L cone response and deuteranope has poor M cone response.

Additional control experiment was performed on a single tritanopic subject (DMCK) to see the intrusion of S cones on the L and M cone isolating conditions. In this experiment, L and M cone responses were compared in two conditions at 30Hz and at 12Hz. In first condition, L and M cone responses were isolated by silencing the rod photoreceptors. In second condition, L and M cone responses were isolated by silencing the S cones. Results are plotted in figure 3.15. From the plots, we can observe that the L and M cone response amplitudes change as function of stimulus condition at 30Hz and at 12Hz. However, it is important to note that for a given stimulus condition, amplitudes show a very little or no variation, whether the ERG is recorded by silencing the rods or silencing the S cones.

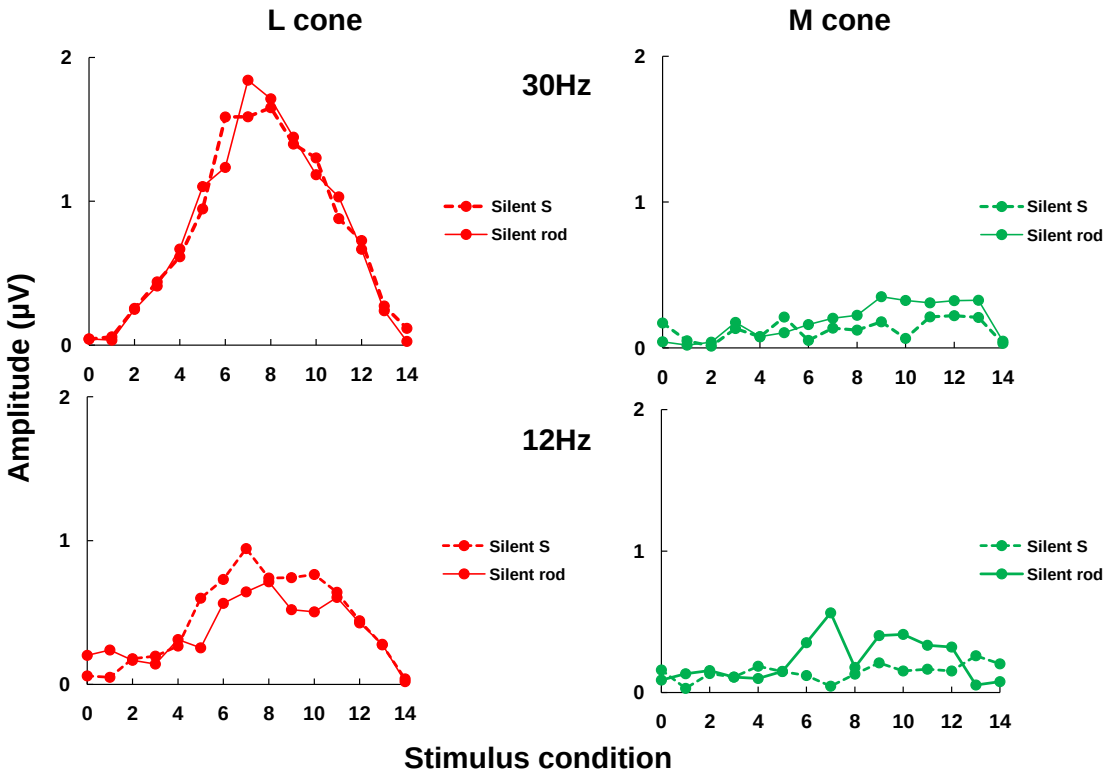

Figure 3.15 L and M cone response amplitudes in a subject as function of retinal regions stimulated. Dashed line represents the responses when S cones are silenced and straight line data represent responses when rod photoreceptors are silenced. Upper traces represent ERG responses at 30Hz and lower traces represent ERG responses at 12Hz.

If there is any cross contamination, the difference in responses could be expected between the two conditions but that was not the case. This control experiment confirms that S cone's contribution is very small to the ERG responses.

3.7 ELECTRODE PLACEMENT AND ERG RECORDING

The electrode placement for ERG recording is as shown in figure 3.16. Active electrode **(**DTL fibre electrode) is mounted close to the corneal limbus. A silver-silver chloride reference electrode was placed at the outer canthus and a ground electrode was placed on the forehead using a Ten 20 conductive paste. Before attaching reference and ground electrode the skin was prepared by cleaning with Omniprep exfoliating fluid isoprep to reduce the resistance between skin and electrodes. Electrode impedances were kept below 5kΩ. Recording equipment and signal acquisition is similar to that used for VEP recordings.

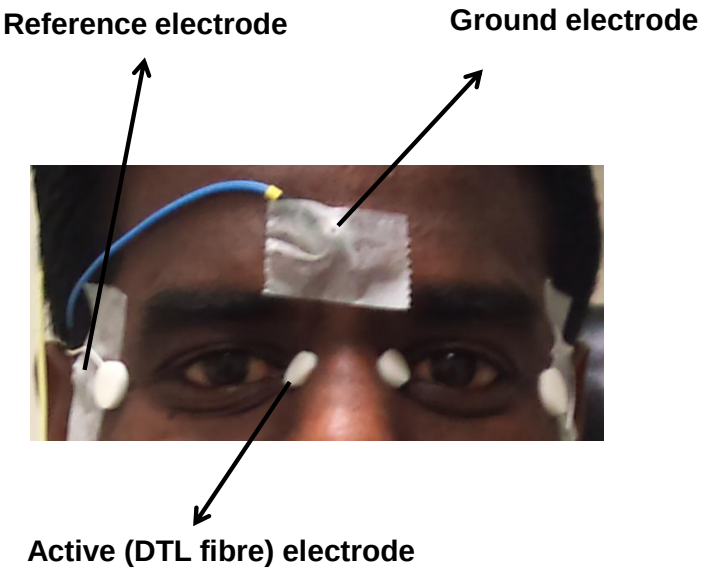

Figure 3.16 A subject shown with electrodes for ERG recording. Note that DTL fibre electrode was used as active electrode for the ERG recordings.

The ERG signals were amplified using a Grass 15A94 amplifier (Astro-Med, Rhode Island, USA) with band pass frequency of 3-100Hz. The signals were sampled at a rate of 1024 Hz over a period of 4 seconds and averaged responses were based upon at least 20 repetitions. Fourier components were extracted from the response using a CED 1401 smart interface (Cambridge

Electronic Design, Cambridge, UK). During recording observers' pupils were dilated with 1% Tropicamide and they viewed the stimuli monocularly from a distance of 10 cm and both a chin and head rest were used. Fixation was maintained on a centrally placed black cross which subtended 2°. Informed consent was received from all the subjects prior to the commencement of the experiments.

3.8 FOURIER ANALYSIS

ERG data is Fourier analyzed as shown in figure 3.17. The left side plot represents the average of 20 ERG responses of a subject. Stimulus was L cone isolating and stimulation rate is 30Hz. Right plot represents the Fourier analysis of the corresponding ERG. First and second harmonic components occurred at 30Hz and 60Hz respectively (see the arrows in the figure). We can also appreciate that the first harmonic (1H) has larger amplitude than the second harmonic (2H). Noise for 1H and 2H was measured at 1H-1Hz (29Hz in below example) and 2H-1Hz (59Hz in below example) respectively.

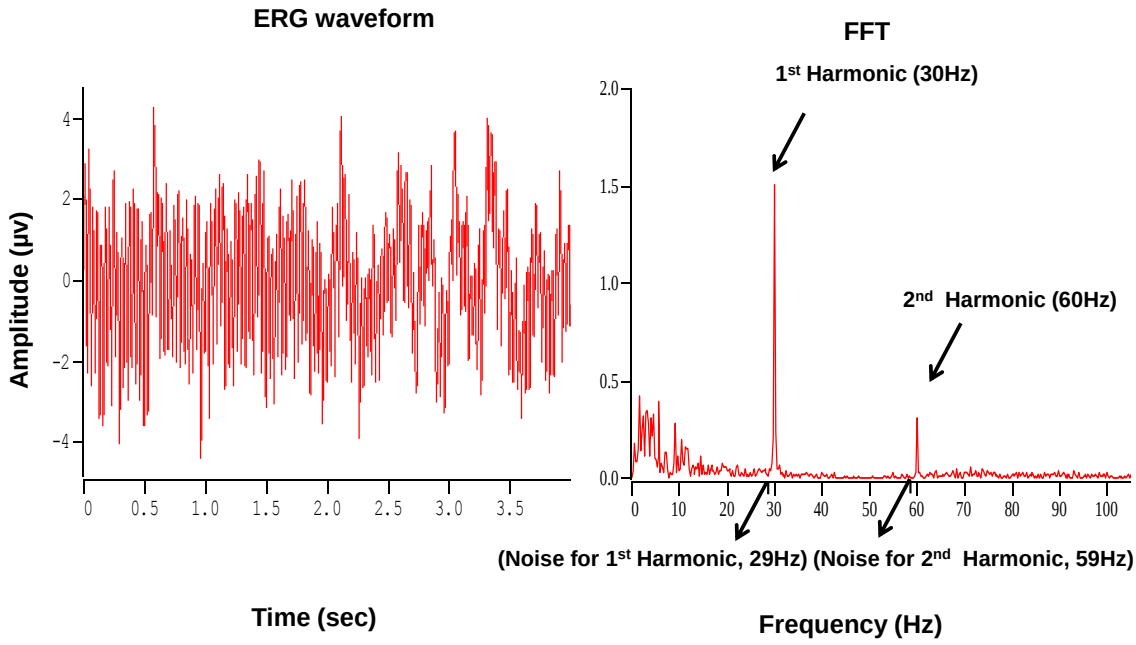

Figure 3.17 ERG waveform (left side) for L cone isolating stimuli (16 samples). Corresponding Fourier components (right side) i.e 1st t harmonic and 2nd harmonic (arrow marks) were marked respectively.

CHAPTER - 4 EFFECT OF LUMINANCE RATIO ON CHROMATIC SPOT VEPS

4.1 INTRODUCTION

Colour forms a distinct sub-speciality within vision and this fact most probably accounts for the success of many studies in eliciting chromatic VEPs from human occipital cortex (Murray et al., 1986; Berninger et al., 1989; Korth et al., 1993; Rabin and Adams, 1992; Rabin et al., 1994; McKeefry et al., 1996; Kulikowski et al., 1997; Suttle and Harding, 1999a; Porciatti and Sartucci, 1999). The main aspect of these studies is the use of isoluminant chromatic patterned stimuli which typically take the form of low spatial frequency sinusoidal or square wave gratings (Kulikowski, 1991b). This is mainly because checker boards do not provide a good means of separation between VEPs elicited by luminance and chromatic modulated stimuli (Regan and Spekreijse, 1974). Chromatic grating stimuli presented in onset-offset mode, elicit VEPs dominated by a negative component with latency at about 120-220ms, depending on the stimulus conditions (Murray et al., 1986; Rabin et al., 1994; Porciatti and Sartucci, 1999). Chromatic VEPs obtained under favourably selective conditions have shown sustained properties and reveal low pass spatial and temporal tuning characteristics (Previc, 1986; Valberg and Rudvin, 1997). These properties replicate known properties of the chromatic system for which the P-cellular system provides the neural substrate. On the other hand, luminance contrast stimuli generate responses dominated by components with similar latency to the chromatic response but with opposite polarity (Murray et al., 1986). Studied have also shown that VEP response was always dominated

by a chromatic component, when used with a mixture of chromatic and achromatic contrast (Crognale et al., 1993; Rabin et al., 1994).

In comparison to chromatic VEPs elicited by gratings, relatively few studies have used isoluminant spot stimuli to elicit the chromatic VEPs (Krauskopf, 1973; Paulus et al., 1984; Paulus et al., 1986; Valberg and Rudvin, 1997). Arguably spot stimuli allow more selective activation of chromatic mechanisms because they are able to stimulate efficiently cells that are colour opponent, but not spatially opponent. Spot stimuli have an added advantage that they are less vulnerable to the effects of chromatic aberrations because of fewer edges. Studies have also shown that the VEPs elicited by pattern stimulus differ in many aspects from those obtained with homogeneous light stimuli (Spekreijse et al., 1977). Pattern VEPs may contain many components which relate to the luminance changes occurring in the stimulus than to spatial contrast as such. For instance, CII (P120) is the clearest component which one can associate with the changes in spatial contrast, especially around sharp contours. If this is the case then the VEPs elicited by isoluminant chromatic gratings elicit different VEPs to that of Isoluminant chromatic homogenous stimuli. VEPs elicited by isoluminant spot stimuli have a prominent negativity at 87ms (N87), which is reduced in amplitude with the introduction of luminance increments or decrements. This factor was taken as evidence of chromatic specificity (Paulus et al., 1984) and subsequent studies supported this view (Valberg and Rudvin, 1997). The N87 component obtained with spot stimuli occurs much earlier than the negativity generated by isoluminant grating stimuli suggesting that it may reflect the activity of neurons in the P-cellular recipient layer of V1 (Paulus et al., 1984). Nevertheless, stimulus contrast determines the relative contributions from M and P- cellular mechanisms (Valberg and Rudvin, 1997). Adding to this,

a large positivity at 100-140ms is observed with spot stimuli, which is not observed in chromatic VEPs elicited by isoluminant grating stimuli. The differences between chromatic VEPs elicited by grating and spot stimuli indicate that different neural populations in chromatic processing are activated by the two stimulus types. This view is also supported by single unit study of neurons in visual cortex (Johnson et al., 2001). According to them, colour-luminance cells in Primary visual cortex are responsible for chromatic processing that is different from the cells that give preferential response to colour, as they show evidence of chromatic opponency, often demonstrate a high degree of orientation selectivity, and have spatial tuning to both colour and luminance. Colour-luminance neurons may respond to cues for form, like boundaries or features, and they may take signals from colour or black and white as needed to define the form cue. They may also provide the needed signals for colour contrast induction because they respond at colour boundaries, but not in the interior of colours regions, because of their spatial selectivity. If this is the case, then colour-luminance cells responds better to sinusoidal grating stimuli than homogeneous isoluminant chromatic spot stimuli because of the orientation cues available from the boundaries of the red and green gratings and also form cues available from the boundaries between the red- green gratings. However, isoluminant chromatic spot stimuli does not have any cues within the stimulus, may mainly activate colour preferring neurons.

4.2 RATIONALE

The effect of luminance contrast on chromatic VEPs elicited by sinusoidal gratings and chromatic spots have been studied previously (Murray et al., 1986; Paulus et al., 1984; Valberg and Rudvin, 1997; Kulikowski, 1991a). These studies have demonstrated that the chromatic activity is maximum at isoluminance and that the morphology of the VEPs change as the luminance contrast content is added to the chromatic stimuli. However, very few studies have investigated the morphology of the VEPs and their components as a function of luminance and chromatic contrast along the different cardinal axes using spot stimuli. So we would like to investigate the following questions using spot stimuli.

1) Are there any morphological differences for chromatic spot VEPs as function of luminance contrast using the same paradigm?
2) Does the luminance contrast and chromatic contrast have different effects on different components of VEPs along the +L-M, -L+M, +S-(L+M) and –S+(L+M) cardinal axes?
3) If different neuronal population is involved in the generation of responses to isoluminant chromatic spot stimuli to that of isoluminant sinusoidal gratings, then the VEPs elicited by chromatic spot stimuli reflect these differences to that of VEPs elicited by sinusoidal grating stimuli?

4.3 METHODS

Full details of the VEP recording procedure are presented in section 3.4. The general stimulus structure is presented in section 3.1. Stimuli were presented at

nine luminance ratios (1.0, 0.8, 0.6, isoluminance+0.02, isoluminance point, isoluminance -0.02, 0.4, 0.2 and 0). The isoluminance point for each chromatic axis was determined subjectively using heterochromatic flicker photometry. VEP responses were elicited along the +L-M, -L+M, +S-(L+M) and –S+(L+M) cardinal axes. The Stimuli subtended 2 degrees at the fovea. For each luminance ratio, VEPs were recorded from Oz. Four subjects, ranging age from 28-42 years, were used. All subjects had best corrected visual acuities of 6/6 or better and all of them were colour normal on Farnsworth Munsell 100 hue colour vision test.

4.4 RESULTS

Figure 4.1, 4.2 and 4.3 shows the group averaged chromatic on-off VEPs for the nine luminance ratios along the +L-M, -L+M, +S-(L+M) cardinal axes respectively. Examination of the data shows that as we change the luminance contrast content there is an effect on the morphology of the VEPs. As the stimulus approaches isoluminance (0.5), the morphology of the VEPs changes dramatically. The N1 component for instance, has varying degree of prominence depending upon the luminance contrast content and it is almost extinguished for luminance ratios of 0 and 1 (i.e. luminance contrast stimuli). The P2 component on the other hand shows maximum amplitude for luminance ratio of 0 and 1. For other luminance ratios P2 amplitude reduces gradually and reaches its minima at isoluminance point. This trend is noticed for the three chromatic axes we studied. Other differences occur in the morphology of the offset response, which is minimal at isoluminance and becomes increasingly well-defined as luminance contrast is introduced to the stimulus. The clearest

component for the luminance contrast stimuli (high luminance ratios of 0 and 1) is the off-set response, a Positive-Negative-Positive complex (see figures 4.4, 4.5 and 4.6), the negativity of which occurs approximately 135ms after onset. The Positive-Negative-Positive (P-N-P) complex for offset response was obvious at higher luminance ratios (0 and 1) and diminished when the stimulus approaches the isoluminance.

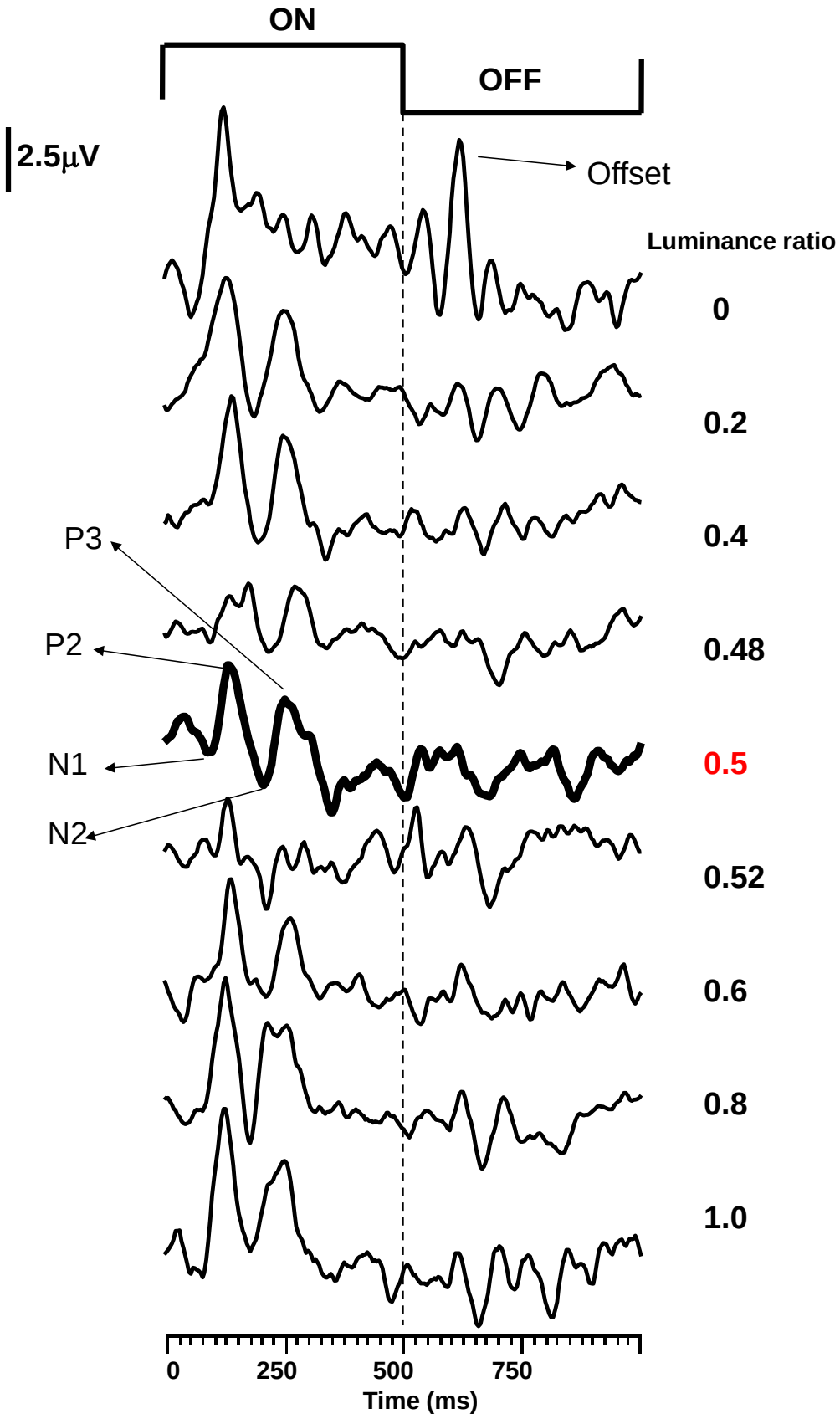

Figure 4.1 Group averaged chromatic onset VEPs for the nine luminance ratios along the +L-M cardinal axes respectively.

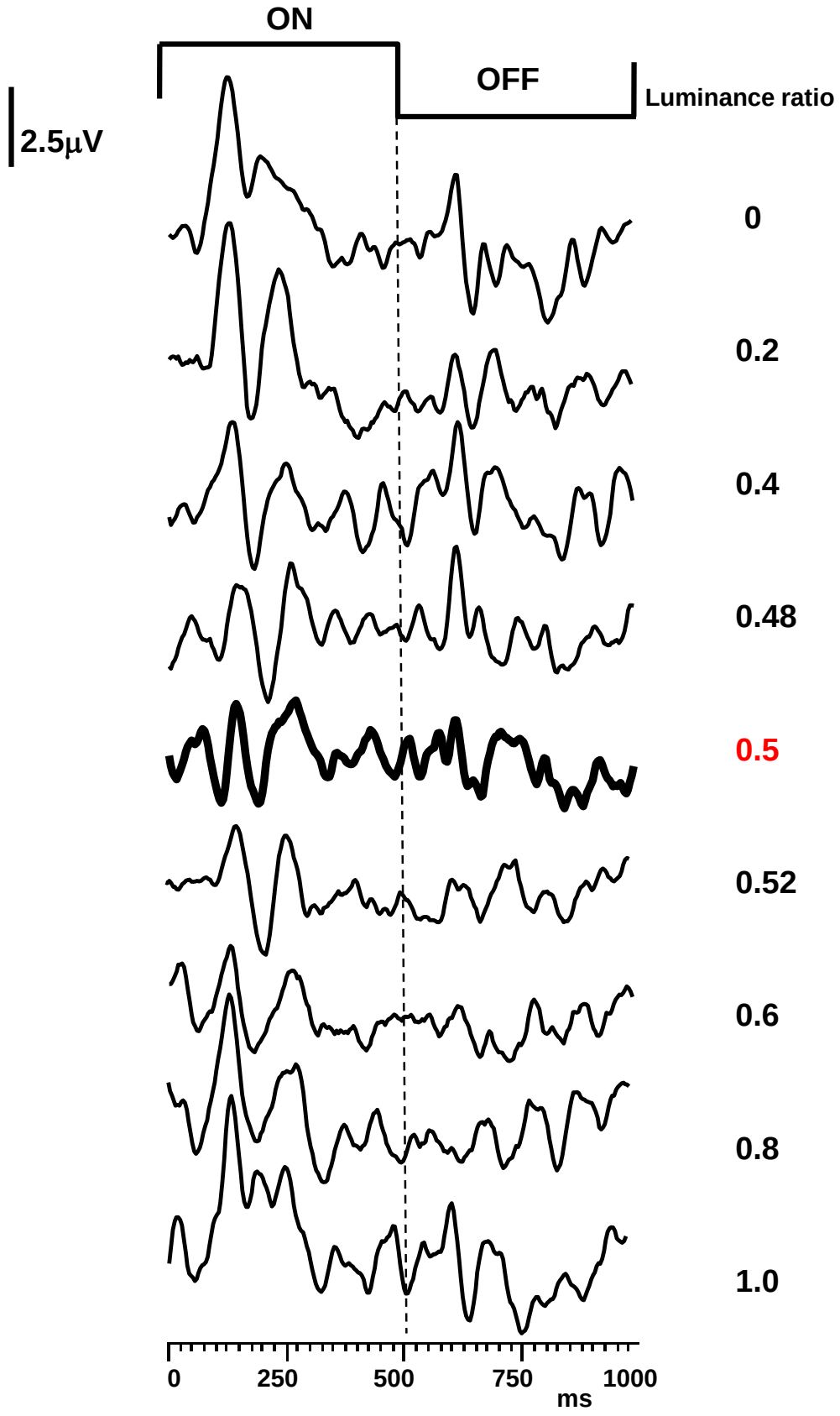

Figure 4.2 Group averaged chromatic onset VEPs for the nine luminance ratios along the –L+M cardinal axes respectively.

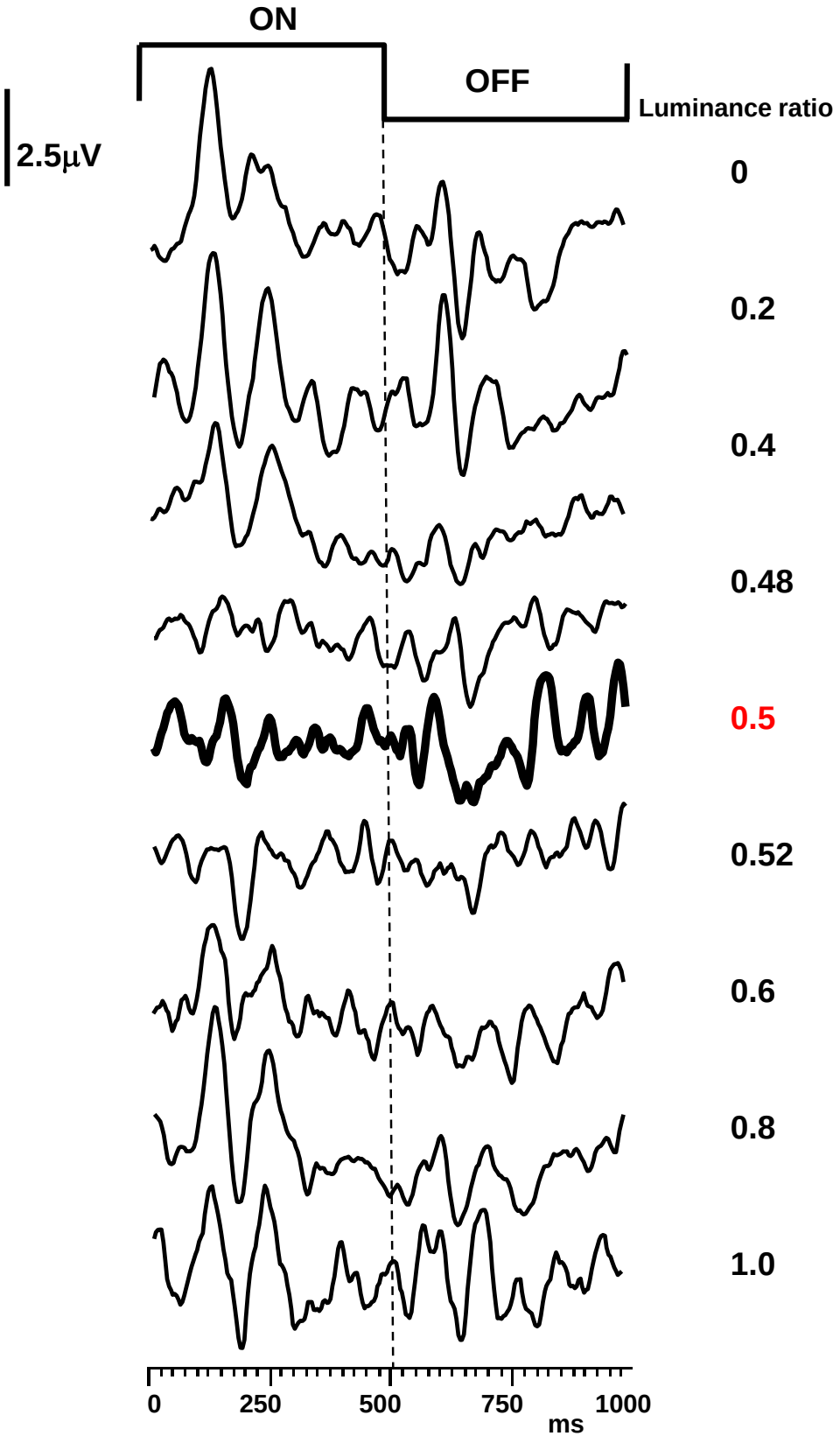

Figure 4.3 Group averaged chromatic onset VEPs for the nine luminance ratios along the S–(L+M) cardinal axes respectively.

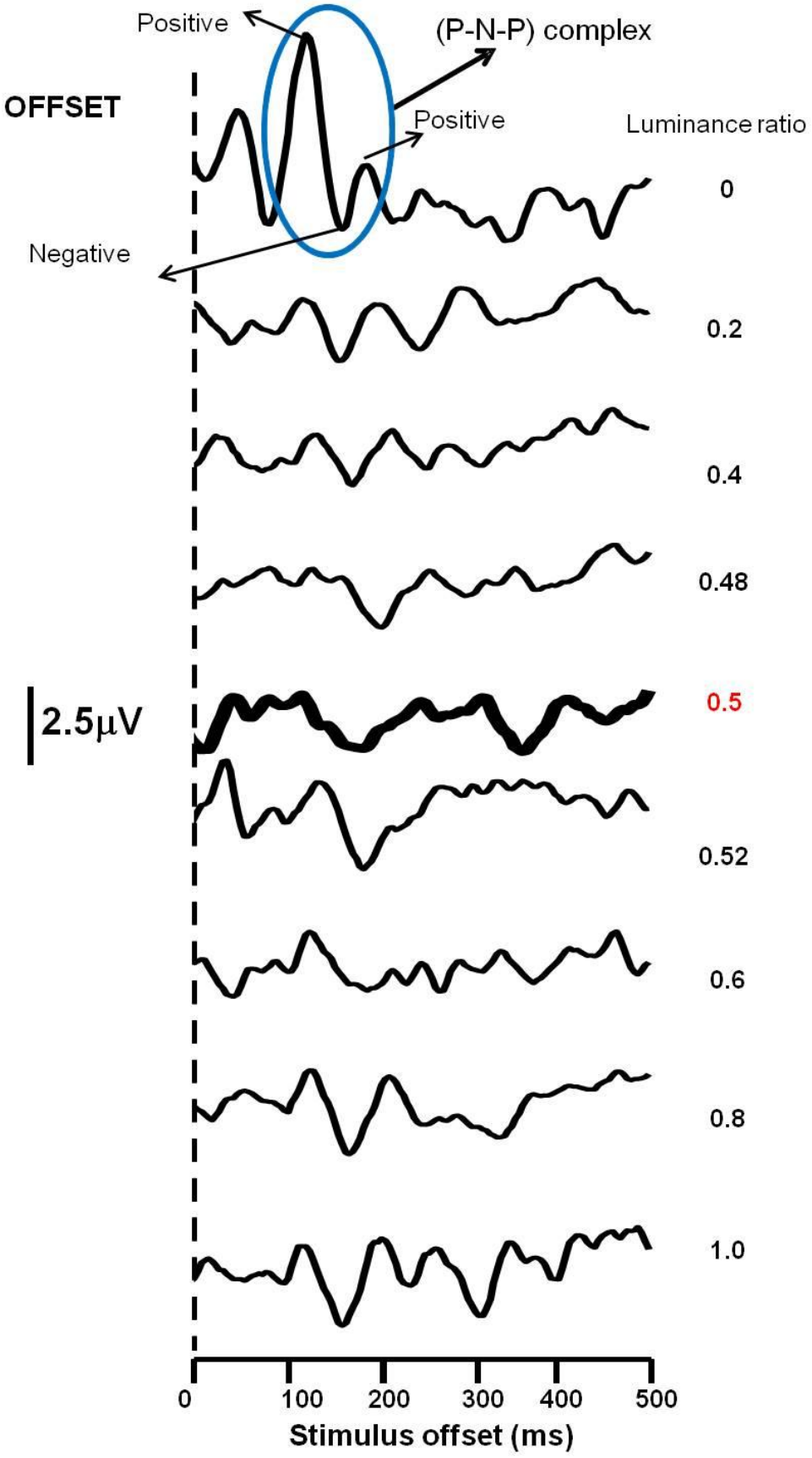

Figure 4.4 Group averaged chromatic off-set responses for the nine luminance ratios along the +L-M cardinal axes respectively.

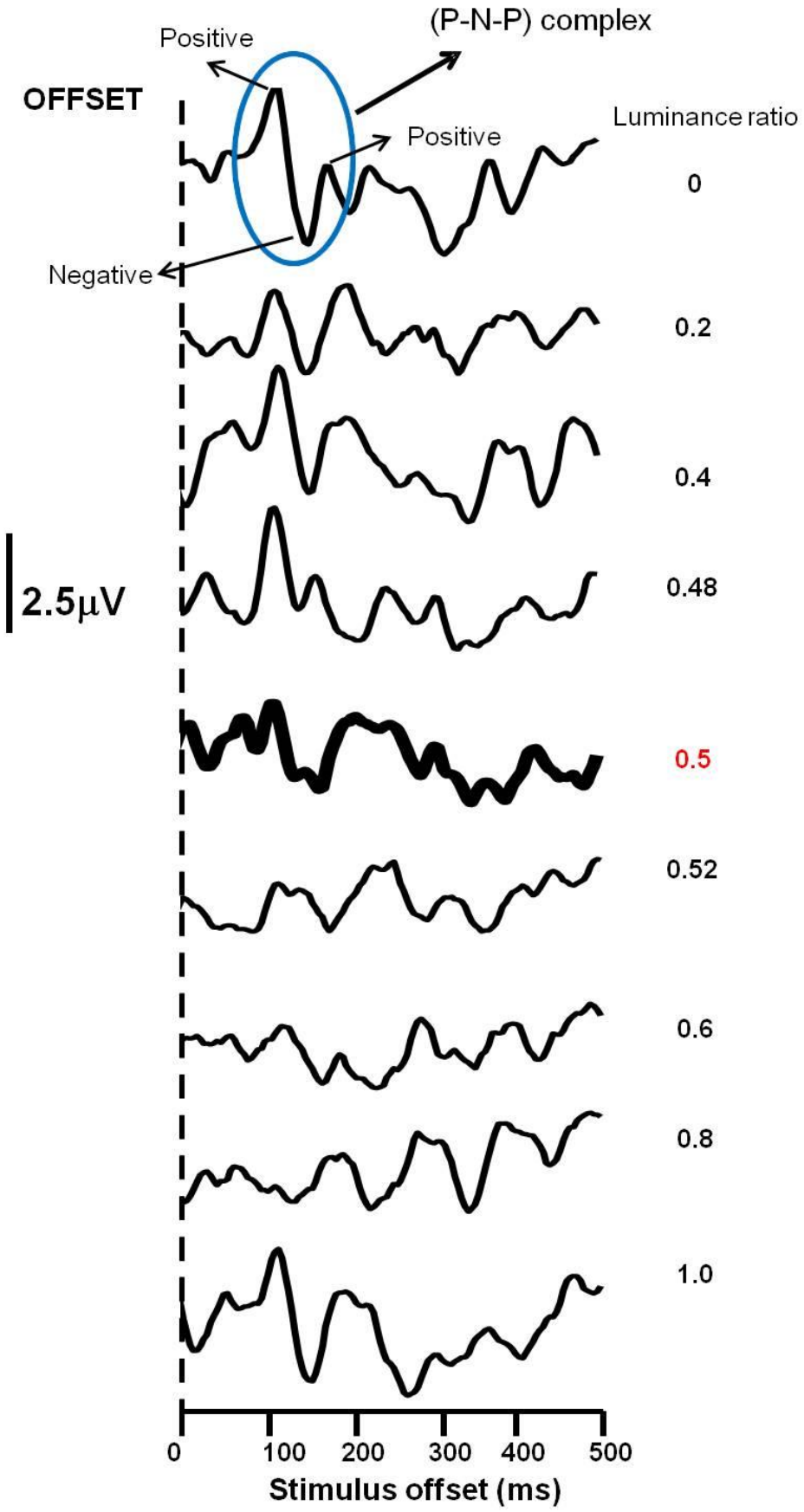

Figure 4.5 Group averaged chromatic off-set responses for the nine luminance ratios along the –L+M cardinal axes respectively.

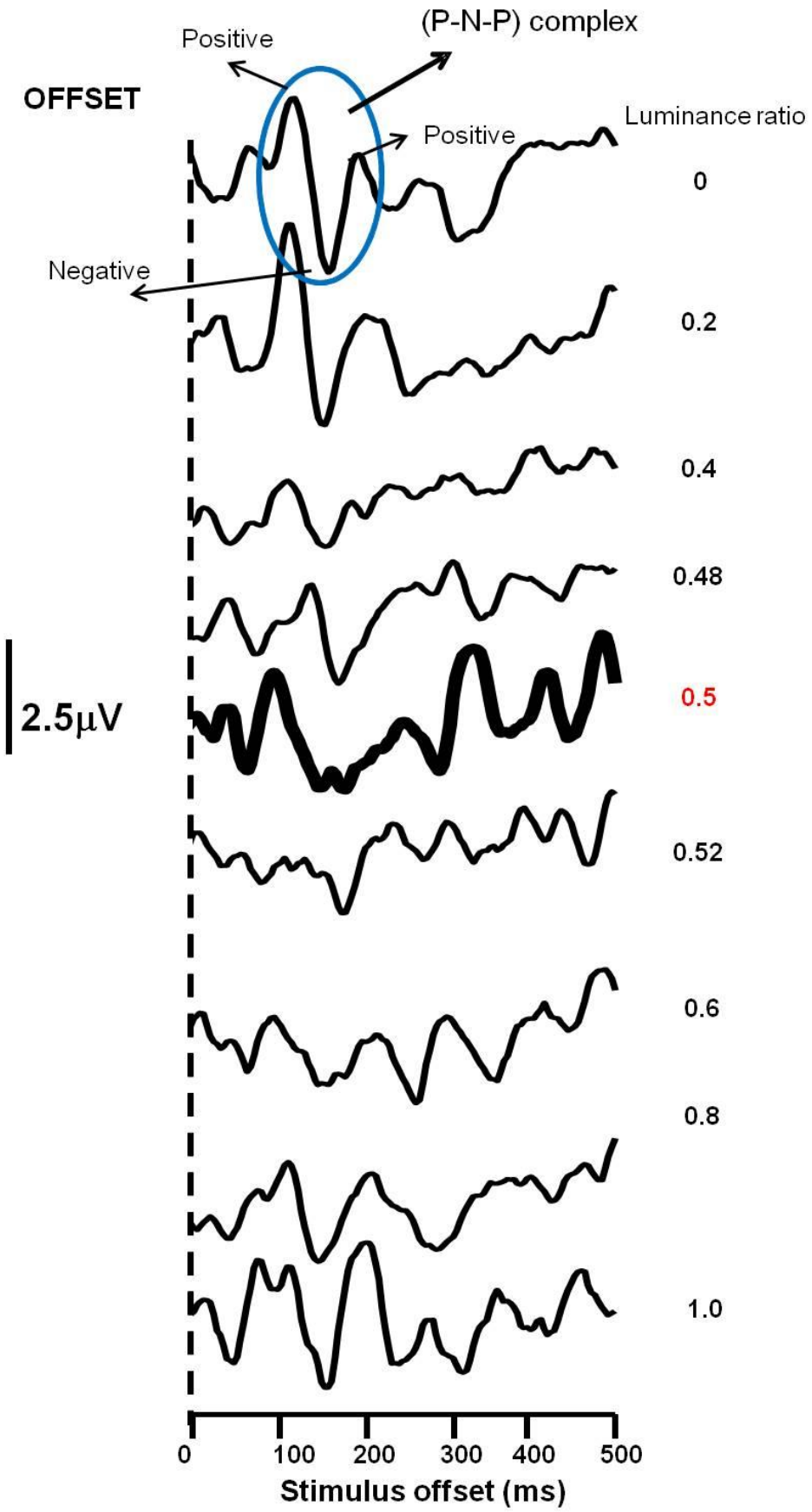

Figure 4.6 Group averaged chromatic off-set responses for the nine luminance ratios along the +S-(L+M) cardinal axes respectively.

4.4.1 Amplitudes

The group averaged amplitudes of N1, P2, N2 and P3 components as function of luminance ratio were plotted in the figure 4.7 for +L-M, -L+M axes, and in figure 4.8 for +S-(L+M) axes. From the plots it can be noticed that the N1 and P2 components have varying degrees of prominence depending upon the luminance ratio of the stimulus. The N1 amplitude reaches a maximum at isoluminance point and gradually decreases with luminance contrast increments or decrements to the isoluminant chromatic stimulus. N1 reaches its minima at luminance ratios 0 and 1. This trend is noticed for all three chromatic axes that were examined. On the other hand, the P2 component shows reverse trend i.e. P2 amplitude reaches a minimum at the isoluminance point and gradually increases with luminance contrast increment or decrement to the isoluminant chromatic stimulus. These results supports the idea of previous studies that the N1 and P2 components are the features of chromatic and luminance components respectively (Murray et al., 1986; Berninger et al., 1989; Kulikowski, 1989; Russell et al., 1991). N2 and P3 components also show a similar trend as the P2 component suggesting that these components also related to luminance content of the stimulus. The P3 amplitude is quite variable across various luminance ratios for 0 and 180 axes, but for axis 90 the amplitude reaches a minimum at isoluminance and gradually increased when the luminance contrast content is changed.

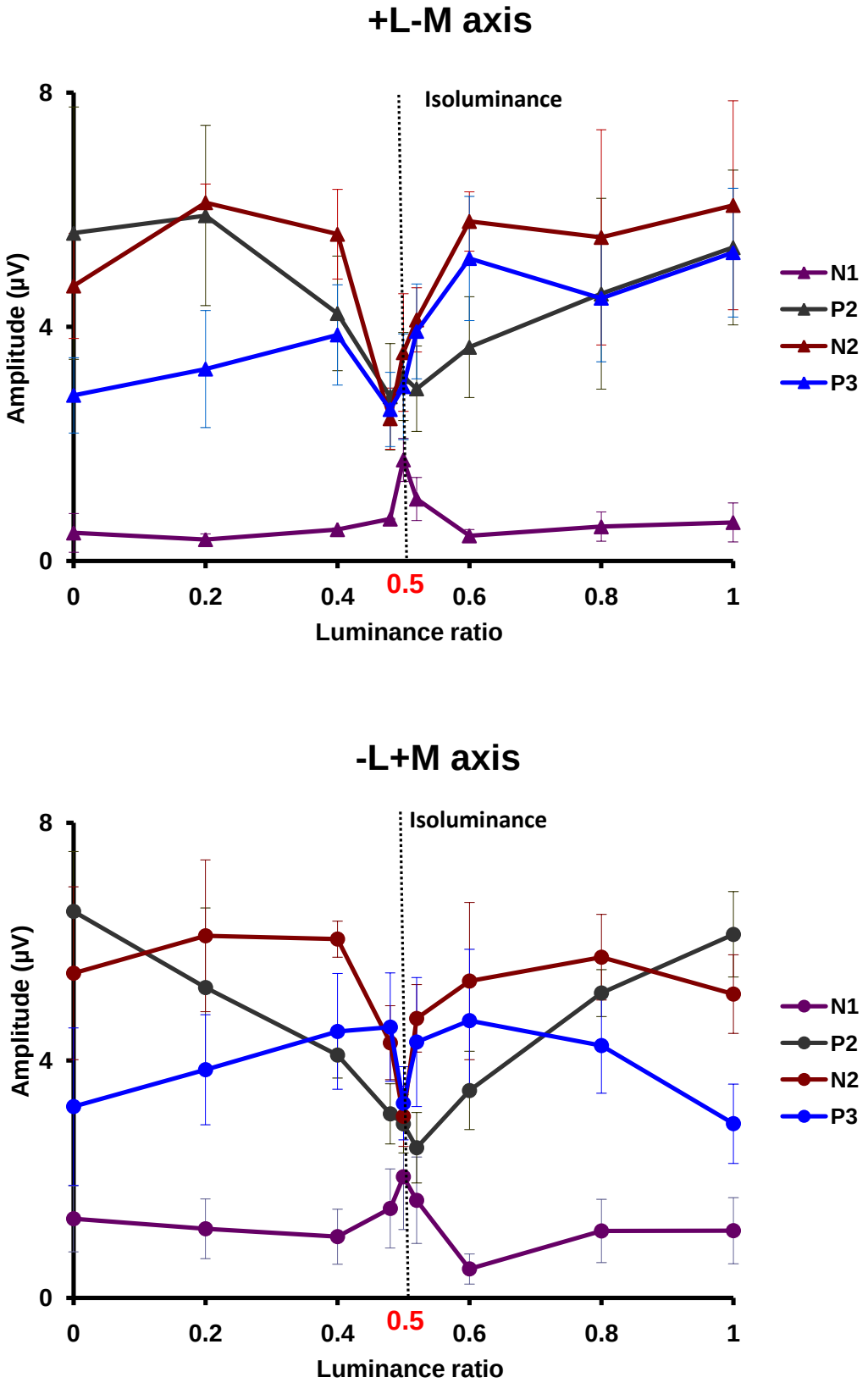

Figure 4.7 Plots of group average amplitudes of the principal components along +L-M axis (upper plot) and -L+M axis (lower plot) as function of luminance ratio.

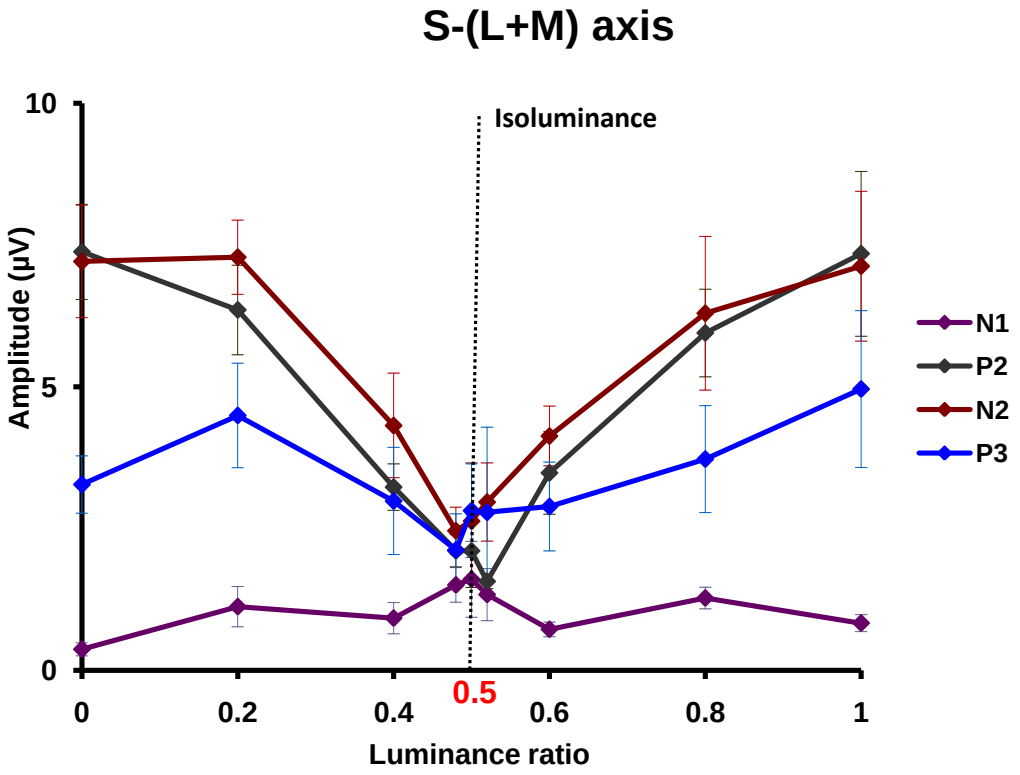

Figure 4.8 Plots of group average amplitudes of the principal components along S-(L+M) axis as function of luminance ratio.

The positive response noted at about 100-110ms after stimulus disappearance was considered as the offset response. The offset amplitude measurement is described in general methods (section 3.4). The group average off-set amplitudes as function of luminance ratio were plotted in the figure 4.9 for +L-M, -L+M axes, and in figure 4.10 for +S-(L+M) axes. From the plots it is obvious that the offset amplitude is minimal at isoluminance and increases as the luminance differences are introduced to the stimulus. Offset amplitudes reach its maxima at two extreme luminance ratios 0 and 1. However, offset amplitudes are not equivalent to the onset (P2) responses.

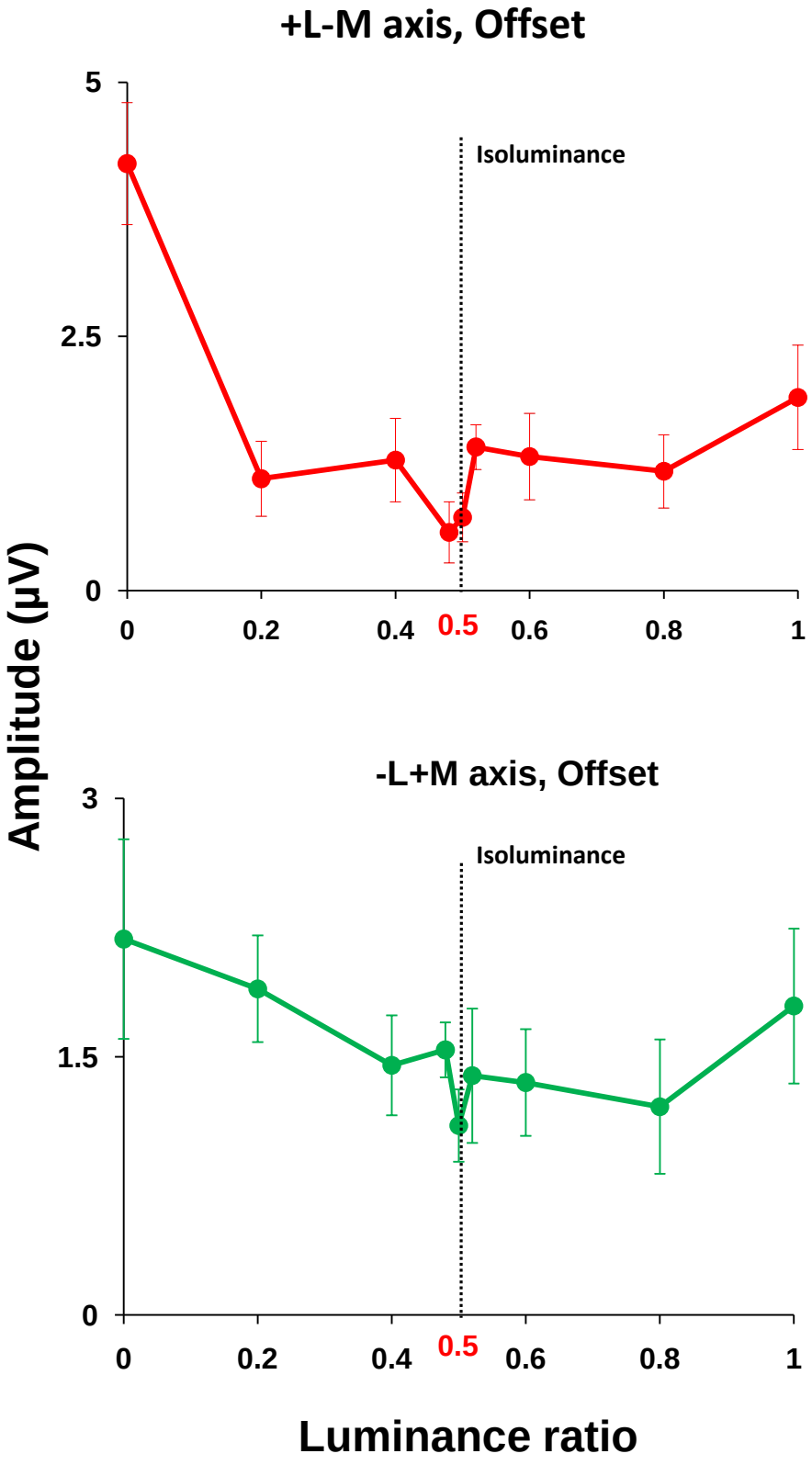

Figure 4.9 Plots of group average offset amplitudes along +L-M axis (upper plot) and -L+M axis (lower plot) as function of luminance ratio.

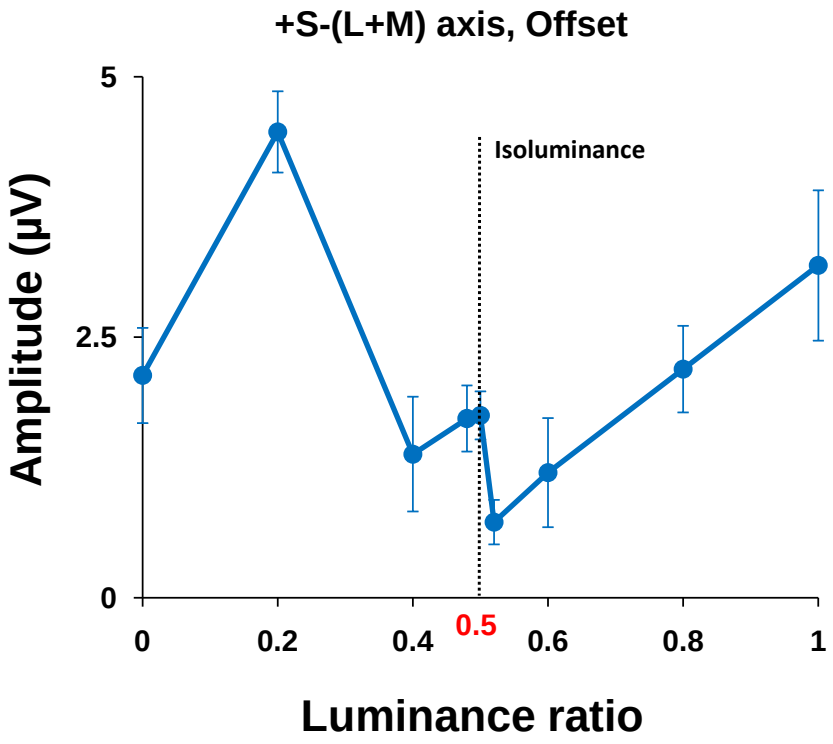

Figure 4.10 Plot of group average offset amplitudes along +S-(L+M) axis as function of luminance ratio.

4.4.2 Latencies

The figure 4.11 and 4.12 shows the latencies of all four components (N1, P2, N2 and P3) plotted against the luminance ratio for the three chromatic axes. As stimulus reaches the isoluminance point there is a definite delay in latency of all these four components. At the two extremities of luminance ratio (i.e. 0 and 1) these components shows shorter latencies as compared to the latencies as we approach the isoluminance point. These results suggest that when luminance contrast content is introduced in the stimulus, the VEP responses are quicker. For 0º and 180º axis, N1 latency differences were about 30-40ms between the isoluminance point and the luminance ratios of 0 and 1. In comparison, along axis 90º, the N1 latency difference is about 50-60ms between the isoluminance

point and the luminance ratios of 0 and 1. These results suggest that the isoluminant VEP response along axis 90º is slower in comparison to the 0º and 180 º axes.

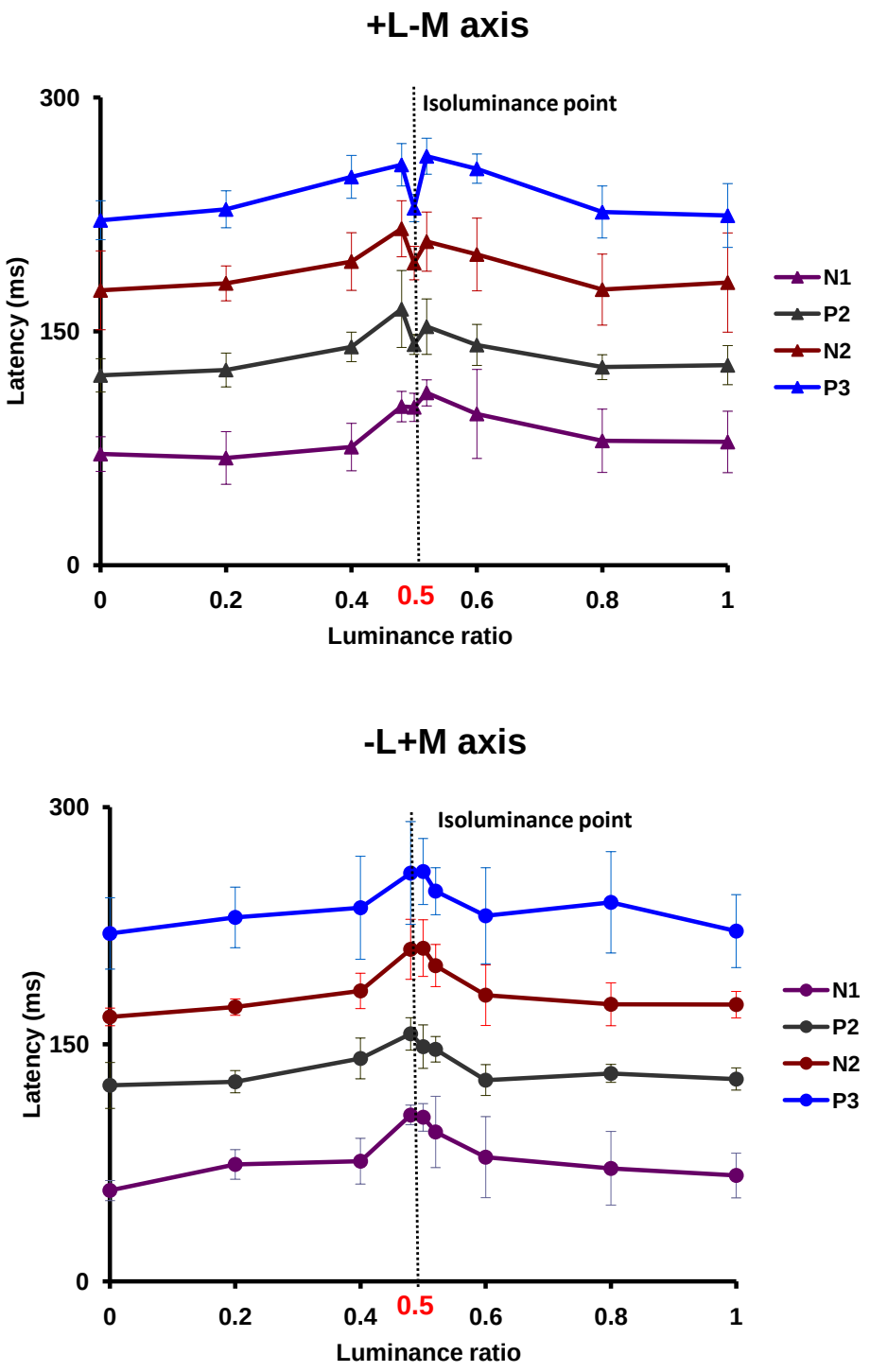

Figure 4.11 Plots of group average latencies of the principal components along +L-M axis (upper plot) and -L+M axis (lower plot) as function of luminance ratio.

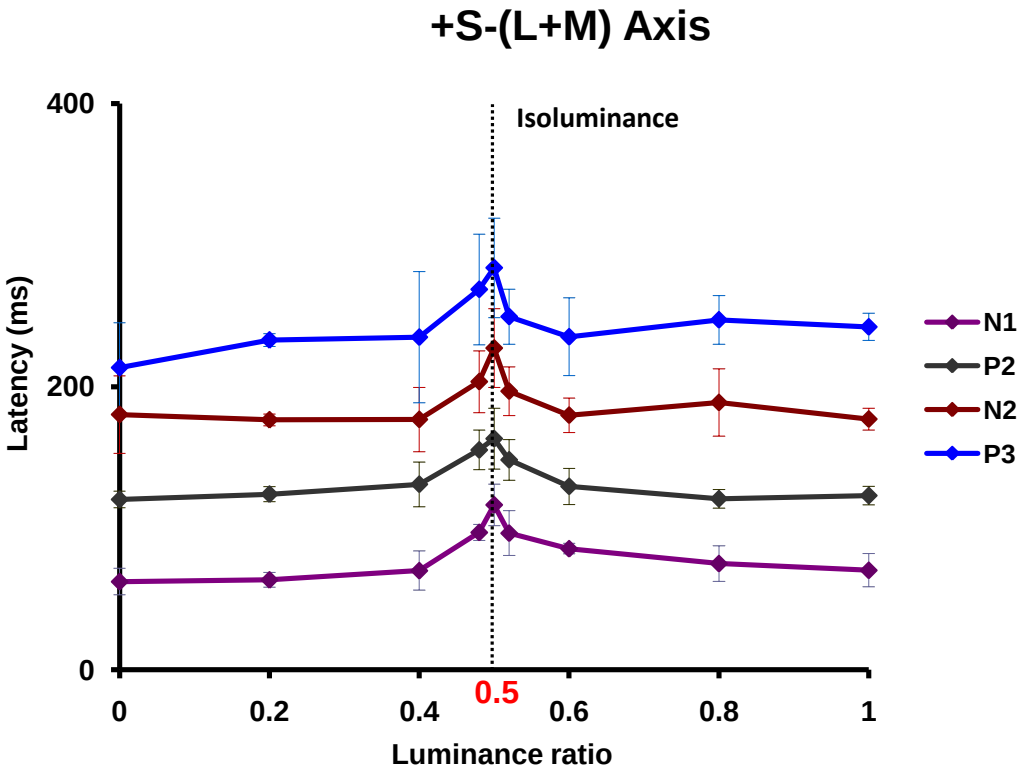

Figure 4.12 Plots of group average latencies of the principal components along S-(L+M) axis as function of luminance ratio.

4.5 DISCUSSION

This experiment has examined the morphology of VEPs elicited by circular, homogeneous, chromatic spots along three chromatic axes, which have undergone changes in luminance contrast content. Consistent with many other studies that have used sinusoidal gratings, the results indicate that luminance contrast changes can elicit qualitatively different responses to those elicited by equiluminant changes in chromatic contrast (Murray et al., 1986; Tobimatsu et al., 1995; Kulikowski, 1991a; Porciatti and Sartucci, 1999).

The studies, which used sinusoidal chromatic gratings and changed the luminance contrast content, observed that the peak response to the chromatic

stimulation is negative going and peak response to luminance onset is positive going (Murray et al., 1986; Suttle and Harding, 1999). We also noted similar observation in our study.

Large N1 amplitude is observed at isoluminant stimulation and its amplitude decreased as luminance contrast content is added to the stimulus. This finding in this study seem to favour the previous idea that N1 reflects colour processing (Murray et al., 1986; Berninger et al., 1989; Paulus et al., 1984; Kulikowski et al., 1989; Russel 1991; Tobimatsu, 1995). The N1 component is believed to reflect the colour processing for two reasons 1) its amplitude was maximal at isoluminance. 2) This component is absent in congenital colour blindness subjects (Murray et al., 1986; Berninger et al., 1989).

The presence of the early negative component (N1) in chromatic spot VEPs elicited along +L-M and –L+M axis seems to be consistent with previous studies that have examined chromatic spot stimuli (Paulus et al., 1984,1986) and would seem to justify their conclusions that the generation of this component is associated with chromatic processing in the early geniculo-recipient layers of the primary visual cortex.

Kulikowski and Vidyasagar (1987) have recorded the field potentials from chromatic sensitive single units in the area of lamina 4C of V1 of monkeys. They observed that the waveforms are similar to the scalp recorded VEPs in man. There is an assumption that the VEPs indirectly reflects multi-unit neuronal responses in the visual cortex (Schroeder et al., 1991), however, exact contribution of sources is still unknown. It can also be speculated that the isoluminant chromatic VEPs recorded in this experiment may be a reflection of

physiological properties of the corresponding group of neurons in the visual cortex.

The second positivity (P2) and the second negativity (N2) are minimal at isoluminance but as the luminance contrast was introduced N2 amplitudes were increased and became well defined at two extreme luminance ratios (0 and 1) for the three chromatic axes studied. Similar changes in morphology of VEPs have been noticed previously to chromatic grating stimuli (Kulikowski, 1989, Suttle and Harding, 1999). This finding suggests that P2 and N2 components are not a response to chromatic contrast rather they are responses to the luminance contrast modulation. The stimulus offset response is minimal at isoluminance point and well defined at higher luminance ratios. This finding is consistent for all three axes. Colour cells in the cortex respond weakly to stimulus offset (Jankov, 1978; Zrenner, 1983) and respond in a sustained fashion primarily to the stimulus offset. The absolute contrast of the stimulus at offset is zero, so the response to this stimulus from chromatic cells is minimal. On the other hand, luminance cells respond to contrast change, which means they respond transiently to both stimulus onset and offset. The properties of chromatic and luminance cells are reflected in the VEP responses of this experiment, with the response to isoluminant chromatic stimulation showing minimal offset response, and the responses away from isoluminance point (which contain luminance contrast) showing maximal offset response. Suttle and Harding (1999) studied VEP offset responses at various luminance ratios using sinusoidal gratings. They noticed similarly minimal offset responses at photometric isoluminance and maximal offset response to isochromatic luminance contrast stimulation. These findings are in agreement with their observations. Though, the offset responses are minimal at isoluminance point

nonetheless still present, suggesting some residual involvement of achromatic activity at isoluminance. It can be assumed that this could be because of small variation in isoluminance point from fovea to 2 degree region. The other possible explanation is that the effect of macular pigmentation. Moreland et al (1998) strongly suggested that the VEPs can reflect the contaminating effects of macular pigment on colour stimuli, even subject specific isoluminance is determined for small fields.

The P-N-P complex observed in the offset response was obvious at higher luminance ratios and diminished at isoluminance point for +L-M and –L+M chromatic axes. The negativity of P-N-P complex was noted approximately at 135 ms after stimulus off-set. At isoluminance, the response to both +L-M and -L+M axes showed a very small P-N-P complex, the negativity of which occurs at approximately 165-170ms after stimulus offset. Suttle and Harding (1999), who used sinusoidal gratings, noted similar offset responses and changes in morphology as the luminance ratio of the chromatic stimulus is varied. However, in their study the negativity of P-N-P complex was occurred at approximately 230ms after stimulus off-set. The speculation from this experiment is that the difference in latency may probably be due to difference in stimuli parameters and differences in onset- offset time periods. For example, Suttle and Harding used sinusoidal gratings and onset-offset time periods were 300 and 700ms respectively. In this study the stimuli were circular homogenous spots with 500ms onset-offset time period.

Latency plots suggest N1, P2, N2, and P3 components have longer latencies at isoluminance and shorter latencies at higher luminance ratios. These findings favour the idea that the isoluminant chromatic stimuli are processed more slowly than the luminance modulated stimuli.

At higher luminance ratios, VEP components along +L-M and –L+M axes have shorter latencies, dominated primarily by positive onset response and have shown large off-set responses. These responses are consistent with transient magno cellular properties. At isoluminance, VEP components have longer latencies, dominated primarily by negative onset response and have shown small offset responses. From these finding it can be speculated that these characteristics of VEPs may reflect the sustained nature of the responses respectively. Furthermore, these responses are derived from the cells of M- and P- pathway respectively. The latency differences between and +S-(L+M) axis and other two chromatic axes (+L-M, –L+M axes) may suggest that these two responses are derived from different cone opponent pathways.

In conclusion, morphological changes in VEP related to the changes in luminance and chromatic contrast can be summarized as follows. Isoluminant chromatic stimuli generate VEP responses with longer latency and minimal offset responses. This sustained nature of the responses is consistent with P cellular processing. On the other hand, VEPs generated by luminance contrast modulation have shorter latencies and large offset amplitudes. The transient nature of the luminance contrast VEP response is consistent with M cellular processing.

CHAPTER - 5 EFFECT OF STIMULUS SIZE ON CHROMATIC SPOT VEPS

5.1 INTRODUCTION

Chromatic VEPs recorded with low spatial frequency and low contrast red-green sinusoidal gratings have been shown to contain a dominant early negative chromatic component at approximately 120ms, which is of opposite polarity to achromatic VEPs (Murray et al., 1986; Kulikowski, 1989; Rabin et al., 1994; Berninger et al., 1989). Isoluminant pattern stimuli are prone to effects of longitudinal and transverse chromatic aberrations (results in lights of different colours being differently focused and magnified) which introduce luminance contrast artefacts (Flitcroft, 1989; Kulikowski, 1991a). In addition to this, S cone isolating stimuli are subjected to the effects of macular pigmentation which varies in density and distribution (Ruddock, 1963; Moreland and Bhatt, 1984).

VEP studies, which used chromatic patterns and homogenous stimuli, have indicated qualitatively different responses to these stimuli. It has been noted that many attributes such as contrast, colour, spatial extent of the stimulus may effect and perhaps encoded in VEPs (Estevez and Dijkhuis, 1983). Colour effects are masked in VEPs by dominating pattern responses (Shipley et al., 1965; Spekreijse et al., 1977; Estevez and Dijkhuis, 1983; Paulus et al., 1984). In addition to this, Spekreijse et al (1977) suggested that pattern VEP may contain components which relate to border sharpness. For instance, the CII component (occurs at a latency about 120ms) can be associated to changes in spatial contrast, especially around sharp contours.

In order to reduce the effect of pattern on VEPs, Paulus and co-workers (1984) used circular spot chromatic stimuli and found that the colour dominated component (N1) is slightly earlier (87ms) than that of chromatic VEPs elicited by the sinusoidal gratings. According to them, circular spot stimuli activate different neuronal population to that of grating stimuli. The only constraint they noticed is, chromatic spot VEPs cannot produce robust VEPs (in terms of amplitudes) like gratings. Adding to this, a study on single unit neurons has also suggested that spot and grating stimuli activate different neural populations for chromatic processing.

Zrenner (1983) claimed that large stimulus fields introduce variations in isoluminance with eccentricity. However, Kulikowski (1991a), using low contrast stimuli, showed VEP responses are similar to small or large fields, suggesting that contrast plays a more important role than the stimulus size for selective activation of M and P mechanisms. These studies recorded VEPs using isoluminant gratings. The research questions we wish to address are 1) Does size have any effect on isoluminant spot VEPs? 2) Are there any changes in VEP morphology with the use of large isoluminance spots? 3) if not, do large size spot stimuli produce large amplitude VEPs similar to those elicited by gratings? In order to answer all these questions we recorded VEPs using isoluminant spots of a range of sizes.

Single unit physiology has characterised the responses of colour opponent P-cellular neurons as sustained whilst those of broad-band neurons are transient (Gouras, 1968; Kaplan and Shapley, 1982; Demonasterio and Gouras, 1975; Shapley and Perry, 1986; Blakemore and Vital-Durand, 1986). Magnocellular (transient or non opponent) neurons respond equally to the onset and offset phases of the stimuli and P-cellular (colour –opponent) neurons on the other

hand, respond mainly to the onset not to the offset of the stimuli (Zrenner, 1983) (see figure 5.1). It implies that if the offset response is smaller than the onset response, then the response is mainly sustained P system (Kulikowski, 1991). The comparison of onset and offset response can produce a measure of the selectivity of sustained chromatic mechanism.

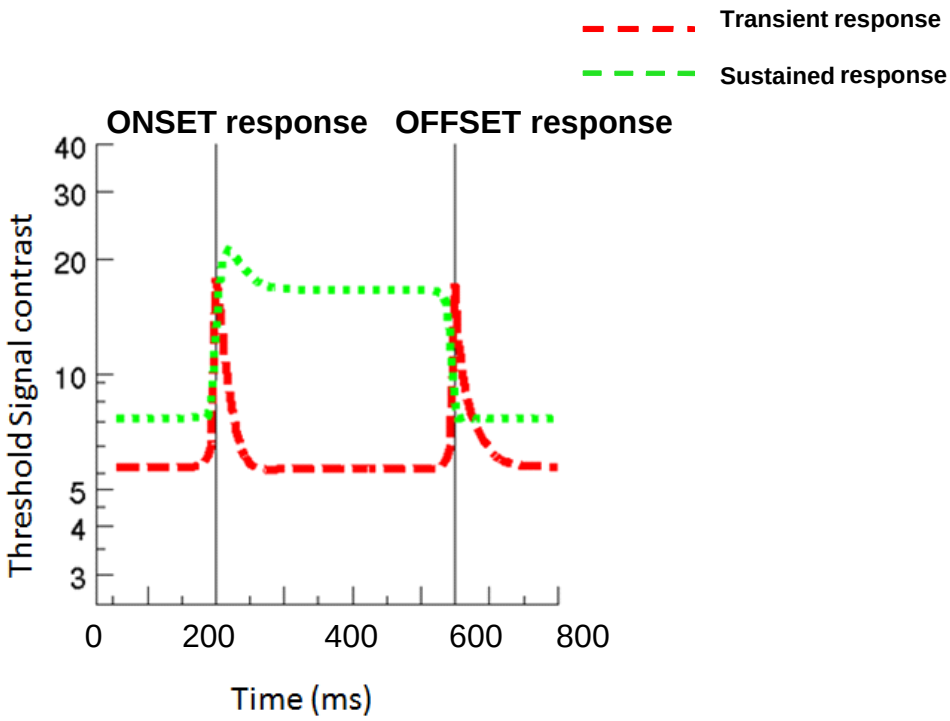

Figure 5.1 Response characteristics of typical M (transient) and typical P (sustained) cells to the onset-offset stimuli. Note that response shown in red-dash line is from the magno cell which has transient character, means respond equally to the onset-offset phases. Green-dash line is the response from P cell which has sustained character, means respond well to the onset but response gradually reduces by the time stimulus is off.

To our knowledge this is the first attempt to examine the effect of stimulus size on chromatic spot VEPs. It would be interesting to see the effect of stimulus size on spot VEPs since these stimuli type are claimed to activate mainly chromatic mechanisms.

5.2 METHODS

5.2.1 Stimuli and VEP recordings

Full details of the VEP recording procedure is presented in section 3.4. General stimulus structure is presented in section 3.3. The VEP stimuli consisted of homogenous circular discs of nine different diameters ranging from 14° to 0.5° degrees which were centred on the fovea. The mean luminance of the discs was 25cd/m^2 and they were surrounded by a grey background of the same mean luminance. The circular stimulus could be made to undergo equiluminant hue modulation over time which involved presenting the target with specific hue for 500ms, then replacing it for the same period with neutral grey stimulus (CIE 1931 chromaticity co-ordinates: x = 0.310, y = 0.316) of same mean luminance. Thus the stimulus had the appearance of circular patch the hue of which was modulated in onset-offset fashion with a square wave temporal profile. A fixation cross was placed in the centre of the stimulus to minimise the influence of eye movements and subjects viewed the stimulus binocularly.

5.3 RESULTS

5.3.1 Morphology of VEPs as function of stimulus size

Individual VEP data are shown in figures 5.2, 5.3 and 5.4 for chromatic stimuli which modulate along +L-M, +M-L and +S-(L+M) axes. Figures 5.5, 5.6 and 5.7 represent the group averaged responses of chromatic VEPs as a function of stimulus size along three cardinal axes. VEPs generated by +L-M and –L+M

axes are similar in appearance and are characterised by a small positive component (P1) with a latency of about 55-80ms, followed by negative component with a latency ranging from 90-115ms based on stimulus size under these experimental conditions. The negative component, referred as N1, seems to be consistent feature in all subjects' waveforms for all chromatic sizes along +L-M and –L+M cone isolating axes. It is likely that N1 is similar to the N87 and N90 components described by Paulus et al (1984) and Valberg & Rudvin (1997). The N1 component is followed by large positive component (P2) that has the latency between 130-175ms. The second negative component (N2) (latency about 180-225ms) and third positive component (P3) (latency at about 230-280ms), seem to be consistent features of VEPs elicited by all stimulus sizes; however their response variation is clearly seen as function of stimulus size. Another important feature noticed is the offset responses, which increased as the size of the stimulus is increased. In this experiment we restricted our analysis to N1 and P2 and Offset components. The above mentioned components have shown variability in latency for S cone isolating stimuli. This variability is discussed in results section.

Figure 5.7 shows chromatic VEPs as function of stimulus size along +S-(L+M) cone isolating axis. N1, P2, N2, P3 and offset components were well preserved up to 6 degree stimuli and from there on the N1 component is almost diminished for small size stimuli. Morphology of VEPs elicited from small spots is different from that of which elicited from large spots. For example N1 component seems to decrease in amplitude as we reduce the size of the stimuli and almost disappeared with small spots. Very small spots (0.5 to 1 degree) haven noisy responses along +S-(L+M) axis. So the responses were analysed for the stimulus size ranging from 14 degrees to 2 degree size. All components

of the VEP along +S-(L+M) axes showed delayed latencies in comparison to the +L-M and (-L+M) axis.

The other morphological difference is seen in offset response with the change in size of the stimuli is P-N-P complex (for detailed explanation see previous chapter), which is more apparent for the large size stimuli and it almost disappeared for small size stimuli especially along the +L-M and -L+M axes.

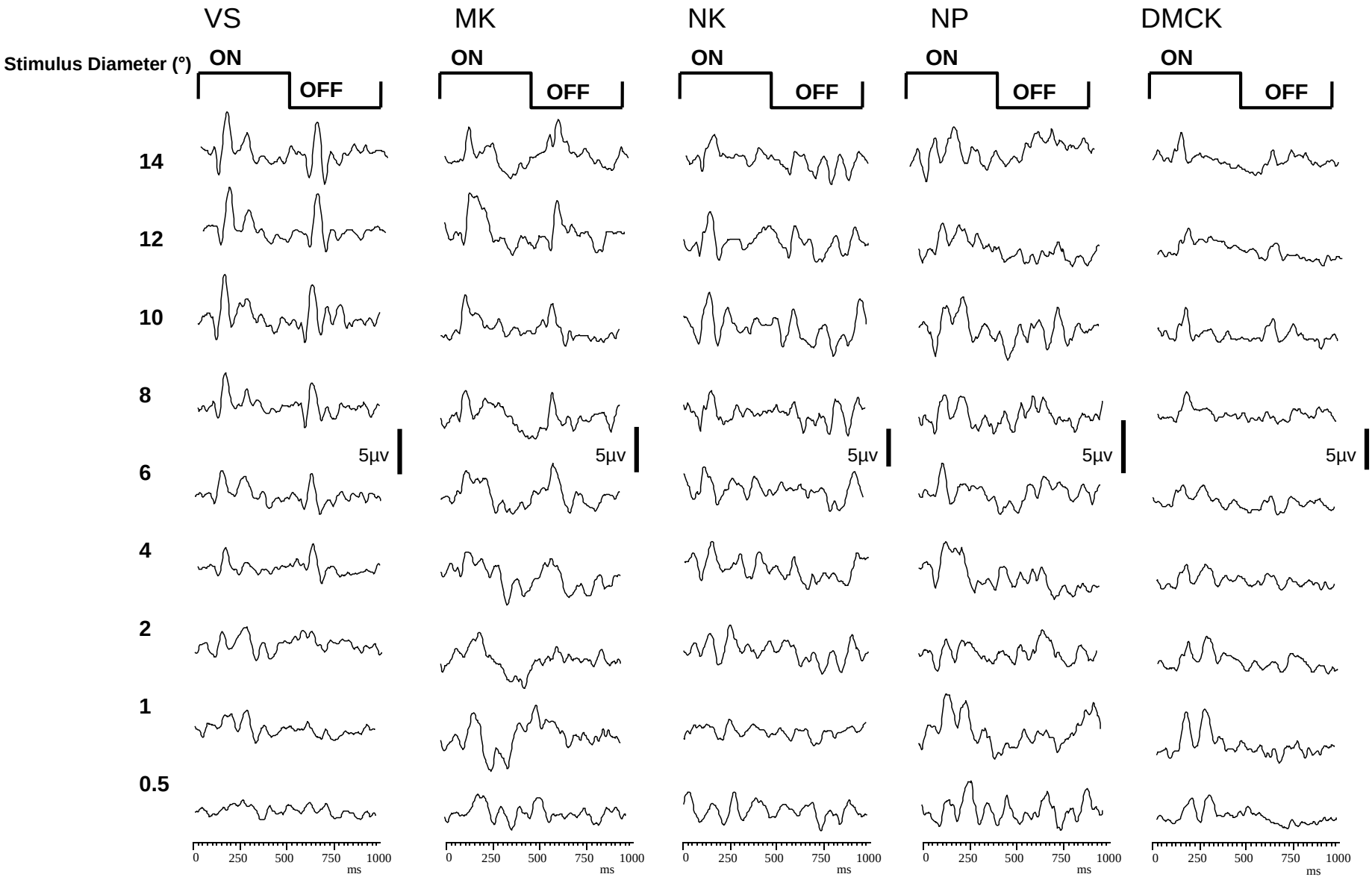

Figure 5.2 Individual VEP responses as function of stimulus size along +L-M axis.

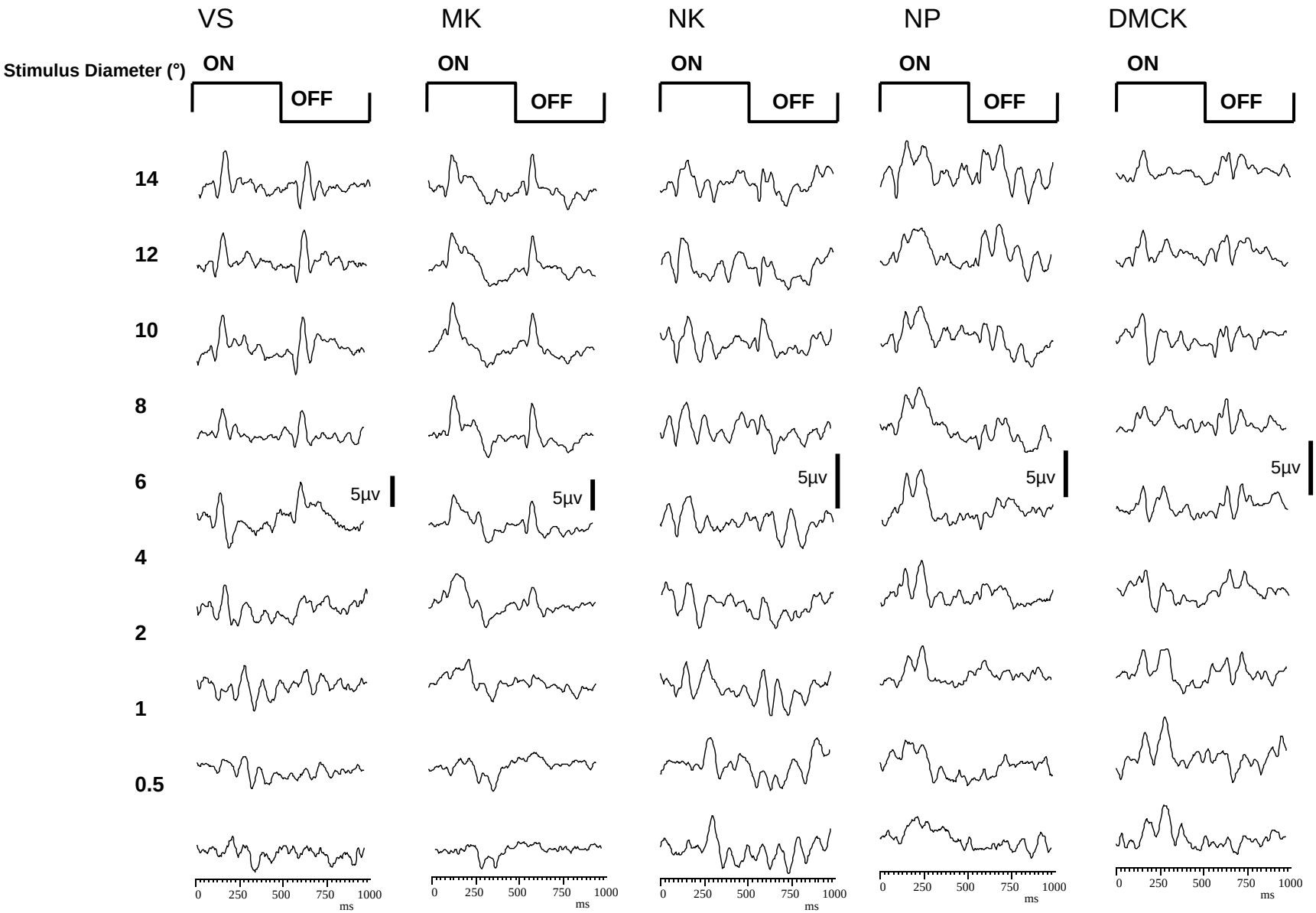

Figure 5.3 Individual VEP responses as function of stimulus size along –L+M axis.

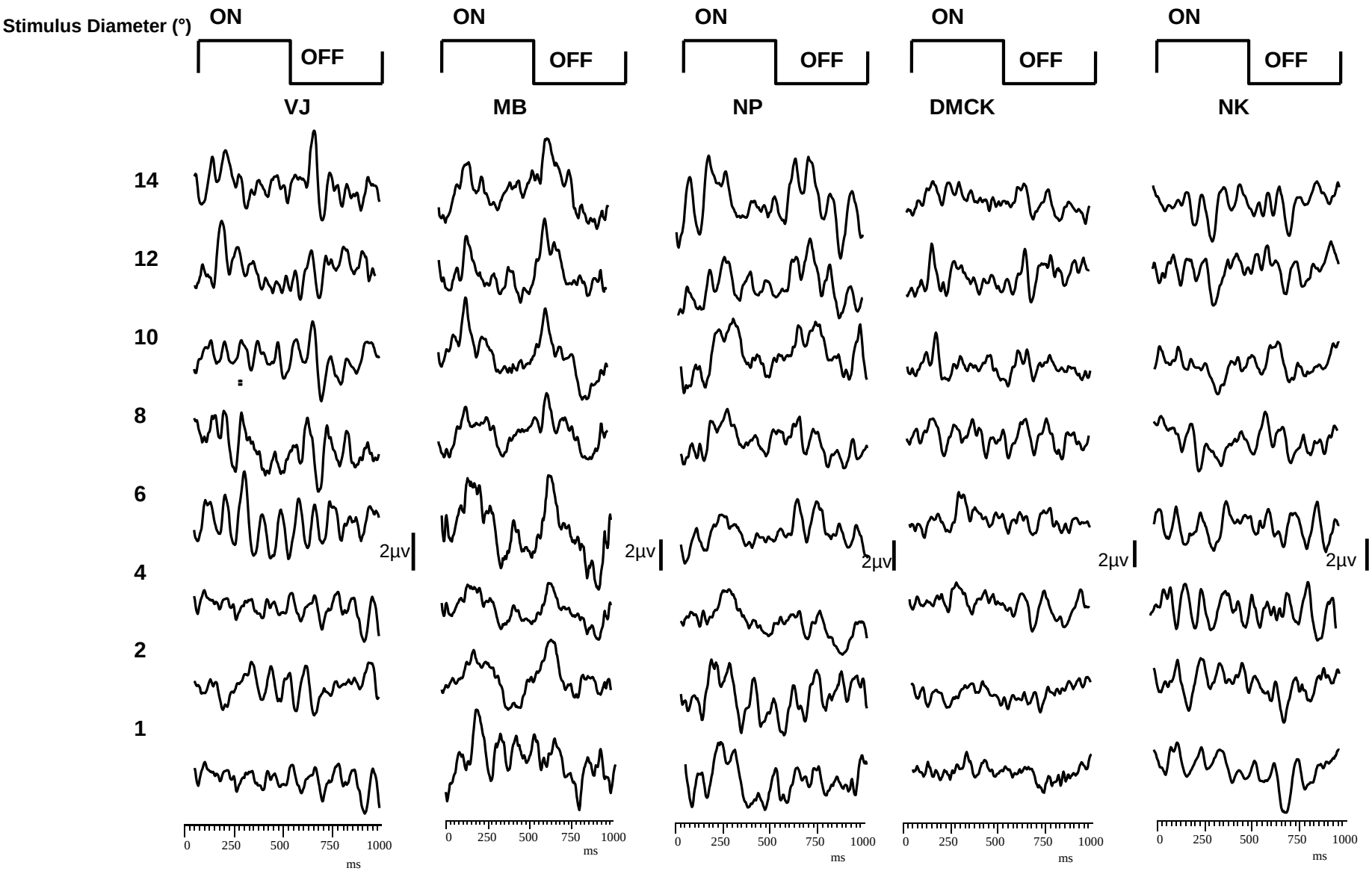

Figure 5.4 Individual VEP responses as function of stimulus size along +S-(L+M) axis.

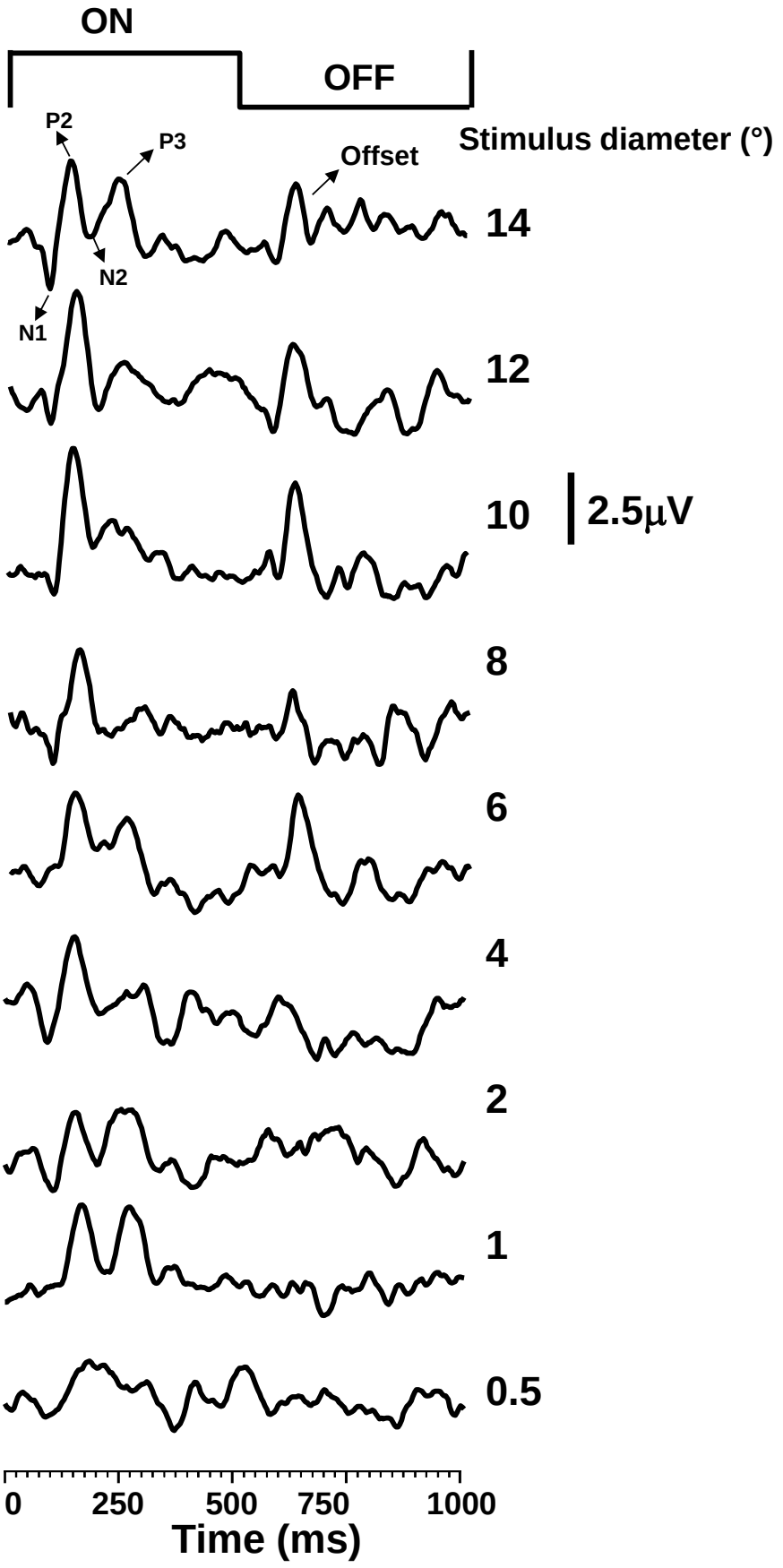

Figure 5.5 Group averaged VEPs (n=5) generated by chromatic spot stimuli of varying sizes along +L- M axis.

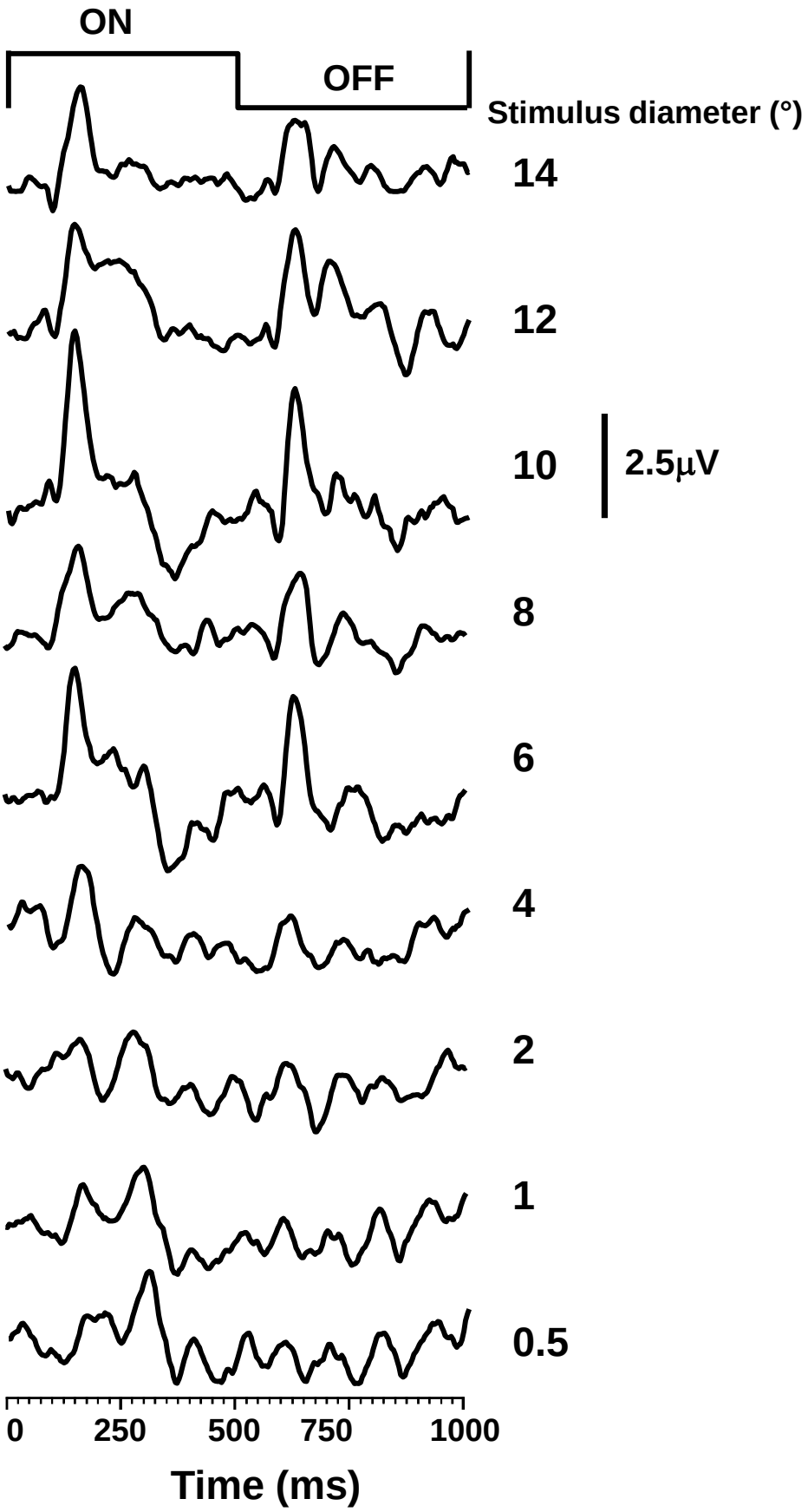

Figure 5.6 Group averaged VEPs (n=5) generated by chromatic spot stimuli of varying sizes along –L+M axis.

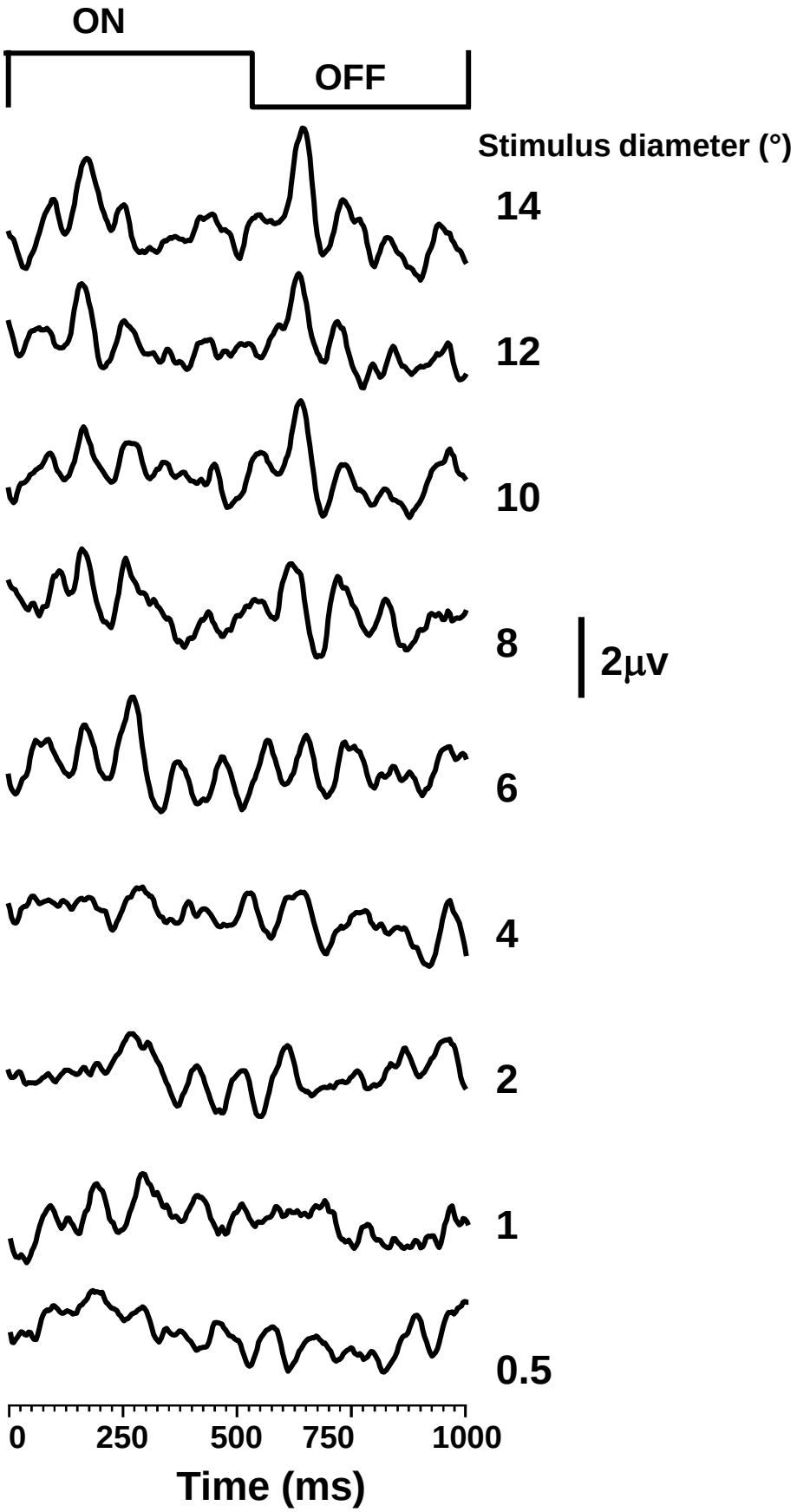

Figure 5.7 Group averaged VEPs (n=5) generated by chromatic spot stimuli of varying sizes along +S-(L+M) cone isolating axis.

5.3.2 Amplitudes

N1, P2 and offset amplitudes as function of stimulus size along +L-M, –L+M and +S-(L+M) chromatic axes were plotted as shown in figure 5.8 and 5.9 and 5.10. From the figures, it can be observed that the change in stimulus size has no significant effect ($p>0.05$) on N1component along the three cardinal axes, whilst P2 and offset component is significantly changed ($p<0.05$) to the variation in spatial configuration of the stimulus. We measured the amount of change in P2 and offset amplitude for every degree increase in stimulus size for +L-M and –L+M chromatic axes. In order to do this, we fitted a regression line that describes the linear model for each chromatic axes. Regression analysis of N1, P2 and offset components for each chromatic axis were presented in table 5.1. Size response functions (slope of the line) describe the change in amplitude for every degree increase in stimulus size. Regression equations are presented in figure 5.8, 5.9 and 5.10, where significant effect of size is noted. Size response functions obtained for P2 component along +L-M and –L+M axes are 0.23µV/° and 0.20µV/° respectively. Size response functions obtained for Offset component along +L-M and –L+M axes is 0.30µV/° and 0.25µV/° respectively.

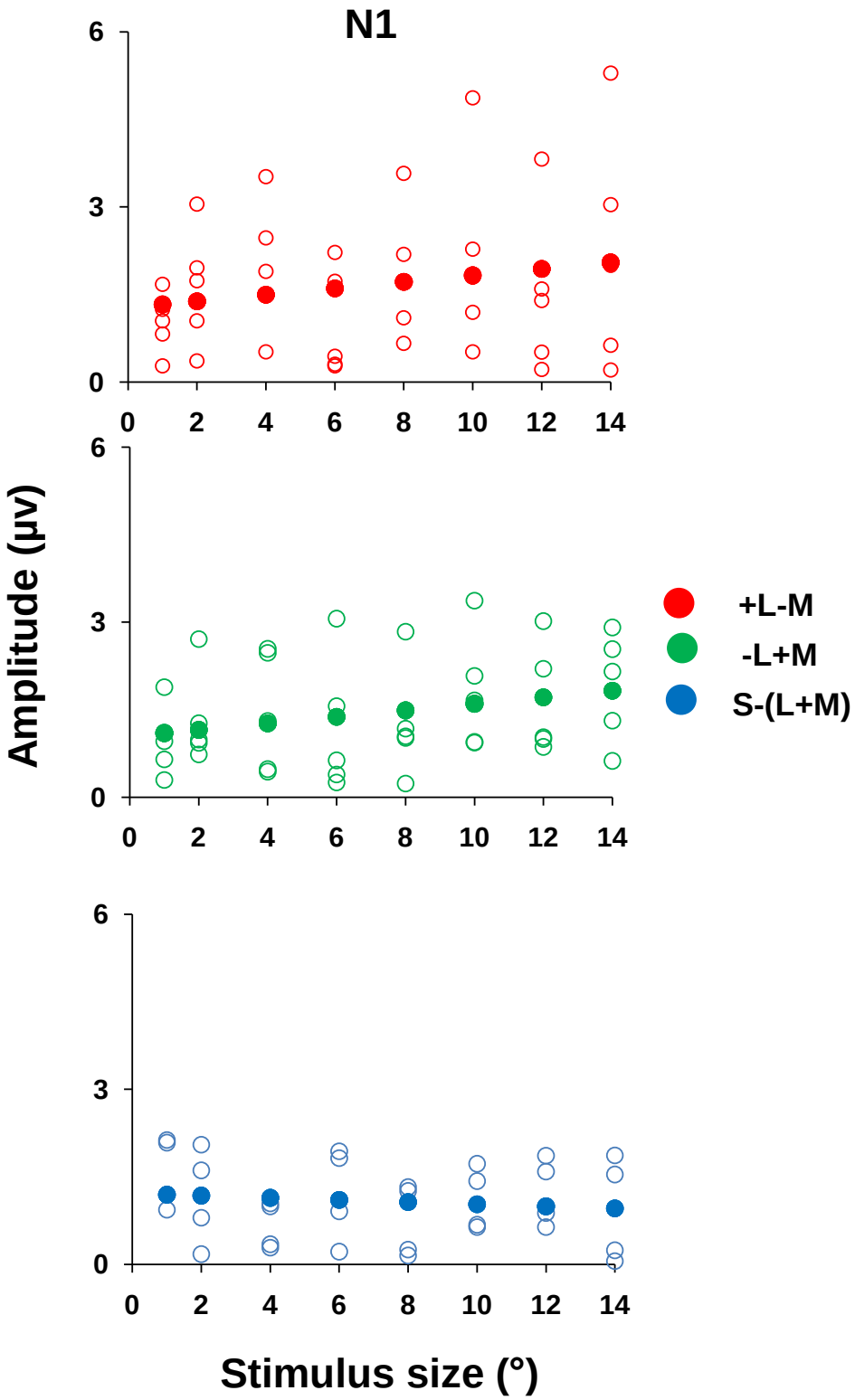

Figure 5.8 N1 amplitudes as function of stimulus size for +L-M, -L+M and +S-(L+M) chromatic axes. Open circles represent raw data of 5 subjects and filled circles represents the group average response data. Stimulus size has no significant effect on VEP responses along three chromatic axes. p values are presented in table 5.1 for reference.

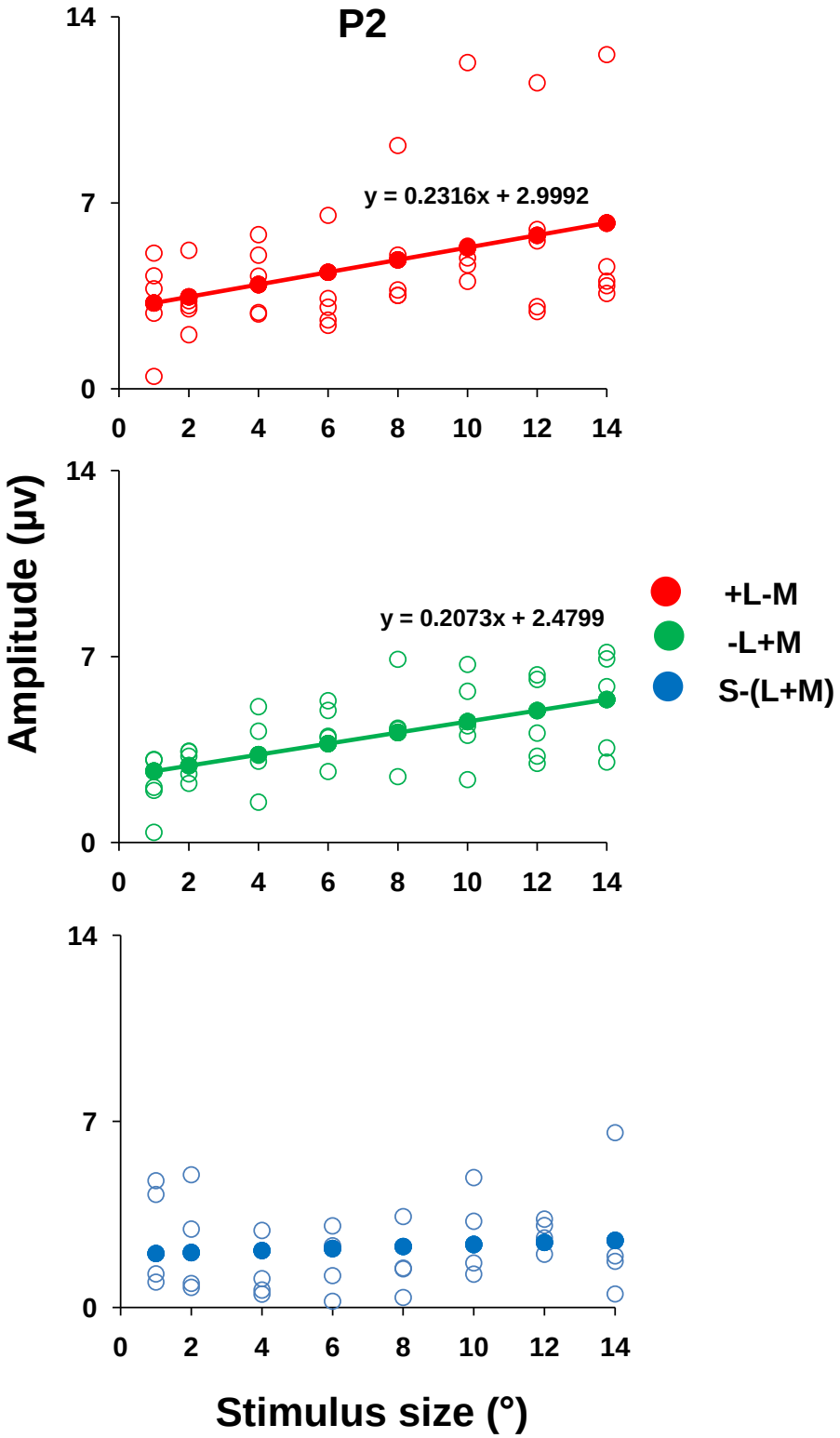

Figure 5.9 P2 amplitudes as function of stimulus size for +L-M, -L+M and +S-(L+M) chromatic axes. Open circles represent raw data of 5 subjects and filled circles represents the group average response data. Stimulus size has significant effect on N1 component along +L-M and –L+M axes. Regression lines are fitted for statistically significant data. p values are presented in table 5.1 for reference.

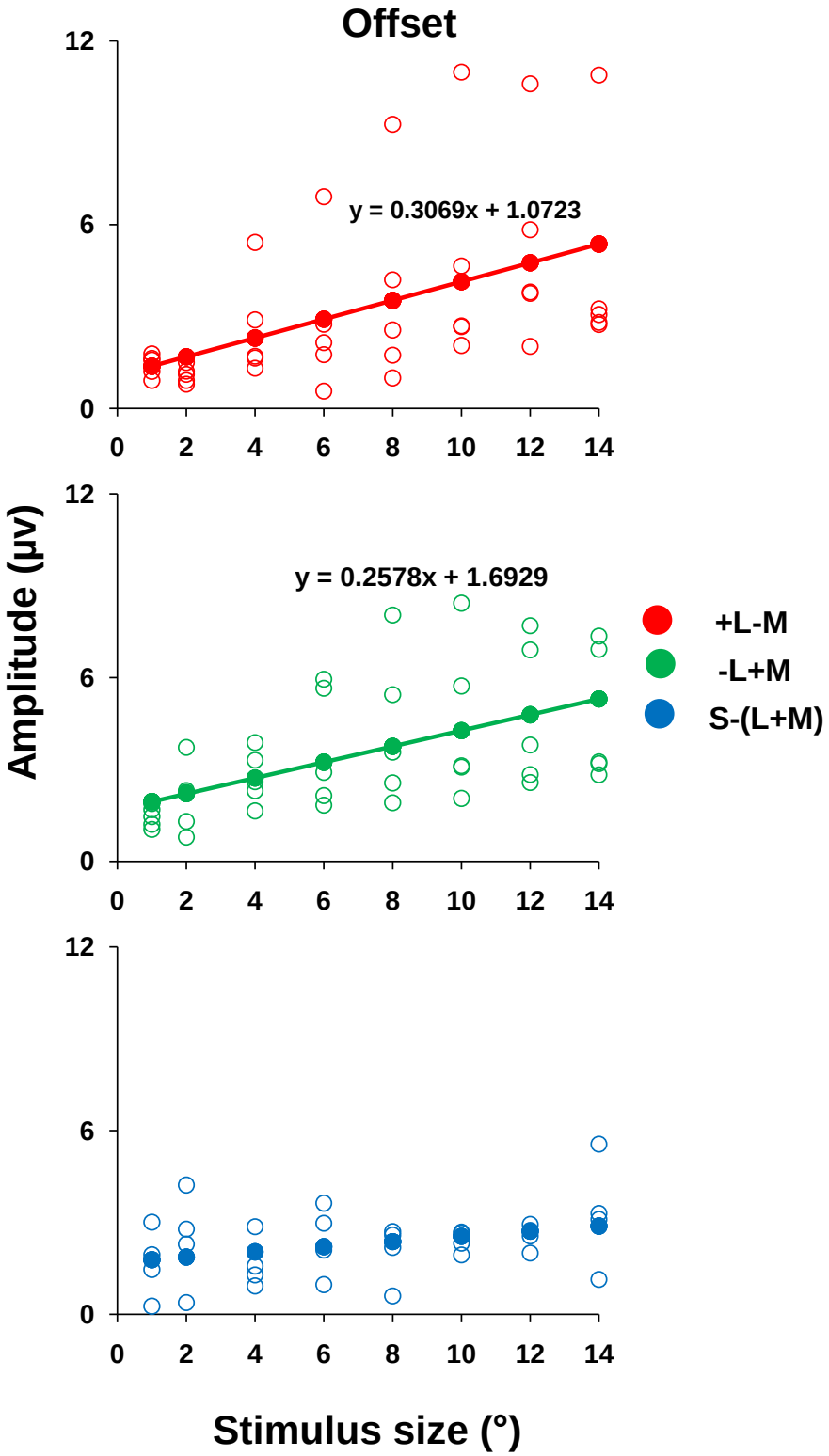

Figure 5.10 Offset amplitudes as function of stimulus size for +L-M, -L+M and +S-(L+M) chromatic axes. Open circles represent raw data of 5 subjects and filled circles represents the group average response data. Stimulus size has significant effect on offset component along +L-M and –L+M axes. Regression lines are fitted for statistically significant data. p values are presented in table 5.1 for reference.

Regression analysis				
Component				
N1		R^2	F Value	p value
	+L-M	0.0381	1.5073	0.2270
	+M-L	0.0755	3.1065	0.0860
	+S-(L+M)	0.0151	0.4602	0.5026
P2				
	+L-M	0.157276	7.0918	**0.0112**
	+M-L	0.330889	18.7914	**0.0001**
	+S-(L+M)	0.011532	0.3499	0.5585
Offset				
	+L-M	0.236053	11.7416	**0.0014**
	+M-L	0.293759	15.8060	**0.0003**
	+S-(L+M)	0.114087	3.8633	0.0586

Table 5.1 Regression analysis of N1, P2 and offset amplitudes along three cardinal axes as function of stimulus size. R^2 suggest the goodness of fit. According to the table, poor fits are noted for N1 component and relatively good fits are noted for P2 and offset component. Statistically significant values ($p<0.05$) were presented in bold letters.

5.3.3 Latencies

The N1 and P2 latencies along +L-M, -L+M and +S-(L+M) chromatic axes are presented in figure 5.11 and 5.12. From the plots we can notice a general trend that there is a negative correlation between stimulus size and the latency for all three cardinal axes. As the stimulus size increases latency decreases. The latency difference of about 20ms was observed for both N1 and P2 components between the smallest and largest stimuli. The N1 and P2 components have longer latencies (approximately 20ms) for +S-(L+M) chromatic axes in comparison to +L-M, -L+M chromatic axes for all sizes examined. N1 latencies are significantly effected by size for all three chromatic axes whilst P2 latencies

are effected by size only along –L+M and +S-(L+M) chromatic axes. Regression equations and lines were presented to the plots where there is significant effect of stimulus size on latency . Regression analysis is summarised in table 5.2.

		Regression analysis		
Component				
N1		R^2	F Value	p value
	+L-M	0.223	10.92899	**0.002074**
	+M-L	0.104	4.451716	**0.041507**
	+S-(L+M)	0.148	5.21604	**0.029628**
P2				
	+L-M	0.043	1.709294	0.198933
	+M-L	0.223	10.92411	**0.002078**
	+S-(L+M)	0.144	5.087085	**0.031556**

Table 5.1 Regression analysis of N1 and P2 latencies along three cardinal axes as function of stimulus size. R^2 suggest the goodness of fit. According to the table, N1 and P2 latencies were significantly changed by increase in stimulus size. Statistically significant values ($p<0.05$) were presented in bold letters.

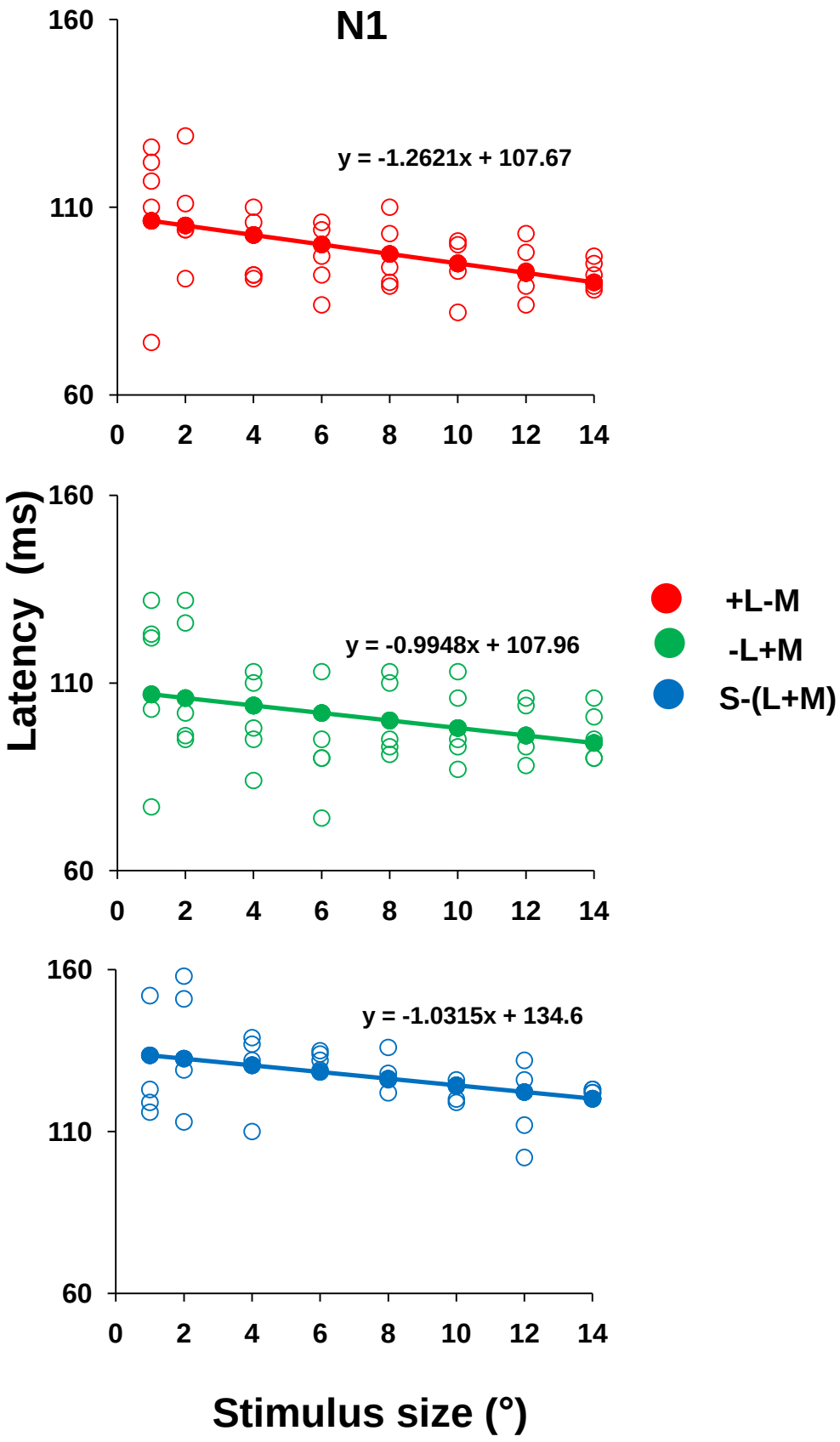

Figure 5.11 N1 (upper plot) and P2 (lower plot) latencies calculated from group average VEP as function of stimulus size for L, M and S cone isolating axis.

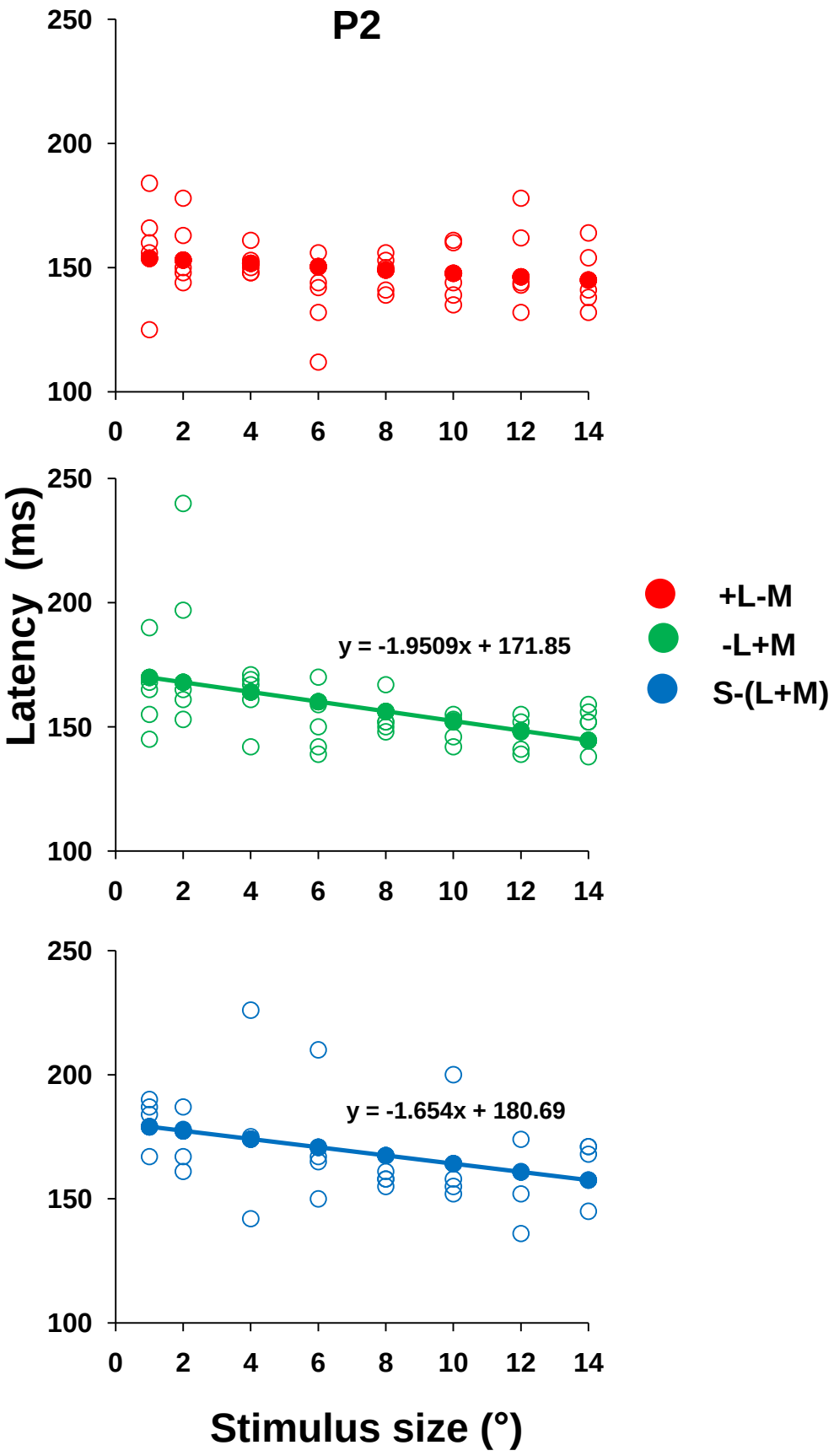

Figure 5.12 N1 (upper plot) and P2 (lower plot) latencies calculated from group average VEP as function of stimulus size for L, M and S cone isolating axis.

5.4 DISCUSSION

This experiment examined the morphology of the circular spot chromatic VEPs for different stimulus sizes along +L-M, -L+M and +S-(L+M) cone axes in MBDKL colour space. It shows that chromatic VEPs generated by circular homogenous spot stimuli of increasing sizes generate responses with different morphologies.

The presence of an early negative component (N1) in the chromatic VEPs elicited by L and M cone isolating stimuli is consistent with previous studies that used chromatic spot stimulus (Paulus et al., 1986; Paulus et al., 1984) and would seem to justify the conclusions of Paulus et al (1984), which ascribed the generation of this N1 component to chromatic processing in the early geniculo-recipient layers of the primary visual cortex. Paulus and his co-workers also considered the P2 component in their study and described it as the luminance dominated component which has its latency at about 120ms. In the present study as well as in Valberg and Rudvin (1997) study, P2 component had a longer latency at about 140-180ms. This is possibly due to differences in experimental conditions between the studies. For example, Paulus and his co-workers used a shorter onset (300ms) stimulus presentation with a yellow adaptation background, where as in this study the onset period is 500ms and the background was grey.

The amplitude and latency data suggest that, all components of the isoluminant chromatic VEPs along +S-(L+M) cone axis have smaller amplitudes and longer latencies compared to the L and M cone cardinal axis. Previous VEP studies, which used isoluminant chromatic gratings, have also noted relatively weak S cone mediated responses (Berninger and Arden, 1991; Kulikowski, 1989). They

suggested that this is because of fewer neurons signalling S-(L+M) as opposed to L-M opponency, in the primary visual cortex (Ts'o and Gilbert, 1988).

Size response functions are greater for P2 component than N1 component and the P2 is more prone to luminance contrast content changes as we noted in chapter 5. This finding suggests the possibility of luminance contributions for P2 component as the stimulus size is increased. Ribeiro and Castle-Branco (2010), using chromatic VEPs, studied the variation in size response functions for L-M and S-(L+M) cone opponent axes. They have noticed differences between the areas of summation observed in L-M and S-(L+M) cone opponent response. But the response differences are large in comparison to our study. This could be because they used sinusoidal grating stimuli (Gabor stimuli) for VEP recordings.

Latency data indicate that all components of the isoluminant chromatic VEPs along +S-(L+M) cone axis have longer latencies compared to the +L-M and –L+M cone cardinal axes. This observation is consistent with previous human VEP studies (Rabin et al., 1994; Robson and Kulikowski, 1998) and psychophysics (Smithson and Mollon, 2004; Wade, 2009). Cottaris and De Valois (1998) proposed that the reason for the longer latency of S cone channel is of cortical origin. According to their viewpoint, the sparse S cone opponent signal in LGN is amplified in the cortex through recurrent excitatory circuit, in which the out-put of striate neuron re-enters the cell to be summed synergistically with new signals. The resulting S-cone signal is quite different from that seen in the LGN, having longer latency and slower dynamics. This process results in sluggish cortical S cone signal.

The speculation from this study is that the VEPs elicited by large chromatic spot stimuli share both transient, achromatic and sustained, chromatic response characteristics. This claim is made based on following observations. Firstly, the large size spot stimuli elicit VEPs with large offset responses. Single unit physiology has shown that, transient cells respond equally to the onset and offset phases of the stimulus and sustained cells respond mainly to the onset of the stimulus not to the offset (Gouras, 1968; Demonasterio and Gouras, 1975; Kaplan and Shapley, 1982; Blakemore and Vital-Durand, 1986). VEPs of equal onset-offset periods optimally reveal the existence of achromatic intrusions (Kulikowski et al., 1997). We think that this aspect can be applied to chromatic onset-offset VEP. If this is true, then the VEPs elicited by larger stimuli have large offset responses suggesting that there is an involvement of transient cells in generation of these responses. Numerous studies related to the chromatic and achromatic onset-offset VEPs have shown that the N1 component that occurs at about 90-135ms can be attributed to the chromatic activity generated by sustained P-cellular mechanism (Murray et al., 1986; Berninger et al., 1989; Kulikowski, 1989; Rabin et al., 1994; Kulikowski, 1991a; Paulus et al., 1984). The second observation is that the P-N-P complex seen in the offset response is large but gradually reduces as the stimulus size is reduced. Suttle and Harding (1999) have noted that the off-set responses have a diminished P-N-P complex at isoluminance, but are more apparent as the luminance contrast is added to the stimulus. Our experiment demonstrates that a well defined P-N-P complex is evident for larger size stimuli suggesting that these stimuli are prone to luminance contamination. In addition, the diminished P-N-P complex for small size stimuli suggests these stimuli mainly activate chromatic opponent neurons. Considering the two observations, it can be assumed that VEPs elicited by large

size spot stimuli reflect the mixed achromatic (transient) and chromatic (sustained) activity.

A noteworthy feature from this experiment is that, small size stimuli generated VEPs with small offset amplitudes in comparison to the onset amplitudes, especially for +L-M and –L+M cone axis. N1 latencies are also delayed in comparison to the responses generated by large stimuli. These points suggest that the responses elicited by small stimuli are mainly activated by slow, sustained, chromatic neurons. These stimuli activate fewer numbers of neurons, so the response initiated by them could be low to be detected in the VEP.

Studies have indicated contradictory views regarding the use of large stimuli in recording S-cone isolating VEPs. Some have suggested large grating stimuli can activate transient activity in the response (Kulikowski et al., 1996; Robson et al., 2006), whilst the others favour that the large stimuli can be still be used for recording chromatic responses with minimal activation of transient activity (Ribeiro and Castelo-Branco, 2010; Switkes et al., 1996). From the observations of this study, it can be speculated that the optimal size for recording VEPs along +S-(L+M) axis would be about 6°. These size stimuli (6°) seem to represent a compromise between the two extremes. Large size S cone stimuli (> 6°) induce large offset responses similar to the onset responses suggesting there is involvement of chromatic, transient activity. Previous studies that elicited S-cone VEPs have also suggested that the large size stimuli elicit large VEPs which reflect the mixed achromatic and chromatic activity. Achromatic activity in the VEPs is attributed to the effects of chromatic aberration (Kulikowski et al., 1997; Robson and Kulikowski, 1995). The VEP is also seem to be variable among the subjects, which gives a tentative clue that the achromatic intrusions are attributed to the inter-subject differences in

macular pigmentation (Robson and Kulikowski, 1996). Small size S cone stimuli on the other hand elicit VEPs that are of low N1 and P2 amplitudes. This could be because of two reasons. 1) Sparse number of S cones. 2) Subjected to macular pigmentation

The results of this experiment recommend that VEPs specific to chromatic processing are suggested by 1) N1 component that should have latency at about 90-120ms. 2) Small offset amplitudes.

In conclusion, the optimal stimulus size to record chromatic spot VEPs along +L-M and –L+M cardinal axis is about 2-4 degrees and for +S-(L+M) cone axis is about 6 degrees. The optimal size stimuli would activate mainly chromatic opponent neurons in visual cortex. On the other hand, large size stimuli are prone to variation in isoluminance point and may mainly activate both transient and chromatic neurons in visual cortex.

CHAPTER - 6 EFFECT OF CHROMATIC AXES ON CHROMATIC SPOT VEPs

6.1 INTRODUTION

Pre-cortically, chromatic information is signalled via two cone-opponent channels; L-M channel which receives opposing inputs from L and M cones and the S-(L+M) channel that receives S-cone input opposed by an additive combination of L and M cones. Studies have indicated that these two channels may have separate anatomical substrates (Dacey and Lee, 1994; Martin et al., 1997; Lee, 1999). The L-M channel has its projection from midget ganglion cells to the P-cellular layers of LGN. S-(L+M) channel is based upon output from small bi-stratified ganglion cells and has their synapse in the koniocellular zones of LGN. At later stage of processing, probably at the cortical level there is a re-organisation of the chromatic pathway from the cardinal, cone-opponent channels leading to the formation of multiple chromatic mechanisms that are tuned to many orientations in colour space. In order to study the influence of these pre-cortical and/or cortical mechanisms, we can define the chromatic stimuli used to elicit VEPs in terms of their location in colour space. One example of such space is MBDKL colour space (see chapter 3). This space can be used to study the chromatic mechanisms, cardinal or non-cardinal, which can be examined in isolation simply by changing the orientation of axis of stimulation. Studies have successfully used such space to study the chromatic VEPs in both colour normal (Rabin et al., 1994) and colour deficient subjects (Crognale et al., 1993). The present experiment uses MBDKL colour space to

study the chromatic VEPs elicited by isoluminant spot stimuli that are free from confounding effects of changes in spatial frequency.

6.2 RATIONALE

MBDKL colour space allows precise control of the activation of the L-M and S-(L+M) mechanisms. The foundation of L-M and S-(L+M) opponent mechanisms are better explained by separate P- and K- cellular pathways. These different underlying mechanisms provide impetus to examine:

1) To examine the morphology of the chromatic VEPs elicited by L-M and S-(L+M) cone isolating stimuli reflect these differences?
2) To assess the influence of L-M and S-(L+M) opponent mechanisms have in the generation of chromatic VEPs.

The novel approach of this experiment is to investigate how the morphology and components of the chromatic spot VEPs were affected as function of chromatic axes. To our knowledge, none of the studies have looked at the effect of chromatic axes on chromatic spot VEPs.

6.3 METHODS

Full details of the stimulus configuration and the VEP procedure, are presented in sections 3.3 and 3.4. Stimuli were modulated along the sixteen chromatic axes in MBDKL colour space that included L-M, -L+M, S+(L-M) and –S+(L+M) cardinal axes and twelve chromatic axes that relatively activate L, M and S cones (see figure 6.1). Stimulus size chosen was 2 degrees. For the each

stimulus, VEPs were recorded from the channel Oz until the response showed a discriminable waveform. Five subjects, ranging in age from 24 to 40 years, were used. All subjects had visual acuities of 6/6 or better (with refractive correction where necessary) and all subjects were found to be colour normal, using the Farnsworth- Munsell 100 Hue colour vision test. The relative amount of L, M and S cone excitations in terms of cone contrast were summarized in general methods section.

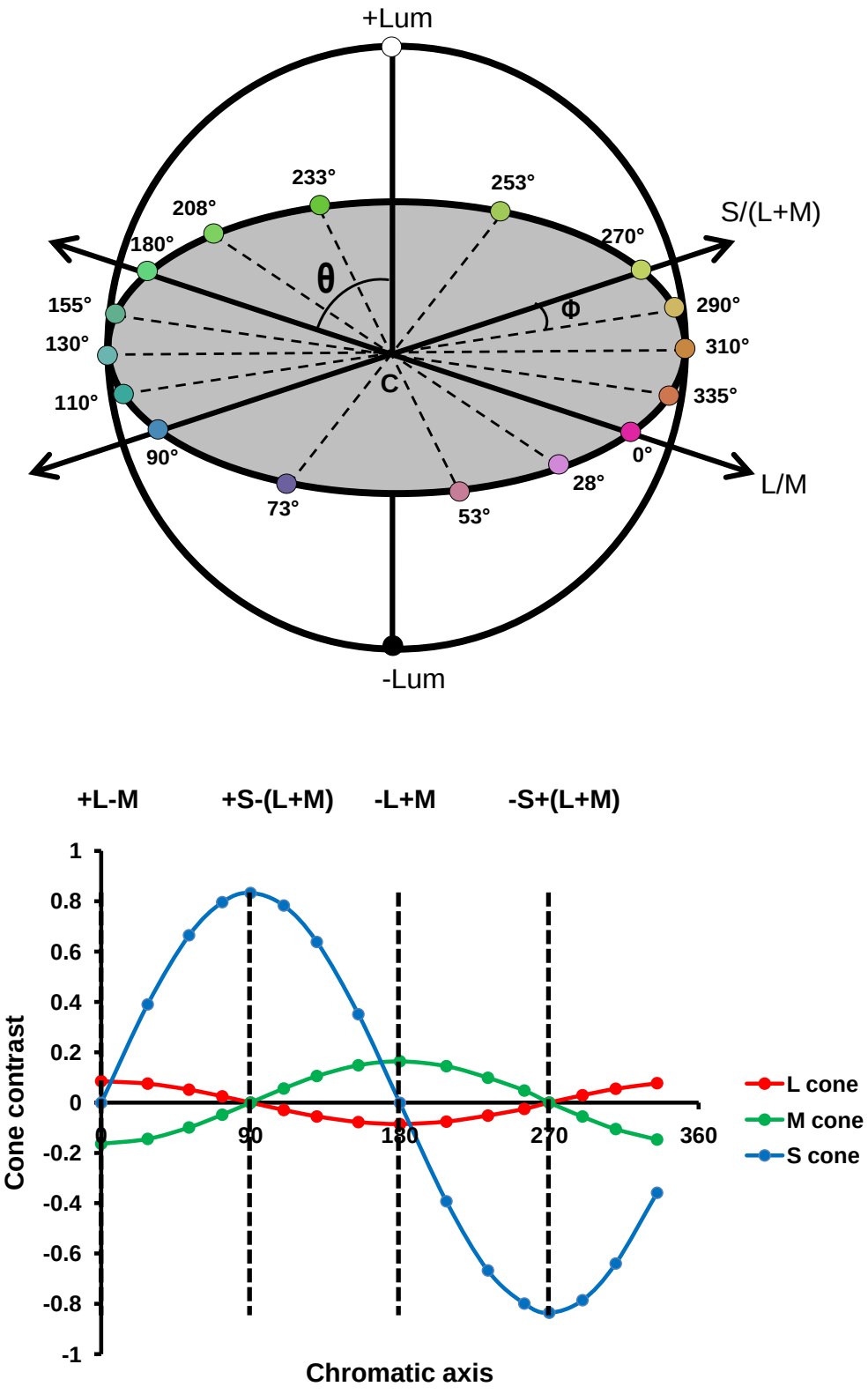

Figure 6.1 Upper plot shows the MBDKL colour space. Lower plot shows relative cone contrasts of L, M and S cone contrasts along different chromatic axis.

6.4 RESULTS

6.4.1 Morphology

Figure 6.2 shows the group averaged chromatic onset VEPs for the 16 chromatic axes investigated. Examination of the data shows that changing the axis of chromatic stimulation does have an effect on the morphology of the VEP waveforms. The N1 component, for example, is a feature of onset response that has a varying degree of prominence depending upon the chromaticity of the stimulus and it almost disappears for +S-(L+M) and –S+(L+M) axes. The P2 component forms a prominent feature of the onset response for most axes of stimulation and can be easily observed in group averaged responses but was clearly diminished for responses elicited by S- cone isolating stimuli. The amplitude of the offset component for L-M cone isolating stimuli show robust responses whilst elicited by S-cone isolating stimuli are reduced in comparison.

6.4.2 Amplitudes:

The amplitudes were measured to the wave peak from the proceeding trough or vice versa. The amplitude of N1 and P2 components as a function of chromatic axis were presented in the figure 6.3. The figure clearly shows that the N1 and P2 components have varying degree of amplitudes depending upon the chromaticity of the stimulus. The amplitude of this two components reach a maximum closer to the +L-M and –L+M cone isolating axes and gradually diminishes as the axis of stimulation shifts towards S-cone isolating axes. This could be attributed to the smaller population of S cones relative to that of the L and M cones (Roorda and Williams, 1999; Brainard et al., 2000). Small

difference in amplitudes of the N1 and P2 components along +L-M and –L+M chromatic axes may be attributed to the difference in numbers of L and M cones (Roorda and Williams, 1999; Brainard et al., 2000) in the retina.

The N2 amplitude (Figure 6.4) reaches its maxima along the +L-M cone isolating axis, reaches a minima at –S+(L+M) axis and seems to vary across other chromatic axes tested. P3 amplitudes, on the other hand, reach its maxima, along +L-M, -L+M chromatic axes and gradually decreases as the axis of stimulation shifts towards S-cone isolating axes. The P3 amplitudes are smaller along -S+(L+M) axis than +S-(L+M) axis.

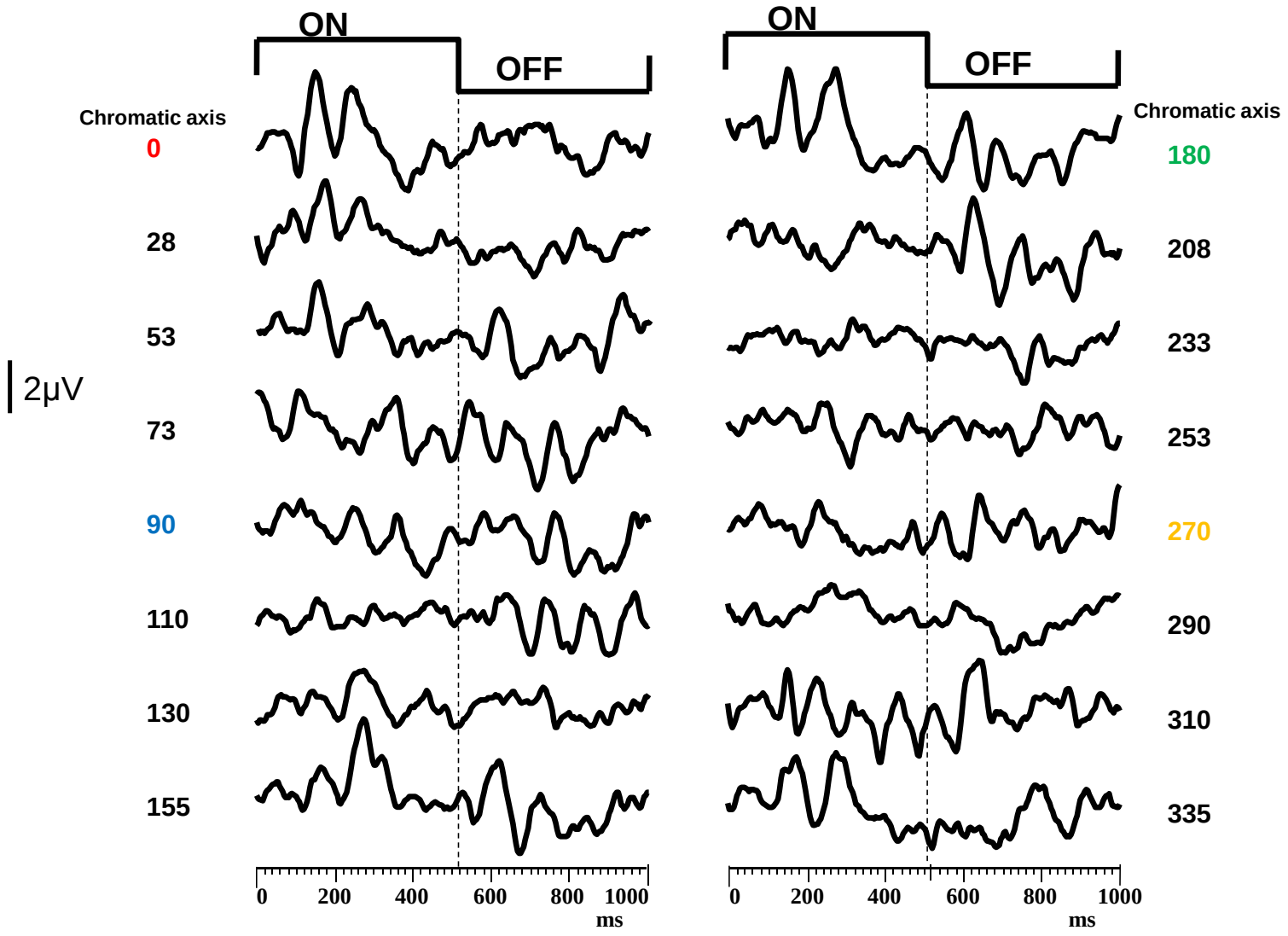

Figure 6.2 Group average (n=5) chromatic VEP responses as function of the sixteen chromatic axes.

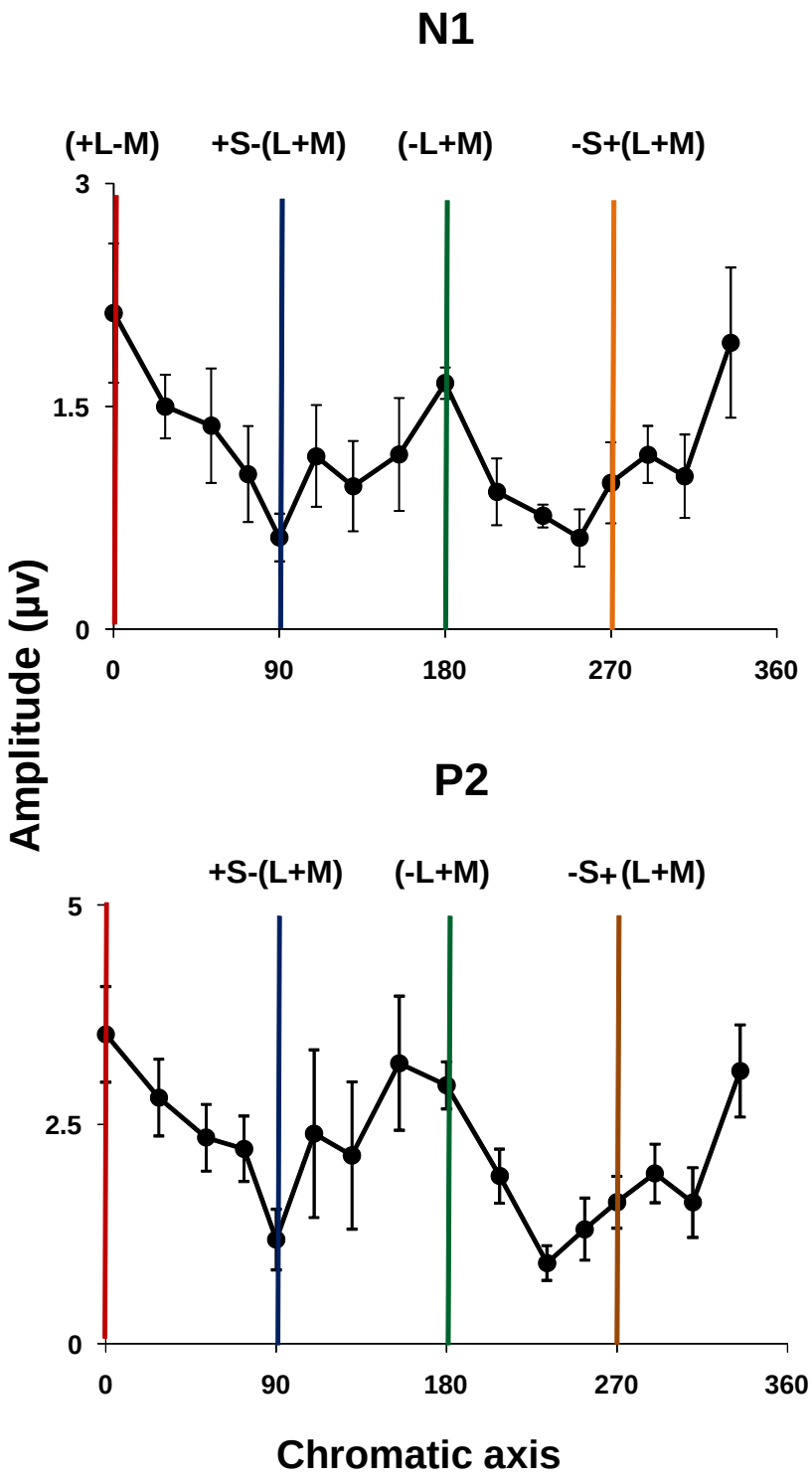

Figure 6.3 Group average data (n=5) of N1 and P2 amplitudes as a function of chromatic axis. Error bars represents ± standard devation.

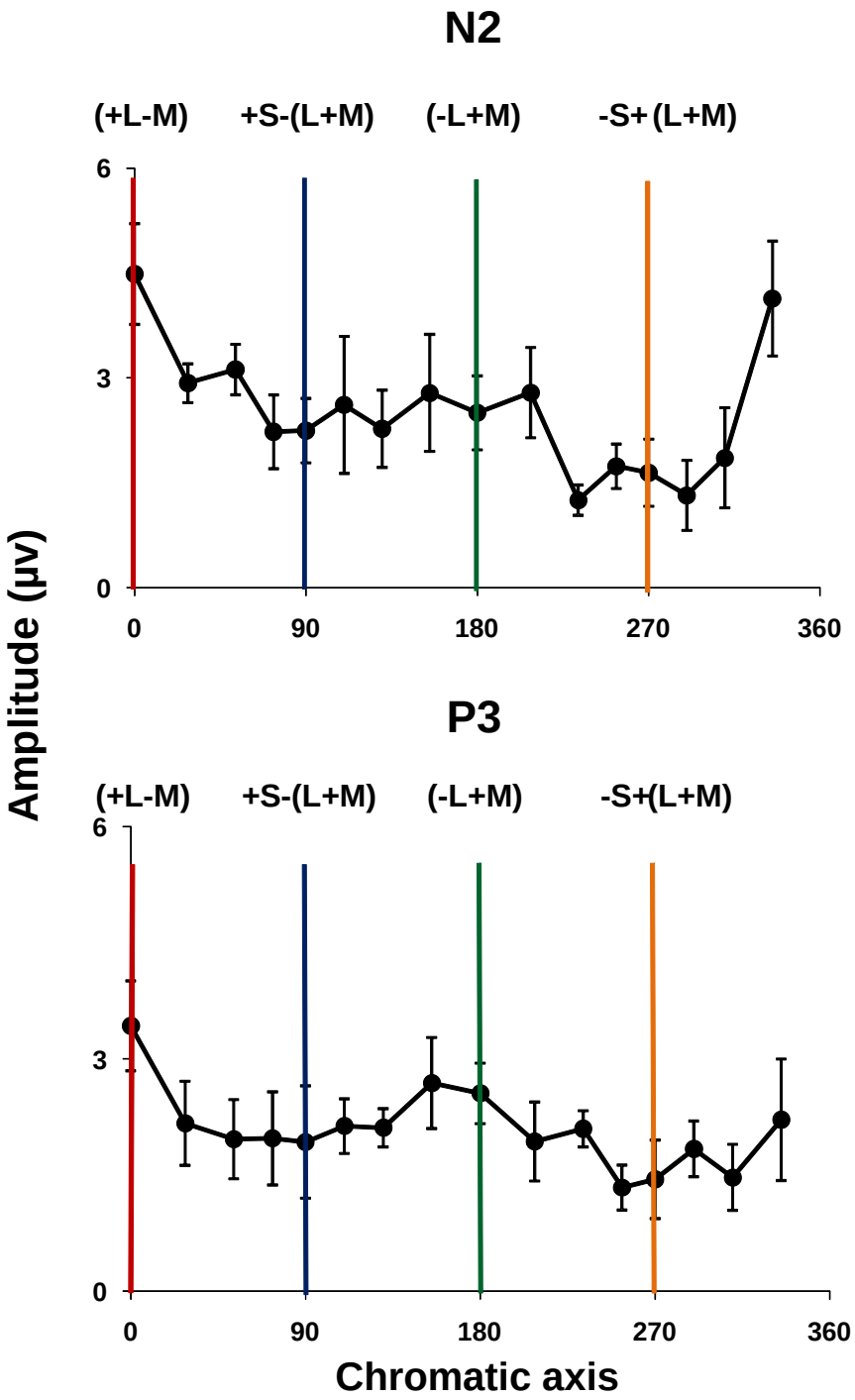

Figure 6.4 Group average data (n=5) of N2 and P3 amplitudes as a function of chromatic axis. Error bars represents ± standard devation.

6.4.3 Latencies

The latency of the N1 component as a function of the chromatic axis is shown in figure 6.5A. The figure shows that shorter latencies for L-M cone isolating axes and delayed latencies for S cone isolating axes. The latency difference of about 30-35 ms was noted between L-M cone isolating axes to S cone isolating axes.

The P2 (Figure 6.5) and N2 (Figure 6.6) components have shown delayed latency along the –S-(L+M) axis. Shorter latencies were observed for these two components along +L-M, –L+M and +S-(L+M) axes. P3 (Figure 6.6) component on the other hand, have shown delayed latency along the chromatic axes 53° and 233°. Relatively shorter latencies were observed along four cardinal axes.

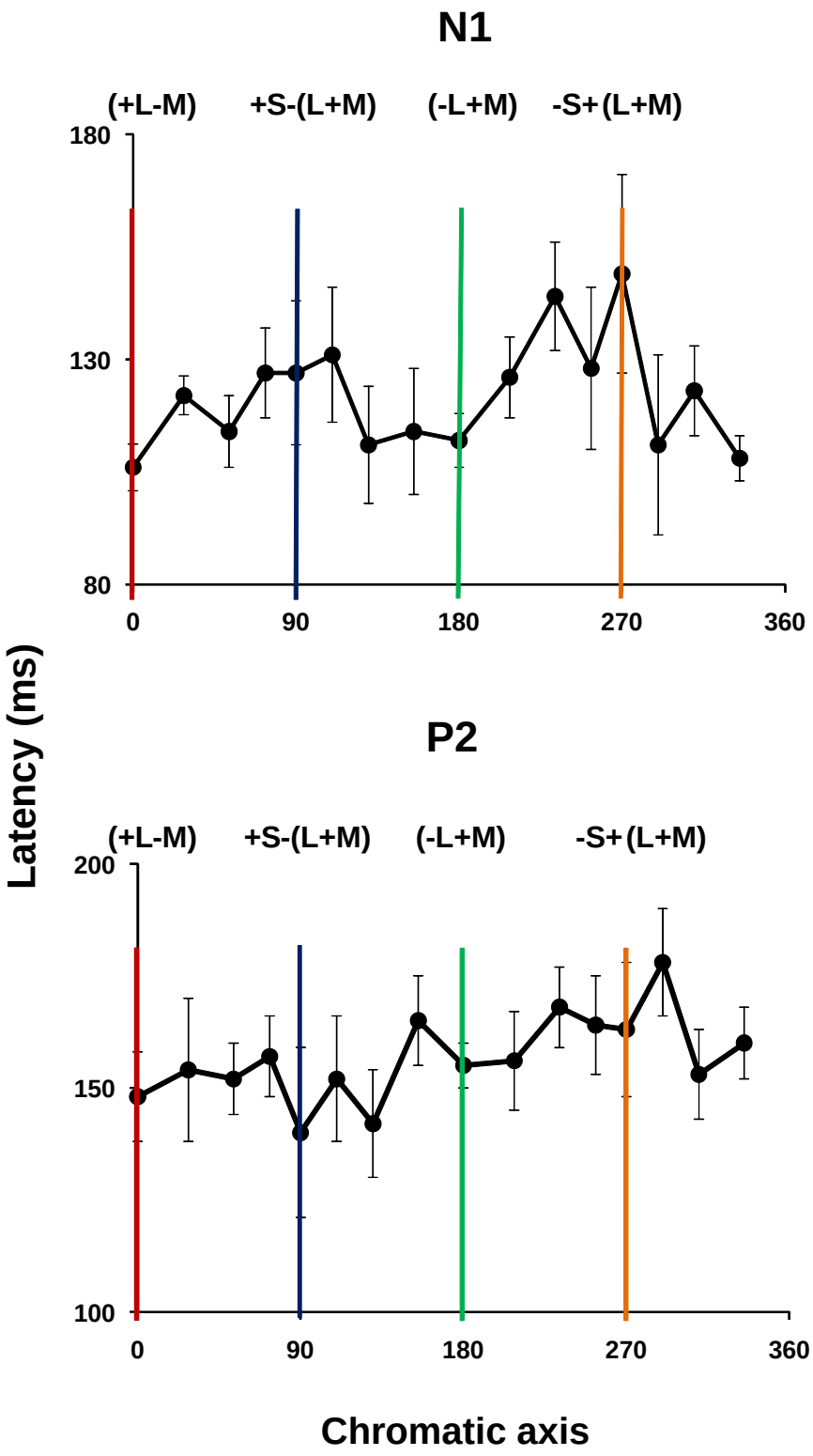

Figure 6.5 N1 (upper plot) and P2 (lower plot) latencies calculated from group average VEP as a function of chromatic axis. The data represents the group average data of 4 subjects.

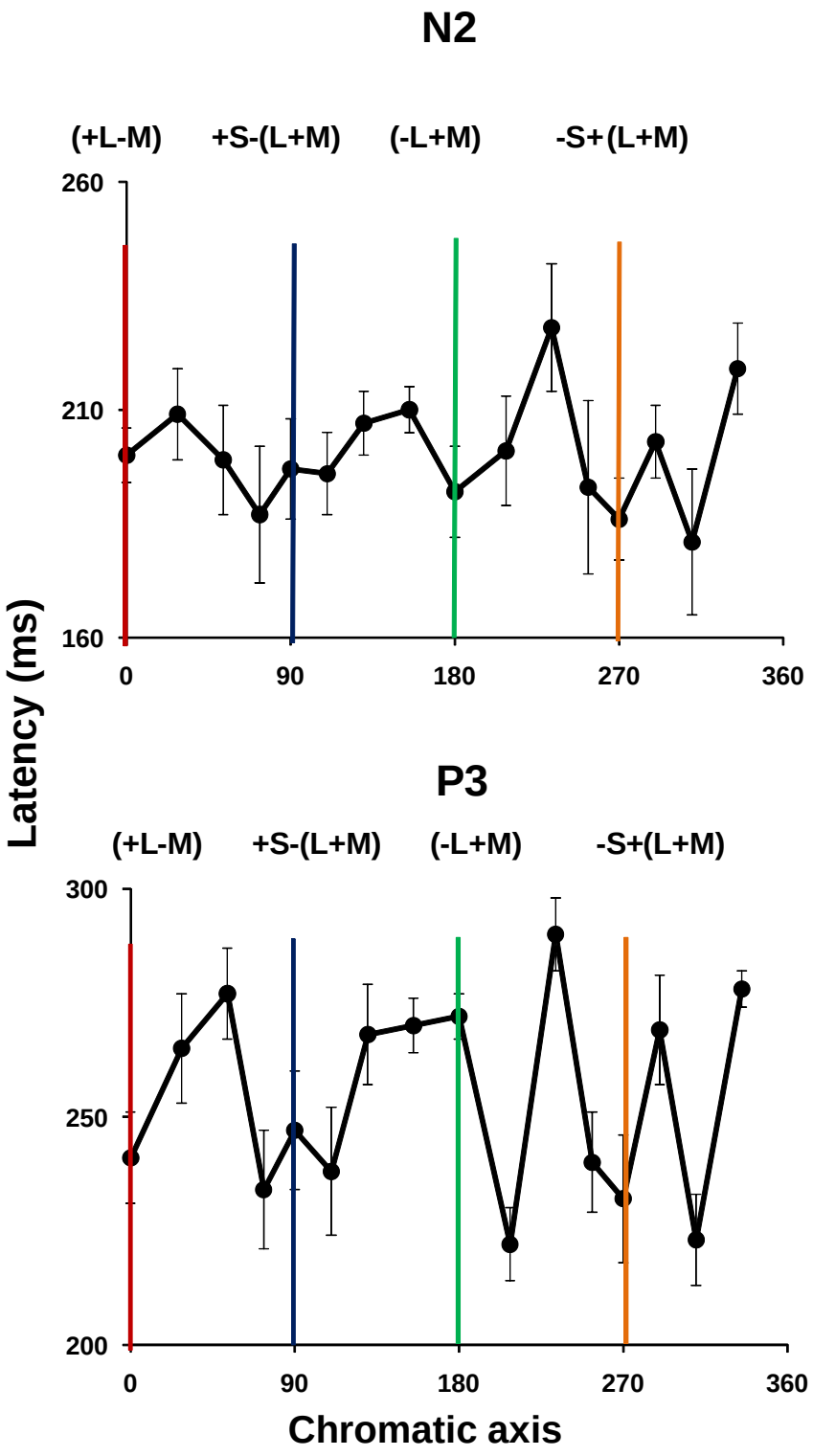

Figure 6.6 Plots of the N2 and P3 latencies calculated from group average VEP as a function of chromatic axis. The data represents the group average data of 4 subjects.

6.5 DISCUSSION

This experiment has examined the morphology of the VEPs elicited by spot stimuli which undergo equiluminant changes in chromaticity in which contributions from the L, M and S cones varied systematically. Changing the axis of chromatic stimulation produces changes in the morphology of the chromatic VEP responses that are dependent upon the degree of activation of L-M or S-(L+M) opponent mechanisms. The morphological differences are consistent with the underlying neuro-antomical pathways being involved in the processing of L-M and S-(L+M) opponent signals. The former originates from midget ganglion cells and relays to the P layer of the LGN, whilst the latter stems from small bi-stratified ganglion cells and projects to the K neurons in the LGN (Dacey and Lee, 1994; White et al., 1998; Calkins, 2001).

Along the L-M cone isolating axes, the chromatic onset VEPs showed prominent N1 and P2 components. The presence of the early negative component (N1) in chromatic VEPs elicited by L and M cone isolating stimuli seems to be consistent with previous studies that have examined chromatic spot stimuli (Paulus et al., 1984; Paulus et al., 1986) and would seem to justify their conclusion that the generation of this component is associated with chromatic processing in the early geniculo-recipient layers of the primary visual cortex. However, VEPs elicited by the S-cone isolating stimuli were unsuccessful in displaying such a predominant N1 component. This suggests that the early negativity may not be a standard marker of colour related activity but instead reflect the chromatic processing that takes place within the P-pathway as opposed to the K- pathway.

Latency data indicate that all components of the isoluminant chromatic VEPs along the S cone axis have longer latencies compared to the +L-M and –L+ M cardinal axis. This observation is consistent with previous human VEP studies (Rabin et al., 1994; Robson and Kulikowski, 1998) and psychophysics (Smithson and Mollon, 2004; Wade, 2009). Previous studies have also compared reaction times for isoluminant stimuli along L-M and S cone axis and have shown that S-cone pathway is sluggish in comparison to L-M cone axis. Whilst McKeefry et al (2003) reported that the S-cone axis has a lag of 40ms; Smithson and Mollon (2004) found that the difference between L-M and S-cone pathway does not exceed 20-30ms.Cottaris and De Valois (1998) proposed that the reason for the longer latency of S cone channel is of cortical origin. According to their viewpoint, sparse S cone opponent signal in LGN is amplified in the cortex through recurrent excitatory circuit, in which the output of striate neuron re-enters the cell to be summed synergistically with new signals. The resulting S-cone signal is quite different from that seen in the LGN, having longer latency and slower dynamics. This process results in sluggish cortical S cone signal. Other proposal was that supports this finding is delayed optic chaismal and antidromic stimulation of the extra striate cortex by K neurons (Norton and Casagrande, 1982; White et al., 2001).

Recently Shinmori and Werner (2008) measured the impulse response functions (IRF) for isoluminant stimuli along S-ON and S-OFF channels. They noted S cone OFF signals are substantially slower than S cone ON signals. Results of our data have shown a latency difference of 35-50 ms for S-OFF and S-ON axes, former being sluggish. Our results seem to be strongly in agreement with the Shinmori and Werner findings. In contrary, the reaction

times measured by Mckeefry et al (2003) find sluggish responses along the S-ON channel. The reason for the discrepancy is unclear.

Differences between the morphologies of the VEPs elicited by blue and yellow patterned stimulation have also been noted in previous studies (Korth et al., 1993 , Korth and Nguyen, 1997). Asymmetries between the blue-on/yellow-off and yellow-on/blue-off mechanisms have also been noted in some psychophysical studies (Shinomori et al., 1999; Vassilev et al., 2000; McLellan and Eskew, 2000), but not others (Smith et al., 1989; DeMarco et al., 1994; Schwartz, 1996). One might hypothesize that the existence of differences in response properties may echo the underlying neurophysiology of the blue-on and off pathways, which are thought to be supported by very different retinal circuitry. The blue-on pathway compromises small bi-stratified ganglion cells that project to the P cells that project to the P- and K- layers of the LGN. Whilst on the other hand, it is thought that blue-off pathway is based on ganglion cells that are midget-like, although this has yet to gain wide acceptance.

Separate ON and OFF processing pathways within the cone opponent mechanisms are well described by recent psychophysical investigations. The studies infer that colour vision may be more accurately thought of comprising of four separate mechanisms (+L-M = ‘red-on/green off’; +M-L = ‘green-on/red-off’; +S-(L+M) = ‘blue-on/yellow-off’ and –S+(L+M) = ‘yellow-on/blue-off’) rather than two opponent mechanisms described previously. The similarity between the red-on/green-off and green-on/red-off VEPs suggests a common, balanced substrate for these responses. However, the VEPs generated by blue-on/yellow off and yellow-on/blue-off stimuli are qualitatively dissimilar in appearance implying that different populations of neurons are involved in their generation.

CHAPTER-7 L AND M CONE ISOLATING ERGs AS FUNCTION OF TEMPORAL FREQUENCY.

7.1 INTRODUCTION

Experimental studies have provided evidence to suggest that ERGs can be used to study post-receptoral retinal activity such as bipolar cell activity or spiking activity of ganglion cells (Holder, 2001; Sieving et al., 1994; Viswanathan et al., 1999; Viswanathan et al., 2000; Viswanathan et al., 2002). Until recently there has been little evidence to indicate that the ERG signals are directly driven by post-receptoral mechanisms. Kremers et al (2000) were the first to propose that flicker ERGs that vary in temporal characteristics can reflect P- and M-cellular post-receptoral mechanisms. According to their model, the high and low temporal ERGs reflect M- and P- cellular properties respectively (see figure 7.1).

The proposed model is strengthened by recent work of Kremers and Link (2008). They have demonstrated (see figure 7.2) that with appropriate choice of temporal stimulation parameters, the ERG can be made to reflect the operation cone-opponent (chromatic) and non-opponent (luminance) post-receptoral mechanisms (Kremers and Link, 2008; Kremers et al., 2009). Low temporal frequency flicker (~12Hz) ERGs have response properties which are consistent with their generation by cone-opponent, chromatic mechanisms. In these responses, the ratio of L- to M-cone driven ERG amplitudes is close to unity and the difference between their response phases is close to 180° (Kremers and Link, 2008). By comparison, ERGs that are elicited by faster flicker frequencies (>30Hz) have response properties that are consistent with their mediation via

non-opponent, luminance post-receptoral mechanisms. For example, the L- and M-cone response ratios for these faster flicker ERGs are greater than unity and highly variable across individuals. They also tend to be abolished by isoluminant stimulation (Kremers et al., 2009).

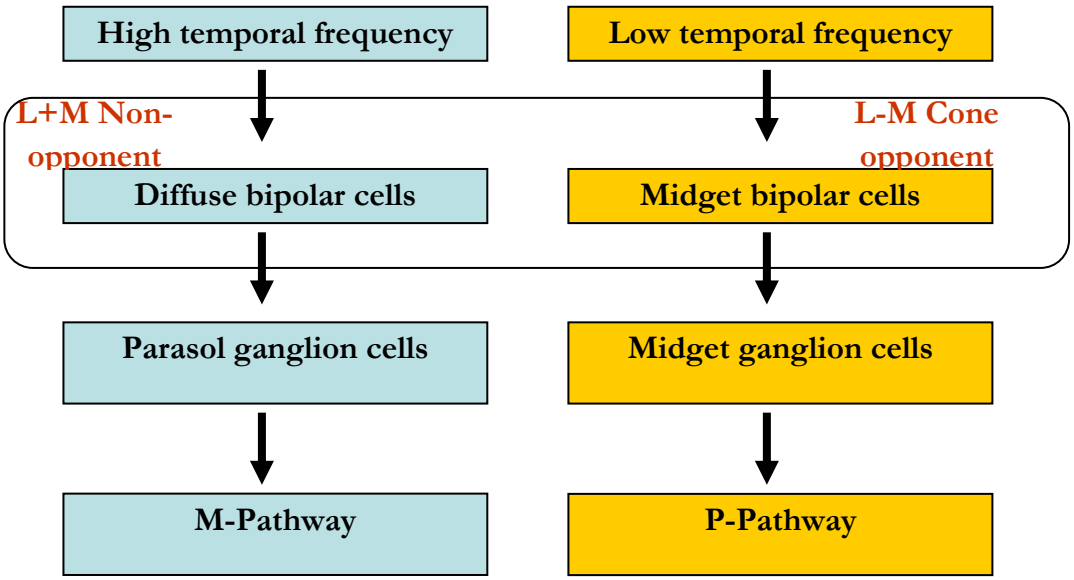

Figure 7.1 Model of the origin of the flicker ERGs at low and high temporal frequencies reflecting P and M pathways in early the visual system. The model is based on Kremers (2003) work.

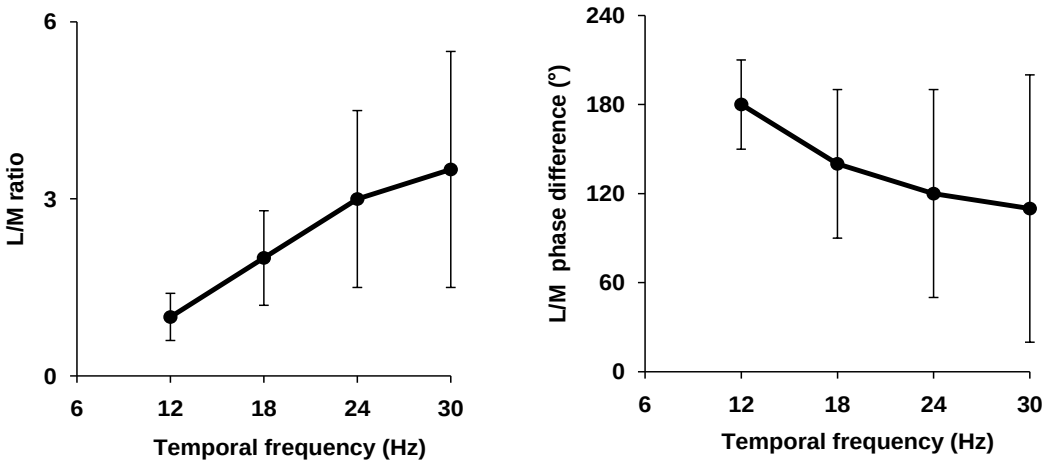

Figure 7.2 Mean L/M ratios (left side plot) and L-M phase differences (right side plot) as function of temporal frequency. The data shows an increase in L/M ratio and decrease in phase difference, with increase in temporal frequency. At 12 Hz, L/M ratio was close to unity and phase difference close to 180°. The upper and lower limits in the L/M ratio plot indicate the standard deviations of the logarithm of the ratios. The picture adapted and modified from Kremers and Link (2008).

7.2 RATIONALE

Based on differences between low and high temporal frequency ERG response properties, we would like to examine the effects of temporal frequency on L and M cone mediated ERG response amplitudes and phases. The amplitude of the L and M cone responses at various temporal frequencies would be useful to measure the L and M cone weightings to post-receptoral mechanism. Similarly, L and M cone response phase would be useful to ascertain whether the L and M cones interact in an additive or opponent fashion.

7.3 METHODS

7.3.1 Stimulus generation

The stimuli comprised temporal exchanges between two colours, the chromaticities and luminance of which were chosen so that some photoreceptor types did not respond to the exchange and are therefore 'silenced' (see: Estevez & Spekreijse, 1974; 1982; Kremers, 2003). All stimuli were presented on a Sony GDM500 CRT monitor (refresh rate = 120Hz) (Sony Corporation, Tokyo, Japan) controlled by a VSG 2/4 graphics card. The time and space averaged luminance of the monitor was 66cd/m2. Spectral characteristics of the CRT phosphors, chromaticity co-ordinates and luminance were calibrated using a PR650 spectrascan spectroradiometer.

The stimuli we employed actually constituted *double* silent substitutions (See section 3.5.2 for silent substitution stimuli). For M-cone isolating stimuli we silenced the L-cones along with rods. For L-cone isolating stimuli we silenced the M-cones along with the rods.

7.3.2 Stimulus configuration

The stimulus configuration used to record the ERGs at six temporal frequencies consists of a circular disc of angular subtense equal to 70° at 10cm viewing distance.

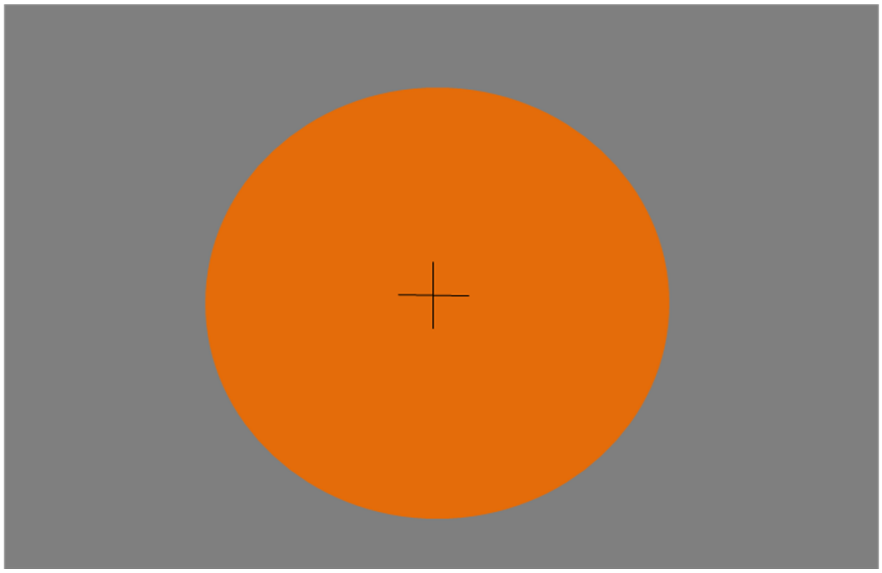

Figure 7.3 Stimulus configuration used to record the ERGs. Note that the background luminance is 66cd/m^2 silent substitution stimulus is flickered at various temporal frequencies to record the ERG responses. Stimulus was subtending 70° at 10cm distance.

Modulation depth and phase were chosen in such a way that either L or M cones were stimulated. Cone contrasts were equalized for each stimulus condition at 20%. The rods were not stimulated in any of these conditions. The isolation of L and M cones by our stimuli were validated for all the conditions in control experiments on dichromats (see methods section).

7.3.3 ERG recordings

A silver-silver chloride reference electrode was placed at the outer canthus and a ground electrode was placed on the forehead. Electrode impedances were kept below 5kΩ. The ERG signals were amplified using a Grass 15A94 amplifier (Astro-Med, Rhode Island, USA) with band pass frequency of 3-100Hz. The signals were sampled at a rate of 1024 Hz over a period of 4 seconds and averaged responses were based upon at least 20 repetitions. Fourier

components were extracted from the response using a CED 1401 smart interface (Cambridge Electronic Design, Cambridge, UK). L cone and M cone isolating ERGs were recorded at 10Hz, 12Hz, 15Hz, 20Hz, 25Hz and 30Hz respectively.

7.3.4 Subjects

Five male observers participated in this study. All were emmetropes or corrected ammetropes and were colour normal according to the Farnsworth Munsell 100 Hue test. During recording observers' pupils were dilated with 1% Tropicamide and they viewed the stimuli monocularly from a distance of 10 cm and both a chin and head rest were used. Fixation was maintained on a centrally placed black cross which subtended 2°. All subjects gave informed consent prior to the commencement of the experiments.

7.3.5 Fourier analysis

Fourier components were extracted from the response using a CED 1401 smart interface. First (1H) and second harmonic (2H) components were used for the analysis. Similarly, 1H-1Hz and 2H-1Hz magnitudes were used as a measure of the noise for corresponding harmonic frequencies for all the conditions. Fourier analysed L and M cone responses from five subjects across six temporal frequencies were examined and presented in figures 7.4, 7.5, 7.6, 7.7 and 7.8. From the FFT data of five subjects it can be observed that the ERG signal energy is large in magnitude at the first harmonic (1H). However, small second harmonic components were also observed.

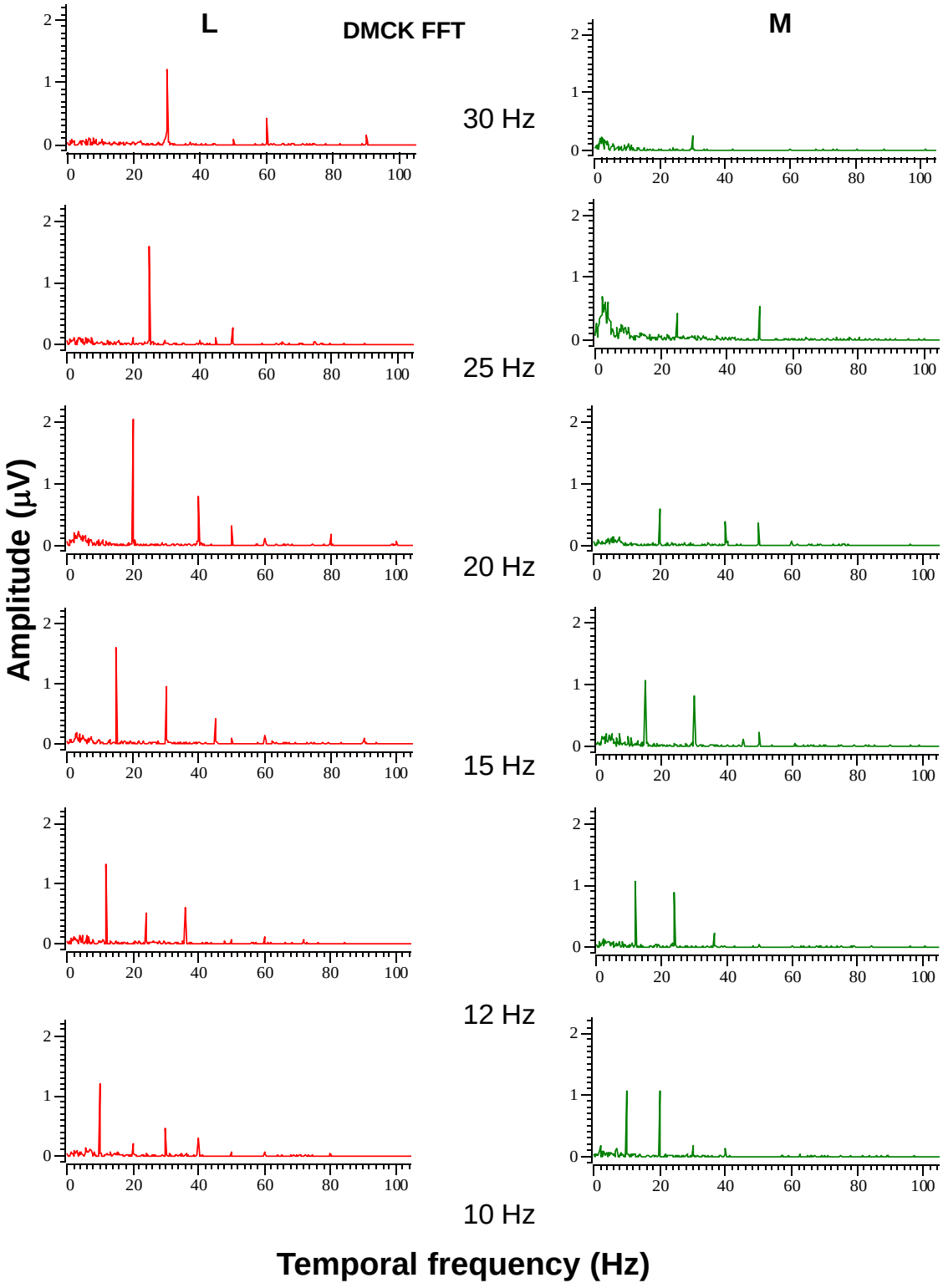

Figure 7.4 FFT analysis of subject 1. Red colour lines indicate the L cone response and green colour lines indicate the M cone response.

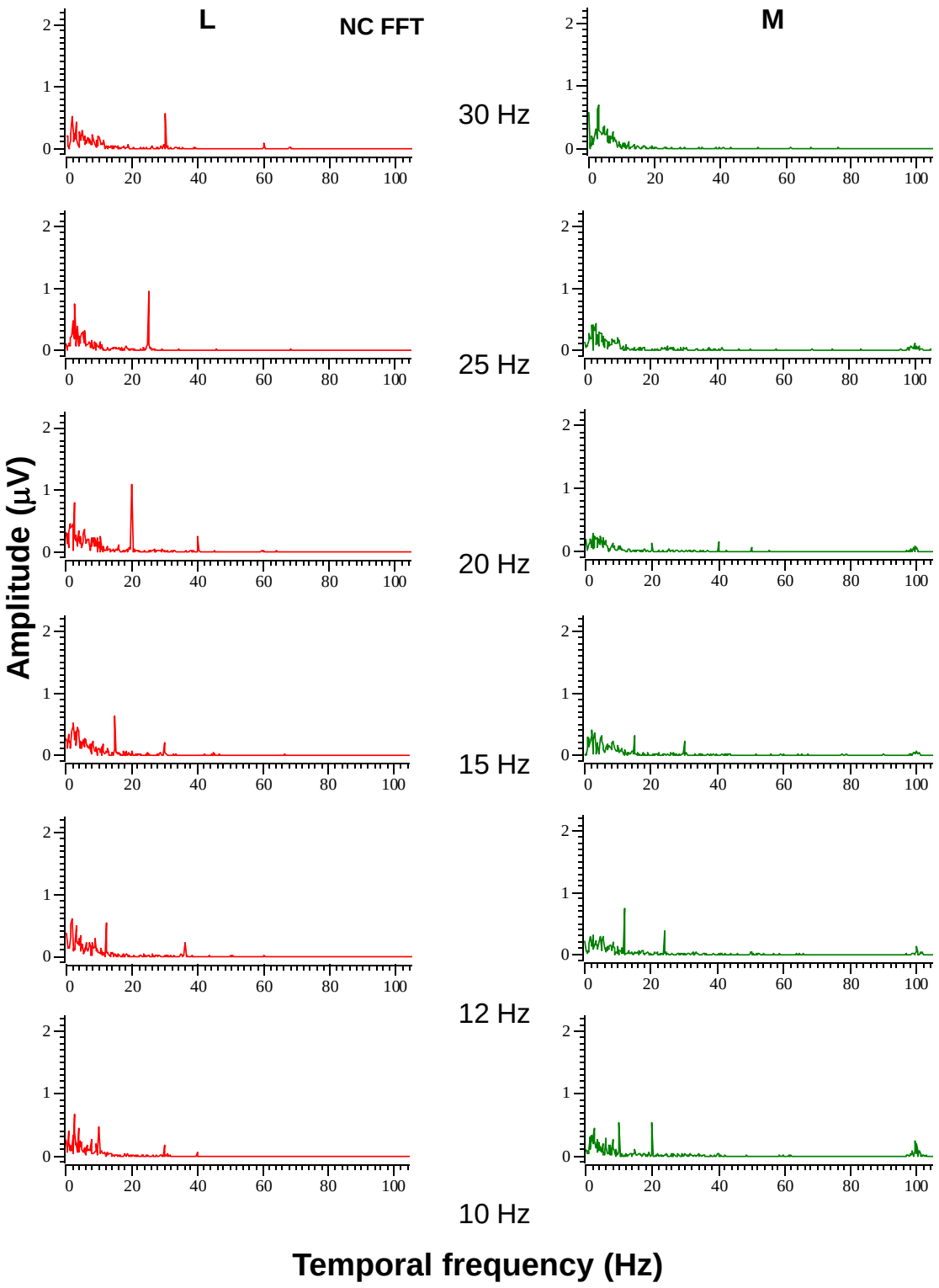

Figure 7.5 FFT analysis of subject 2. Red colour lines indicate the L cone response and green colour lines indicate the M cone response.

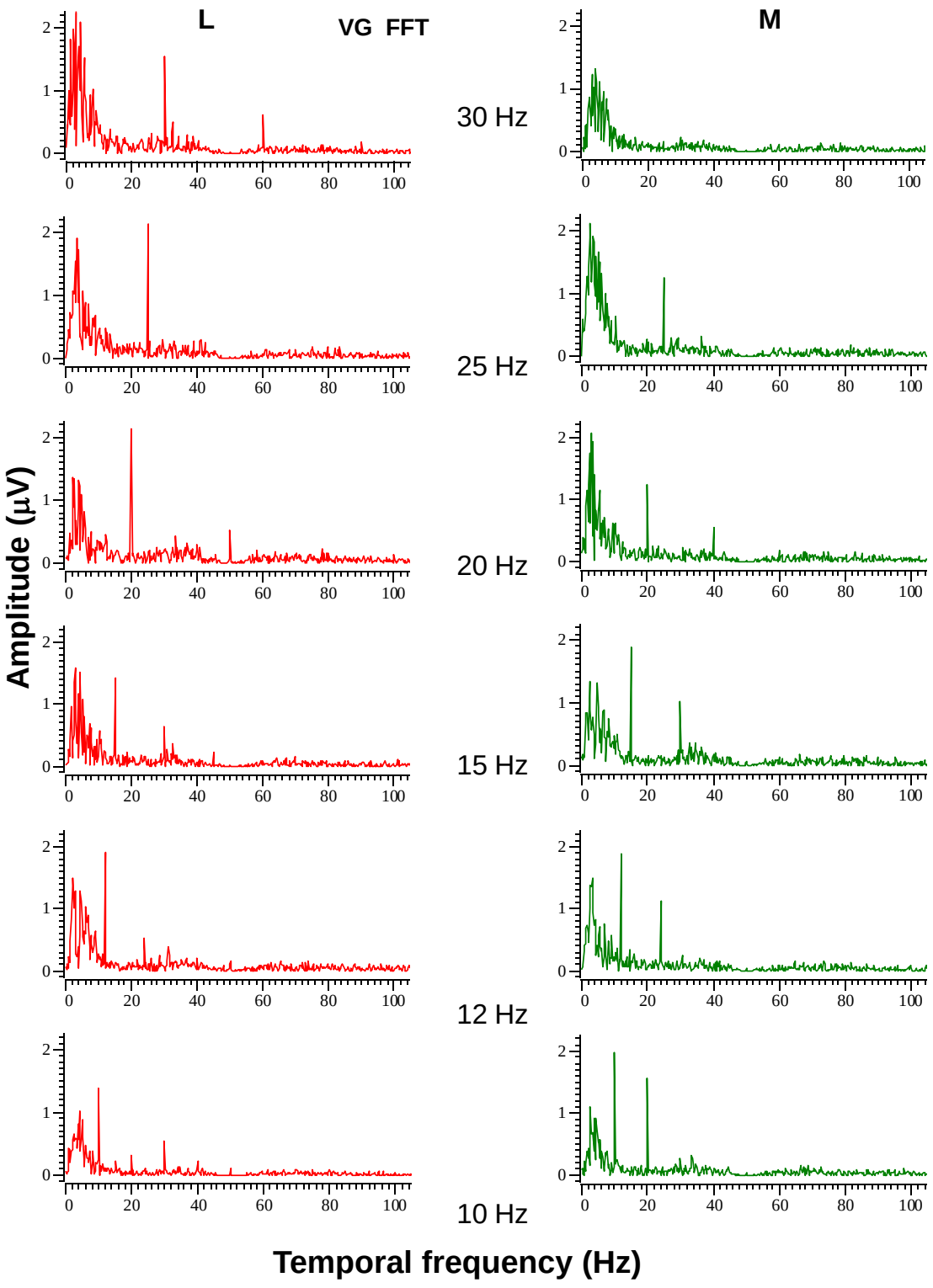

Figure 7.6 FFT analysis of subject 3. Red colour lines indicate the L cone response and green colour lines indicate the M cone response.

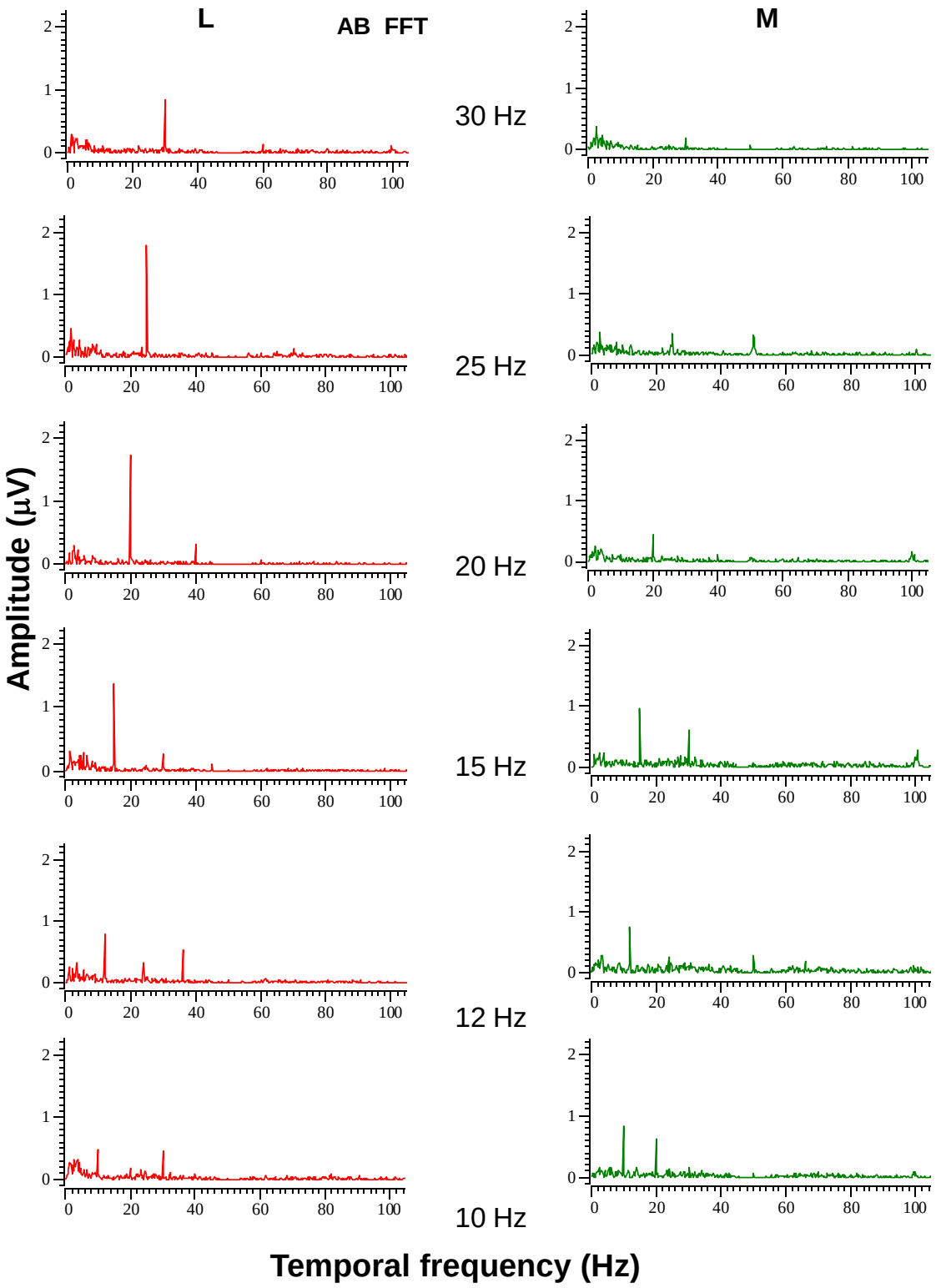

Figure 7.7 FFT analysis of subject 4. Red colour lines indicate the L cone response and green colour lines indicate the M cone response.

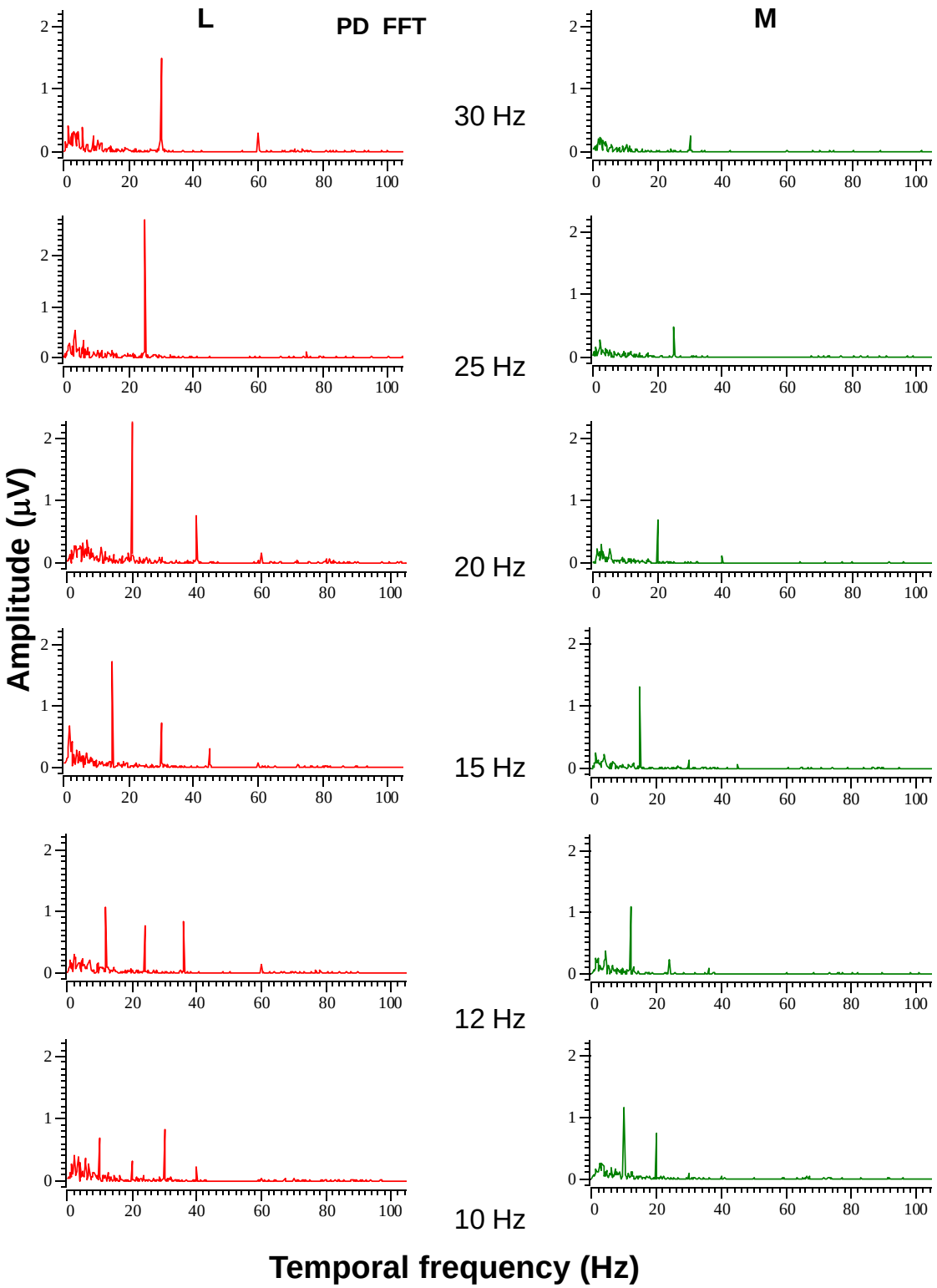

Figure 7.8 FFT analysis of subject 5. Red colour lines indicate the L cone response and green colour lines indicate the M cone response.

7.4 RESULTS

7.4.1 First Harmonic Amplitudes

The first harmonic amplitudes of the L and M cone mediated responses were plotted against temporal frequency. Individual data is plotted in figure 7.9 and the group averaged data in figure 7.10. From the group average plot it can be seen that the L cone response shows a band pass function with its maxima at 20Hz (1.977μV ± 0.61) and M cone response shows a low pass function. The amplitude for M cone response at 10Hz is 1.240μV ± 0.44. The M cone response at high temporal frequency (i.e. 30Hz) is almost negligible.

7.4.2 Second harmonic amplitudes

The second harmonic amplitudes of L and M cone mediated responses were plotted against temporal frequency is as shown in the figure 7.11 for five different subjects. Second harmonic L and M cone responses of five subjects were small in comparison to the first harmonic responses at all temporal frequencies tested. Similar to the first harmonic responses, the group averaged plot of the second harmonic data is shown in figure 7.12. From the plots it can be observed that the L cone responses show a band pass function with its maxima at 15Hz (0.559μV ± 0.295) and M cone responses show a low pass function with its maxima at 10Hz (0.940μV± 0.415). The mean data of second harmonics shows that the L and M cone responses were equal at temporal frequency of 15Hz. However, it is important to note that the second harmonic

responses were closer to the noise levels, so cautious interpretation was necessary to interpret the results.

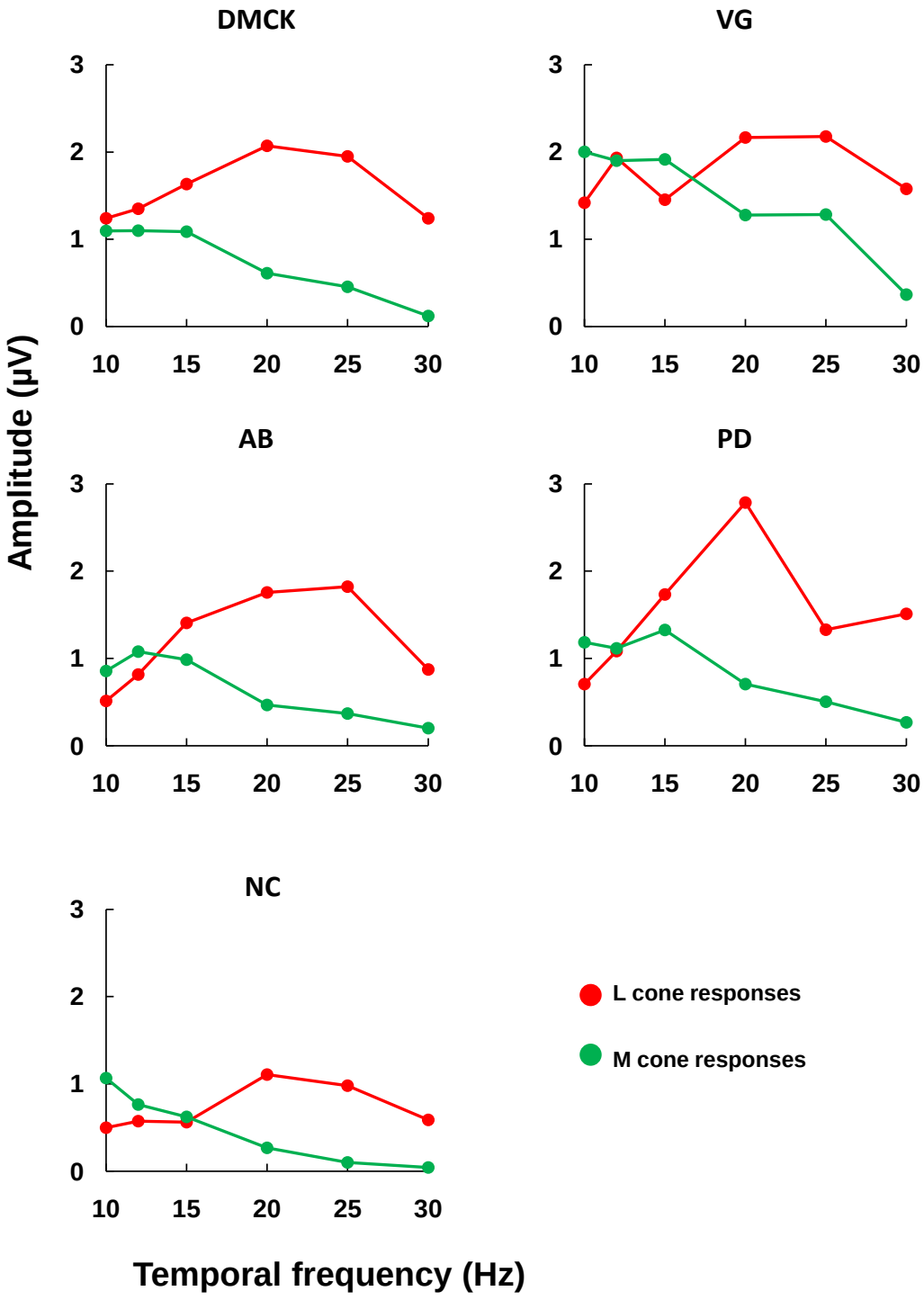

Figure 7.9 L and M cone 1st harmonic response amplitude as a function of temporal frequency in five different subjects. Note that red circles indicate the L cone responses and green circles indicate the M cone responses.

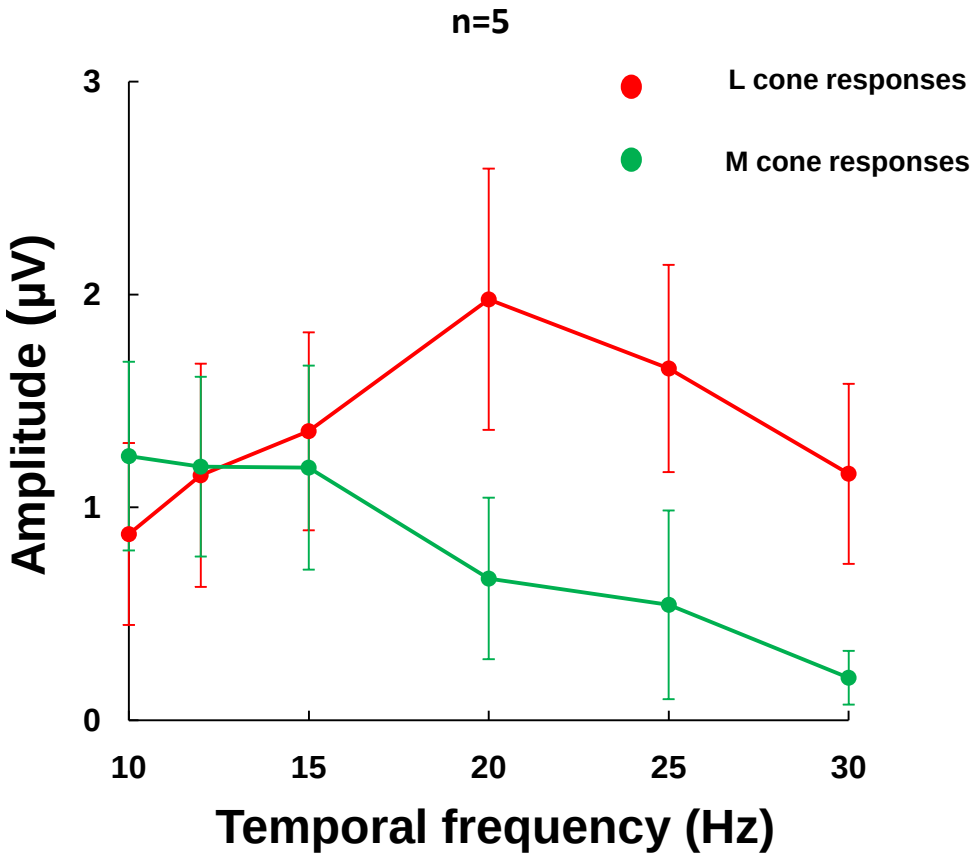

Figure 7.10 Mean of five subjects L and M cone 1st harmonic response amplitude as a function of temporal frequency. Errors bars show the standard deviation of responses among subjects. Note that red circles indicate the L cone responses and green circles indicate the M cone responses.

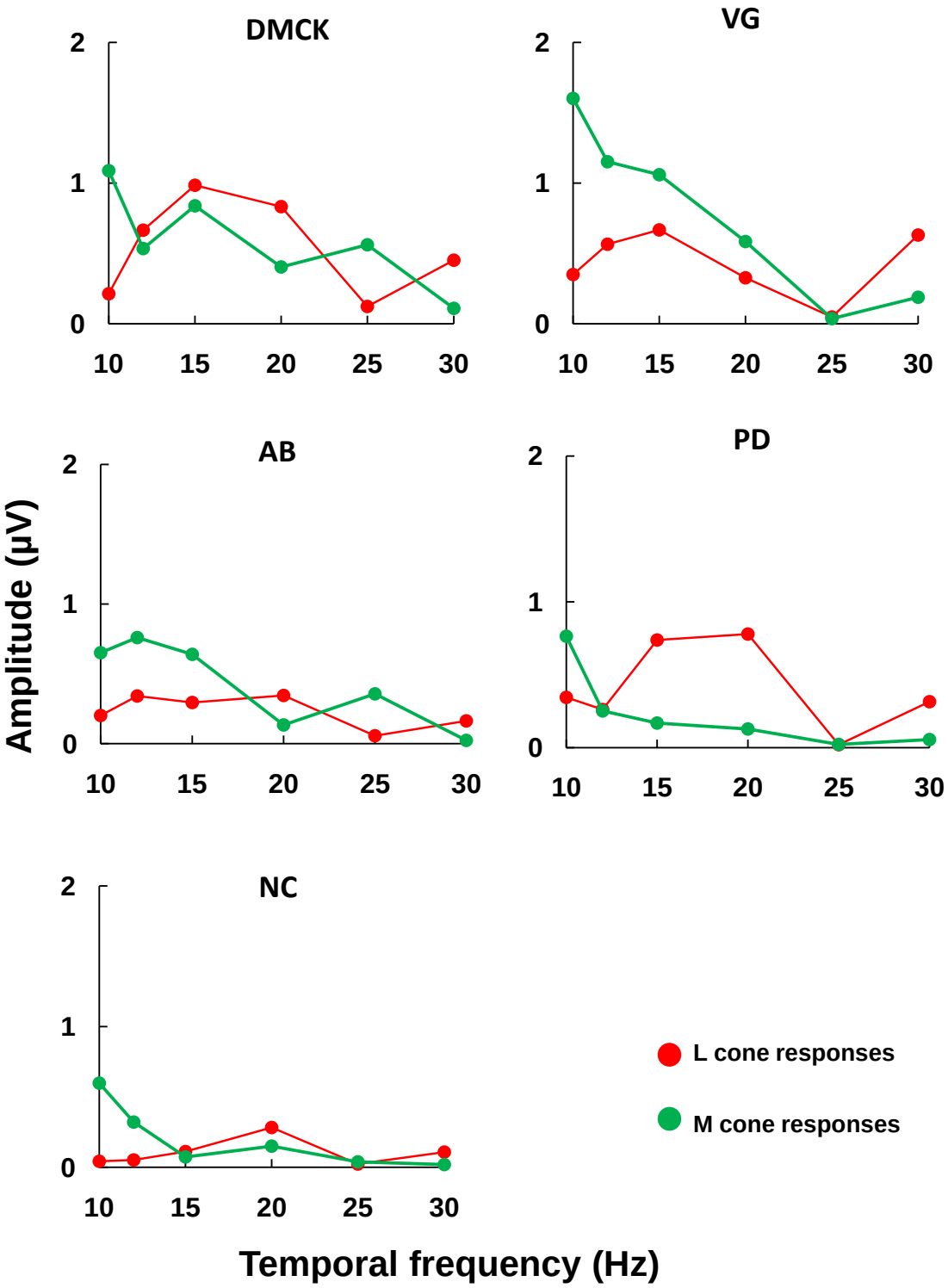

Figure 7.11 L and M cone 2nd harmonic response amplitude as a function of temporal frequency in five different subjects. Note that red circles indicate the L cone responses and green circles indicate the M cone responses.

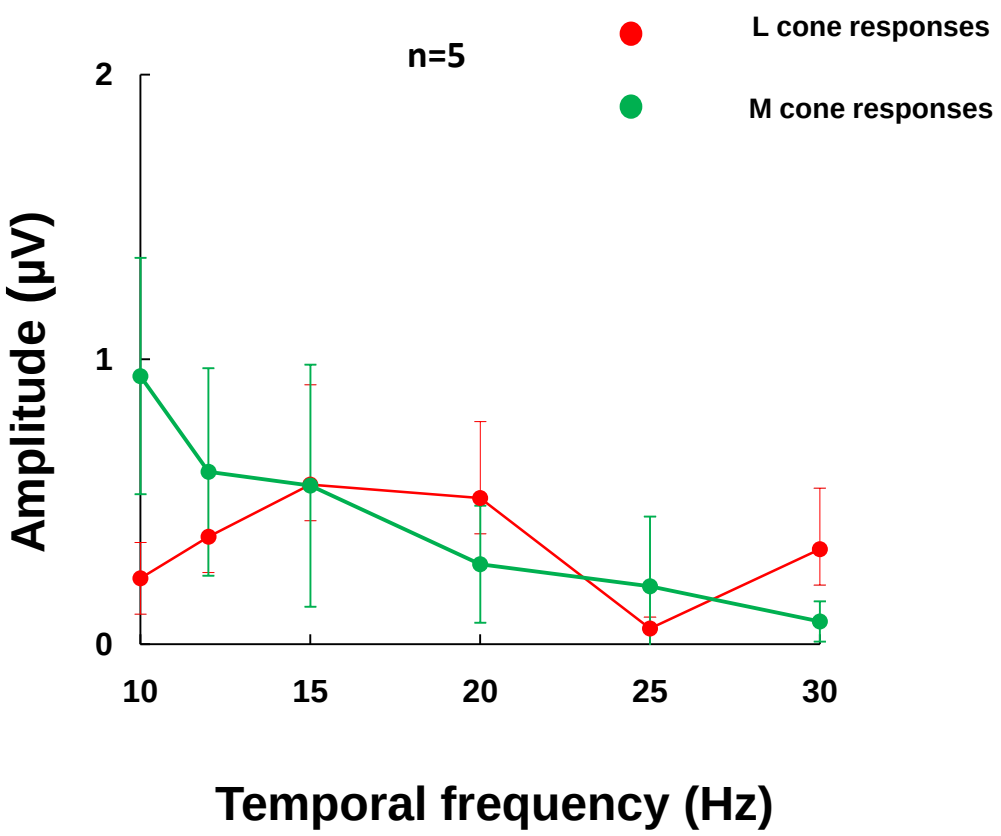

Figure 7.12 Mean of five subjects L and M cone 2nd harmonic response amplitude as a function of temporal frequency. Errors bars show the standard deviation of responses among subjects. Note that red circles indicate the L cone responses and green circles indicate the M cone responses.

7.4.3 L:M cone ERG ratios

As stated earlier, L:M cone response amplitude ratio can be used to assess the relative L and M cone contributions to the post-receptoral mechanisms at various temporal frequencies. The L:M cone response amplitude ratio can be calculated by dividing the L cone ERG amplitude at particular temporal frequency by the M cone ERG amplitude at the same temporal frequency. The first harmonic L and M cone ERG response ratio as function of temporal frequency of 5 subjects is plotted in figure 7.13 and group average data is plotted in figure 7.14. The group average plot (figure 7.14) shows that the L:M cone response ratio is nearly unity at lower temporal frequencies (10-12Hz) and gradually increases with increasing temporal frequency. On the other hand, at higher temporal frequencies L:M cone ratios are more than unity (25-30Hz) and shows large inter-subject variation. At the highest temporal frequency (30Hz) the mean L:M ratio is 7.630 ± 4.183, the highest being 13.651 and the lowest being 4.230. At the lowest temporal frequency (10Hz) the mean L:M ratio is 0.710 ± 0.199, highest being 1.132 and lowest being 0.468.

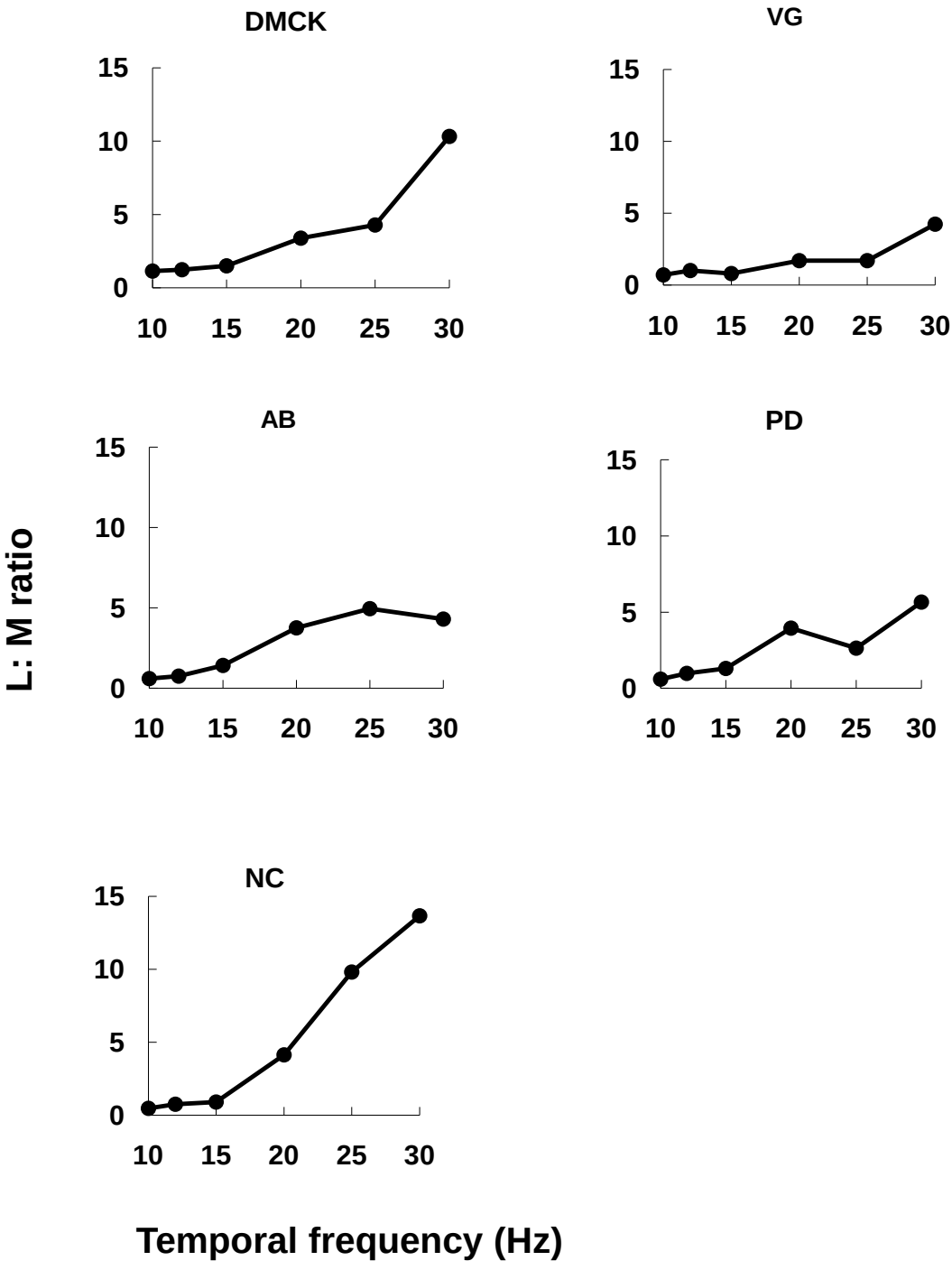

Figure 7.13 L:M cone ratios (calculated from L and M cone ERG 1st harmonic amplitudes) as function of temporal frequency in five different subjects.

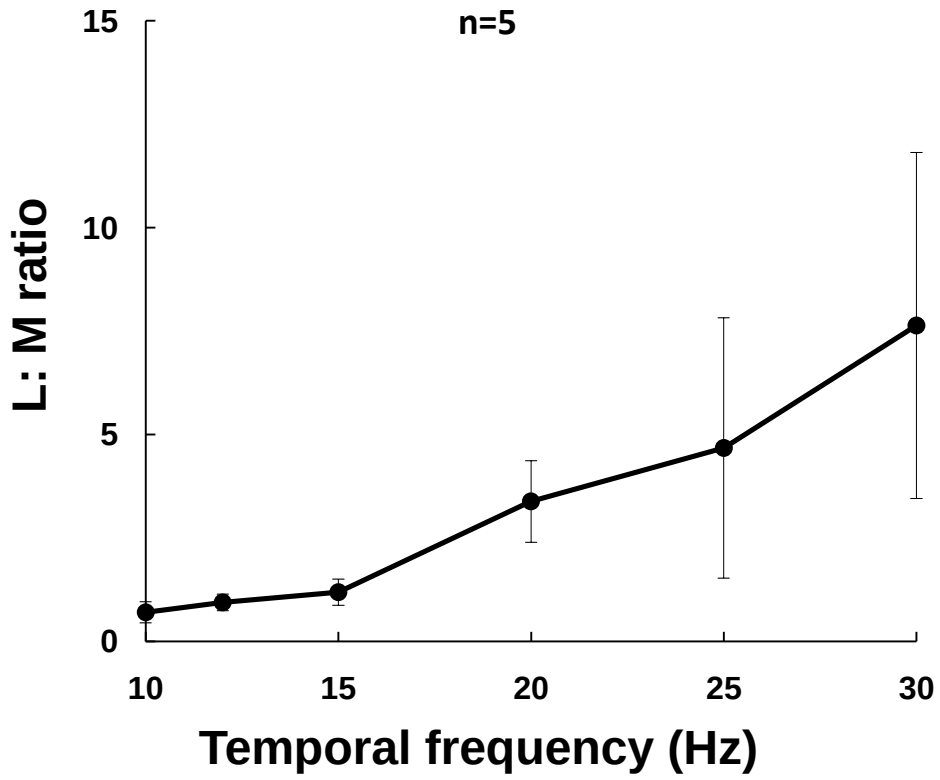

Figure 7.14 Mean of five subjects L: M cone ratios (calculated from L and M cone ERG 1st harmonic amplitudes) as function of temporal frequency. Error bars shows standard deviation among subjects.

7.4.4 L and M cone response phase differences

The L and M cone response phase difference was analysed to see how these two cones interact as a function of temporal frequency. For example L and M cone response phase difference is 180°, suggest that they interact in an opponent manner. Similarly, L and M cone response phase difference is close to 90, means that the L and M cones interact in non-opponent fashion.

The Group average data and individual data of phase differences between L and M cones as function of temporal al frequency is plotted in figure 7.15 and 7.16 respectively. Group average data (see figure 7.15) shows that the L and M cone response phase difference is close 180° at 12Hz (170.75° ± 3.30) which means at this temporal frequency, L and M cone interact in an opponent manner. On the other hand, at highest temporal frequency (30Hz), L and M cone response phase difference is close to 90° (111.75°± 58.48) suggests that L and M cones interact in non-opponent manner. The phase differences at 12Hz display less inter individual variation than at other temporal frequencies.

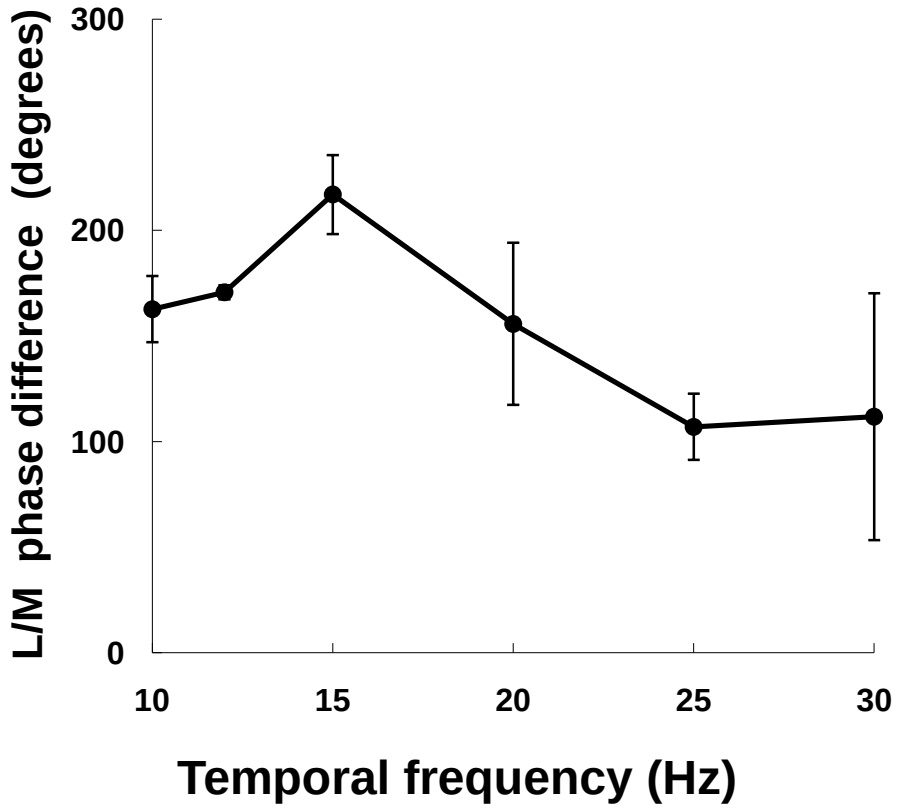

Figure 7.15 Mean data of L/M phase difference (calculated from L and M cone ERG 1st harmonic phases) as function of temporal frequency. Error bars shows standard deviation among subjects. Note that large error bars at 30Hz suggest large variation among subjects; small error bars at 12Hz suggest a small variation among subjects.

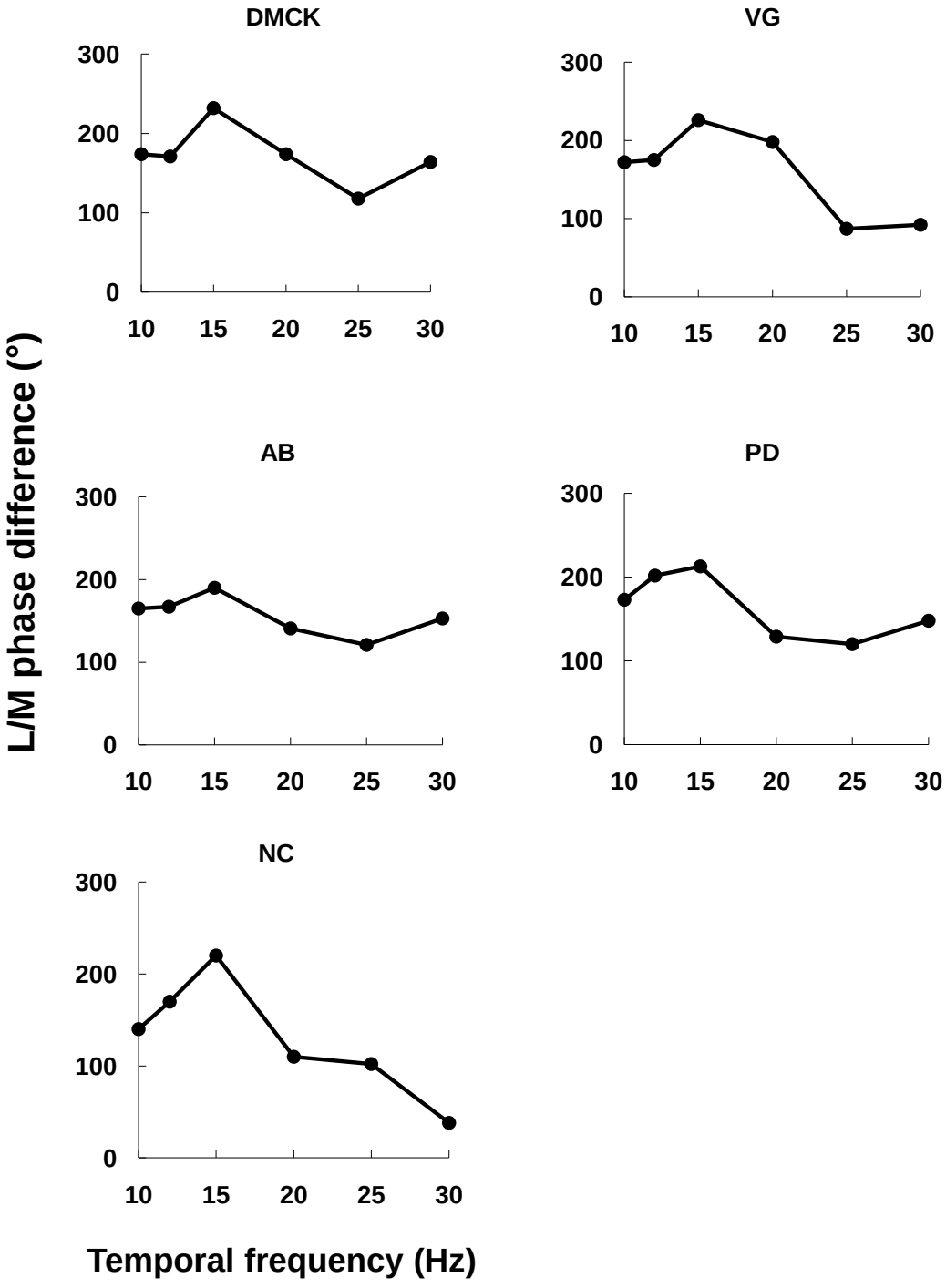

Figure 7.16. L/M cone phase differences (calculated from L and M cone ERG 1st harmonic phases) as function of temporal frequency in five different subjects.

7.4.5 L and M cone Response Phases

Response phase is the relationship between the phases of the signal input (example sinusoidal input) to the phases of the output signal. We would like to examine the response phase behaviour in L and M cone stimuli as a function of temporal frequency. The Group average data for L and M cone response phase as a function of temporal frequency is presented as shown figure 7.17.

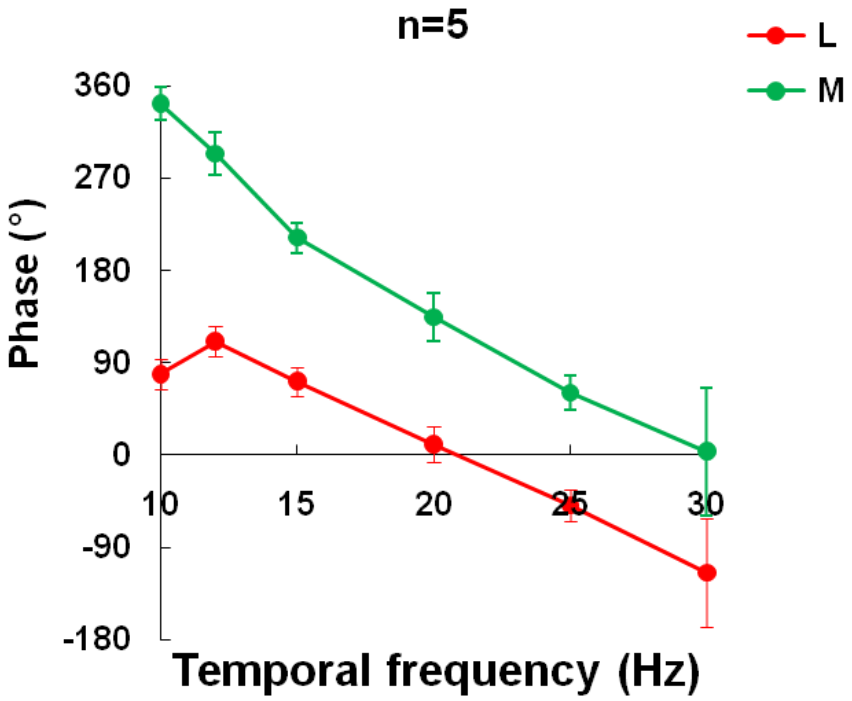

Figure 7.17 Group average data of L and M cone response phase as a function of temporal frequency. Note that the error bars are large at 30Hz for both L and M cone phases, suggesting large variability in phases among the observers.

From the plots of figure 7.17, it can be seen that there is a constant phase decline for both L and M cone responses as the temporal frequency is increased.

7.5 DISCUSSION

The present experiment used L and M cone isolating stimuli at various temporal stimulation rates (ranging from 10 Hz to 30Hz) to examine the L and M cone response properties. Our results suggest that L and M cones have different temporal properties. As a function of temporal frequency, L cone response shows a band pass function, whilst M cone response shows a low pass function.

In order to investigate the L and M cone inputs to ERGs at various temporal frequencies we measured the L:M ratios by dividing the L cone ERG response to M cone ERG response (L:M cone ratio). Our results demonstrate that at a 12Hz, the L:M cone ratio is close to unity and the L/M phase difference is close to 180°. The existence of L:M ratio close to unity for 12Hz response would appear to indicate that there is balanced contribution from L and M cones to this response consistent with idea that it is mediated by cone-opponent, P-cellular processing pathways. Earlier work has already shown that there is a good correlation between the ERG cone amplitude ratios and L:M ratios measured by anatomical means (Stockman et al., 1993b; Kremers et al., 2000; Kremers, 2003; Usui et al., 1998; Kremers et al., 2003). In normal dichromats L:M cone ratios have been shown to vary widely across different subjects (Brainard et al., 2000; Carroll et al., 2002; Hofer et al., 2005). Yet despite such large variations in the relative numbers of L and M cones in the human retina it has been persistent puzzle that colour perception remains stable across observers. For example, the studies of Miyahara et al (1998) and Brainard et al (2000) have shown that there is very little variation in the wavelength of unique yellow across the observers in spite of large

differences in their L:M ratios. The L:M cone opponent mechanism appears to be able to ignore the large inter-subject variations in the number of L and M cones and combine them in a more uniform and balanced fashion (Neitz et al., 2002).

The L:M ratios obtained for the 30Hz ERG are different to those obtained for the 12Hz response. For this stimulation frequency L:M ratios are greater than unity ranging from 3 to 11 across the observers. The higher L:M ratios obtained for the 30Hz are more likely to reflect the anatomical ratios of L and M cones and their input to non-opponent, luminance processing mechanisms (Stockman et al., 1993b; Kremers et al., 2000; Kremers, 2003; Usui et al., 1998; Kremers et al., 2003). The hypothesis put forward by Brainard (2000) suggests that individual variability in L:M cone ratio underlies individual variability in photopic luminous efficiency.

Sankeralli and Mullen (1996) measured the L and M cone input weights to luminance (non-opponent) and red-green (opponent) mechanisms using psychophysically determined detection threshold contours in cone contrast space. They proposed that the luminance mechanism has a cone weighting equal to *k*L +M where *k* varies from 3 to 5 at high temporal frequencies. On other hand, for the red-green mechanism L and M cones have equal but opposite weights. Our study also show that the L cone input is 3 to 11 times more than M cone for the luminance mechanism (at 30Hz) but for the chromatic mechanism (at 12Hz) there is equal and opposite input from L and M cones. Our findings are consistent with their study.

Pokorny et al, (1991) suggested a possible explanation for the differences in L:M ratios for luminance and chromatic processing lies in the fact that a person adjusts the relative contribution of L and M cones to the red-green mechanism by experience and therefore may be environmentally determined. This adjustment can be during ongoing development or throughout the whole of life. Since chromatic mechanisms are opponent, a mechanism response of zero provides a natural reference level for calibration. On the other hand, the luminance mechanism is additive, so there is no adjustable reference level for calibration. It may be possible that the luminance mechanism preserves individual differences in the L:M cone ratios due to the inability of visual system to compensate for their differences. The differences in L:M ratios for chromatic and luminance mechanisms found in our results seem to support the Pokorny's statement.

One of the key findings of this experiment is that at 30Hz, L cone ERG response amplitude is large, whilst the M cone response is almost negligible. The poor M cone response for luminance mechanisms has also been noted by various groups (example, (Pokorny, 1987; Pokorny, 1991; Kremers et al., 2000; Brainard et al., 2000)) studied the L and M cone responses at higher temporal frequencies. In addition to this, Whitmore and Bowmaker (1995) studied the L and M cone temporal properties under a range of light adapting conditions in a human observer using electrophysiological techniques. They observed that the L and M cone temporal properties are different and this difference is constant irrespective of state of light adaptation. Their results suggest that light adaptation has a little influence on the kinetics of transduction in human cones. They have also noted that at 33Hz, L cones have response amplitude in order of 100nV whilst M cones have response

amplitude in order of 30nV. The reasons they suggest for the difference in relative amplitude of L and M cones is the difference in the relative numbers of L and M cones in the retina. The other possibility is that L and M cones are attenuated by different amounts at high temporal frequency (33Hz).

Earlier suction electrode work on macaque photoreceptors (Schnapf et al., 1990) has shown that there is a difference in temporal characteristics between the three cone classes. According to their data, time to peak of the photocurrent impulse response of L cones is 55±18 ms, M cones is 51±13ms and S cones is 61±1 ms, and the integration time for L cones is 28±14ms, M cones is 19±10ms and 34±17ms. In spite of large standard deviation there is a uniform trend that suggests decreased integration time and time to peak from S cones through M cones to L cones. Adding to this, the spectral sensitivity of human L and M cones measured by suction electrode recordings (Schnapf et al., 1987), impulse responses of L and M cones have shown the same pattern. In addition to this Whitmore and Bowmaker (1995) have noted the phase difference of 12ms between L and M cones at 33Hz. Our results have also shown that there is difference in phase behaviour of L and M cone pathways at higher temporal frequencies. Independent of whether the data collected from single cones or mass response of the cells which has same spectral composition, all results together recommend that the temporal properties of L and M cone pathways are different. The obvious questions that are raised by the above observations are 1) what would be the molecular basis for the difference in temporal properties of L and M cones 2) which level in the transduction cascade might the measured differences occurs? The answer might lie in the properties of the pigments themselves (Whitmore and Bowmaker, 1995),

perhaps due to differences in time course of activation by light and the rate at which the excited pigment can in turn activate transducin. There are studies in the direction that supports this idea. For example, rate of formation and decay of meta II photoproducts of chicken rod and cone pigments differ (Okada et al., 1994; Shichida et al., 1994). If this is ultimately shown to be the case, then there is a possibility that the polymorphism of primate visual pigments may be reflected in a polymorphism of temporal properties (Whitmore and Bowmaker, 1995).

7.6 PSYCHOPHYSICAL INVESTIGATION OF L:M CONE RATIO AT VARIOUS TEMPORAL FREQUENCIES

7.6.1 Introduction

Previously, it has been noted that cells in the visual cortex show decreases in their responses with increase in temporal frequency. Their response is diminished even at frequencies to which the cells in LGN respond vigorously (Hawken et al., 1996; Holub and Morton-Gibson, 1981; Saul and Humphrey, 1992; Sclar, 1987). Recently, Lee (2010) has also observed that the psychophysical sensitivity to red-green stimuli falls off above 4Hz and above 10-12Hz the chromatic alternation cannot be seen. However, ganglion cells robustly respond to at least 30Hz. From these observations, it is clear that the pre-cortical chromatic signals undergo temporal filtering at the level of cortex.

The ERG is an electrical by-product of retinal processing and therefore may not be a true reflection of the processes that lead to visual perception. Psychophysical tasks can be used to estimate the subject's perception. If we can establish a correlation between psychophysical and ERG measurements then we are able to understand the mechanisms that lead to perception. Flicker ERGs that are mediated by the chromatic and luminance channels cannot be directly compared to psychophysical measures, because of cortical filtering of temporal chromatic signals. In order to exploit the chromatic and luminance driven signals, we need to use different temporal parameters for the ERG and psychophysical task.

Recent work (Kremers and Link, 2008) has shown that the temporal frequencies which separate the luminance and chromatic channels for psychophysical

procedure are different from the ERGs. Kremers and Link (2008) have suggested that the cone modulation thresholds at low temporal frequency (about ≤ 4Hz) and high temporal frequencies (≥ 20Hz) can separate chromatic and luminance mechanisms respectively. So we would like to verify psychophysically, the temporal parameters that separate the chromatic and luminance mechanisms using flicker detection thresholds for L and cone isolating stimuli. In addition to this, we would like to compare the results of psychophysics data to the ERG data. We chose L and M cone isolating stimuli which are representative of central and peripheral retina. We looked at the flicker detection sensitivities of L and M cones at temporal frequencies of 4, 8, 10, 12, 16 and 20Hz.

7.6.2 Methods

7.6.2a Stimuli

The stimulus configurations used to measure flicker detection thresholds were circular spot stimuli of angular substance 10° and 70-60° diameter (see figure 7.18) respectively. Modulation depth and phase were chosen in such a way that either L- or M-cones were stimulated and cone contrasts were equalized for each stimulus condition at 20%.

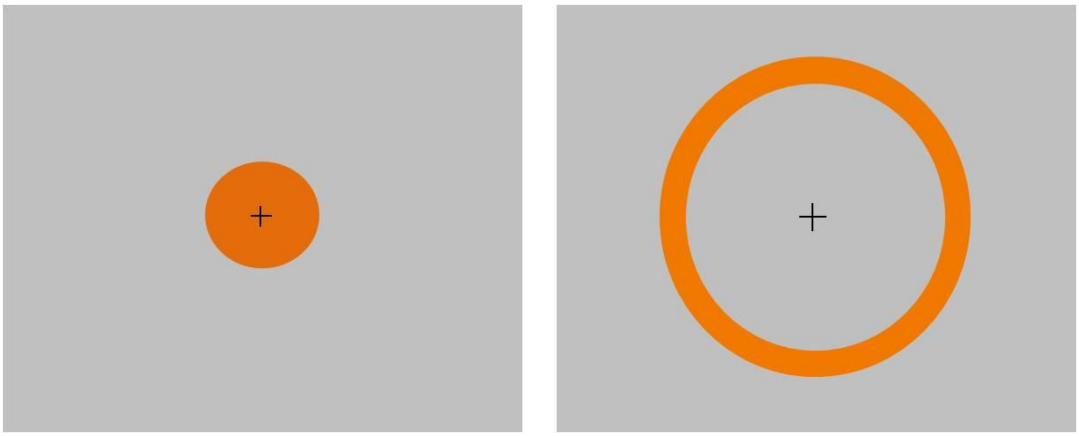

Figure 7.18 Stimulus configurations used for L and M cone detection thresholds A) 10° disc B) 70° disc centrally ablated 60°.

The rods were not stimulated in any of these conditions. Preference is given to silence the rods rather than S cones, because S-cones make little contribution to the detection of flicker for the stimuli that modulate L and M cones (Kulikowski and VidyaSagar, 1987). The time averaged luminance of the monitor was 66 cd/m^2. Spectral characterstics and luminances were calibrated using PR650 spectrascan spectroradiometer.

7.6.2b Psychophysical procedure

Flicker detection thresholds for the L and M cone isolating stimuli were measured using a two temporal alternative forced choice procedure (2AFC). In this procedure a flickering stimulus was presented in one of two temporal intervals (see figure 7.19). The observer had to indicate by button press (CB3 response box, Cambridge Research systems, Cambridge, UK) in which interval the stimulus was present.

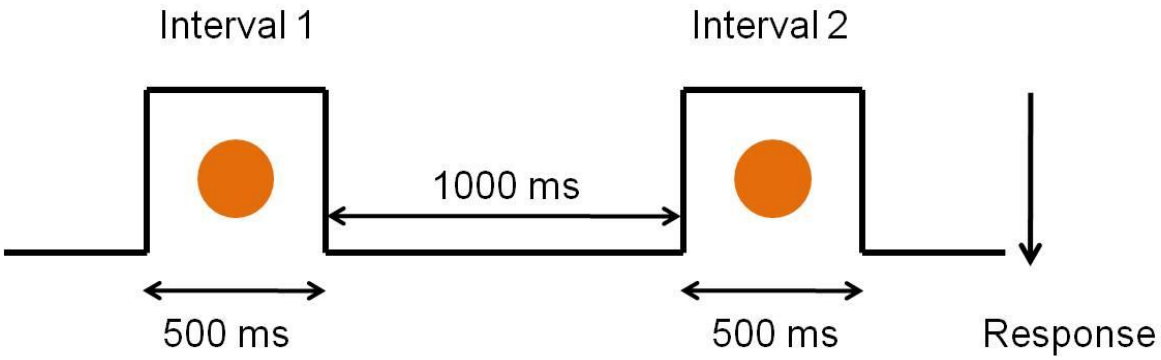

Figure 7.19 Stmulus presentation in 2 temporal alternate force choice procedure. Stimulus is presented in interval 1 or interval 2 and subject has to report in which the stimulus is present. The timing of stimulus onset and inter-stimulus interval are also shown in the figure.

The cone isolating stimuli were presented at 7 contrast levels ranging from sub-threshold to supra-threshold levels, the range of which was determined in preliminary experiments. Twenty repeats of each stimulus were used to generate psychometric functions. Threshold was set at 75% seen. Psychometric curves (see figure 7.20) were obtained from the data utilising Bootstrap software (Foster and Bischof, 1991) from which the threshold estimates (75% seen) were obtained. Threshold estimates were obtained in decibels. These values are converted into contrast percentage using the equation 7.1:

$$Contrast\ in\ (\%) = -\frac{1}{20}\ Anti\log\ (detection\ threshold\ in\ decibles) X\ 100 \text{----- (7.1)}$$

This procedure was repeated for L and M cone isolating conditions at temporal frequencies of 4, 8, 10, 12, 16, and 20Hz.

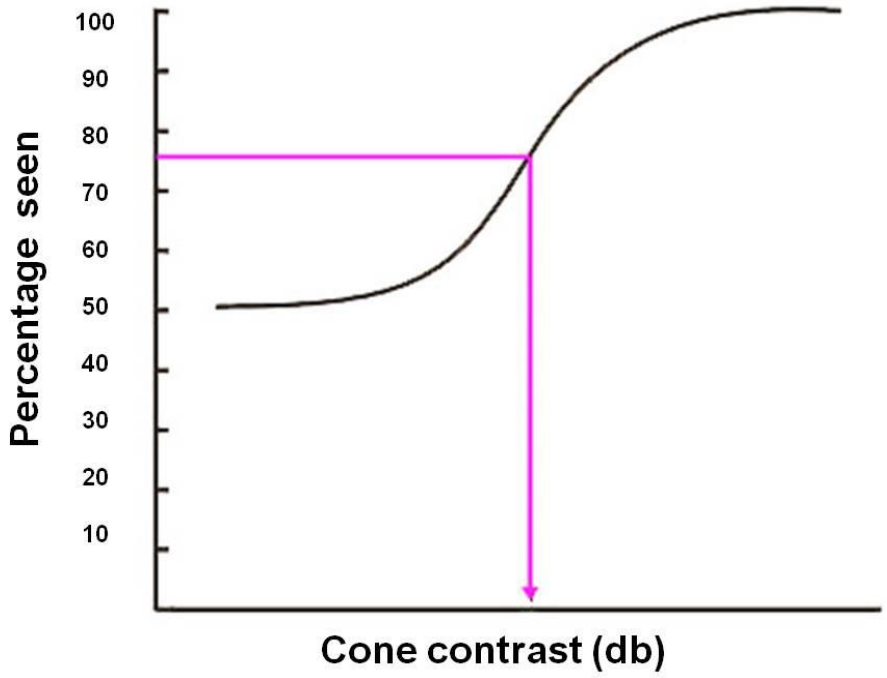

Figure 7.20 Psychometric functions for 2AFC. Threshold is taken at the 75% seen level.

7.6.2c Subjects

Two male observers (DM, NC) were participated in this study. One was an emmetrope and the other was a corrected myope. Both subjects were colour-normal according to the Farnsworth Munsell 100 Hue test. Observers viewed the stimuli monocularly maintaining fixation on a centrally placed cross. Subjects gave informed consent prior to the commencement of the experiment.

7.6.3 Results

7.6.3a L and M cone contrast thresholds

Group average flicker detection thresholds for L and M cone isolating stimuli for central and peripheral retina were plotted as a function of temporal frequency (figure 7.21). Individual data is presented in figure 7.22 for the reference. From the group average plots (figure 7.22), it can be observed that the L cone contrast thresholds are relatively constant across all temporal frequencies. On the other hand, M cone contrast thresholds were similar to L cone thresholds at lower temporal frequencies and gradually increased with increasing temporal frequency.

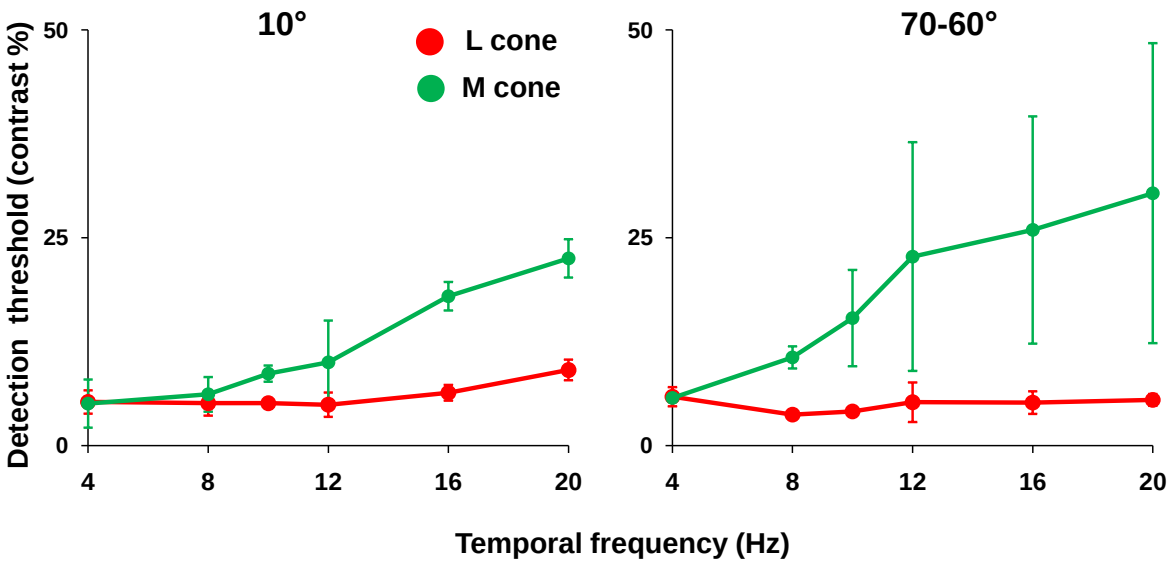

Figure 7.21 Mean (n=2) L and M cone contrast flicker detection thresholds as function of temporal frequency. Left and right panels represent the results of the central and peripheral retina respectively.

At 4Hz, L and M cones have similar detection thresholds for both central and peripheral stimulus conditions. In contrast, at 20Hz, M cones have large detection thresholds than L cones for both central and peripheral stimulus conditions. Moreover, M cone detection thresholds are lot higher for peripheral stimulus than central stimulus particularly for subject NC.

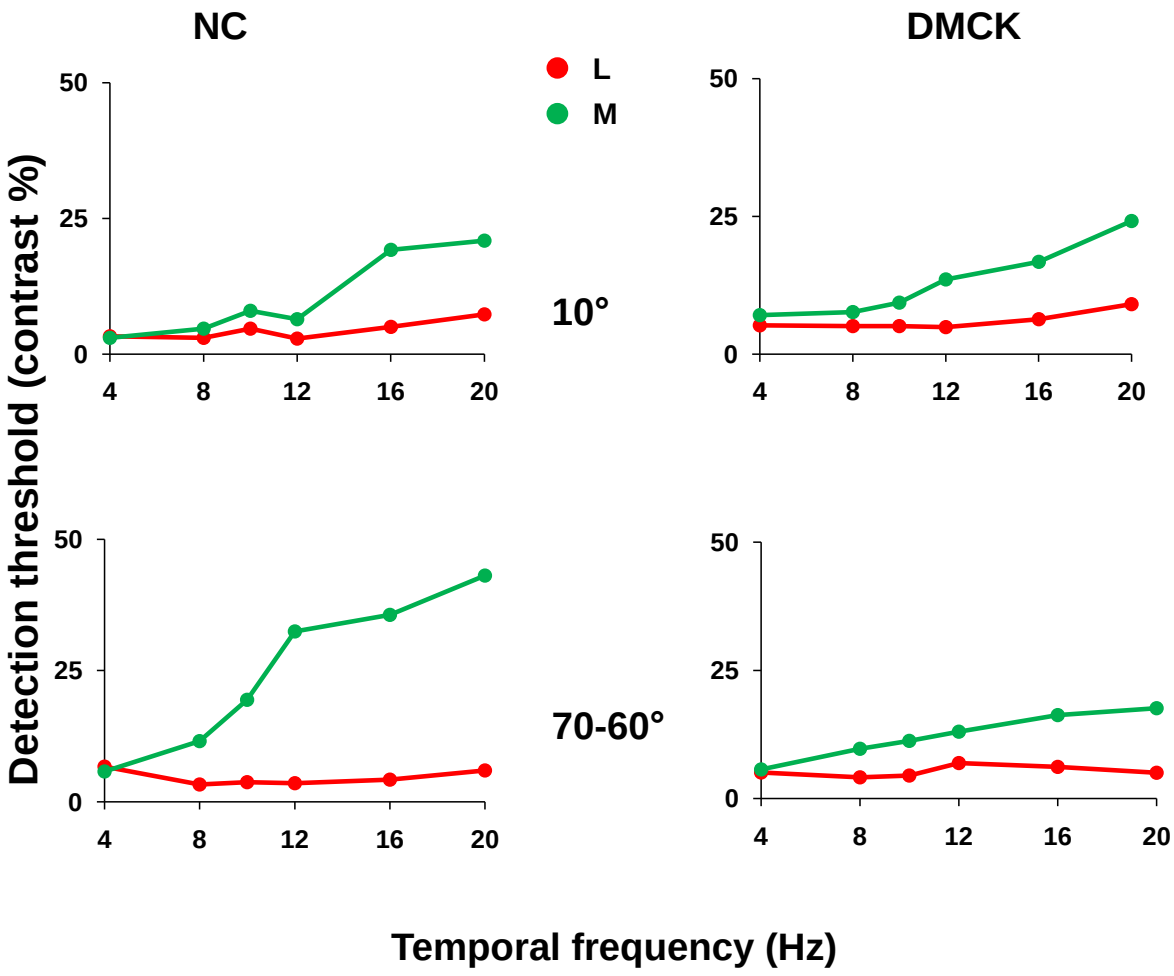

Figure 7.22 L and M cone contrast flicker detection thresholds as function of temporal frequency Left plot represents the data of subject NC and right plot represents the data of subject DMCK. Top and bottom panels represent the results of the central and peripheral retina respectively.

7.6.3b L:M ratios

L:M ratios were calculated by dividing the M cone contrast threshold by L cone contrast thresholds (since the threshold is reciprocal of sensitivity). The mean L:M ratio of the two subjects as function of temporal frequency for central and peripheral stimuli were plotted in figure 7.23. From the plot, it can be appreciated that the L:M ratio gradually increases as we increase the temporal frequency. At 4Hz, L:M cone ratios are close to unity for both central and peripheral stimulus conditions in both subjects whist at 20Hz the L:M ratios are more than unity and these ratios are not same for central and peripheral stimulus conditions. The individual variation of L:M ratio for central and peripheral stimuli were plotted in figure 7.24.

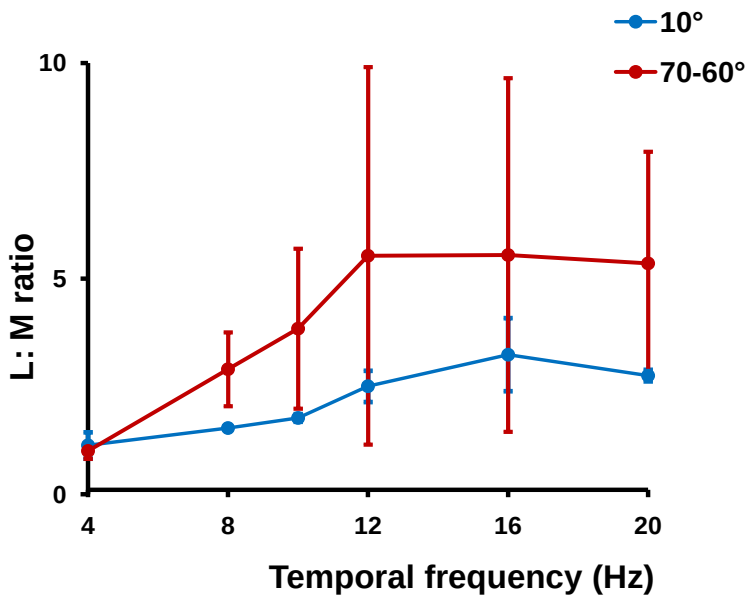

Figure 7.23 Mean (n=2) L:M cone ratios as function of temporal frequency is plotted for two stimulus conditions.

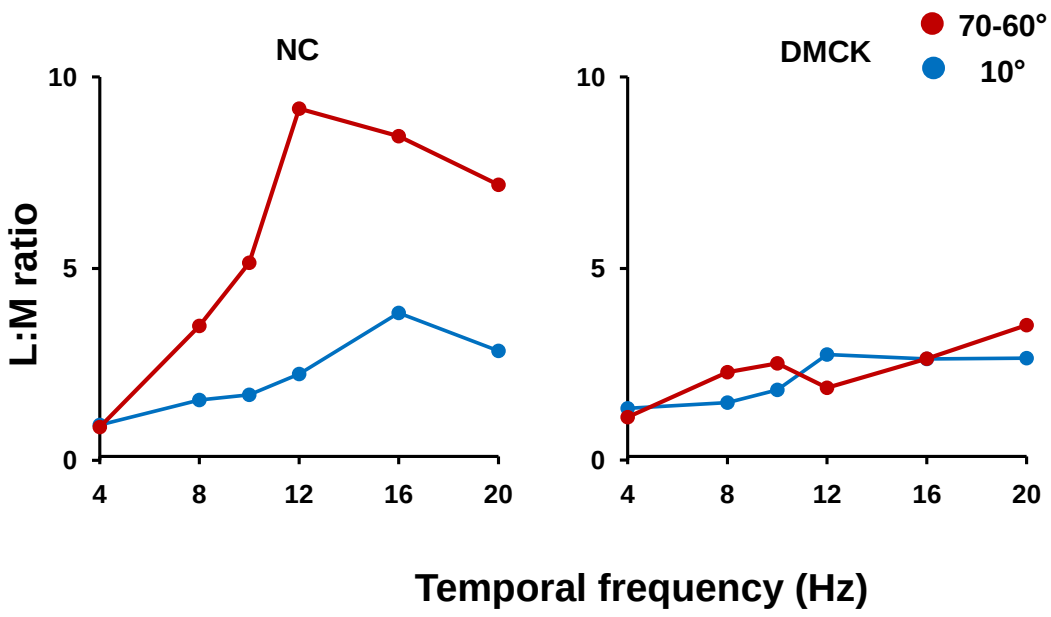

Figure 7.24 L:M cone ratios as function of temporal frequency is plotted for two stimulus conditions in two different subjects.

7.6.4 Discussion

This experiment measured the flicker detection thresholds for L and M cone isolating stimuli at various temporal frequencies. Results suggest that the flicker detection thresholds for L and M cone isolating stimuli do vary as function of temporal frequency in similar fashion to the ERG responses. Moreover, these variations are noticeable at low and high temporal frequencies. Our results suggest that the psychophysical task at 4Hz and 20Hz is mediated by chromatic and luminance mechanisms. The claim is based on following findings; at 4Hz, L and M cones have equal detection thresholds for both central and peripheral stimuli

conditions and have shown L and M cone ratio of unity, which correlate to the ERGs that tap the chromatic mechanism. On the other hand at 20Hz, L and M cone have different detection thresholds (M > L). L:M ratio is more than unity for both central and peripheral stimulus conditions, which is in correlation to the 30Hz ERG that tap the luminance mechanism. Our results presented here are in concordance with previous idea that cone modulation thresholds measured at low temporal frequency is mediated by the red-green chromatic channel and those measured at high temporal frequency is mediated by the luminance channel (Kremers and Link, 2008)

Another important observation is that M cone detection thresholds increase with increase in temporal frequency, whilst the L cone detection thresholds remain stable. This finding suggests that at high temporal frequencies M cone sensitivity decreases. Poor M cone amplitudes were also noted at higher temporal frequencies in 30Hz ERGs, suggesting its poor response to luminance mechanism. Recently, Stockman et al (2005) have suggested various contributions to the achromatic flicker perception as L, M or S, according to cone type from which the signal originate, prefixed by either ‘f’ or‘s’, according to the relative phase delay of the input signal, and by either ‘+’ or ‘-’according to whether the inputs are non-inverted or inverted with respect to the fast signal. According to their findings, fast (f) and slow (s) M cone input signals of the same polarity (+sM and +fM) sum at low temporal frequencies, but then they destructively interfere near 16Hz because of the delay between them. In contrast to this fast and slow L cone input signals of opposite polarity (-sL and –fL) cancel at low temporal frequencies, but then constructively interfere near 16Hz. If we apply the stockman et al findings to our

results, we speculate that the reason for poor M cone response at higher temporal frequency is because of the destructive interference of fast (f) and slow (s) M cone input signals.

Our results have shown a large discrepancy between L:M ratios of the two subjects at higher temporal frequencies. Such individual variation in L:M ratios at higher temporal frequencies was also noted in our ERG measurements. Various groups have estimated L:M cone ratios for the luminance channel using different approaches such as flicker ERG measurements (Hofer et al., 2005; Kremers and link, 2008; Brianard et al, 2000; Kremers et al., 2000), psychophysical measurements (Kremers et al., 2000; Jacobs, 1993; Jacobs et al., 1996; Nerger and Cicerone, 1992; Krauskopf, 2000), retinal densiometry measurements (Krauskopf, 2000; Williams, 1999) unique yellow measurements (Otake et al., 2000; Brainard et al., 2000). All these studies have shown that the L:M cone ratio may vary from 1.4:1 to 9:1 in different individuals suggesting their inter subject variability.

The Mean L:M ratios measured by flicker ERGs at 30Hz are similar to the mean L:M ratios measured by psychophysics at 20Hz. Earlier studies have suggested that the flicker ERGs reflect the post-recptoral processing and L:M ratios measured by flicker ERGs reflects the L and M cone weighting to the post-receptoral processing (Kremers et al., 1999; Kremers and Link, 2008; Kremers et al., 2000). Psychophysical studies have speculated that L:M ratios measured at high temporal frequencies are probably related to actual cone numbers that have been measured anatomically (Brainard et al., 2000; Kremers et al., 2000). If this is the case, then the actual cone numbers in the retina measured anatomically is same as their

weightings to the post-receptoral pathway that is mediated by luminance mechanism.

CHAPTER - 8 L- AND M- CONE INPUT TO 12Hz AND 30Hz FLICKER ERGs ACROSS THE HUMAN RETINA

8.1 INTRODUCTION

Quantitative models of human colour vision can be constructed from an understanding of the relative numbers of three types of cones in the retina which mediate long wavelength (L), medium wavelength (M) and short wavelength (S) light responses. Density and distribution of the S cones have been described by various studies (Ahnelt et al., 1987; Curcio et al., 1991). In addition, S cone distribution estimated by anatomical means correlate well with psychophysical estimations in humans (Williams et al., 1981) and in primates (Marc and Sperling, 1977; DeMonasterio et al., 1981; Mollon and Bowmaker, 1992). By comparison, the relative numerosity of L and M cones is less well established. However, new techniques have been developed to measure the relative numbers of L and M cones. Roorda and Williams (1999) studied two human retinae by direct imaging and found that L/M cone ratios were 1.15 and 3.79. Analysis of messenger RNA expressed in retinas from 100 male eye donors showed that there is considerable inter individual variation in L/M cone ratio (Hagstrom et al., 1998). The L/M ratio in this group of donors was found to vary from 0.82 to 9.71. Anatomical imaging studies have also noted significant differences in L and M cone ratios in different individuals (see figure 8.1).

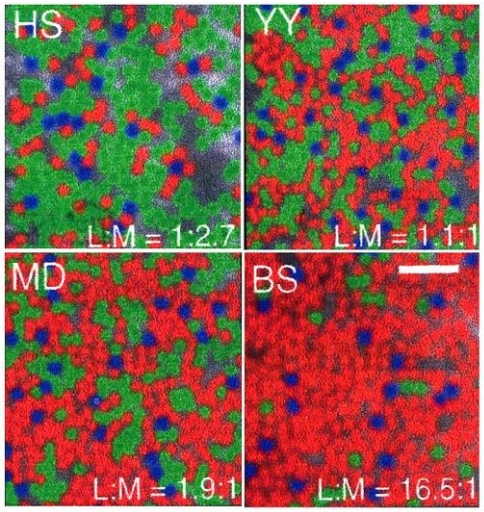

Figure 8.1 Adaptive optics imaging of L (red dots), M (green dots) and S cone (blue dots) mosaic in four colour normal individuals. It is obvious from picture that individual L, M cone ratios vary significantly. The corresponding L:M ratios of individuals are specfied in each box seperately.

Source:http://www.ncbi.nlm.nih.gov/books/NBK11537/figure/ch22color.F21/?report=objectonly

Several groups have looked at the contribution of L and M cone signals to the ERG in normal trichromats (Kremers et al., 1999; Kremers et al., 2000; Brainard et al., 2000; Carroll et al., 2000). Responses derived from photoreceptor stimulation and their amplitude ratios were found to be closely correlated with known cone spectral sensitivities and L:M cone ratios determined by direct anatomical imaging techniques (Stockman et al., 1993b; Kremers et al., 2000; Kremers, 2003; Usui et al., 1998; Kremers et al., 2003; Brainard et al., 2000). Furthermore, Knau et al (2000) measured the L:M cone ratios at different retinal eccentricities using heterochromatic flicker photometry which showed that L:M cone ratios for each subject was nearly constant at all measured eccentricities, with the individual values ranging from 0.9:1 to 3.4:1. In contrast to this finding, psychophysical

studies that measured the relative number of L and M cones provided indirect evidence that the L:M cone ratio is not stable across the retina. Other studies have measured colour appearance (Boynton et al., 1964), wavelength discrimination (Weale, 1951), and spectral sensitivity for small and dim test lights (Uchikawa et al., 1982). All of These studies indicated that M cone sensitivity decreases with retinal eccentricity suggesting that the relative number of M cones decreases with retinal eccentricity.

Individual variation in L:M cone ratios might have consequences for vision. Functional tasks such as the ability to detect lights of different spectral composition (Cicerone and Nerger, 1989; Vimal et al., 1989; Wesner et al., 1991), the appearance of brief, small flashes of lights (Krauskopf and Srebro, 1965) and hyper-acuity measurements for small spots of different spectral composition (Gowdy and Cicerone, 1998) all reflect variation in L:M cone ratio. There is considerable individual variation in the relative strength of L and M cone input to mechanisms that mediate both psychophysical flicker photometry (Rushton and Baker, 1964; Pokorny, 1991; Kremers et al., 2000) and flicker ERG (Jacobs and Neitz, 1993; Jacobs and Deegan, 1997; Usui et al., 1998; Kremers et al., 1999; Brainard et al., 2000). This variation may be attributed to the relative number of L and M cones.

8.1.1 ERG as measure of inner retinal function

Traditionally, the ERG is used as a measure of distal retinal function because of the belief that photoreceptors are the main source of the fast flicker ERG

responses in primates (Granit, 1947; Donovan and Baron, 1982; Seiple et al., 1992). The origin of this idea comes from two main observations: one involving intra-retinal microelectrode studies in the primates and the other is intracellular recordings from Müller cells in vertebrates. However, studies have shown that ERGs can be used to study the inner retinal function (Baron, 1980; Donovan and Baron, 1982; Bush and Sieving, 1996; Viswanathan et al., 1999; Viswanathan et al., 2000; Viswanathan et al., 2002).

Baron (1980) was the first to report that the slow potential in foveal local ERG correlates well with the absolute logarithmic difference between L and M cone sensitivities. Later Donovan and Baron (1982) recorded steady state ERGs using long wavelength sinusoidal flickering stimuli. Their ERG analysis revealed two primary components which are affected differently by illuminance, temporal frequency and chromatic adaptation. They also noted similarities between corneal ERG and local foveal ERG with regards to the amplitude and phase. In addition to these studies, work by Mills and Sperling (1990, 1991) has also demonstrated that the ERG signal can be an index of some aspects of cone opponent processing and may be correlated with colour vision. They have also shown that the inner retina contributes to the ERGs. These ERG studies have improved our understanding of the post-receptoral processing, in particular cone inputs to the ganglion cell receptive fields.

8.1.2 Architecture of cone inputs to the ganglion cell receptive fields

Long (L), medium (M) and short (S) wavelength cones combine in various ways to form a chromatic (colour-opponent) and luminance (non-opponent) channels that carry visual information further along of the primate visual pathway (see figure 8.2). Cone-opponent mechanisms arise when outputs from the long (L), middle (M) and short-wavelength (S) sensitive cones are combined in a subtractive or opponent manner. L/M opponency is established by the segregation of L versus M cone signals to the centre and the surround of a ganglion cell's receptive field (RF), whereas in the S/(L+M) mechanism the S-cone signals are opposed to a combined L+M cone signal. In addition, there is a third luminance (non-opponent) or achromatic mechanism in which ganglion cells receive combined L and M (i.e. additive) cone input (De Valois et al., 1966; Derrington et al., 1984; Dacey, 2000a). Information processing in the L/M cone-opponent pathway is mediated by the midget ganglion cells (MGC).

Currently, there are conflicting views regarding the architecture of the L- and M-cone inputs to the centre and surrounds of the midget ganglion cell receptive fields and how this input might change from the fovea to the peripheral retina (see figure 8.3). One school of thought proposes that with increasing retinal eccentricity, there is a loss in the cone specific nature of inputs to the centres and surrounds to the midget ganglion cells with both receptive field centres and surrounds receiving mixed spectral inputs ('random-wiring' hypothesis) (Shapley and Perry, 1986; Lennie et al., 1991; Mullen and Kingdom, 1996; Dacey et al., 2000a; Dacey, 2000b). Another view is that selective connectivity by L- and M-cones to the centres and surrounds of the receptive fields is maintained ('cone-selective'

hypothesis) (Reid and Shapley, 1992; Reid and Shapley, 2002; Martin et al., 2001; Lee et al., 1998).

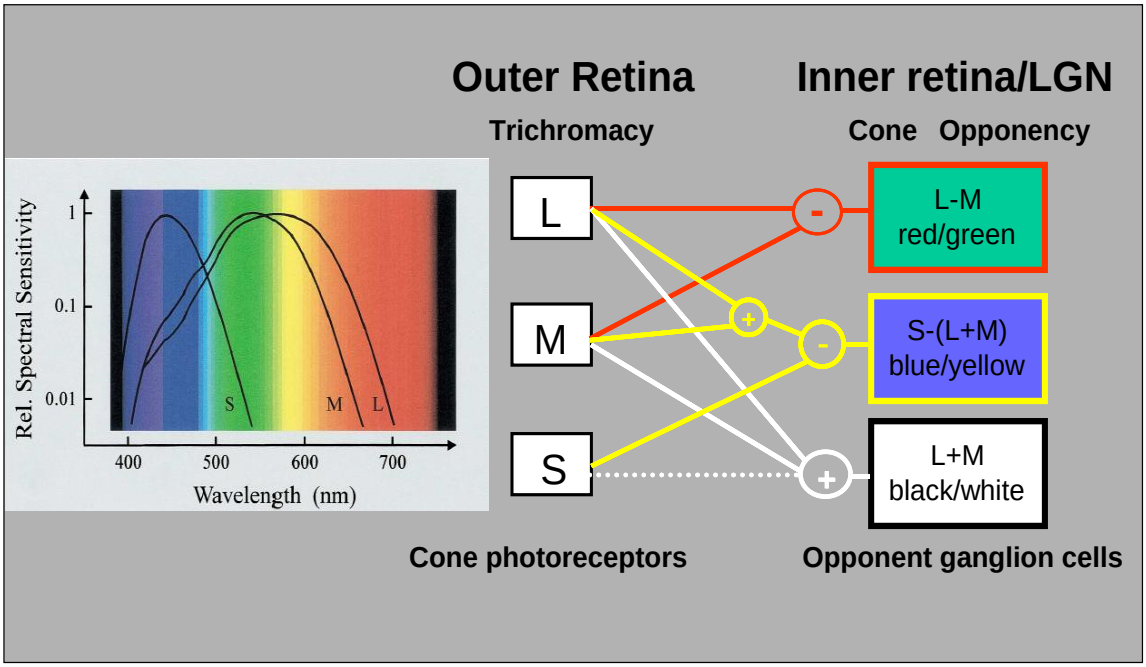

Figure 8.2 Cone opponent mechanisms in the visual system. Left trace of the picture shows the spectral sensitivty of L, M and S cones. Right side picture shows the corresponding input to the ganglion cell to form non-opponent (black/white) and opponent channels (red-green and blue-yellow).

Regardless of whether cone inputs are organised in selective or random fashion, cone opponency exists in the central retina by virtue of the fact that the centres receive input from a single type of cone. This is also termed as a private line arrangement. However, in the retinal periphery there is an increase in receptive field size. As a consequence of this, if the random wiring theory holds, there is the potential for both the centres and surrounds to receive input from multiple cone types. This is likely to result in a shift away from balanced L- and M-cone input, with increasing retinal eccentricity. Conversely, if cone selectivity holds in the peripheral retina, segregated and balanced L- and M-cone inputs to the RF centres

and surrounds will occur, maintaining an L:M cone input ratio close to unity, similar to that found in the foveal retina.

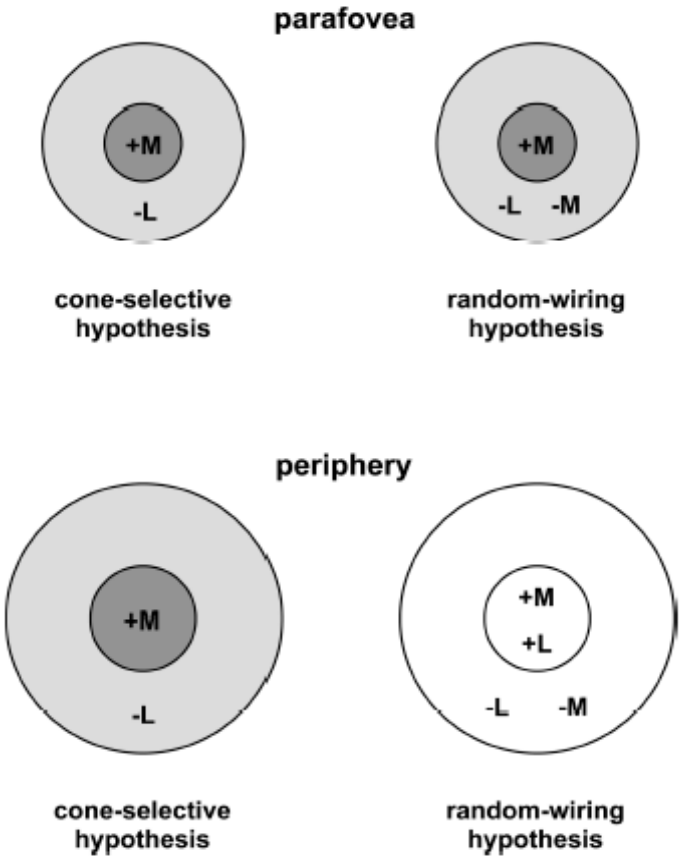

Figure 8.3 Architecture of cone input to the ganglion cell receptive fields in central (upper image) and peripheral retina (lower image). Cone selective hypothesis (left side of the image) predicts that L and M cones feed to the receptive field centre and surround of the ganglion cell respectively. In contrast, random wiring theory (right side of the image) predicts that selective input is lost and mixed spectral inputs to the receptive field centre and surround of the gaglion cells. Picture adapted from Vakrou et al (2005).

8.1.3 Implications of cone inputs to the ganglion cell receptive fields

Many inferences can be made by understanding the cone inputs to the ganglion cell receptive fields. For instance, the type of cone input to the receptive fields of midget ganglion cells can be partially attributed to the perceptual differences in colour from central to peripheral retina in human (Ayama and Sakurai, 2003; Moreland and Cruz, 1959; Abramov et al., 1991; Nerger et al., 1995; Sakurai et al., 2003; Parry et al., 2006; McKeefry et al., 2007). Human behavioural studies, for example, have demonstrated differential losses in sensitivity between the L-M and S-(L+M) cone opponent mechanisms, with the former becoming more functionally compromised than the latter with increasing retinal eccentricity (Mullen and Kingdom, 2002; Mullen et al., 2005; Murray et al., 2006). The L-M cone-opponent pathway is mediated by midget ganglion cells (MGC) in the retina, which project to the P-cellular layers of the LGN. On the other hand, S-(L+M) cone-opponent pathway is mediated by small bistratified ganglion cells (SBS) in the retina which project to the K layers of LGN.

In the light of these different views regarding cone inputs to the receptive fields of ganglion cells, we wanted to examine how L and M cone amplitude ratios vary across the human retina using cone isolating flicker ERGs. Our earlier experiment has demonstrated that with appropriate choice of temporal stimulation parameters, the ERG can be made to reflect the operation of cone-opponent (chromatic or P-cellular) and non-opponent (luminance or magnocellular) post-receptoral mechanisms. At 12Hz, ERGs have response properties which are consistent with their generation by cone-opponent, chromatic mechanisms. In these responses the ratio of L to M cone driven ERG amplitudes is close to unity and the difference

between their response phases is close to 180°. By comparison, ERGs that are elicited by faster flicker frequencies (≥25Hz) have response properties that are consistent with their mediation via non-opponent, luminance post-receptoral mechanisms. For example, the L and M cone response ratios for these faster flicker ERGs are greater than unity and highly variable across individuals and presumably reflect the relative numbers of L and M cones.

8.2 RATIONALE

We used fast (30Hz) and slower (12Hz) rate ERGs in order to assess how the contributions of L- and M-cones, expressed in terms of L:M response amplitude ratios, vary for non-opponent (luminance) and cone-opponent (chromatic) processing when different regions of the retina are stimulated. As yet no studies have examined how the ratio of L to M cone contributions to the ERG might vary with retinal location for cone-opponent processing and how this might differ from luminance processing. The cone selective versus random wiring theories make two different predictions as to how L:M ratios might vary across the retina. On the one hand, if selectivity is maintained we might expect that a ratio close to unity would result in both the central and peripheral retina. Alternatively, if a more random pattern of cone connectivity exists we might expect that the L:M ratio to depart from unity and exhibit a greater degree of variability as different numbers of L and M cones are activated. We also evaluated L and M cone phase shifts for different regions of the retina are stimulated and also how this differs for chromatic and luminance processing.

8.3 METHODS

Stimulus generation is similar to that used in earlier experiment (see section 7.3.1). However, different stimulus configurations were used to record the ERGs and these could be grouped into two main types: (1) Circular stimuli of different angular substance which increased in 10° steps from 10° up to 70° in diameter, and (2) annular stimuli with a 70° outer diameter but gradually ablated from the centre in 10° steps (see figure 8.4). These stimuli were presented in a single sequence of 15 steps which included blank trials at the beginning and the end. Modulation depth and phase were chosen in such a way that either L- or M-cones were stimulated and cone contrasts were equalized for each stimulus condition at 20%.

8.3.1 ERG recordings

A silver-silver chloride reference electrode was placed at the outer canthus and a ground electrode was placed on the forehead. Electrode impedances were kept below 5kΩ. The ERG signals were amplified using a Grass 15A94 amplifier (Astro-Med, Rhode Island, USA) with band pass frequency of 3-100Hz. The signals were sampled at a rate of 1024 Hz over a period of 4 seconds and averaged responses were based upon at least 20 repetitions. Fourier components were extracted from the response using a CED 1401 smart interface (Cambridge Electronic Design, Cambridge, UK). L cone and M cone isolating ERGs were recorded at 12HZ and 30Hz respectively.

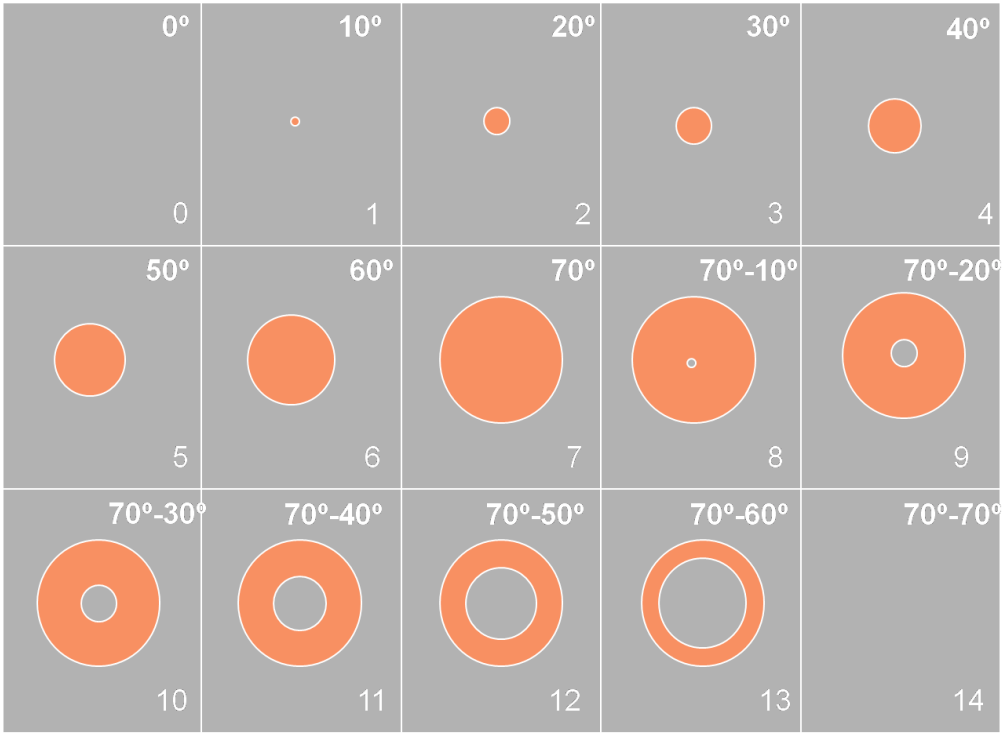

Figure 8.4 A representation of 15 different spatial configurations used for the L- and M-cone isolating stimuli that were used to elicit ERGs. Condition 1-7 comprise of circular stimuli of different angular subtense which increase in 10° steps to 70° in diameter. Conditions 8-13 are annular stimuli with 70° outer diameters the centres of which are gradually ablated in 10° steps. Condition 0 and 14 contain no stimuli. The background was uniform grey with luminance of 66cd/m^2.

8.3.2 Observers

Five male observers participated in this study. All were either emmetropes or corrected ammetropes and were colour normal according to the Farnsworth Munsell 100 Hue test. During recording observers' pupils were dilated with 1% tropicamide. They viewed the stimuli monocularly from a distance of 10 cm and both a chin and head rest were used. Fixation was maintained on a centrally

placed black cross which subtended 2°. All subjects gave informed consent prior to the commencement of the experiments.

8.3.3 Validation of isolation of L and M cone responses

The isolation of L and M cone stimuli were validated for all the conditions in additional control experiments on two dichromats (one protanope and one deuteranope). From the figure 8.5, It can be observed that protanope has very small L cone amplitudes for L cone isolating stimuli and in contrast, deuteranope has very small M cone amplitudes for M cone isolating condition. This data suggests that isolating conditions revealed minimal cross contamination that may have resulted from any errors in calculations or calibrations of cone isolating stimuli. If there is any contamination of the responses, we would expect the response from M cones for L cone isolating conditions in a protanope and L cone contamination for M cone isolating stimulus for a deuteranope. However, this was not the case.

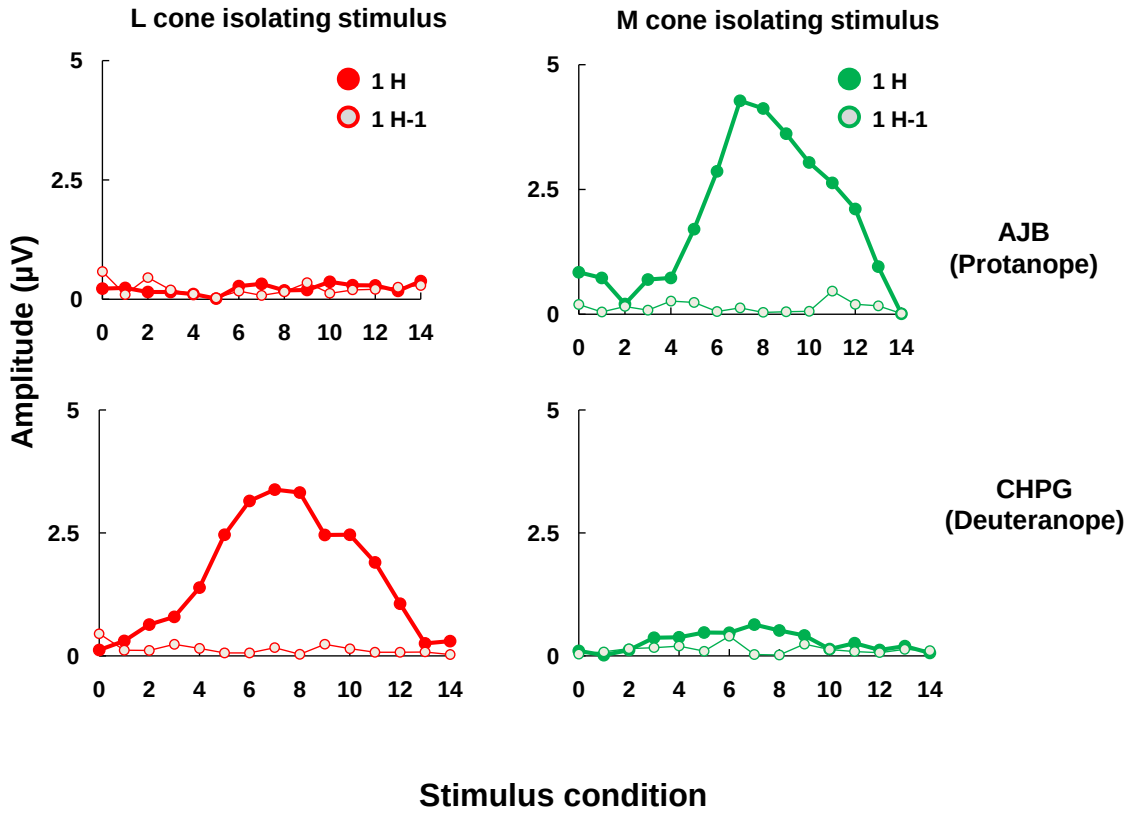

Figure 8.5 L and M cone response amplitudes in a protanope (see the first row plots) and deuteranope (see the second row plots) as function of retinal regions stimulated at 30Hz. Filled circles represent the first harmonic (1H) responses and open circles represent the measure of noise (1H-1). It is obvious from the figure that protanope has poor L cone response and deuteranope has poor M cone response.

Additional control experiment was performed on a single subject (DMCK) to see the intrusion of S cones on the L and M cone isolating conditions. In this experiment, L and M cone responses were compared in two conditions at 30Hz and at 12Hz. In first condition, L and M cone responses were isolated by silencing the rod photoreceptors. In second condition, L and M cone responses were isolated by silencing the S cones. Results are plotted in figure 8.6. From the plots, it can be observed that the L and M cone response amplitudes change as function of stimulus condition at 30Hz and at 12Hz. However, it is important to note that for

a given stimulus condition, amplitudes show a very little or no variation, whether the ERG is recorded by silencing the rods or silencing the S cones.

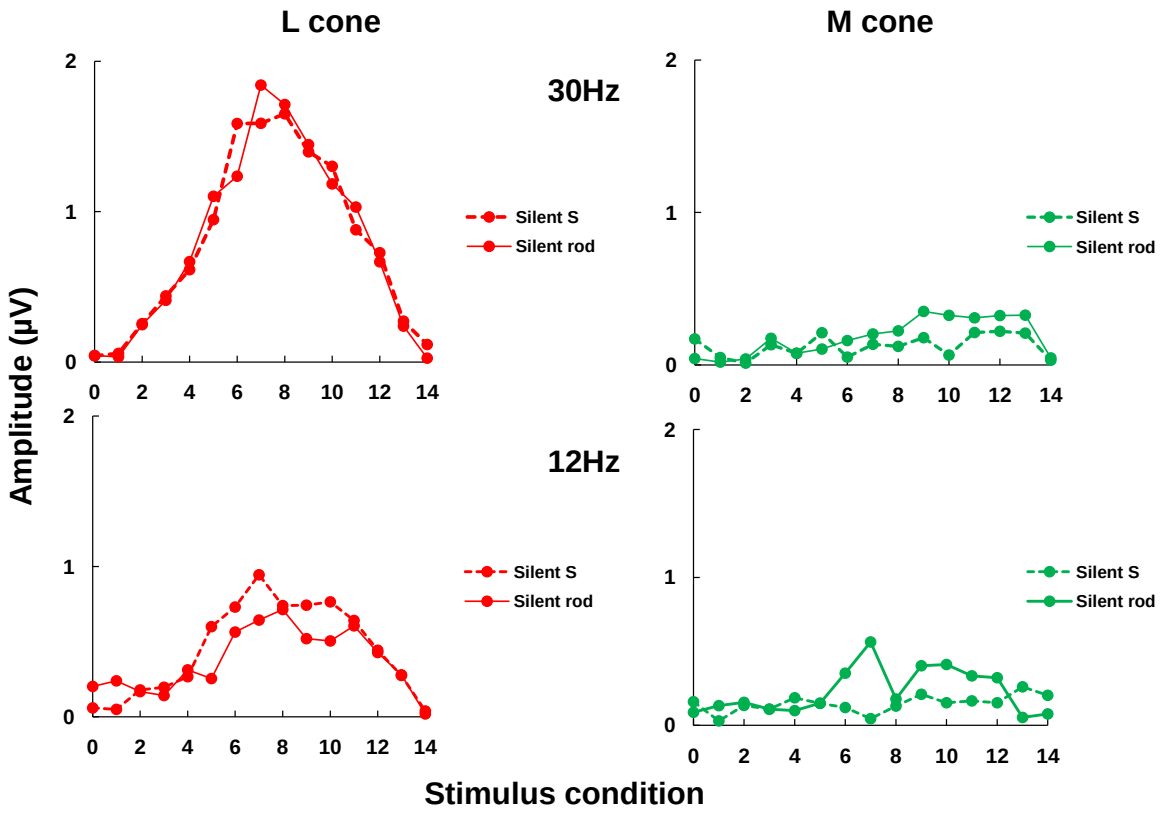

Figure 8.6 L and M cone response amplitudes in a subject as function of retinal regions stimulated. Dashed line represents the responses when S cones are silenced and straight line data represent responses when rod photoreceptors are silenced. Upper traces represent ERG responses at 30Hz and lower traces represent ERG responses at 12Hz.

8.4 RESULTS

8.4.1 Amplitudes

Figure 8.7, 8.8, 8.9, 8.10 and 8.11 shows typical data obtained in the experiment for five different subjects. The graphs plot the magnitude of the fundamental ERG amplitudes (1H) and a measure of noise (1H -1) as a function of the 15 stimulus conditions (note that conditions 0 and 14 contain no stimulus). For the 12 Hz stimulus the amplitudes of the ERG responses elicited by the L and M cone isolating stimuli vary across all conditions but are similar to each other. Typically, the responses increase up to a maximum for condition 8 (the largest circular stimulus), then decrease in amplitude as the area of central ablation gets larger. For the 30 Hz stimulus the magnitudes of the L and M cone responses are very different. At this faster stimulation rate the L cone isolating stimulus generates robust responses across virtually all stimulus conditions. In contrast, the responses elicited by the M cone isolating stimulus are greatly reduced at this frequency. This trend is seen in all five subjects. In addition to this, we can also notice that the noise (1H-1) is well below the signal in especially from condition 2 to 12.

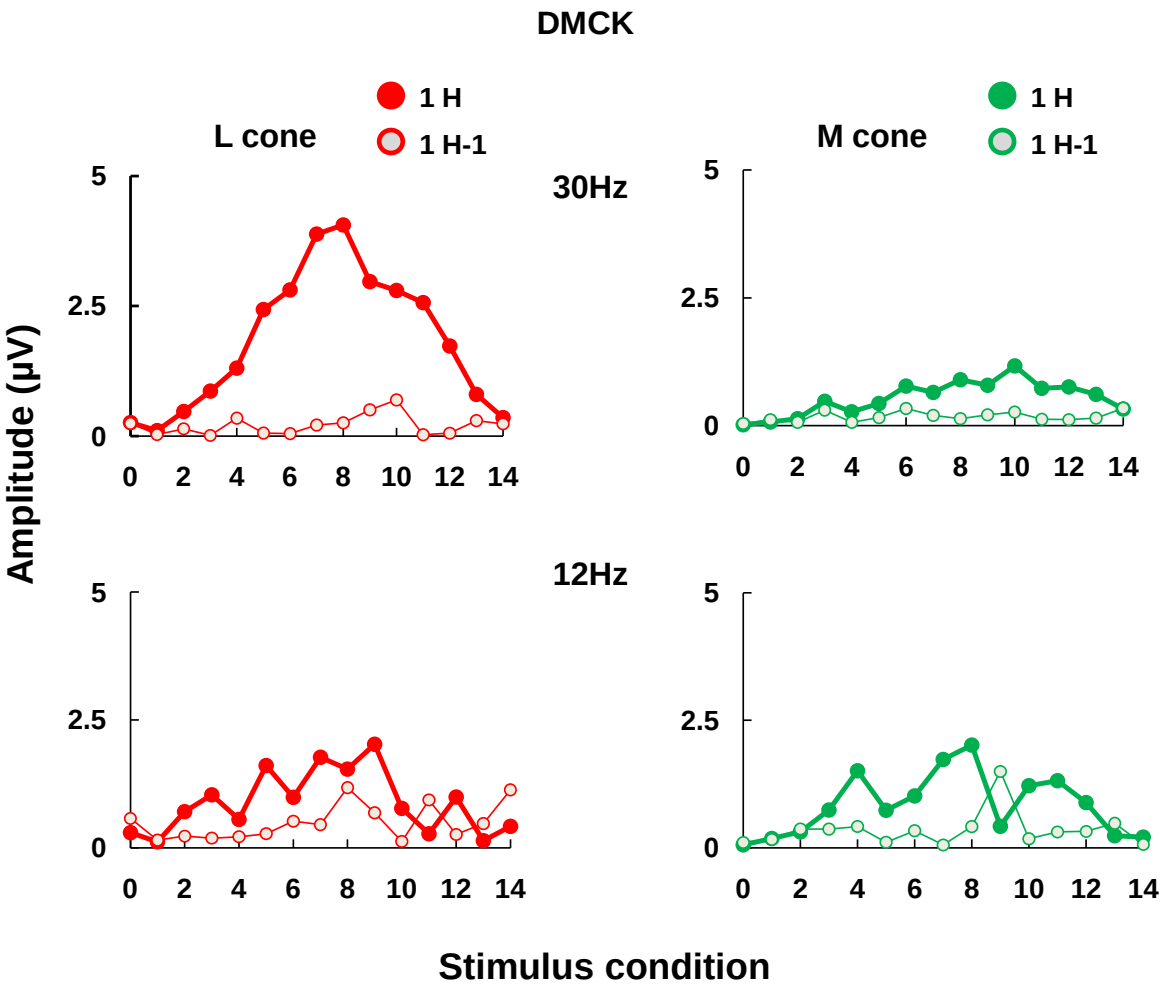

Figure 8.7 L and M cone response amplitudes as function of retinal regions stimulated at two modulation rates (12Hz and 30Hz) for subject 1. Filled circles represent the first harmonic (1H) responses and open circles represent the measure of noise (1H-1).

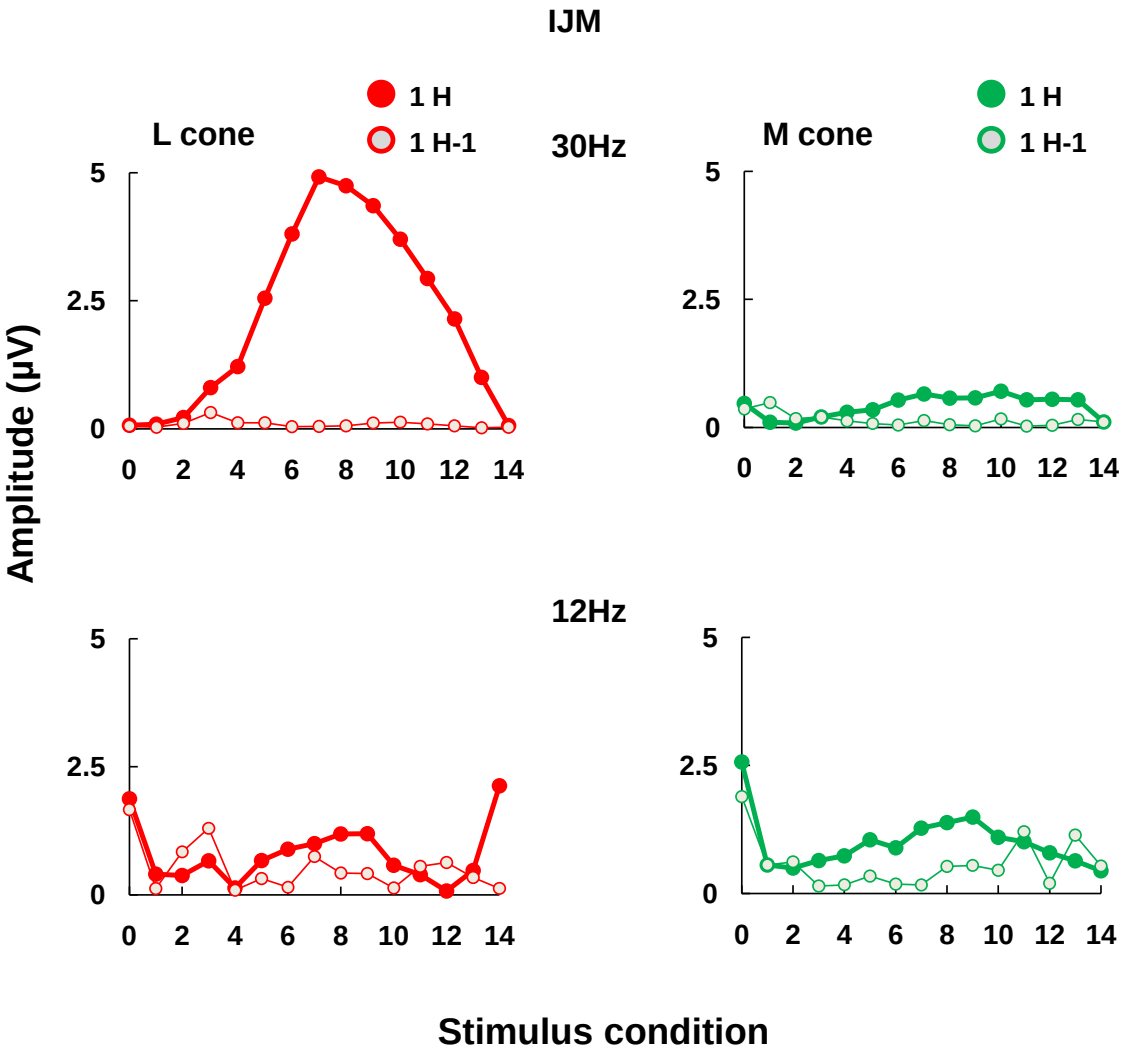

Figure 8.8 L and M cone response amplitudes as function of retinal regions stimulated at two modulation rates (12Hz and 30Hz) for subject 3. Filled circles represent the first harmonic (1H) responses and open circles represent the measure of noise (1H-1).

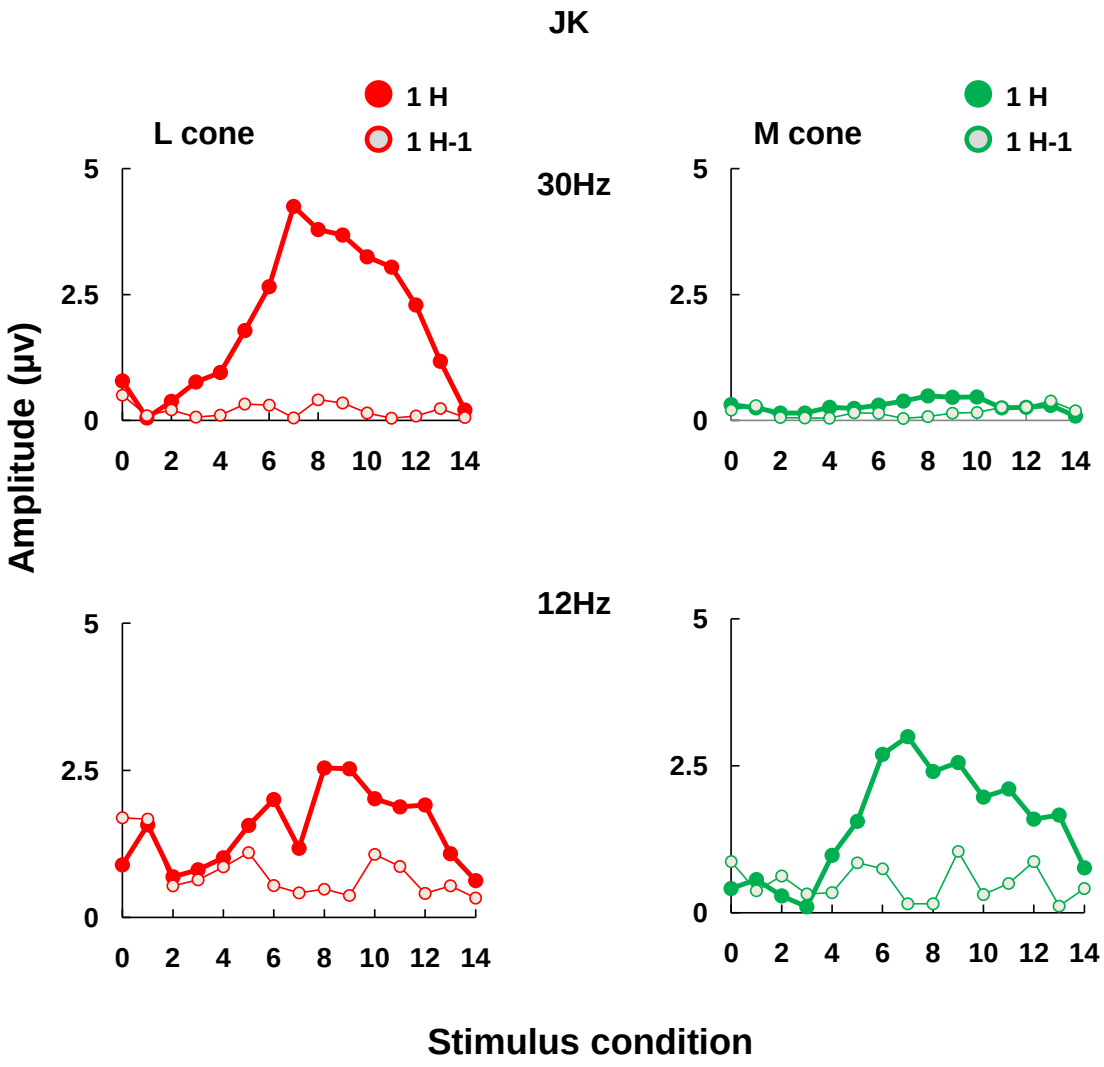

Figure 8.9 L and M cone response amplitudes as function of retinal regions stimulated at two modulation rates (12Hz and 30Hz) for subject 3. Filled circles represent the first harmonic (1H) responses and open circles represent the measure of noise (1H-1).

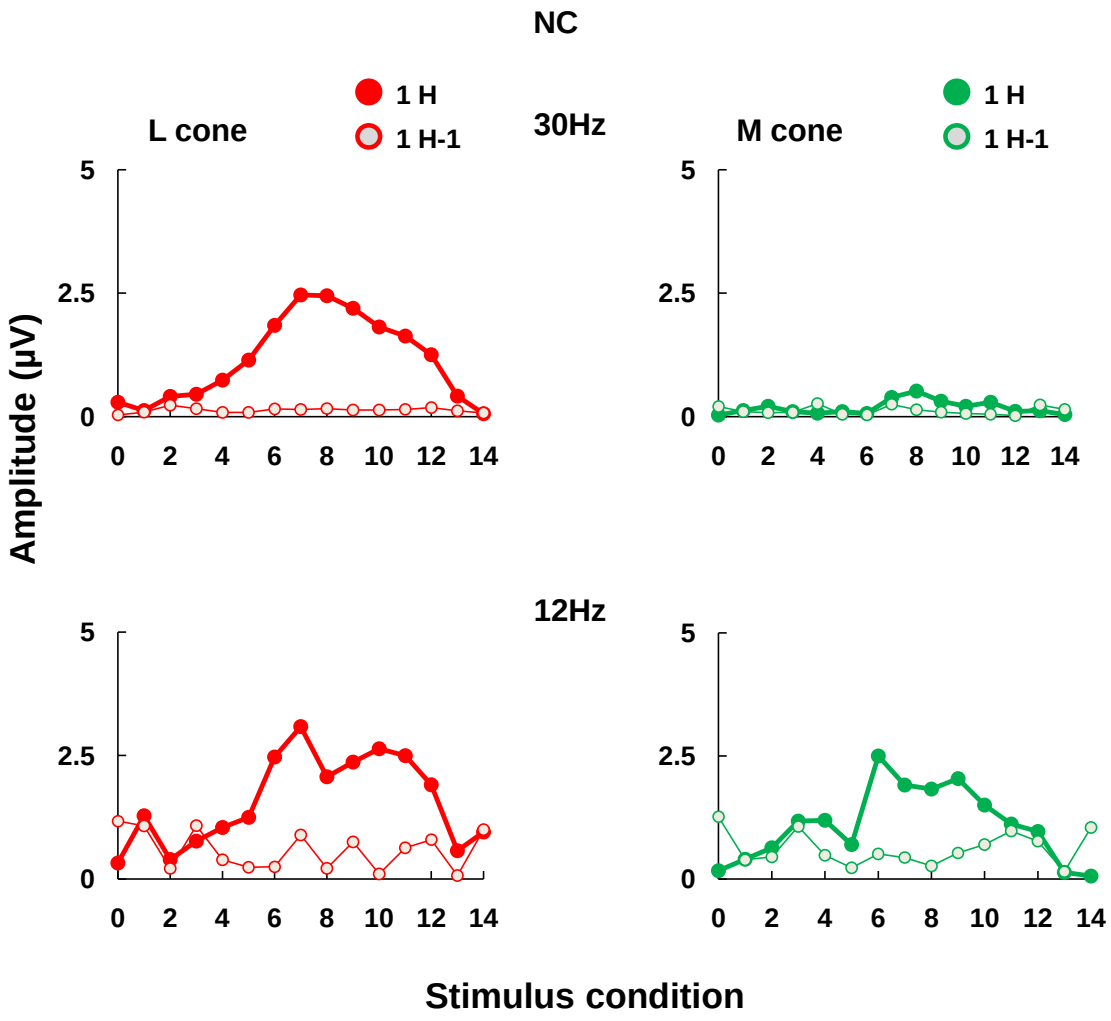

Figure 8.10 L and M cone response amplitudes as function of retinal regions stimulated at two modulation rates (12Hz and 30Hz) for subject 4. Filled circles represent the first harmonic (1H) responses and open circles represent the measure of noise (1H-1).

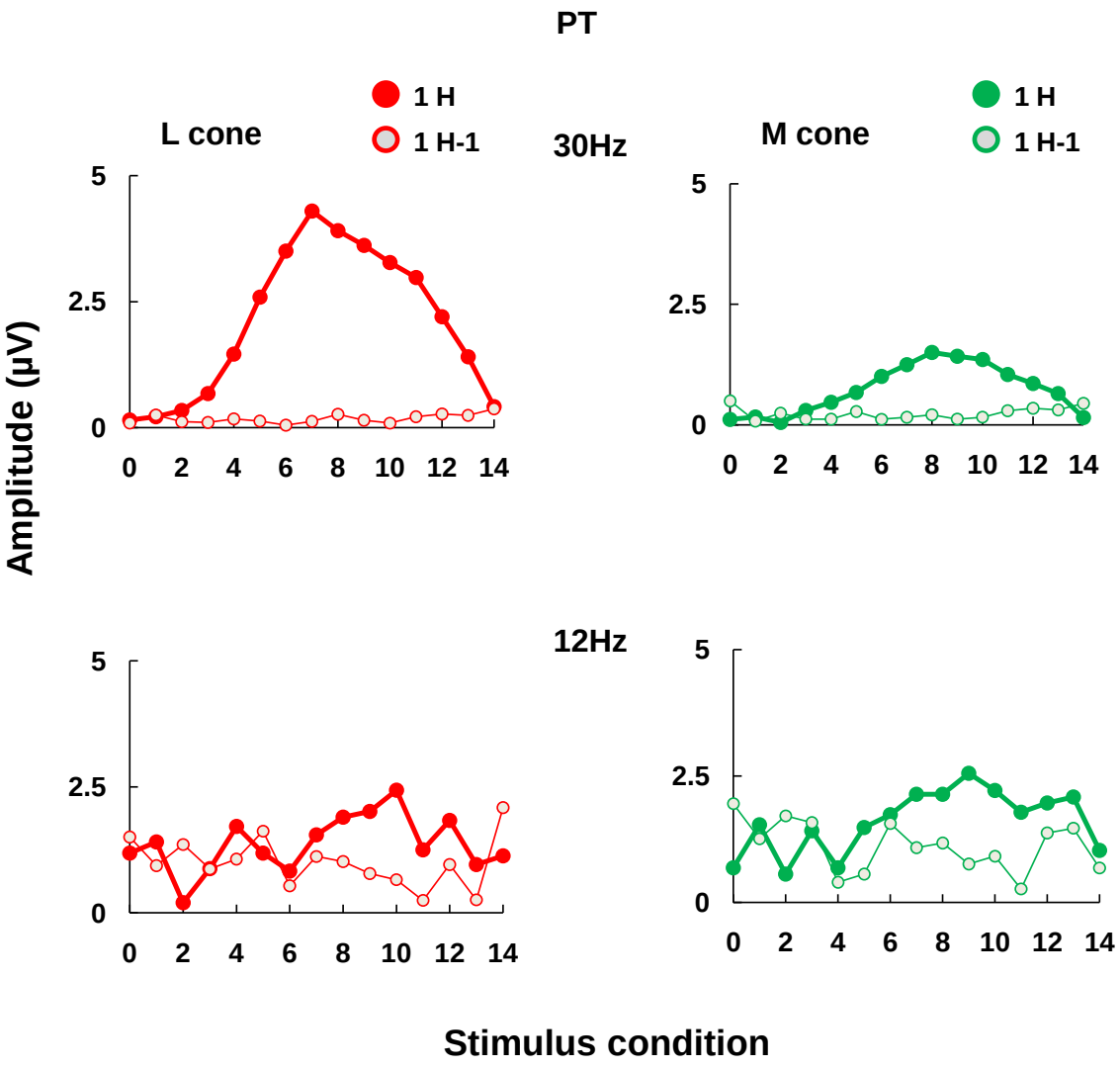

Figure 8.11 L and M cone response amplitudes as function of retinal regions stimulated at two modulation rates (12Hz and 30Hz) for subject 5. Filled circles represent the first harmonic (1H) responses and open circles represent the measure of noise (1H-1).

Figure 8.12 shows the group average data of L and M cone ERG responses for 30Hz and 12Hz respectively. Figure 8.13 and 8.14 shows individual data that compare L and M cone ERG responses at 30Hz and 12Hz stimulation rates respectively, for all stimulus conditions. From mean data (figure 8.12) we can be observe that L cone responses are robust at the faster stimulation rate (30Hz)

than for the slower stimulation rate (12Hz). In contrast, M cone responses are larger at a slower stimulation rate (12Hz) than at a faster stimulation rate (30Hz). Both L and M cone responses, typically, increase up to a maximum for condition 8 (the largest circular stimulus), then decrease in amplitude as the area of central ablation gets larger. It is obvious from 30Hz data that the L cone amplitudes are larger than M cone amplitudes across all stimulus conditions. On the other hand, 12Hz data shows nearly equal L and M cone amplitudes for all stimulus conditions.

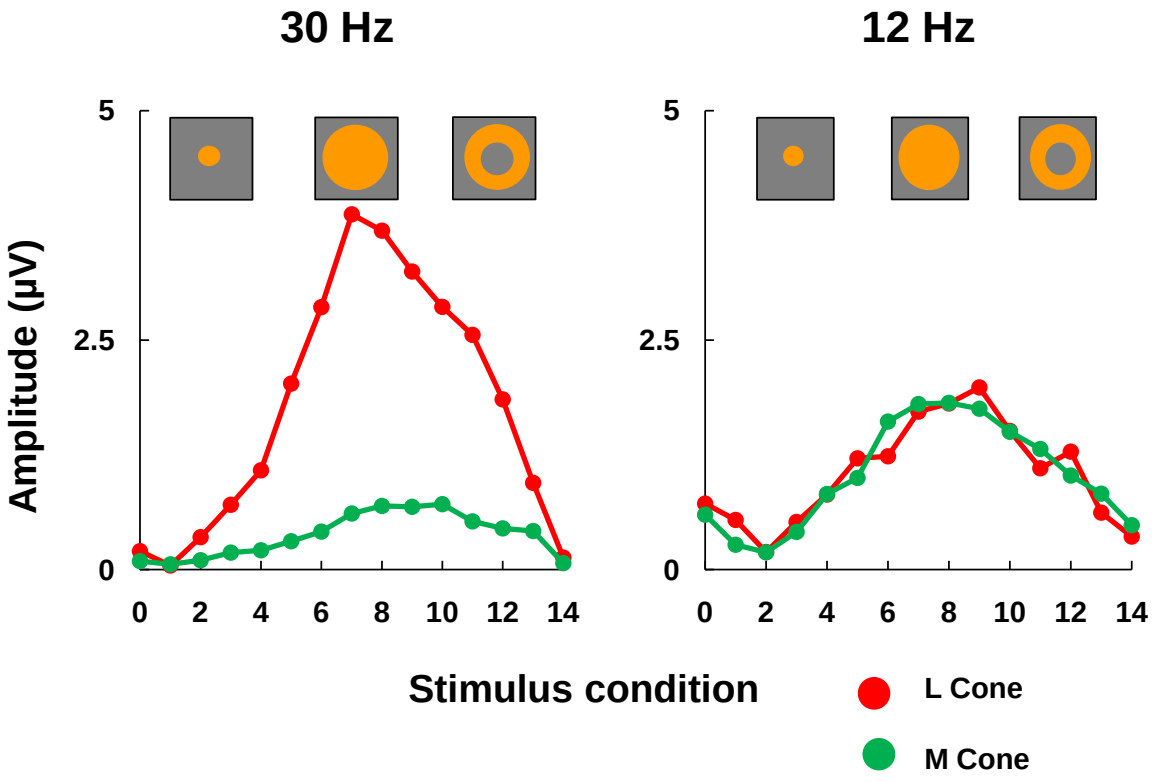

Figure 8.12 Mean L and M cone response amplitudes as function of retinal regions stimulated at two modulation rates. Red circles represent the L cone responses and green circles represent the M cone responses. We can notice hat at 30Hz responses are dominated by L cones and in contrast, at 12Hz, L and M cones have nearly equal amplitudes.

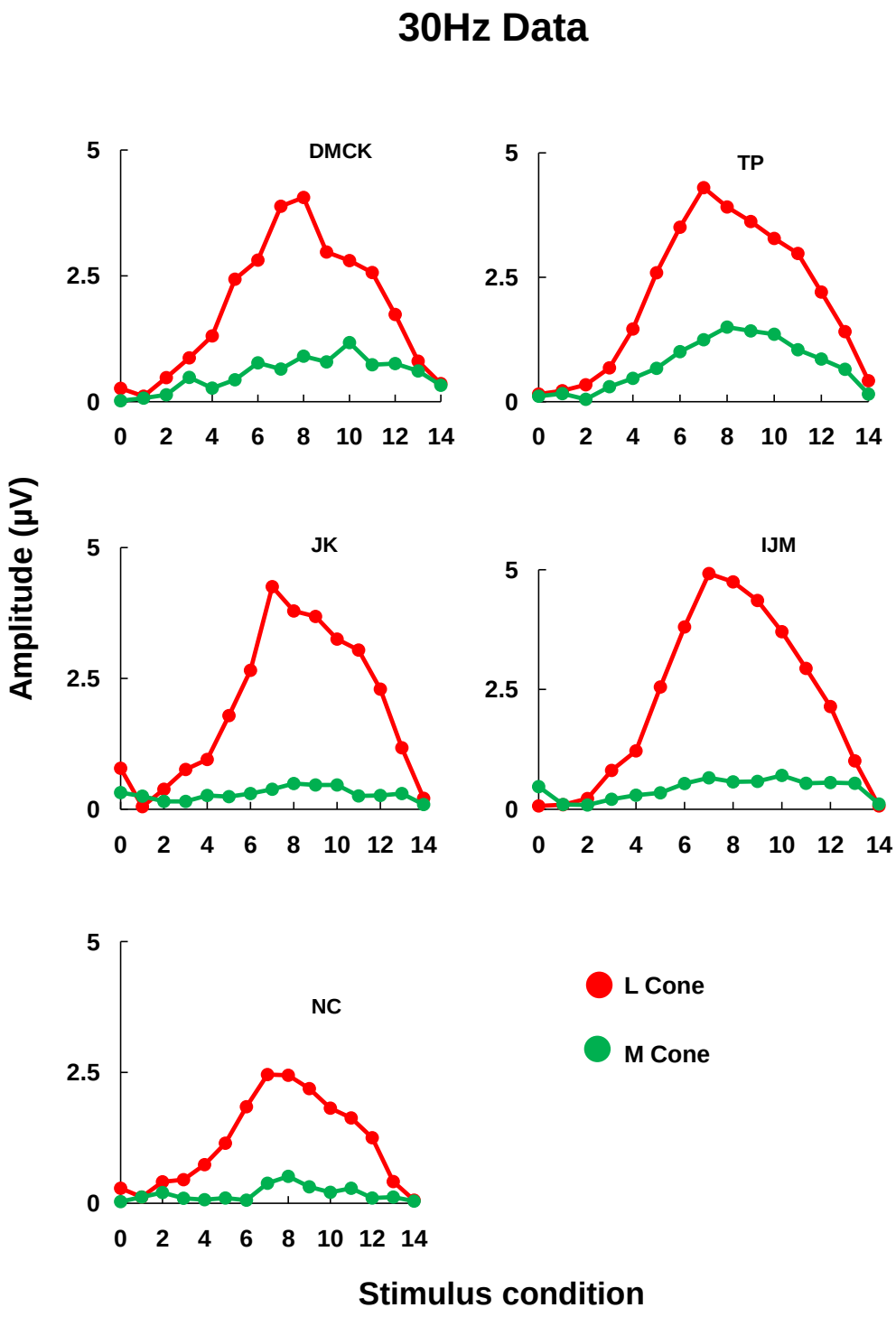

Figure 8.13 L and M cone response amplitudes as function of retinal regions stimulated at 30Hz modulation rates for 5 subjects. Red circles represent the L cone responses and green circles represent the M cone responses. We can notice that all subjects have large L cone responses and poor M cone responses.

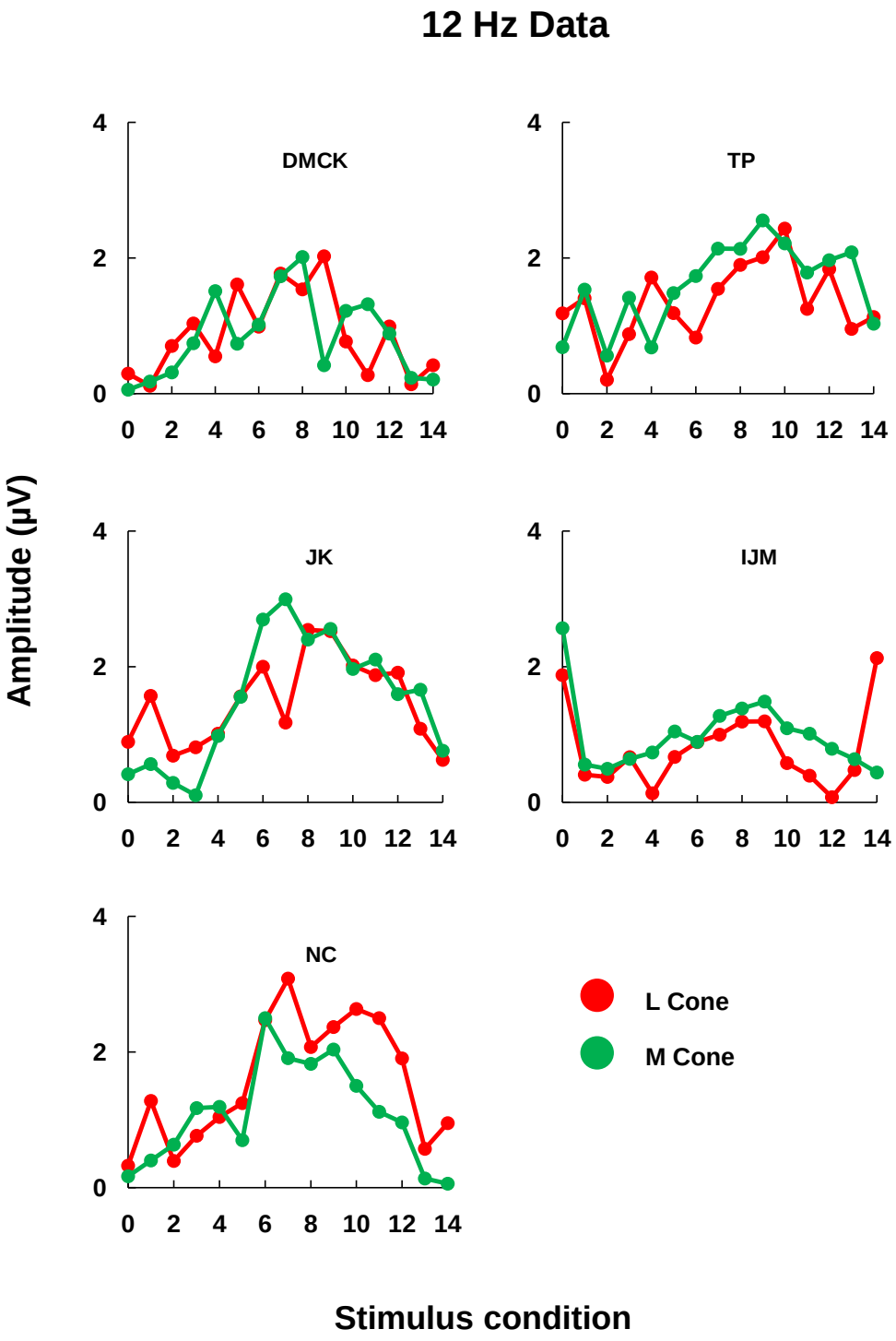

Figure 8.14 L and M cone response amplitudes as function of retinal regions stimulated at 12 Hz modulation rates for 5 subjects. Red circles represent the L cone responses and green circles represent the M cone responses.

8.4.2 L:M ratios

We used the above data to calculate L:M cone response amplitude ratios (L:M ratios), and plotted as a function of stimulus condition (see figure 8.16) for five subjects. This has been done only for conditions 2– 12 where the fundamental response in all observers remains well above the amplitude of the noise. In figure 8.12, it can be observed that the variation in L:M ratio as a function of retinal area stimulated is different for the 12Hz compared to the 30 Hz response. For the former, L:M ratio remains close to unity (i.e. the L and M cone ERGs have similar amplitudes) for most of the stimulus conditions. In comparison the L:M ratios for the 30Hz stimulation are consistently greater than unity for all five observers across all stimulus conditions.

Figure 8.15 represents the group average (mean) data of L:M cone ratios as a function for the two stimulation rates (30HZ and 12Hz). For the 12Hz stimulus, L:M ratio remains close to unity (i.e. the L- and M-cone ERGs have similar amplitudes) for all stimulus conditions ; central circular as well as more peripheral annular configurations. In comparison, the L:M ratios for the 30Hz stimulation are consistently greater than unity across all stimulus conditions. At this stimulation rate (30Hz) there is a systematic variation in L:M ratios depending upon what region of the retina is being stimulated. For smaller (≤ 30°) circular stimuli mean L:M ratios are of the order of approximately 3:1. As the size of the stimulus increases up to a maximum diameter of 70° (condition 7) the L:M increase up to a maximum of over 7:1. Then as increasingly larger central areas of the stimulus are ablated and the stimulus becomes a narrower annulus (conditions 9 – 12) the L:M ratio falls back down to a level similar to that found for the smaller circular central

stimuli. The mean data shows large error bars for 30Hz data suggesting the large variation in L;M ratios among individuals. In contrast, 12Hz data shows small error bars across all stimulus conditions suggesting minimum variation among the subjects.

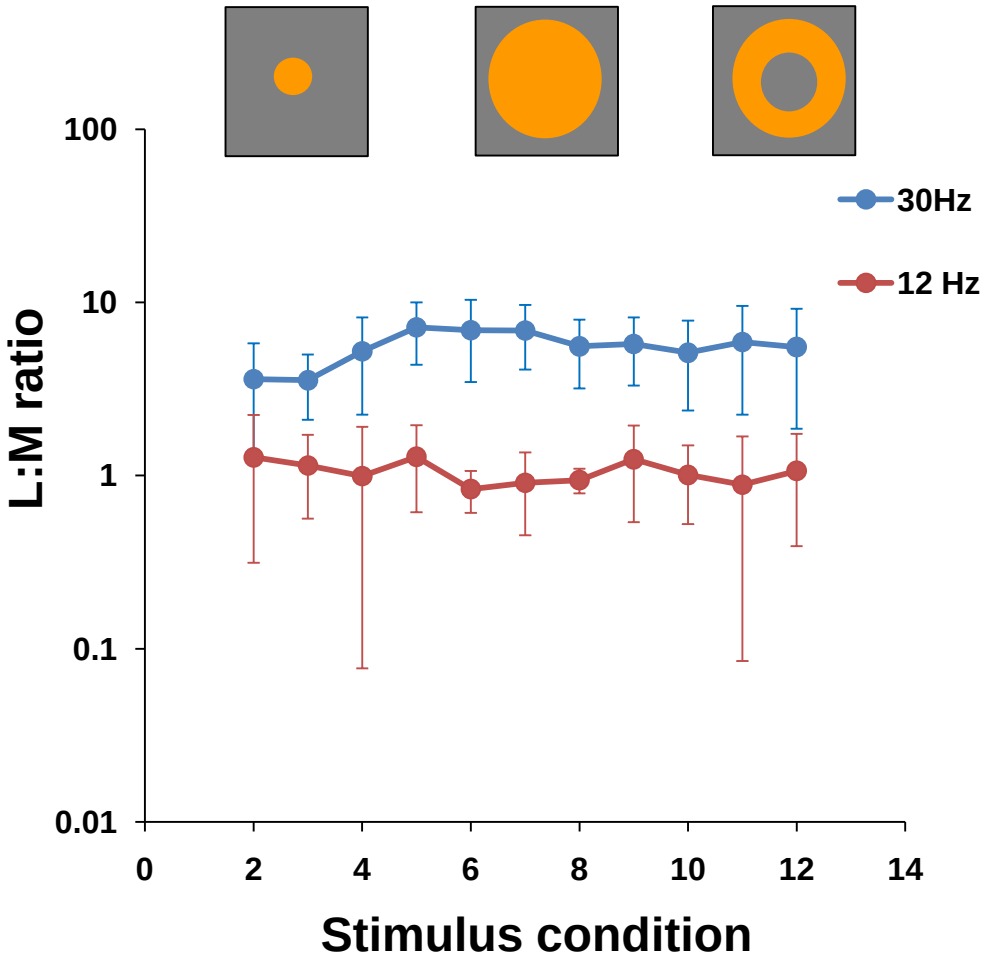

Figure 8.15 Group average data of L:M cone ratios as function of retinal regions stimulated at two modulation rates. Blue circles represent the L:M ratios at 30Hz. Brown red circles represent the L:M ratios at 30Hz. We can notice that at 30Hz L:M ratios are greater than unity and at 12Hz, L:M ratios are nearly unity for all stimulus conditions. Note that vertical scale is plotted on log scale.

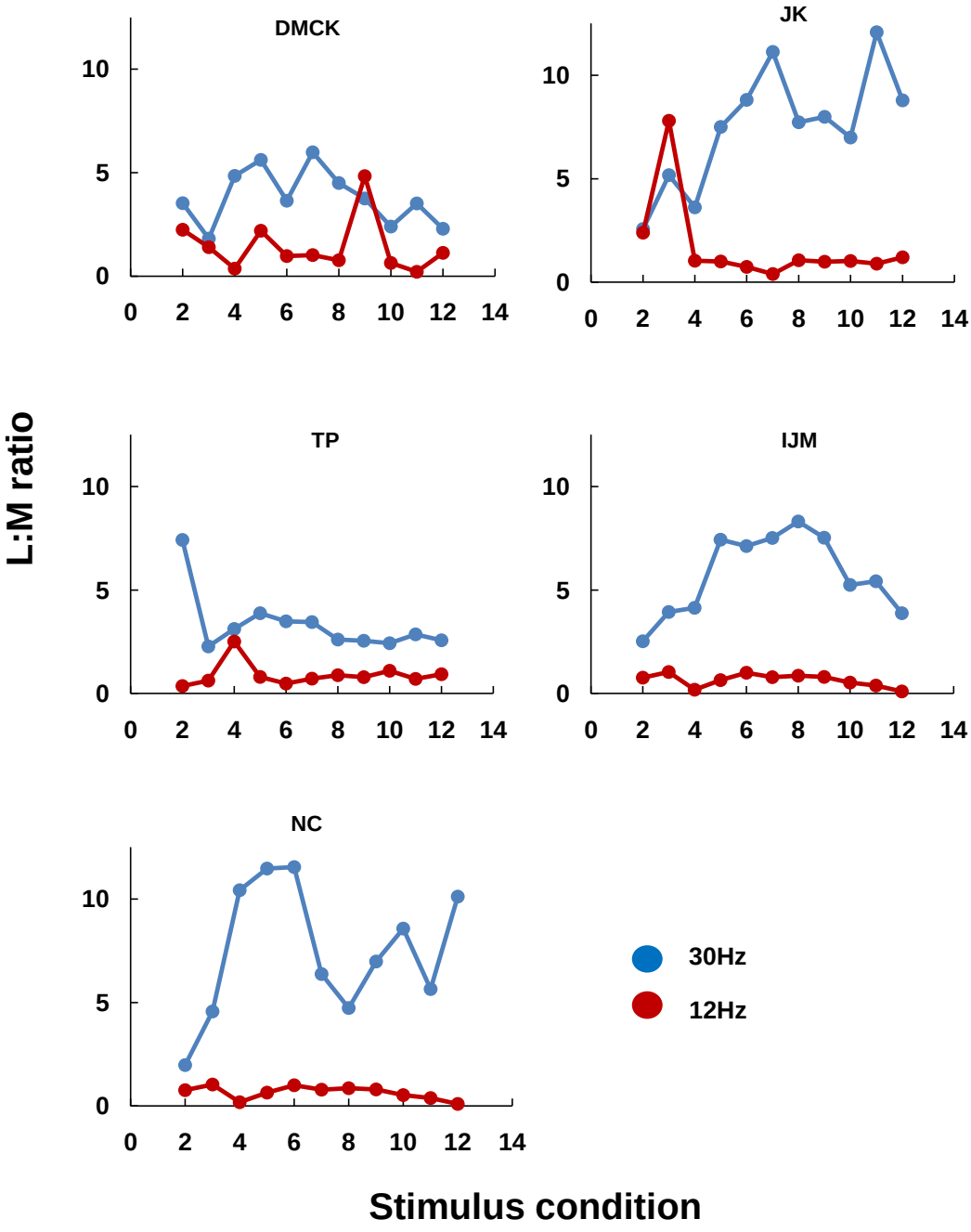

Figure 8.16 L:M cone ratios as function of retinal regions stimulated at two modulation rates for 5 subjects. Blue circles represent the L:M ratios at 30Hz. Brown red circles represent the L:M ratios at 30Hz. We can notice that at 30Hz L:M ratios are greater than unity and at 12Hz, L:M ratios are nearly unity for all stimulus conditions in all five subjects.

Considering the large standard deviation of L:M ratios for 30Hz data we want to see whether the positive trend (that is increase the stimulus size increase in L:M ratios) is real for all the five subjects. In order to test this we derived regression plots (see figure 8.17) of L:M ratios as function of stimulus size for five subjects from condition 2 to condition 7 for the 30Hz data.

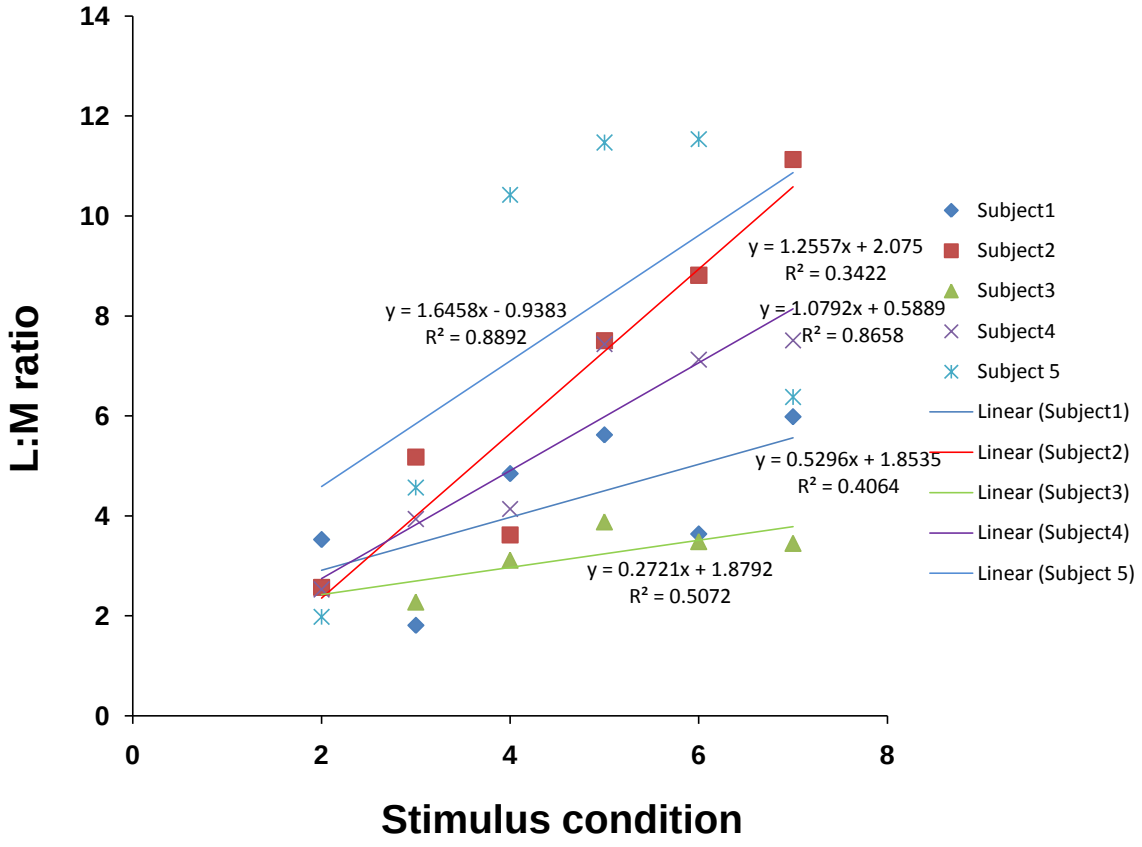

Figure 8.17 L:M ratios as function of stimulus condition (2-7) in five different individuals. Regression lines are fitted for each individual. One way ANOVA (analysis of variance) was performed to compare the slopes of five individuals. Analysis shows no significant difference (p= 0.235, p>0.05) in slopes between individuals suggesting similar trend in all subjects.

We performed one way ANOVA from summary data (interactive statistics, for information see **http://statpages.org/anova1sm.htmlpage)** to compare the slopes

of individual subjects. Results suggest there is no significant difference (p=0.235) in the slopes of five subjects. It means all subjects follow similar trend (positive correlation coefficients) in L:M ratios as we increase the stimulus size. We also fitted regression line using all observers L:M ratio data to see the type of effect of stimulus size on L:M ratios of all five subjects (see figure 8.18). The regression analysis (see table 8.1) shows that the L:M ratios are significantly different (p=0.006, F value = 8.676) as we change the spatial configuration of stimulus. These statistical results put together it can be said that, by increase in stimulus size L:M ratio increases significantly.

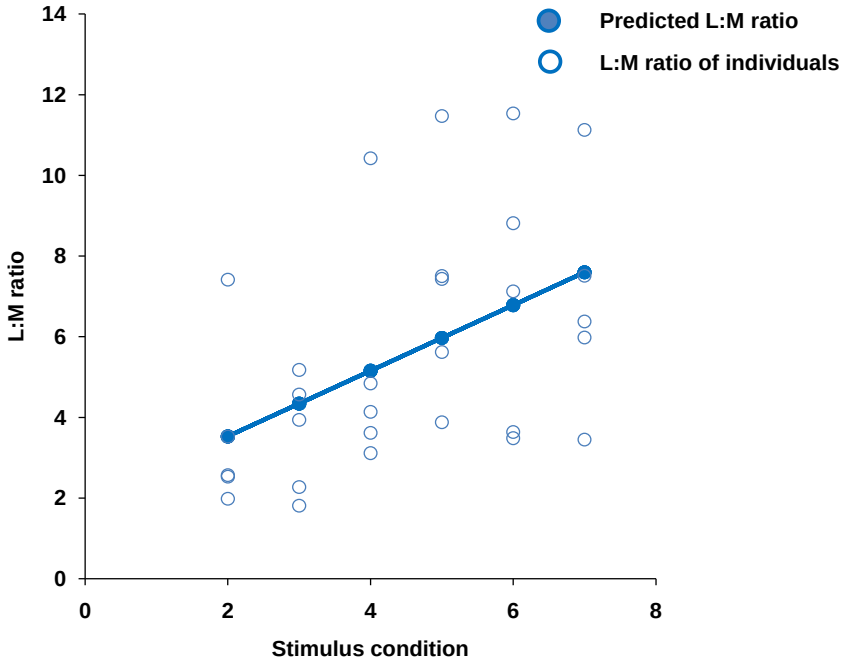

Figure 8.18 L:M ratios as function of stimulus condition (2-7) in five different individuals for 30Hz data. Regression lines are fitted from the overall data points. Regression line shows positive trend. Analysis shows significant difference (p= 0.0064, p<0.05) suggesting that, as the stimulus size is increased L:M ratio also increase significantly. Note that open circles in raw data of L:M ratios of all five subjects. Filled circles indicates predicted L:M ratio from the all the data points.

Regression Statistics					
Multiple R	0.4863				
R Square	0.2365				
Adjusted R Square	0.2092				
Standard Error	2.5847				
Observations	30				
ANOVA					
	df	*SS*	*MS*	*F*	*Significane.*
Regression	1	57.9657	57.9657	8.6760	**0.0064**
Residual	28	187.07162	6.6811		
Total	29	245.0373			

Table 8.1 Regression analysis of the five subjects data from condition 2 to condition 7(total observations 30). Analysis shows significant difference (shown in bold numbers) suggesting that, change in the spatial configuration of the stimulus has a significant effect on L:M ratio.

8.4.3 L and M cone response phase

Important feature of the data shown in figure 8.12 is the relatively low amplitude responses that are obtained from the M cones in response to the 30 Hz cone isolating stimuli. By comparison, the L cone response still appears to be robust at this temporal rate. A possible reason for this lies in the fact that there are differences in the phase of the M cone responses as a function of the retinal area being stimulated. Figure 8.19 shows the group average phase of the L and M cone ERGs plotted as a function of stimulus condition for the 12and 30Hz stimulation rates.

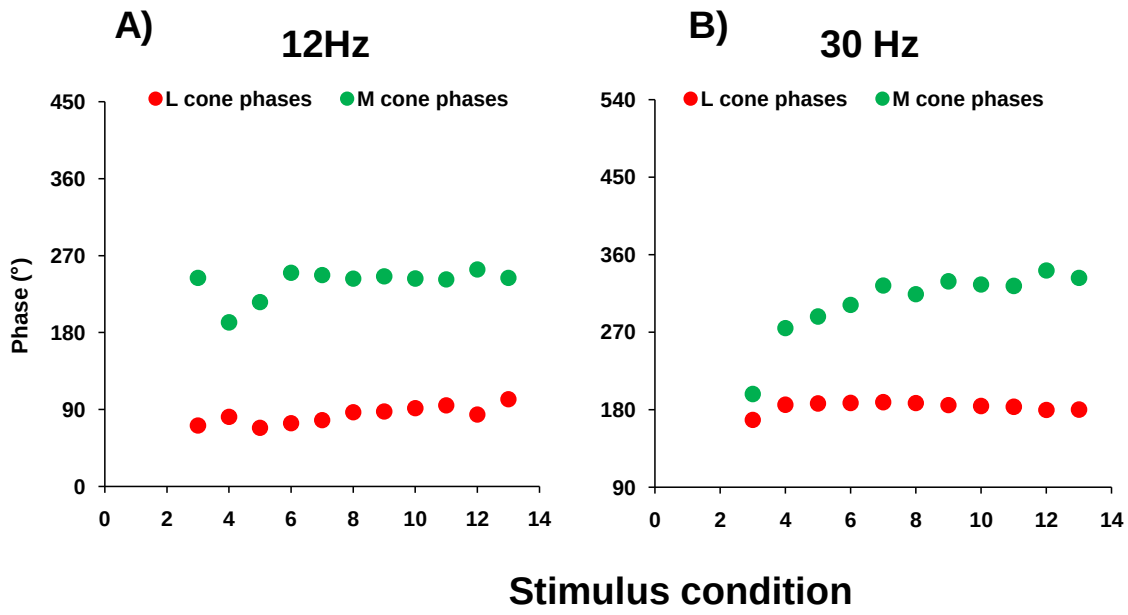

Figure 8.19 The mean (n=5) variation in the phase of L and M cone ERGs as function of stimulus condition. A) Phase variation for 12 Hz stimulation B) Phase variation for 30Hz stimulation.

Figure 8.20 and Figure 8.21 shows the Individual phase data for L and M cone ERGs plotted as a function of stimulus condition for the 12 and 30Hz stimulation rates.

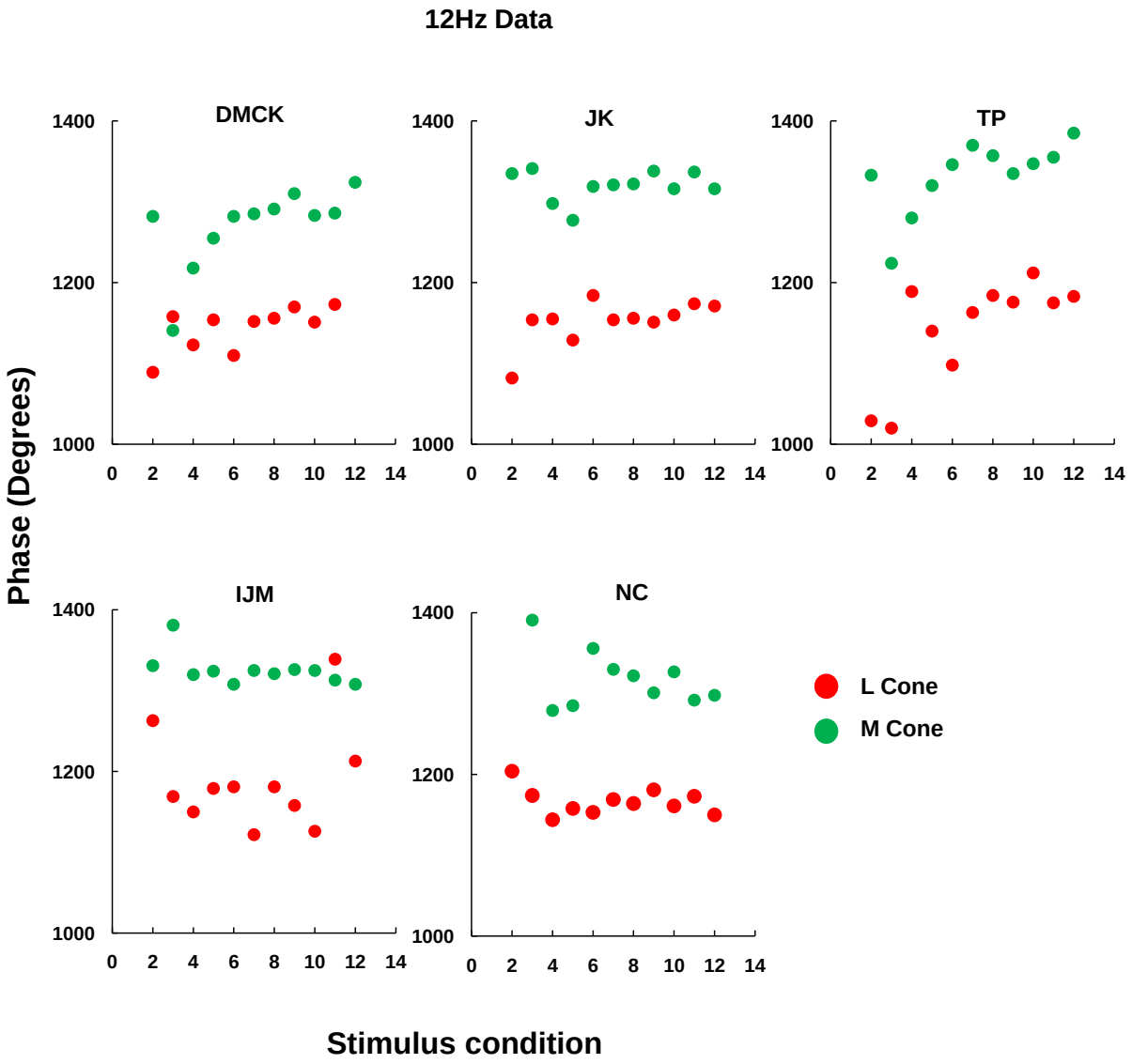

Figure 8.20 L and M cone phases as function of retinal regions stimulated at 12Hz modulation rates for 5 subjects. Red circles represent the L cone phases and green circles represent the M cone phases. The L and M cone phases are nearly constant across all conditions except the variation in M cone phases for the observer TP and DMCK. Note that the large phase values (phases plus 3-4 full cycles) represents the raw data.

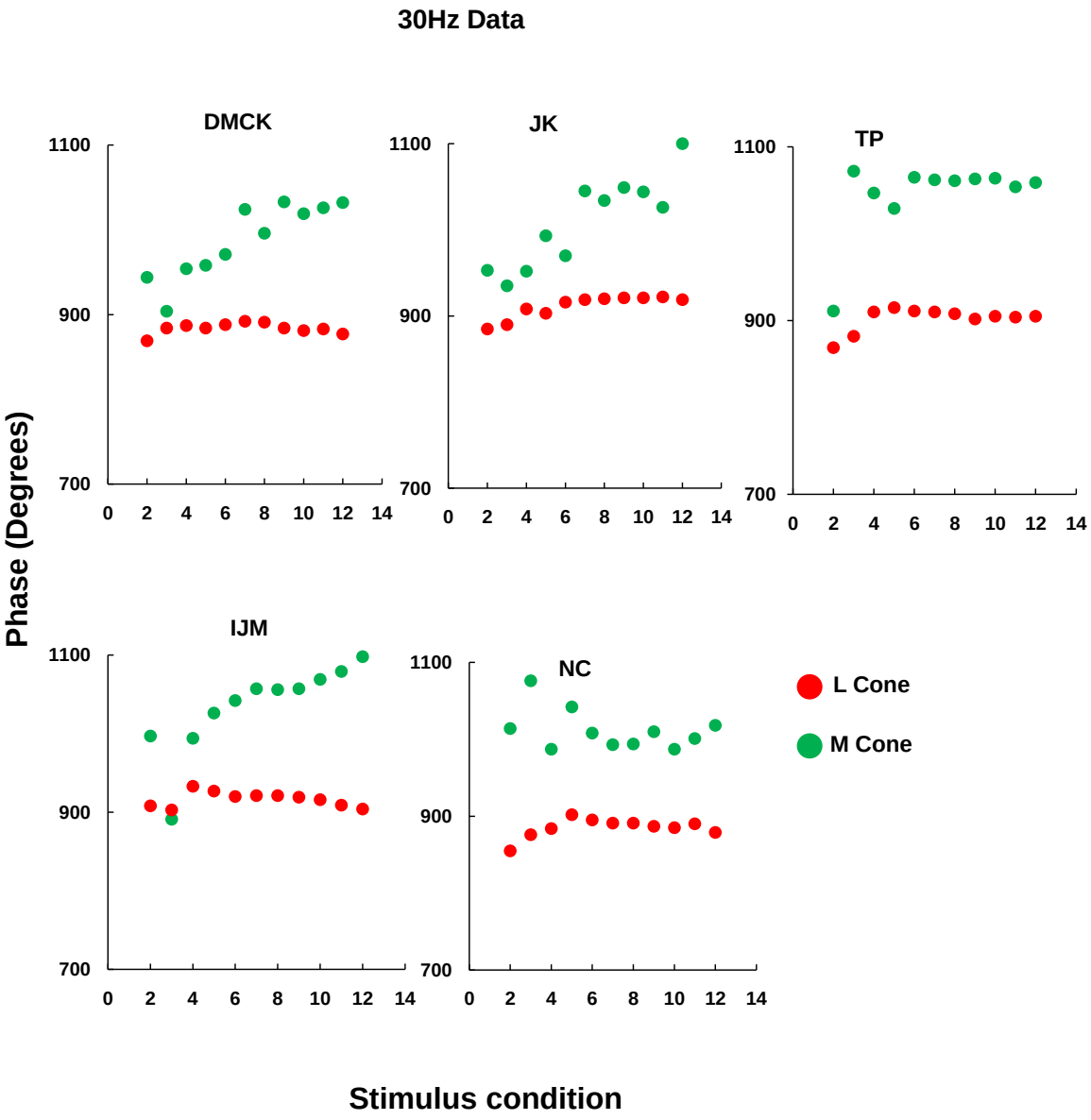

Figure 8.21 L and M cone phases as function of retinal regions stimulated at 30Hz modulation rates for 5 subjects. Red circles represent the L cone phases and green circles represent the M cone phases. The L cone phases are nearly constant across all conditions. In contrast M cone phases are nearly phase advanced by 150° for largest stimulus (stimulus condition 7). However subject TP and NC has relatively constant M cone phases. Note that the large phase values (phases plus 2-3 full cycles) represents the raw data.

For 12Hz modulation the phases of L and M cone responses are relatively constant as function of stimulus condition. For 30Hz, whilst the phase of L cone is stable across conditions, M cone phase undergoes an advance of 100° between conditions 3-13. Existence of phase differences or 'phase smearing' between the responses elicited from the central retinal areas by the small circular stimuli, and those elicited from more peripheral retinal areas by the annular stimuli, means that when M cone ERGs are elicited by large diameter (70°) stimuli there will be destructive interference between the response from these different retinal areas. As a result of this what we observe is a reduction in M cone ERG response amplitude, which in turn will lead to an increase in the measured L:M ratios, particularly for the larger stimuli. This point is demonstrated in figure 8.22, where the amplitudes of the ERGs obtained from the large 70° circular stimulus (condition 7) are compared to the scalar sum of the amplitudes obtained for conditions 4 (30° circular stimulus) and 10 (the annular stimulus with outer diameter = 70° but with a central ablation of 30°). This summing of responses from conditions 4 and 10 effectively discounts the phase differences that exist between the ERGs elicited from these two retinal regions. If additivity holds across the retina for the ERG then the amplitudes for condition 7 should equal the sum of those obtained for conditions 4 and 10. This is close to being the case for the L-cone response at 30 Hz where, for all observers, the summed response constitutes over 90% of the response amplitude obtained for condition 7 alone. (This additivity, incidentally, is also a good indicator that we are getting responses from localized retinal regions and that stray light is not a major contributory factor in the generation of these responses). For the M cone response the summed amplitudes from conditions 4 and 10 are greater than those obtained for condition 7 for all except observer 5.

This failure of additivity for the M cone response we consider to be a consequence of the phase smearing between central and more peripheral M cones. Interestingly, for observer 5 the 30 Hz M cone phase exhibits the least variation as a function of stimulus condition.

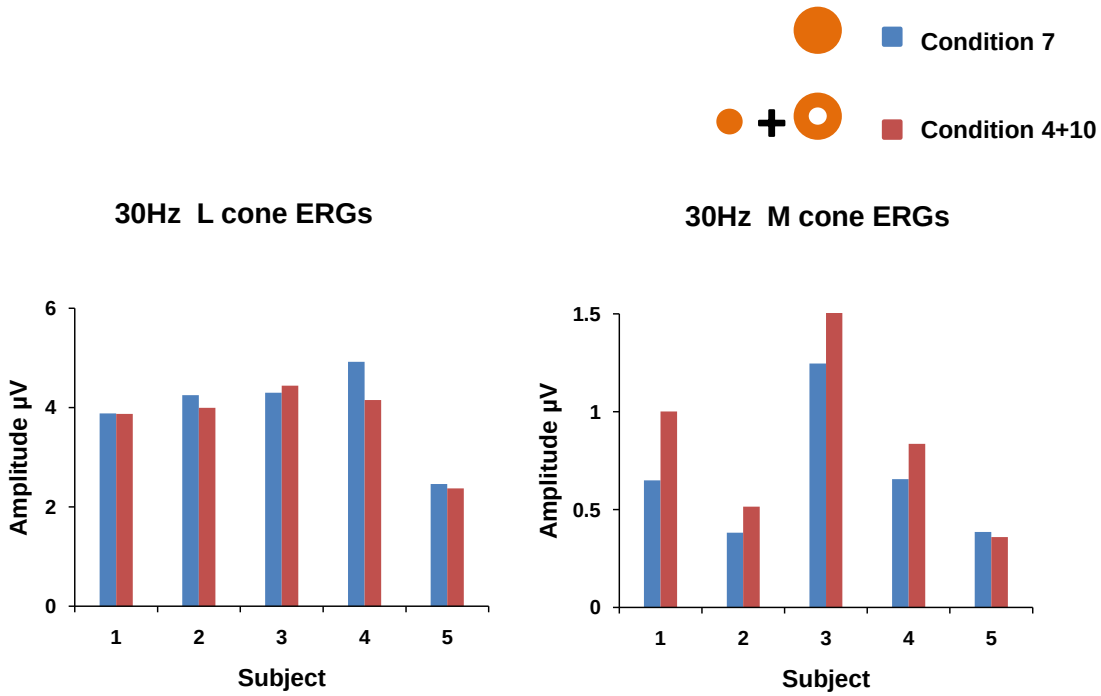

Figure 8.22 Graphs for each of the 5 observers showing the difference in response amplitude between ERGs obtained from the largest stimulus (70° circular stimulus - condition 7) compared to those obtained by summing the response amplitudes obtained from conditions 4 (30° circular stimulus) and 10 (annular stimulus with a 70° outer diameter and a 30° inner diameter). a) The comparison between the equal areas of stimulation is shown for the 30 Hz L-cone response. For each observer the summed response accounts for approximately 90% of that obtained by the single large stimulus. b) The same comparison is shown for the 30 Hz M-cone responses. In this case for 4 of the 5 observers the summed response is greater than that obtained for the large single stimulus, indicating a failure of additivity.

8.4.4 M cone response phase in a trichromat and a protanope

We observed the variation in M cone response phase as a function of stimulus condition for 30Hz ERG in trichromats. We were also interested to find whether the phase behaviour of M cones in protanope is the same? This would allow studying the response phase of M cone pathways in the absence of L cones. We plotted the M cone response phase as function of stimulus condition in a protanope and a trichromat as shown in figure 8.23. From the plots we can observe that, protanope has a relatively constant M cone phase response as function of stimulus condition whilst trichromat showed advance in M cone response phase as a function of stimulus condition. These results in protanope suggest that the phase behaviour of M cone pathways changes in the absence of L cones.

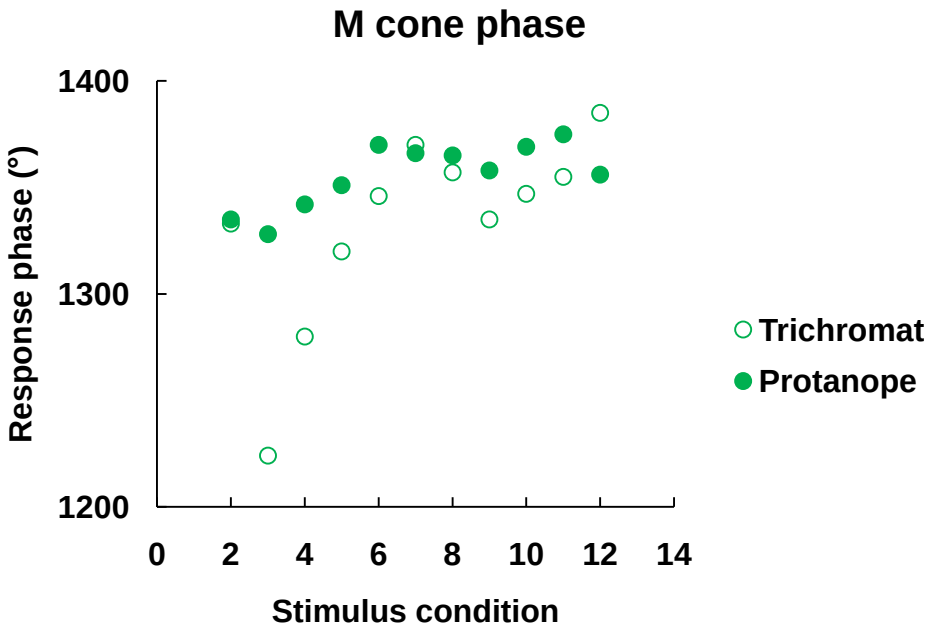

Figure 8.23 M cone response phases of a trichromat and a protanope for different stimulus configurations. In a protanope, M cone response phase is relatively constant across all the conditions and in a trichromat M cone response phase is significantly varied as stimulus condition is changed.

8.4.5 Temporal properties of L and M cones for various stimulus conditions

The other possible reason for the poor M cone responses at 30Hz would be the temporal properties of the M cones itself. In order to verify this we recorded L and M cone ERGs for three stimulus conditions at five modulation rates in a single subject. It can be noted from the left plot of the figure 8.24 that the L cone amplitudes show a band pass function at about 20Hz for central and peripheral stimuli. On the other hand M cone amplitudes (see figure 8.24, right plot) reduced significantly as temporal frequency is increased for all stimulus conditions. We can also observed from the data that the temporal properties of M cones are different from L cones Moreover, compromised M cone responses are noted at higher temporal frequencies at different retinal regions tested. One more observation from the data is temporal characteristics of central L and M cones are not so different from peripheral L and M cones.

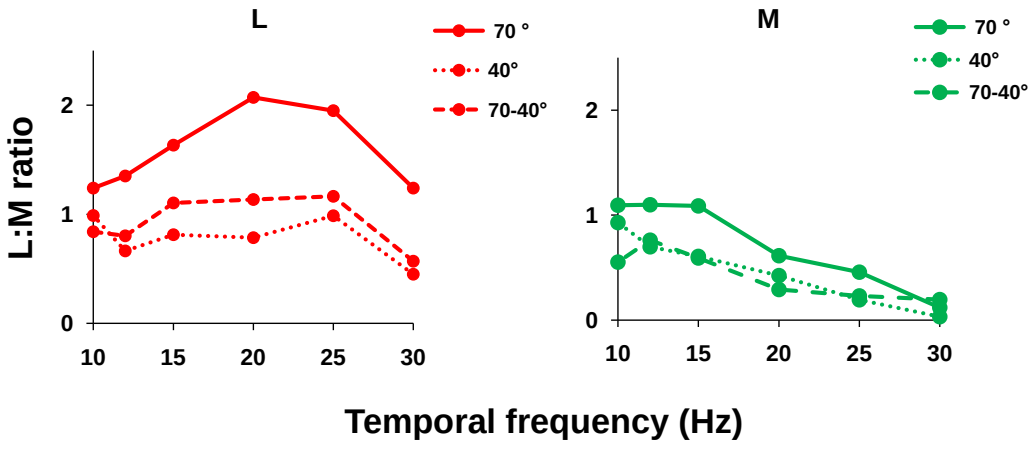

Figure 8.24 L and M cone response amplitudes as function of temporal frequency at various retinal regions stimulated. Left plot represent L cone response and right plot represents M cone responses. See the difference in the temporal characteristics of L and M cone responses.

8.5 DISCUSSION

In this experiment we have used L and M cone isolating stimuli at two different temporal modulation rates (30 & 12 Hz) in order to study how cone inputs to non-opponent (luminance) and cone-opponent (chromatic) mediated ERGs vary across different regions of the retina. Our results illustrate that for the cone-opponent mediated (12 Hz) ERG, measured L:M ratios are close to unity and that this ratio remains constant across the different retinal areas that were stimulated. The existence of an L:M ratio close to unity and L/M phase difference of nearly 180° for the 12Hz response indicate that there is a balanced and opponent contribution from L- and M-cones to this response consistent with the idea that it is mediated by cone-opponent, P pathway (Kremers & Link, 2008).

ERG cone amplitude ratios have been shown to be directly correlated with L:M cone ratios determined by anatomical means (Stockman et al., 1993b , Kremers et al., 2000 , Kremers, 2003 , Usui et al., 1998 , Kremers et al., 2003). In normal trichromats L:M cone ratios have been shown to vary widely across different subjects (Brainard et al., 2000; Carroll et al., 2002; Hofer et al., 2005). In spite of such large variations in the relative numbers of L and M cones in the human retina it has been a persistent puzzle that how perception of colour remains remarkably stable across observers. For an instance, the wavelength of unique yellow shows little variation across observers in spite of large differences in L:M cone ratios (e.g. Brainard et al., 2000; Miyahara et al 1998). The L-M cone-opponent mechanism appears to be able to ignore the large inter-subject variation in the numbers of L and M cones and combine them in a more uniform and balanced fashion (Neitz et al., 2002).

In relation the ‘cone-selective’ versus ‘random wiring’ theories of opponency in the primate retina, the 12Hz ERG data we presented in this experiment provides electrophysiological evidence for the existence of this more balanced and selective weighting of L and M cone contributions to the cone-opponent response across different regions of the retina. If a random pattern of L and M cone input existed then we would have seen a shift in 1:1 relationship and the L:M ratio would have been reflected the local dominance of one or other of the photoreceptors (most likely the L cones). Such a shift is not observed in the present experimental data suggesting a cone selective pattern of connectivity is maintained for the L-M opponent system across the central 70° of the retina. The suggestion that cone-selective input is maintained across the retina is also supported by psychophysical data. For an example, in size scaling experiments Vakrou et al (2005) have shown that deficits in sensitivity to peripherally presented L-M cone-opponent Gabor stimuli can be negated simply by changes in stimulus size. They showed that if a peripheral chromatic stimulus is made large enough so that the sensitivity to that stimulus can be comparable to that obtained for foveal viewing. The implication of this result lies in the fact that it demonstrates that chromatic sensitivity is preserved in the retinal periphery and must be supported by selective L and M cone inputs to the centre and surrounds of MGC receptive fields. Physiological data from the primate retina also point to the preservation of L-M chromatic sensitivity up to an eccentricity of approximately 40° (Martin et al., 2001). This psychophysical and single unit physiological data, alongside the ERG data presented here, all point to the existence of the cone-selective wiring that is necessary to support chromatic sensitivity in the peripheral retina. However, this is not to say that colour

perception in the retinal periphery remains similar to that experienced for foveal viewing, clearly it does not.

The data obtained for 30Hz ERG are different to those obtained for 12Hz response. For this stimulation frequency L:M ratios are greater than unity, ranging from approximately 4:1 for the smaller central and more peripheral annular stimuli, increasing up to 8:1 for the largest 70° diameter stimuli. The higher L:M ratios obtained for 30Hz are more likely to reflect anatomical ratios of L and M cones and their inputs to non-opponent, luminance processing mechanisms (Stockman et al., 1993b; Kremers et al., 2000; Kremers, 2003; Usui et al., 1998; Kremers et al., 2003). However, it is the variation of the L:M ratio as a function of the region of the retina that is stimulated that is of note here. Does this variation represent a genuine variation in the relative numbers of the L and M cones in these different retina areas? Previous studies, using a psychophysical as well as ERG-based methods, have provided an inconsistent picture as to how L:M cone ratios vary in the peripheral retina. Psychophysical studies have demonstrated that L:M ratios remain relatively constant with increasing retinal eccentricity (Cicerone and Nerger, 1989; Nerger and Cicerone, 1992; Otake and Cicerone, 2000; Knau et al., 2000). Similarly, certain ERG studies have reported a constant ratio (Jacobs and Neitz, 1993) whilst others have indicated that the L:M might in fact increase at greater retinal eccentricities (Kremers et al., 1999). An increase in L:M ratio has also been reported for the peripheral retina based on the analysis of variation in opsin mRNA in post-mortem human eyes (Hagstrom et al., 1998). Unfortunately, the data presented here do not resolve these inconsistencies. Whilst the L:M ratios for 30Hz stimulation do appear to vary as a function of stimulus condition, we consider this variation to be a result of the global response properties of the M-

cone ERG. We have shown that phase differences exist between 30Hz M-cone responses derived from central retina stimulation compared to more peripheral retinal stimulation. These phase differences result in a reduction in the amplitude of M-cone isolating ERG responses when the spatial extent of retinal stimulation encompasses both central and more peripheral retinal regions. The reductions in M cone relative to L cone responses means the measured L:M ratios will artificially high and may explain the increases observed for the 30Hz data. Importantly, the results demonstrate that estimates of L:M cone ratios using electrophysiological methods have to be undertaken with caution, particularly when extensive areas of retinal stimulation are employed.

We used *double* silent substitution in which we silenced the rods and other specific cone type (i.e either L or M). The possibility of S cone contribution to the L and M cone responses may be small but not be neglected. Recent study has shown that the phases of both L and M cone driven ERG difference between conditions in which S cones or rods are silenced (Kremers et al., 2009). The best way to solve this problem is to use of *triple* silent substitution method. This could be only possible with LED ganzfeld stimulators, not with the CRT monitors which have three phosphors to control three photoreceptors only. There are other advantages of LEDs over CRTs. First is larger retinal areas can be stimulated using ganzfeld and second is narrow band widths of LEDs emission spectra would allow changing the cone contrasts in wider range.

In summary, the cone weightings in the chromatic channel do not depend on the spatial parameters of the stimulus, suggesting that there is compensatory mechanism for changes in the L and M cone numbers across the retina and also across the observers. Moreover, balanced L and M cone input to the chromatic channel suggest that there is maintenance of cone-selective input in

the peripheral human retina for chromatic vision. The phases of luminance driven ERGs depend on the eccentricity when driven by M cones and not when driven by L cones. The reason for this is not clear. However the phase behaviour of non-opponent mechanism can be attributed to the relative number of L and M cones in retina. M cones are normally less in number than L cones.

8.6 PSYCHOPHYSICAL INVESTIGATION OF L:M CONE RATIOS ACROSS THE RETINA

8.6.1 Introduction

Relative numbers of L and M cones vary largely among different individuals and also at different regions of the retina. L:M ratios in the foveal area of normal human retina have been estimated by various psychophysical procedures such as i) probability detection functions for small targets (Cicerone and Nerger, 1989; Nerger and Cicerone, 1992); ii) heterochromatic flicker photometry (Knau et al., 2000); iii) comparison of L and M cone spectral sensitivity functions (Walraven, 1974); iv) detection of monochromatic lights (Cicerone and Nerger, 1989; Vimal et al., 1989 , Wesner et al., 1991; Gowdy and Cicerone, 1998). The mean L:M ratio estimated from all these psychophysical studies is 2:1. However, it is important to note that the L:M ratios estimated is not only vary between the studies but also among the individuals. This variability in L:M ratios has its range from 0.3:1 to 10:1. Out of all these tasks that were used to estimate the L:M ratios, high estimations were found especially with flicker photometry and flicker sensitivities for red and green lights.

Cone ratios estimated from psychophysical cone modulation thresholds at lower temporal frequencies, which modulate chromatic channel, are always unity for all subjects. (See chapter 3) (Kremers et al., 2000). In addition, Brianard et al (2000) have shown that unique yellow variation is not significantly different between the two observers who have significantly different L:M ratios. All these studies point towards the idea that the L:M ratios effect the luminance channel but not the chromatic channel. All these studies were based on stimuli which correspond to central retina. It is good idea to use stimuli that corresponds to

different retinal regions, so that L/M ratios can be measured in different parts of the retina.

8.6.2 Rationale

Previous experiment results have shown that the psychophysical task mediated by chromatic and luminance mechanisms can be studied at temporal frequencies of 4Hz and 20Hz respectively. However, these findings are based on two stimuli conditions which are representative of central and peripheral retina. We would like to apply these two temporal frequencies in order to find the L:M ratios across the various regions of the retina. This approach would allow us to find any variation in L:M ratios as function of retinal eccentricity for luminance and chromatic channel. In addition, we can also address the question as to whether L:M ratios obtained with flicker ERGs correlate well with psychophysical task?

8.6.3 Methods

8.6.3a Stimuli

Silent substitution stimuli for L- and M-cones were presented on a CRT monitor. The details of the silent substitution were explained in (section 3.5). Stimulus description and is similar to that used for ERG recordings (see section 8.3). However the stimulus configuration is different to that used for the ERG recordings. Seven stimulus configurations were used to record flicker detection thresholds and could be grouped into two main types: (1) Circular stimuli of different angular substance which increased in 20° steps from 10° up to 70° in diameter, and (2) annular stimuli with a 70° outer diameter but gradually ablated

from the centre by 10°, 30°, 50° (see figure 8.23). Stimulus conditions were named as similar to the ERG stimulus configurations to compare the data between ERG and psychophysics.

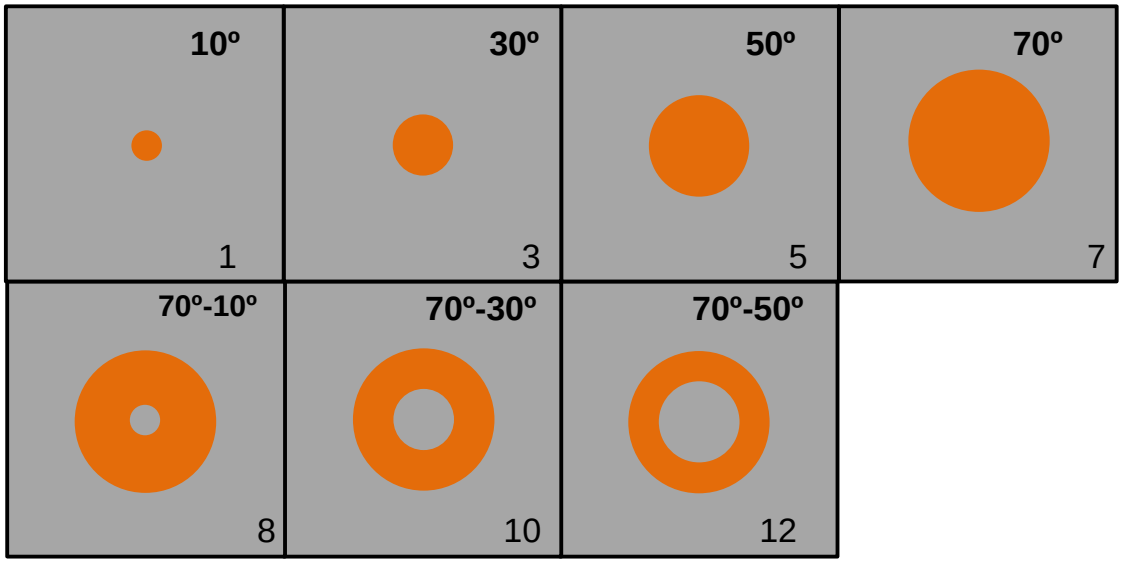

Figure 8.23 Representation of 7 different spatial configurations used to elicit flicker detection thresholds for L and M cone isolating stimuli. Condition 1, 3, 5 and7 comprise of circular stimuli of different angular subtense of 10°, 30°, 50°, and 70° in diameter respectively. Conditions 8, 10 and 12 are annular stimuli with 70° outer diameter whose centres are ablated 10°, 30°, and 50° respectively. The background was uniform grey with luminance of 66cd/m^2.

8.6.3b Subjects

Three male observers participated in this study. One was an emetrope and other two were corrected ametropes. All three were colour normal according to the Farnsworth Munsell 100 Hue test. All three observers viewed the stimuli monocularly maintaining fixation on a centrally placed cross. Subjects gave informed consent prior to the commencement of the experiment.

8.6.3c Psychophysical procedure

Flicker detection thresholds for the L and M cone isolating stimuli were measured using a two temporal alternative forced choice procedure (2AFC). In this procedure a flickering stimulus was presented in one of temporal intervals (see figure 8.24). The observer had to indicate by button press in which interval the stimulus is present.

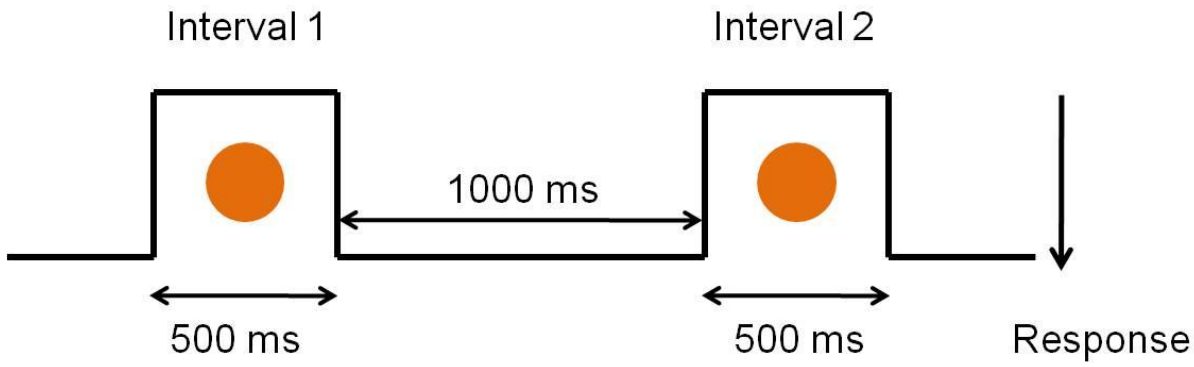

Figure 8.24 Stimulus presentations in 2 temporal alternate force choice procedure. Stimulus is presented in interval 1 or interval 2 and subject has to report in which interval the stimulus is present. The time period of the interval 1, 2 and inter-stimulus interval were also shown in the figure.

The cone isolating stimuli were presented at 7 contrast levels ranging from sub-threshold to supra-threshold levels, the range of which was determined in preliminary experiments. Twenty repeats of each stimulus were used to generate a psychometric function. Threshold was set at 75% seen. Psychometric curves were obtained from the data utilising Bootstrap software (Foster and Bischof, 1991) from which the threshold estimates (75% seen) were obtained. This procedure is repeated for L and M cone isolating conditions at 4 and 20Hz across all stimulus conditions.

8.6.4 Results

8.6.4a L and M cone detection thresholds

Group averaged L and M cone flicker detection thresholds for all seven conditions (covers central and peripheral retinal locations) at 4Hz and 20Hz stimulation rates were plotted in figure 8.25. From the plots, it can be observed that at 4Hz, L and M cone contrast thresholds are approximately equal across the retina, on the other hand, at 20 Hz, M cone thresholds were higher than L cone thresholds. M cone threshold is smallest for largest stimulus condition. We can also note that the M cone response shows large inter-individual variation. It is also interesting to note that L cone thresholds were almost invariant across all stimulus conditions. Individual L and M cone flicker detection thresholds for the three subjects as function of stimulus condition for chromatic (4Hz) and luminance (20Hz) mechanisms were also in figure 8.26.

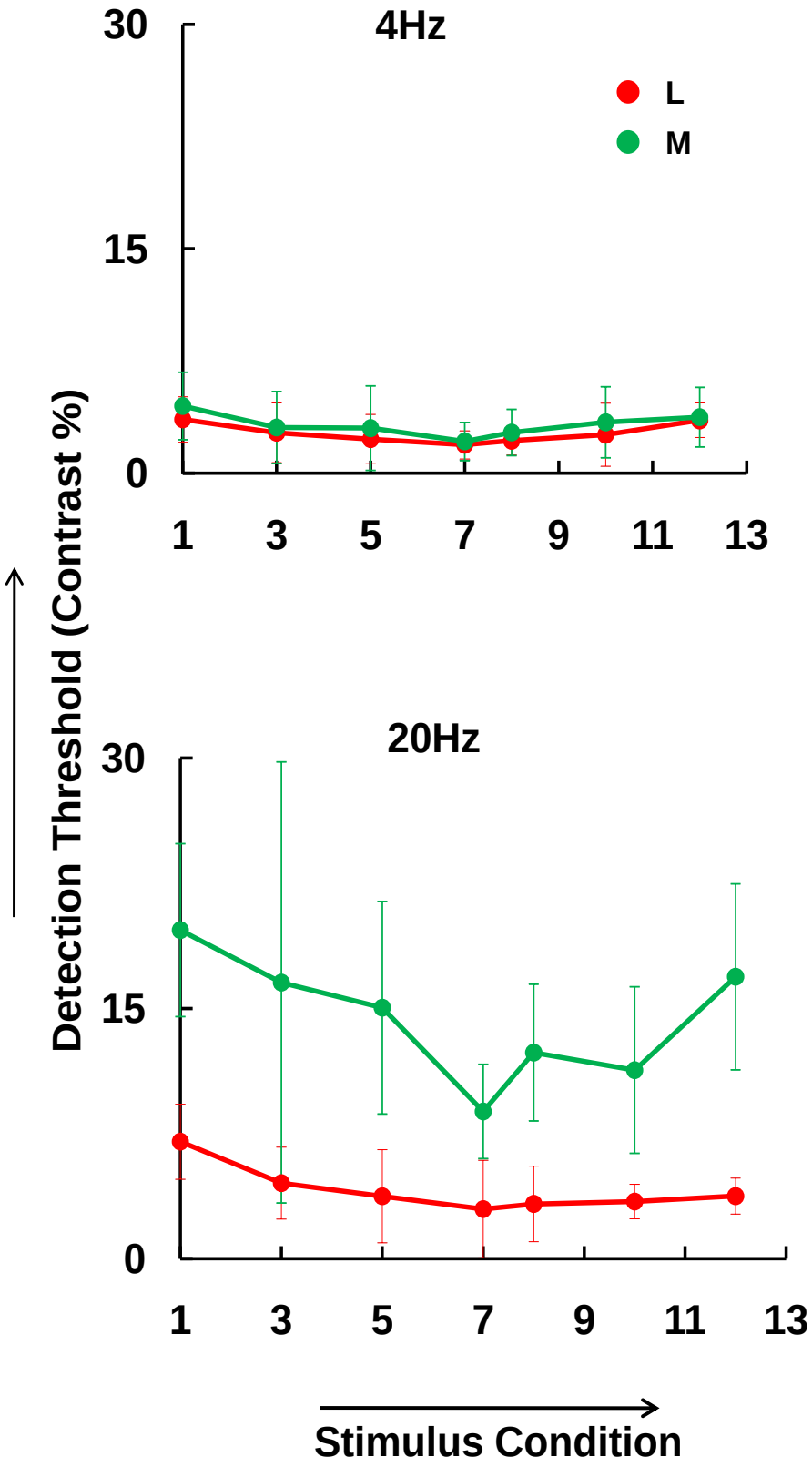

Figure 8.25 Group average (n=3) L and M cone flicker detection thresholds for seven stimulus conditions (covers central and peripheral retinal locations) were plotted at 4Hz (Upper plot) and 20Hz (Lower plot).

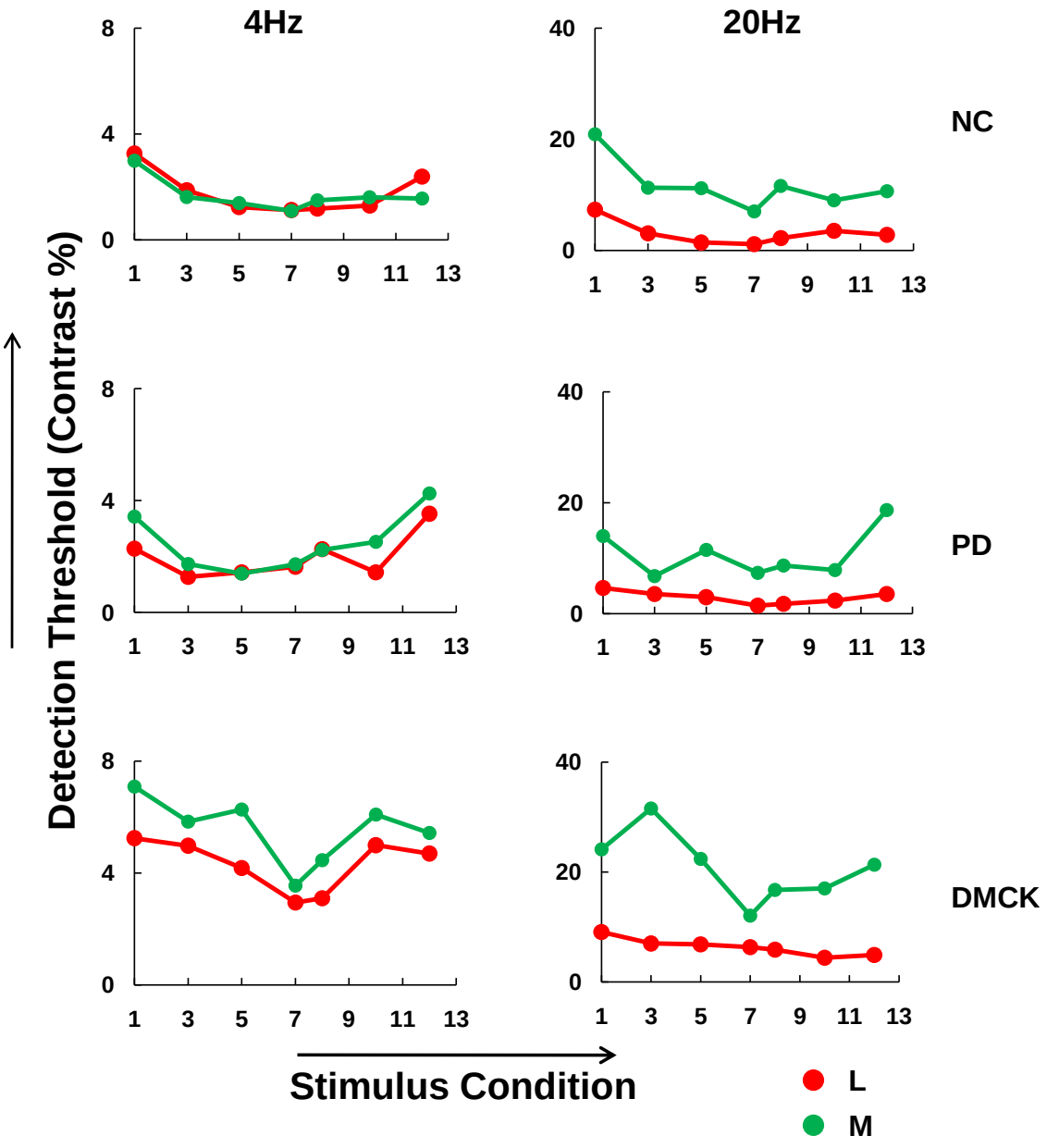

Figure 8.26 Individual L and M cone detection thresholds of three subjects as function of stimulus condition for chromatic (4Hz) and luminance (20Hz) mechanisms. Note that for chromatic mechanism, both L and M cone detection thresholds are similar to each other across all stimulus conditions. In contrast, for luminance channel, M cone detection thresholds were significantly higher than L cones for all stimulus conditions. It is also obvious that the L cone thresholds are invariant across the retina.

8.6.4b L:M ratios

L:M ratio were calculated by dividing the M cone detection threshold with L cone contrast thresholds. The average L:M ratio of three subjects as function of retinal region were plotted as shown in figure 8.27 The graph shows that at 4Hz the L:M ratios were close to unity across all regions of the retina stimulated. In addition to this, small error bars for all seven stimulus conditions at this modulation rate suggest small inter-individual variability. In contrast at 20Hz, L:M ratios are variable as function of area being stimulated. As the stimulus size is increased, L:M ratios were increased and the ratio is maximum with largest stimuli (70°). As the centre of the stimulus is ablated, L:M ratios were decreased. Individual L:M ratios for the three subjects across the retina were presented in figure 8.28 for the reference.

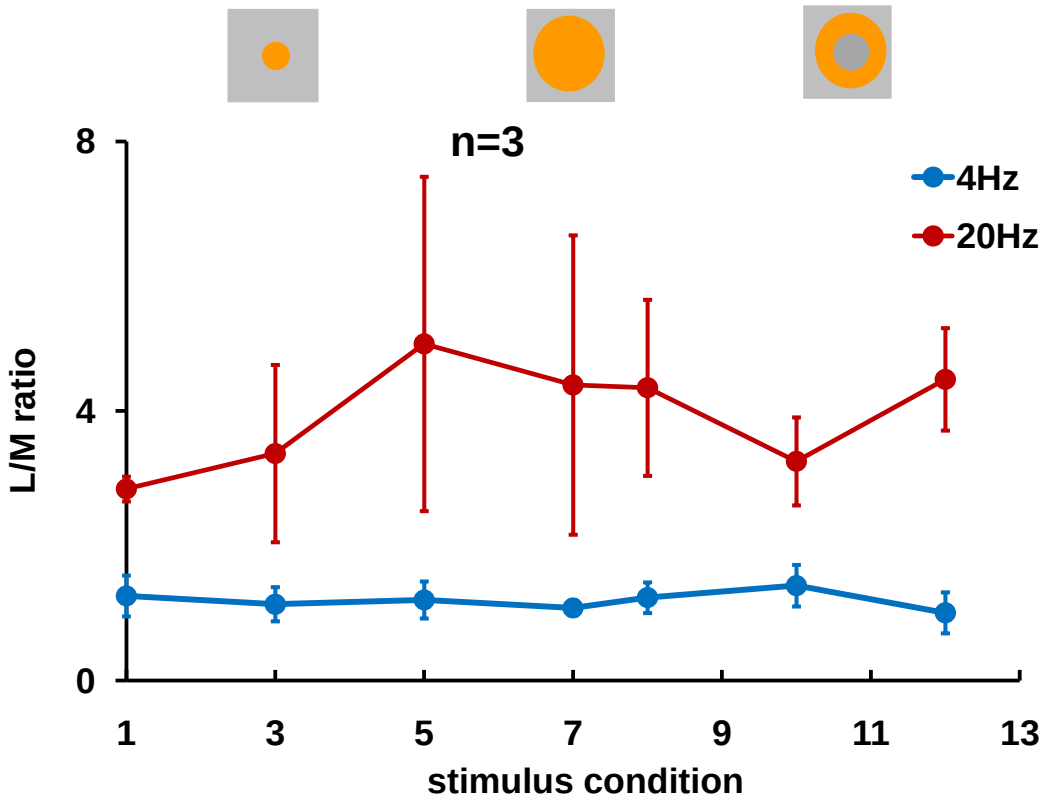

Figure 8.27 Group average L: M cone ratios as function of stimulus condition for chromatic (4Hz) and luminance (20Hz) mechanisms. At 4 Hz the L:M ratio is close to unity and small error bars suggest a small inter-individual variability. In contrast, At 20 Hz, L:M ratios are variable depending on the area of retina being stimulated. Large error bars suggest large inter-individual variability among the subjects.

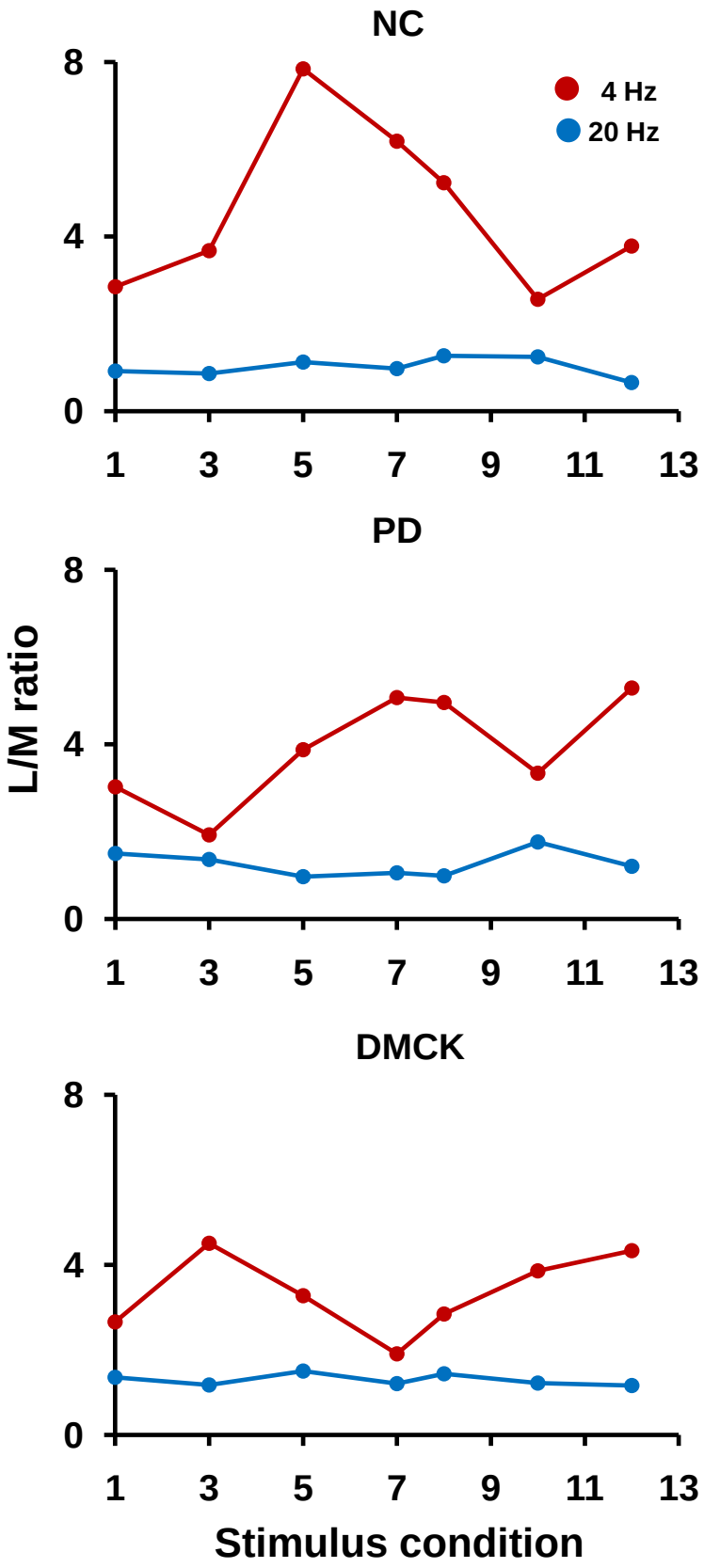

Figure 8.28 Individual L and M cone ratios of three subjects as function of stimulus condition for chromatic (4Hz) and luminance (20Hz) mechanisms.

8.6.5 Discussion

This experiment measured the flicker detection thresholds for L and M cone isolating stimuli as function of retinal eccentricity. Results indicate that the flicker detection thresholds not only vary as function of retinal eccentricity but also depend upon whether the chromatic or luminance channel mediates this detection. Flicker detection task at 4Hz is mediated by chromatic channel and at 20Hz by luminance channel. The L:M ratios estimated from the detection thresholds are different for both chromatic and luminance channel. For the chromatic channel that mediates detection, the L:M ratios were 1:1 and this ratio is invariant across the retina. In addition to this, inter- individual variability is very small for all retinal regions tested. These findings are in close correlation to the flicker ERGs at 12Hz. On the other hand, for luminance channel, average L:M ratios are from 3:1 to 5:1 depending on the area of retina being stimulated. These ratios have also shown large inter-individual variability (ranging from 2:1 to 8:1).

Our results are consistent with the previous idea that the psychophysical task mediated by red-green chromatic system have L:M ratios of unity for all subjects, including the protanope and deuteranope carriers (Miyahara et al.,1998). In addition to this, red-green chromatic system display less inter individual variability than the luminance channel (Krauskopf, 2000; Brainard et al., 2000; Kremers et al., 2003; Kremers and Link, 2008).

Earlier work have also estimated L:M ratios at various retinal locations. For example, Cicerone and Nerger (1989) estimated that the mean L:M cone ratio of three subjects using the probability detection functions for small targets with arc diameters ranging from 1.87’ to 8.12’ minutes of arc. They suggested that

the L cones are twice the M cone numbers. They also noted that this ratio is almost invariant from the fovea to 4 °eccentricity. Knau et al (2000) employed HFP task to estimate the L:M ratios at three retinal eccentricities (0°, 25° and 40°) and found that estimates of L:M ratios were nearly constant at all three eccentricities with values ranging from 0.9:1 to 3.4:1. Hagstrom et al (1998) measured L to M cone opsin mRNA in post-mortem eyes, at different patches of the retina that corresponds to different retinal locations. Their estimation at fovea (patch which centred on fovea) was about 1.5:1; whereas, at 41° visual angle it is about 3.1:1. Yamaguchi et al used similar method in 51 eyes across the retina and found that L to M cone opsin mRNA is 4:1 with the values ranging from 1:1 to 10:1. They also noted that L cone opsin expression is consistently higher throughout the retina with increase in L to M cone opsin RNA in the extra foveal region. The study of Jacobs and Neitz (1993) who used flicker ERGs over a large retina area (53°), reported that the L:M ratio of 2:1 with large inter-individual variability ranging from 0.7:1 to 9:1. Cone isolating ERGs obtained with large viewing fields (124° x 108°) have also indicated higher L:M ratios (4.2:1) with large inter-individual variation (0.3:1 to 8.7:1). As a matter of fact, all these studies have shown different results, some suggesting L:M ratios are invariant as function of retinal eccentricity and other suggesting L:M ratio do vary as function of retinal eccentricity. Our results may not solve the existing contraversary about the L:M ratios but shed a new light that the variation of L:M ratios as function of retinal eccentricity depends upon whether the task is mediated by chromatic or luminance mechanism.

Various groups measured colour appearance (Boynton et al., 1964), wavelength discrimination (Weale, 1951), and spectral sensitivity for small and dim test lights (Uchikawa et al., 1982). These studies have indicated that M

cone sensitivity decreases with retinal eccentricity suggesting that this could be partially because of the relative number of M cones contributing to the perceptual and detection task. Our results strongly favour the idea that M cone sensitivity decreases significantly in peripheral retina especially for luminance detection task.

CHAPTER - 9 FINAL DISCUSSION AND CONCLUSIONS

The main aim of the study was to examine the cortical and retinal contributions to colour vision processing in human trichromatic vision using VEPs and ERGs.

9.1 VEPs

Many studies have elicited the VEPs using chromatic gratings to study the cortical contributions to colour processing (Murray et al., 1986; Berninger et al., 1989; Rabin and Adams, 1992; Suttle and Harding, 1999). The main aspect of these studies is the use of isoluminant chromatic patterned stimuli which typically take the form of low spatial frequency sinusoidal or square wave gratings (Kulikowski, 1991b). All these studies have shown that chromatic VEPs differ in their morphology compared to that of achromatic VEPs. In addition to this, it was also been noted that the morphological variations are prominent when the stimulus has both the colour and luminance contrast. Various groups have also looked at the effect of size, luminance and hue on chromatic VEPs. Results from these studies have shown that the spatial frequency, luminance contrast content and hue have greater influence on chromatic VEPs, and size has no influence on chromatic VEPs. However, the grating stimuli are prone to the effects of transverse and longitudinal chromatic aberrations there by contaminating the contribution of colour to the cortical response.

In comparison to chromatic VEPs elicited by gratings, relatively few studies have used isoluminant spot stimuli to elicit the chromatic VEPs (Krauskopf, 1973; Paulus et al., 1984; Paulus et al., 1986; Valberg and Rudvin, 1997).

These studies speculate that spot stimuli allow more selective activation of chromatic mechanisms because they are able to stimulate efficiently the cells that are colour opponent, but not spatially opponent. In addition, spot stimuli are less vulnerable to the effects of chromatic aberrations because of fewer edges. In spite of having such advantages, very few studies have used chromatic spot VEPs to elicit the cortical response to the colour. Considering the advantages of isoluminant spot stimuli, we studied the effect of size, luminance contrast and hue on chromatic VEPs. So we examined the effects of luminance contrast and size along +L-M, –L+M and S-(L+M) cardinal axis, and hue on chromatic VEPs along the sixteen chromatic axes of MBDKL colour space.

The results of chapter 4 indicate that morphology of the chromatic spot VEP changes significantly when luminance contrast content is added to the stimulus. Especially N1, P2 and offset components are significantly different in terms of their amplitudes and latencies when the luminance contrast content is added to the stimulus. N1 amplitude reaches its maxima at isoluminance and reduces its amplitude as the luminance contrast is added to the stimulus. In contrast to this, P2 and offset components have smaller amplitudes at isoluminance and gradually increases as the luminance contrast content is added to the stimulus. All these components have longer latencies at isoluminance and shorter latencies at both extremes of luminance contrast content. Morphological changes in VEP related to the changes in luminance and chromatic contrast can be summarized as follows. Isoluminant chromatic spot stimuli generate VEP responses with longer latency and minimal offset responses. This sustained nature of the responses is consistent with P-cellular processing. On the other hand, VEPs generated by luminance contrast modulation have shorter

latencies and large offset amplitudes. The transient nature of the luminance contrast VEP response is consistent with M-cellular processing.

The results of chapter 5 suggest that, unlike VEPs elicited by isoluminant chromatic gratings, size has significant influence on isoluminant chromatic spot VEPs. Larger size stimuli generate Larger offset components in the VEPs. These stimuli, along +L-M, –L+M and S-(L+M) cardinal axis, shows large offset responses suggesting the transient chromatic activity to the cortical responses. Especially along the +S-(L+M) axis, small size stimuli seem to elicit attenuated cortical responses with delayed latencies. Firstly, this can be due to the low number of S cones and secondly, such stimuli are prone to filtering effect of macular pigment density in the central retina. Our results recommend, to elicit the chromatic spot VEPs optimal stimulus size would be 2-4° along the +L-M and –L+M axis, and 6° along S-(L+M) axis.

Chapter 6 examined the morphology of the VEPs elicited by spot stimuli which undergo equiluminant changes in chromaticity in which the contributions from the L, M and S cones varied systematically. Changing the axis of chromatic stimulation produces changes in the morphology of the chromatic VEP responses that are dependent upon the degree of activation of L-M or S/(L+M) opponent mechanisms. The morphological differences are consistent with the underlying neuro-antomical pathways being involved in the processing of L-M and S/(L+M) opponent signals. The former originates from midget ganglion cells and relays to the P layers of the LGN, whilst the latter stems from small bi-stratified ganglion cells and projects to the K neurons in the LGN (Dacey and Lee, 1994; White et al., 1998; Calkins, 2001).

Latency data indicate that all components of the isoluminant chromatic VEPs along the S cone axis have longer latencies compared to the +L-M and –L+ M cardinal axis. This observation is consistent with previous human VEP studies (Rabin et al., 1994; Robson and Kulikowski, 1998) and psychophysics (Smithson and Mollon, 2004; Wade, 2009). Previous studies have compared reaction times for isoluminant stimuli along L-M and S cone axis and have shown that S-cone pathway is sluggish in comparison to L-M cone axis. Whilst McKeefy et al (2003) reported that the S-cone axis has a lag of 40ms; Smithson and Mollon (2004) found that the difference between L-M and S-cone pathway does not exceed 20-30ms.Cottaris and De Valois (1998) proposed that the reason for the longer latency of S cone channel is of cortical origin. According to their viewpoint, sparse S cone opponent signal in LGN is amplified in the cortex through recurrent excitatory circuit, in which the out-put of striate neuron re-enters the cell to be summed synergistically with new signals. The resulting S-cone signal is quite different from that seen in the LGN, having longer latency and slower dynamics. This process results in sluggish cortical S cone signal. Other proposal is that the delayed optic chaismal and antidromic stimulation of the extra striate cortex by K neurons (Norton and Casagrande, 1982 , White et al., 2001).

An important observation resulting from chapter 6 is the differences between the morphology of the VEPs elicited by blue and yellow stimulation. Separate ON and OFF processing pathways within the cone opponent mechanisms have been highlighted in recent psychophysical investigations (Shinomori et al., 1999; McLellan and Eskew, 2000). These studies infer that colour vision may be more accurately thought of comprising of four separate mechanisms (+L-M = ‘red-on/green off’; +M-L = ‘green-on/red-off’; +S-(L+M) = ‘blue-on/yellow-off’ and

-S+(L+M) = ‘yellow-on/blue-off’) rather than two opponent mechanisms described previously. The similarity between the red-on/green-off and green-on/red-off VEPs suggests a common, balanced substrate for these responses. However, the VEPs generated by blue-on/yellow off and yellow-on/blue-off stimuli are qualitatively dissimilar in appearance. In addition to this, the latency data presented in the experiment 6 shows that the components of the isoluminant chromatic VEPs along +S-(L+M) cone axis have longer latencies compared to the –S-(L+M) cone axis. All these results strongly suggest that different neuronal populations are involved in generation of these responses. Asymmetries between the blue-on/yellow off and yellow-on/blue-off mechanisms were also noted in some psychophysical studies (Shinomori et al., 1999; McLellan and Eskew, 2000; Vassilev et al., 2000), but not in others (Smith et al., 1989; DeMarco et al., 1994; Schwartz, 1996). One might hypothesize that the existence of differences in response properties may echo the underlying neurophysiology of the blue-on and off pathways, which are thought to be supported by very different retinal circuitry. The blue-on pathway compromises small bi-stratified ganglion cells that project to the P cells that project to the P- and K-cellular layers of the LGN. Whilst on the other hand, it is thought that blue-off pathway is based on ganglion cells that are midget-like, although this has yet to gain wide acceptance.

In spite of such interesting observations, use of chromatic spots in eliciting cortical responses has few limitations.

1) The spot stimuli produce very small amplitude cortical responses compared to those obtained from grating stimuli.
2) There is a large inter-individual variability in the VEP responses.

3) The VEP responses recorded from POz and Pz locations are of low signal to noise ratio. So we could not analyse the data from these channels.
4) The VEP responses recorded along -S+(L+M) axis have very low signal to noise ratio. So we could not analyse the data along this axes in luminance ratio and size experiments. However, in the chromatic axes experiments we are able to elicit the VEPs, along -S+(L+M) chromatic axis, after many samples were averaged from each subject.

These all factors put together suggest that the chromatic spot VEPs have a limited clinical value.

9.2 ERGs

The second phase of the thesis examined retinal contributions to colour vision processing in trichromatic vision using flicker ERG method. Earlier work had suggested that post-receptoral contributions to chromatic and achromatic processing can be studied using flicker ERGs. More recent work of Kremers and Link (2008) have suggested that low (12Hz) and high (30Hz) temporal flicker ERGs can be used to isolate the chromatic and achromatic post-receptoral processing in the retina using silent substitution technique. Moreover, low and high temporal frequency ERGs reflects the known properties of P- and M- processing pathways respectively, in the retina. The L:M ratios obtained from low temporal flicker ERGs are unity and the phase difference between L and M cone isolating ERGs is close to 180° suggest that 12Hz flicker ERGs reflect cone-opponent, chromatic processing. In contrast to this, L:M ratios

obtained from high temporal flicker ERGs are greater than unity and the phase difference between L and M cone isolating ERGs is <180°. There is also large inter-individual variability in these findings, which strengthen the idea that 30Hz flicker ERGs reflect non-opponent, achromatic processing in the retina. In addition to this, psychophysically obtained L:M ratios for non-opponent and opponent channels have also shown similar results to the ERG results. Our results in the experiment 7 seem to be in strong agreement with the previous literature that the low and high temporal frequency ERGs reflect the chromatic, cone-opponent and achromatic, non-opponent pathway in the retina.

Recent work has suggested that the flicker ERGs reflect post-receptoral processing (Kremers and Link, 2008). If that is true, from the results of chapter 7 we would speculate that the L: M ratios obtained for cone-opponent and non-opponent processing reflect L and M cone input to the post-receptoral processing to the ganglion cell receptive fields. The immediate question that arises from these results is; Does L and M cone inputs to the cone-opponent and non-opponent channel is same across the retina? The answer to this question would be helpful to solve the two issues. Firstly, to understand the currently existing controversy of cone-selective or random wiring cone input to the ganglion cell receptive fields. Secondly, the difference in colour processing across the retina could be explained on the basis of cone input to the ganglion cells. In order to answer these two questions, in experiment 8, we measured the L:M ratios using 12Hz and 30Hz flicker ERGs across the retina. The results of experiment 8 suggest that for cone-opponent, chromatic processing, the L:M ratios are unity across the retina. The phase difference between L and M cone ERGs is close to 180° across all stimulus conditions. These results have shown the balanced L and M cone opponent input to the ganglion cell receptive fields

across the retina. Our results support the idea of cone selective theory for the chromatic, cone-opponent processing pathway in the retina. In contrast, 30Hz flicker ERGs that reflects non-opponent and achromatic pathway, L:M ratios are more than unity and variable across the retina and also across the individuals. These results suggest unbalanced L and M cone input to the ganglion cell receptive fields across the retina for achromatic channel.

In addition to the above findings, there is a poor M cone pathway response to 30Hz flicker ERGs even with large size stimuli, which resulted in large L:M ratio. We speculate that the reason for this seems to lie in the phase behaviour of M cones. M cone phase advances with increasing stimulus size and seems to be continuing even after the central ablation of the stimulus, where as L cone response is constant across the retina. This phase advancement in M cones implies that peripheral M cone mechanisms are faster in response to that of central M cones. The possibility of destructive interference between central and peripheral M cone retinal mechanisms would have caused poor M cone ERGs for large stimuli, which resulted in higher L:M ERG ratios. The other possible reason for poor M cone response lies in the temporal behaviour of M cone pathway itself. Our results have shown that independent of stimulus size, M cone ERGs are significantly poor at higher temporal frequency. This point suggests the poor temporal behaviour of M cone mechanisms. The interesting observation from control experiment is that the protanope, where L cones are absent, have shown strong M cone ERG even at higher temporal frequency independent of stimulus condition. In addition to this, M cone phase response is stable across the stimulus conditions suggest that the central and peripheral M cone mechanisms have equal phase behaviour. It was not the case in tritanope. These results suggest that in the absence of L cones, M cone pathways would

change their temporal behaviour. We speculate this could be developmental or learning behaviour of human retina.

L:M ratios measured by psychophysics, across the retina, have also shown similar pattern to that measured by ERGs across the retina suggesting the right approach in measurement. However, direct correlations cannot be made between the two methods because of limited participation of subjects in psychophysical procedure and also subjects were not the same in both the methods of measurements.

From the ERG and psychophysical experiments, we conclude that the achromatic, non-opponent pathway is processed by the unbalanced L and M cone input to the ganglion cell receptive fields in the retina. The difference in L and M cone input across the retina and also across the individuals suggests a random wiring hypothesis for the achromatic visual processing. In contrast, chromatic, cone-opponent pathway is processed by the balanced L and M cone input to the ganglion cell receptive fields across the retina and across the individuals. These findings suggest a cone selective hypothesis for the chromatic processing. Both these pathways are further processed by M- and P-processing pathways.

Future Work

Present thesis have measured L:M ratios using both Electrophysiological and psychophysical methods. However, the correlation between the two techniques was not possible due to different subjects involved in two methods of measurements. So, the future work includes measuring L:M ratios for the same group of subjects in both methods of measurements. This would allow seeing the correlation between ERGs and Psychophysical methods. It would also be helpful in determine which method would be more appropriate to measure the L:M ratios. Same experiments can be done in colour anomalous subjects such as protanopes and deuteranopes.

During the early stages of the thesis the aim was to measure the L:M ratios both in colour normals and also patients suffering from various retinal diseases[4]. However, it was not possible to extend the ERG experiments on patients with above conditions due to time limitations. So, it would be interesting to extend the same ERG experiments in subjects with retinal diseases. This would permit to evaluate how the post-receptoral processing for chromatic and luminance mechanism is effected in these conditions. Group of studies have also shown that the phase behaviour of L and M cones change in different conditions (Kremeres, 2003). Considering the importance of L and M response phases, it would be interesting to the study the response phase of L and M cones in different retinal degenerations. This work would create a pathway to incorporate new strategies for early diagnosis of these conditions.

[4] Retinal diseases include Retinitis pigmentosa, cone dystrophy, rod-cone dystrophy, age related macular degeneration, etc..

The thesis have certain limitations such as; only two of the three photoreceptors can be silenced at the same time (since three phosphors only available in CRT); and also the *silent substitution* can be achieved only at limited luminance level. So this issue can be solved by using LED stimulators. LED stimulators have already shown to be having advantages of silencing three photoreceptors at the same time and also over wide range of luminance (Shapiro et al., 1996; Shapiro, 2002; Murray et al., 2008).

We also would like to extend our ERG experiments using single flashes to obtain L and M cone responses. This would allow comparing the single flash L and M cone responses to generally used single flash cone responses and also the contribution of each cone to the combine cone response.

REFERENCES

Abraham, F. A., & Alpern, M. (1984). Factors influencing threshold of the fundamental electrical response to sinusoidal excitation of human photoreceptors. *Journal of Physiology, 357(1)*, 151-172.

Abramov, I., Gordon, J., & Chan, H. (1991). Color appearance in the peripheral retina: effects of stimulus size. *Journal of Optical Society of America A, 8*(2), 404-414.

Adrian, E. D. (1945). The electric response of the human eye. *Journal of Physiology, 104*(1), 84-104.

Ahnelt, P., & Kolb, H. (1994). Horizontal cells and cone photoreceptors in primate retina: a Golgi-light microscopic study of spectral connectivity. *Journal of Comparative Neurology, 343*(3), 387-405.

Ahnelt, P. K., Kolb, H., & Pflug, R. (1987). Identification of a subtype of cone photoreceptor, likely to be blue sensitive, in the human retina. *Journal of Comparative Neurology, 255*(1), 18-34.

Allison, T., Begleiter, A., Mccarthy, G., Roessler, E., Nobre, A. C., & Spencer, D. D. (1993). Electrophysiological Studies of Color Processing in Human Visual-Cortex. *Electroencephalography and Clinical Neurophysiology (Suppl), 88*(5), 343-355.

Anderson, S. J., Holliday, I. E., Singh, K. D., & Harding, G. F. A. (1996). Localization and functional analysis of human cortical area V5 using magneto-encephalography. *Proceedings of the Royal Society London B: Biological Sciences, 263*(1369), 423-431.

Armington, J. C. (1976). Spectral sensitivity of low level electroretinograms. *Vision Research, 16*(1), 31-35.

Ayama, M., & Sakurai, M. (2003). Changes in hue and saturation of chromatic lights in the peripheral visual field. *Color Research and Applicaion, 28*, 413-424.

Baizer, J. S. (1982). Receptive field properties of V3 neurons in monkey. *Investigative Ophthalmology and Visual Science, 23*(1), 87-95.

Baron, W. S. (1980). Cone difference signal in foveal local electroretinogram of primate. *Investigative Ophthalmology and Visual Science, 19*(12), 1442-1448.

Bartels, A., & Zeki, S. (2000). The architecture of the colour centre in the human visual brain: new results and a review. *European Journal of Neuroscience, 12*(1), 172-193.

Baseler, H. A., & Sutter, E. E. (1997). M and P components of the VEP and their visual field distribution. *Vision Research, 37*(6), 675-690.

Baylor, D. A., Lamb, T. D., & Yau, K. W. (1979). Responses of retinal rods to single photons. *Journal of Physiology, 288*, 613-634.

Baylor, D. A., Nunn, B. J., & Schnapf, J. L. (1987). Spectral sensitivity of cones of the monkey Macaca fascicularis. *Journal of Physiology, 390*, 145-160.

Berninger, T. A., & Arden, G. B. (1991). Visual evoked potentials with chromatic stimuli. In J. R. Heckenlively & G. B. Arden (Eds.), *Principles and practise of clinical electro-physiology and vision* (pp. 147-150). St. Louis: Mosby Year Book.

Berninger, T. A., Arden, G. B., Hogg, C. R., & Frumkes, T. (1989). Separable Evoked Retinal and Cortical Potentials from Each Major Visual Pathway - Preliminary-Results. *British Journal of Ophthalmology, 73*(7), 502-511.

Berson, E. L. (1993). Retinitis pigmentosa. The Friedenwald Lecture. *Investigative Ophthalmology and Visual Science, 34*(5), 1659-1676.

Berson, E. L., & Goldstein, E. B. (1970). The early receptor potential in sex-linked retinitis pigmentosa. *Investigative Ophthalmoogy, 9*(1), 58-63.

Berson, E. L., & Kanters, L. (1970). Cone and rod responses in a family with recessively inherited retinitis pigmentosa. *Archives of Ophthalmology, 84*(3), 288-297.

Birch, D. G., & Anderson, J. L. (1992). Standardized full-field electroretinography. Normal values and their variation with age. *Archives of Ophthalmology, 110*(11), 1571-1576.

Blakemore, C., & Vital-Durand, F. (1986). Organization and post-natal development of the monkey's lateral geniculate nucleus. *Journal of Physiology, 380*, 453-491.

Blasdel, G. G., & Lund, J. S. (1983). Termination of afferent axons in macaque striate cortex. *Journal of Neuroscience, 3*(7), 1389-1413.

Blasdel, G. G., Lund, J. S., & Fitzpatrick, D. (1985). Intrinsic connections of macaque striate cortex: axonal projections of cells outside lamina 4C. *Journal of Neuroscience, 5*(12), 3350-3369.

Born, R. T. (2001). Visual processing: parallel-er and parallel-er. *Current Biology, 11*(14), 566-568.

Bornschein, H., & Schubert, G. (1953). [The photopic flicker-electroretinogram in man. *Journal of Biology, 106*(3), 229-238.

Boycott, B. B., & Wassle, H. (1991). Morphological Classification of Bipolar Cells of the Primate Retina. *European Journal of Neuroscience, 3*(11), 1069-1088.

Boynton, R. M., Schafer, W., & Neun, M. E. (1964). Hue-Wavelength Relation Measured by Color-Naming Method for Three Retinal Locations. *Science, 146(3644)*, 666-668.

Brainard, D. (1996). Cone contrast and Opponent modulation colour spaces. In P. Kaiser & R. M. Boynton (Eds.), *Human Colour Vision* (pp. 563-579). Washington, D.C: Optical Society of America.

Brainard, D. H., Roorda, A., Yamauchi, Y., Calderone, J. B., Metha, A., Neitz, M., Neitz, J., Williams, D. R., & Jacobs, G. H. (2000). Functional consequences of the relative numbers of L and M cones. *Journal of Optical Society of America A: Optics, Image Science and Vision, 17*(3), 607-614.

Bresnick, G. H., Smith, V. C., & Pokorny, J. (1989). Autosomal dominantly inherited macular dystrophy with preferential short-wavelength sensitive cone involvement. *American Journal of Ophthalmology, 108*(3), 265-276.

Brown, K. T., & Murakami, M. (1964a). Biphasic Form of the Early Receptor Potential of the Monkey Retina. *Nature, 204*, 739-740.

Brown, K. T., & Murakami, M. (1964b). A New Receptor Potential of the Monkey Retina with No Detectable Latency. *Nature, 201*, 626-628.

Brown, K. T., Watanabe, K., & Murakami, M. (1965). The early and late receptor potentials of monkey cones and rods. *Cold Spring Harb Symp Quant Biol, 30*, 457-482.

Brown, K. T., & Wiesel, T. N. (1961a). Analysis of the intraretinal electroretinogram in the intact cat eye. *Journal of Physiology, 158*, 229-256.

Brown, K. T., & Wiesel, T. N. (1961b). Localization of origins of electroretinogram components by intraretinal recording in the intact cat eye. *Journal of Physiology, 158*, 257-280.

Buchner, H., Weyen, U., Frackowiak, R. S. J., Romaya, J., & Zeki, S. (1994). The Timing of Visual-Evoked Potential Activity in Human Area V4. *Proceedings of the Royal Society London B: Biological Sciences, 257*(1348), 99-104.

Buckley, M. J., Gaffan, D., & Murray, E. A. (1997). Functional double dissociation between two inferior temporal cortical areas: perirhinal cortex versus middle temporal gyrus. *Journal of Neurophysiology, 77*(2), 587-598.

Bush, R. A., & Sieving, P. A. (1996). Inner retinal contributions to the primate photopic fast flicker electroretinogram. *Journal of Optical Society of America A: Optics, Image Science and Vision, 13*(3), 557-565.

Calkins, D. J. (2001). Seeing with S cones. *Progress in Retinal Eye Research, 20*(3), 255-287.

Calkins, D. J., Schein, S. J., Tsukamoto, Y., & Sterling, P. (1994). M and L cones in macaque fovea connect to midget ganglion cells by different numbers of excitatory synapses. *Nature, 371*(6492), 70-72.

Carden, D., Kulikowski, J. J., Murray, I. J., & Parry, N. R. A. (1985). Human Occipital Potentials-Evoked by the Onset of Equiluminant Chromatic Gratings. *Journal of Physiology-London, 369*(Dec), P44.

Carroll, J., McMahon, C., Neitz, M., & Neitz, J. (2000). Flicker-photometric electroretinogram estimates of L:M cone photoreceptor ratio in men with photopigment spectra derived from genetics. *Journal of Optical Society of America A: Optics, Image Science and Vision, 17*(3), 499-509.

Carroll, J., Neitz, J., & Neitz, M. (2002). Estimates of L:M cone ratio from ERG flicker photometry and genetics. *Journal of Vision, 2*(8), 531-542.

Casagrande, V. A. (1994). A third parallel visual pathway to primate area V1. *Trends in Neuroscience, 17*(7), 305-310.

Chatterjee, S., & Callaway, E. M. (2003). Parallel colour-opponent pathways to primary visual cortex. *Nature, 426*(6967), 668-671.

Chelazzi, L., Miller, E. K., Duncan, J., & Desimone, R. (2001). Responses of neurons in macaque area V4 during memory-guided visual search. *Cerebral Cortex, 11*(8), 761-772.

Cicerone, C. M., & Nerger, J. L. (1989). The relative numbers of long-wavelength-sensitive to middle-wavelength-sensitive cones in the human fovea centralis. *Vision Research, 29*(1), 115-128.

Ciganek, L. (1961). The EEG response (evoked potential) to light stimulus in man. *Electroencephalography and Clinical NeurophysiologySuppl, 13*, 165-172.

Cobb, W. A., & Morton, H. B. (1954). A new compononent of the human electroretinogram. *Journal of Physiology, 123*, 36-37.

Cone, R. A. (1964). Early Receptor Potential of the Vertebrate Retina. *Nature, 204*, 736-739.

Conway, B. R. (2003). Colour vision: a clue to hue in v2. *Current Biology, 13*(8), 308-310.

Conway, B. R., & Tsao, D. Y. (2006). Color architecture in alert macaque cortex revealed by fMRI. *Cerebral Cortex, 16*(11), 1604-1613.

Cottaris, N. P., & De Valois, R. L. (1998). Temporal dynamics of chromatic tuning in macaque primary visual cortex. *Nature, 395*(6705), 896-900.

Creutzfeldt, O. D., Lee, B. B., & Elepfandt, A. (1979). A quantitative study of chromatic organisation and receptive fields of cells in the lateral geniculate body of the rhesus monkey. *Experimental Brain Researchearch, 35*(3), 527-545.

Crognale, M. A. (2002). Development, maturation, and aging of chromatic visual pathways: VEP results. *Journal of Vision, 2*(6), 438-450.

Crognale, M. A., Switkes, E., Rabin, J., Schneck, M. E., Haegerstrom-Portnoy, G., & Adams, A. J. (1993). Application of the spatiochromatic visual evoked potential to detection of congenital and acquired color-vision deficiencies. *Journal of the Optical Society of America A Optics, Image Science and Vision, 10*(8), 1818-1825.

Croner, L. J., & Kaplan, E. (1995). Receptive fields of P and M ganglion cells across the primate retina. *Vision Research, 35*(1), 7-24.

Curcio, C. A., Allen, K. A., Sloan, K. R., Lerea, C. L., Hurley, J. B., Klock, I. B., & Milam, A. H. (1991). Distribution and morphology of human cone photoreceptors stained with anti-blue opsin. *Journal of Comparative Neurology, 312*(4), 610-624.

Dacey, D., Packer, O. S., Diller, L., Brainard, D., Peterson, B., & Lee, B. (2000). Center surround receptive field structure of cone bipolar cells in primate retina. *Vision Research, 40*(14), 1801-1811.

Dacey, D. M. (1993). The mosaic of midget ganglion cells in the human retina. *Journal of Neuroscience, 13*(12), 5334-5355.

Dacey, D. M. (1999). Primate retina: Cell types, circuits and color opponency. *Progress in Retinal and Eye Research, 18*(6), 737-763.

Dacey, D. M. (2000a). Parallel pathways for spectral coding in primate retina. *Anual Reviews of Neuroscience, 23*, 743-775.

Dacey, D. M. (2000b). Parallel pathways for spectral coding in primate retina. *Anual Reviews of Neuroscience, 23*, 743-775.

Dacey, D. M., & Lee, B. B. (1994). The 'blue-on' opponent pathway in primate retina originates from a distinct bistratified ganglion cell type. *Nature, 367*(6465), 731-735.

Dacey, D. M., & Packer, O. S. (2003). Colour coding in the primate retina: diverse cell types and cone-specific circuitry. *Current Opinion in Neurobiology, 13*(4), 421-427.

Dawson, G. D. (1951). A summation technique for detecting small signals in a large irregular background. *Journal of Physiology, 115*(1), 2-3.

Dawson, G. D. (1954). A summation technique for the detection of small evoked potentials. *Electroencephalography and Clinical Neurophysiology(Suppl), 6*(1), 65-84.

Dayhoff, M. O. (Cartographer). (1972). Atlas of protein sequence and structure.

Dewar, J., & McKendrik, J.G. (1873). On the physiological action of light. *Proceedings of the Royal Society (Edinburg). 8, 179-182.*

De Valois, R. L., Abramov, I., & Jacobs, G. H. (1966). Analysis of response patterns of LGN cells. *Journal of Optical Society of America, 56*(7), 966-977.

De Yoe, E. A., Caraman , G. J., Bandettini, P., Glickman, S., Weiser, J., Cox , R., Miller, D., & Neitz, J. (1996). *Mapping striate and extrastriate visual areas in human cerebral cortex.* Paper presented at the Proceedings of the National Academy of Sciences U S A, USA.

DeMarco, P. J., Jr., Smith, V. C., & Pokorny, J. (1994). Effect of sawtooth polarity on chromatic and luminance detection. *Visual Neuroscience, 11*(3), 491-499.

Demonasterio, F. M., & Gouras, P. (1975). Functional Properties of Ganglion-Cells of Rhesus-Monkey Retina. *Journal of Physiology-London, 251*(1), 167-195.

DeMonasterio, F. M., Schein, S. J., & McCrane, E. P. (1981). Staining of blue-sensitive cones of the macaque retina by a fluorescent dye. *Science, 213*(4513), 1278-1281.

Derrington, A. M. (1984). Development of Spatial-Frequency Selectivity in Striate Cortex of Vision-Deprived Cats. *Experimental Brain Researchearch, 55*(3), 431-437.

Derrington, A. M., Krauskopf, J., & Lennie, P. (1984). Chromatic mechanisms in lateral geniculate nucleus of macaque. *Journal of Physiology, 357*, 241-265.

Desimone, R., Albright, T. D., Gross, C. G., & Bruce, C. (1984). Stimulus-Selective Properties of Inferior Temporal Neurons in the Macaque. *Journal of Neuroscience, 4*(8), 2051-2062.

Desimone, R., & Schein, S. J. (1987). Visual properties of neurons in area V4 of the macaque: sensitivity to stimulus form. *Journal of Neurophysiology, 57*(3), 835-868.

DeValois, R. L., DeValois, K. K., Switkes, E., & Mahon, L. (1997). Hue scaling of isoluminant and cone-specific lights. *Vision Research, 37*(7), 885-897.

DeYoe, E. A., & Van Essen, D. C. (1985). Segregation of efferent connections and receptive field properties in visual area V2 of the macaque. *Nature, 317*(6032), 58-61.

Dodt, E. (1951). Cone electroretinography by flicker. *Nature, 168*(4278), 738.

Dong, C. J., & Hare, W. A. (2000). Contribution to the kinetics and amplitude of the electroretinogram b-wave by third-order retinal neurons in the rabbit retina. *Vision Research, 40*(6), 579-589.

Donner, K. O., & Rushton, W. A. (1959). Retinal stimulation by light substitution. *Journal of Physiology, 149*, 288-302.

Donovan, W. J., & Baron, W. S. (1982). Identification of the R-G-cone difference signal in the corneal electroretinogram of the primate. *Journal of Optical Society of America, 72*(8), 1014-1020.

Dow, B. M., & Gouras, P. (1973). Color and spatial specificity of single units in Rhesus monkey foveal striate cortex. *Journal of Neurophysiology, 36*(1), 79-100.

Drasdo, N., Aldebasi, Y. H., Chiti, Z., Mortlock, K. E., Morgan, J. E., & North, R. V. (2001). The s-cone PHNR and pattern ERG in primary open angle glaucoma. *Investigative Ophthalmology and Visual Science, 42*(6), 1266-1272.

Dreher, B., Fukada, Y., & Rodieck, R. W. (1976). Identification, classification and anatomical segregation of cells with X-like and Y-like properties in the lateral geniculate nucleus of old-world primates. *Journal of Physiology, 258*(2), 433-452.

Dustman, R. E., & Beck, E. C. (1969). The effects of maturation and aging on the wave form of visually evoked potentials. *Electroencephalography and Clinical Neurophysiology(Supp)l, 26*(1), 2-11.

Einthoven, W., & Jolly, W. A. (1908). The form and magnitude of the electrical response of the eye to stimulation by light ar various internsities. *Quarterly Journal of Experimental Physiology, 1*, 373-416.

Eisner, A., & Macleod, D. I. (1981). Flicker photometric study of chromatic adaption: selective suppression of cone inputs by colored backgrounds. *Journal of Optical Society of America, 71*(6), 705-717.

Enroth-Cugell, C., Hertz, B. G., & Lennie, P. (1977). Convergence of rod and cone signals in the cat's retina. *Journal of Physiology, 269*(2), 297-318.

Enroth-Cugell, C., Robson, J. G., Schweitzer-Tong, D. E., & Watson, A. B. (1983). Spatio-temporal interactions in cat retinal ganglion cells showing linear spatial summation. *Journal of Physiology, 341*, 279-307.

Essen, D. C., & Zeki, S. M. (1978). The topographic organization of rhesus monkey prestriate cortex. *Journal of Physiology, 277*, 193-226.

Estevez, O., & Dijkhuis, T. (Eds.). (1983). *Human pattern evoked potentails and colour coding*. London: Academic press.

Estevez, O., & Spekreijse, H. (1982). The "silent substitution" method in visual research. *Vision Research, 22*(6), 681-691.

Estevez, O., & Spekreijse, H. (1974). A Spectral compensation method for determining the flicker characterstics of human colour mechanisms. *Vision Research, 14*, 823-830.

Faber, D. S. (1969). *Analysis of the slow trans-retinal potentials in response to light.* Unpublished Ph.D Thesis, State University of New York, Buffalo.

Famiglietti, E. V., Jr., & Kolb, H. (1976). Structural basis for ON-and OFF-center responses in retinal ganglion cells. *Science, 194*(4261), 193-195.

Field, G. D., Sampath, A. P., & Rieke, F. (2005). Retinal processing near absolute threshold: from behavior to mechanism. *Annual review of physiology, 67*, 491-514.

Fitzpatrick, D., Lund, J. S., & Blasdel, G. G. (1985). Intrinsic connections of macaque striate cortex: afferent and efferent connections of lamina 4C. *Journal of Neuroscience, 5*(12), 3329-3349.

Flitcroft, D. I. (1989). The interactions between chromatic aberration, defocus and stimulus chromaticity: implications for visual physiology and colorimetry. *Vision Research, 29*(3), 349-360.

Foster, D. H., & Bischof, W. F. (1991). Thresholds and Psychometric functions: superiority of bootstrap to incremental probit variance estimators. *Pschological Bulletin, 109*, 152-159.

Frishman, L. J., Freeman, A. W., Troy, J. B., Schweitzer-Tong, D. E., & Enroth-Cugell, C. (1987). Spatiotemporal frequency responses of cat retinal ganglion cells. *Journal of General Physiology, 89*(4), 599-628.

Gattass, R., Sousa, A. P. B., & Gross, C. G. (1988). Visuotopic Organization and Extent of V3 and V4 of the Macaque. *Journal of Neuroscience, 8*(6), 1831-1845.

Gegenfurtner, K. R. (2003). Cortical mechanisms of colour vision. *Nature Reviews Neuroscience, 4*(7), 563-572.

Gegenfurtner, K. R., & Kiper, D. C. (2003). Color vision. *Anual Reviews of Neuroscience, 26*, 181-206.

Gegenfurtner, K. R., Kiper, D. C., & Levitt, J. B. (1997). Functional properties of neurons in macaque area V3. *Journal of Neurophysiology, 77*(4), 1906-1923.

Girard, P., & Morrone, M. C. (1995). Spatial structure of chromatically opponent receptive fields in the human visual system. *Visual Neuroscience, 12*(1), 103-116.

Givre, S. J., Arezzo, J. C., & Schroeder, C. E. (1995). Effects of wavelength on the timing and laminar distribution of illuminance-evoked activity in macaque V1. *Visual Neuroscience, 12*(2), 229-239.

Goodale, M. A., & Milner, A. D. (1992). Separate visual pathways for perception and action. *Trends in Neuroscience, 15*(1), 20-25.

Gotch, F. (1903). The time relations of the photo-electric changes in the eyeball of the frog. *Journal of Physiology, 29*(4-5), 388-410.

Gouras, P. (1968). Identification of cone mechanisms in monkey ganglion cells. *Journal of Physiology, 199*(3), 533-547.

Gouras, P. (1969). Antidromic responses of orthodromically identified ganglion cells in monkey retina. *Journal of Physiology, 204*(2), 407-419.

Gouras, P. (1974). Opponent-Color Cells in Different Layers of Foveal Striate Cortex. *Journal of Physiology-London, 238*(3), 583-602.

Gouras, P., & Carr, R. E. (1964). Electrophysiological Studies in Early Retinitis Pigmentosa. *Archives of Ophthalmology, 72*, 104-110.

Gouras, P., & Link, K. (1966). Rod and cone interaction in dark-adapted monkey ganglion cells. *Journal of Physiology, 184*(2), 499-510.

Gouras, P., & MacKay, C. J. (1990). Electroretinographic responses of the short-wavelength-sensitive cones. *Investigative Ophthalmology and Visual Science, 31*(7), 1203-1209.

Gowdy, P. D., & Cicerone, C. M. (1998). The spatial arrangement of the L and M cones in the central fovea of the living human eye. *Vision Research, 38*(17), 2575-2589.

Granit, R. (1933). The components of the retinal action potential in mammals and their relation to the discharge in the optic nerve. *Journal of Physiology, 77*(3), 207-239.

Granit, R. (1947). *Sensory mechanisms of the retina*.Unpublished manuscript, London.

Granit, R., & Munsterhjelm, A. (1937). The electrical responses of dark-adapted frogs' eyes to monochromatic stimuli. *Journal of Physiology, 88*(4), 436-458.

Green, D. G., & Kapousta-Bruneau, N. V. (1999). A dissection of the electroretinogram from the isolated rat retina with microelectrodes and drugs. *Visual Neuroscience, 16*(4), 727-741.

Grunert, U., Martin, P. R., & Wassle, H. (1994). Immunocytochemical analysis of bipolar cells in the macaque monkey retina. *Journal of Comparative Neurology, 348*(4), 607-627.

Gurevich, L., & Slaughter, M. M. (1993). Comparison of the waveforms of the ON bipolar neuron and the b-wave of the electroretinogram. *Vision Research, 33*(17), 2431-2435.

Hadjikhani, N., Liu, A. K., Dale, A. M., Cavanagh, P., & Tootell, R. B. (1998). Retinotopy and color sensitivity in human visual cortical area V8. *Nature Neuroscience, 1*(3), 235-241.

Hagstrom, S. A., Neitz, J., & Neitz, M. (1998). Variations in cone populations for red-green color vision examined by analysis of mRNA. *Neuroreport, 9*(9), 1963-1967.

Hart Jr, W. (1987). The temporal responsiveness of vision. In R. A. Moses & W. M. Hart (Eds.), *Adlers Physiology of the eye, Clinical Application.* St. Louis: The C. V. Mosby Company.

Hawken, M. J., Shapley, R. M., & Grosof, D. H. (1996). Temporal-frequency selectivity in monkey visual cortex. *Visual Neuroscience, 13*(3), 477-492.

Heynen, H., Wachtmeister, L., & van Norren, D. (1985). Origin of the oscillatory potentials in the primate retina. *Vision Research, 25*(10), 1365-1373.

Hicks, T. P., Lee, B. B., & Vidyasagar, T. R. (1983). The responses of cells in macaque lateral geniculate nucleus to sinusoidal gratings. *Journal of Physiology, 337*, 183-200.

Himstedt, F., & Nagel, W. A. (1901). Uber die Einwirkung der Becquerel-undder Rontgenstrahlen auf das Auge. *Physikalische Zeitschrift, 2*, 363.

Holder, G. E. (2001). Pattern electroretinography (PERG) and an integrated approach to visual pathway diagnosis. *Progress in Retinal Eye Research, 20*(4), 531-561.

Holliday, T. A. (2003). Volume conduction in clinical neurophysiology. *Veterinary Neurology and Neurosurgery online, 5*(1).

Holmgren. (1865). Metod att objektivera effektenav ljusintryck pa retina. *Upsala lakaref. Forhandl, 1*, 177-191.

Holub, R. A., & Morton-Gibson, M. (1981). Response of Visual Cortical Neurons of the cat to moving sinusoidal gratings: response-contrast functions and spatiotemporal interactions. *Journal of Neurophysiology, 46*(6), 1244-1259.

Horton, J. C. (1984). Cytochrome oxidase patches: a new cytoarchitectonic feature of monkey visual cortex. *Philosophical Transactions of the Royal Society B: Biological Sciences, 304*(1119), 199-253.

Hubel, D. H., & Wiesel, T. N. (1966). Effects of varying stimulus size and color on single lateral geniculate cells in Rhesus monkeys. *Proceedings of the National Academy of Sciences U S A, 55*(6), 1345-1346.

Hubel, D. H., & Wiesel, T. N. (1968). Receptive fields and functional architecture of monkey striate cortex. *Journal of Physiology, 195*(1), 215-243.

Hubel, D. H., & Wiesel, T. N. (1972). Laminar and columnar distribution of geniculo-cortical fibers in the macaque monkey. *Journal of Comparative Neurology, 146*(4), 421-450.

Jacobi, P. C., Miliczek, K. D., & Zrenner, E. (1993). Experiences with the international standard for clinical electroretinography: normative values for clinical practice, interindividual and intraindividual variations and possible extensions. *Documenta Ophthalmologica, 85*(2), 95-114.

Jacobs, G. H., & Deegan, J. F., 2nd. (1997). Spectral sensitivity of macaque monkeys measured with ERG flicker photometry. *Visual Neuroscience, 14*(5), 921-928.

Jacobs, G. H., & Neitz, J. (1993). Electrophysiological estimates of individual variation in the L/M cone ratio. In B. Drum (Ed.), *Colour Vision Defeciencies* (pp. 107-112). Dordrecht: Kluwer Academic Publishers.

Jacobs, G. H., Neitz, J., & Krogh, K. (1996). Electroretinogram flicker photometry and its applications. *Journal of Optical Society of America A: Optics, Image Science and Vision, 13*(3), 641-648.

Jankov, E. (1978). [Spectral sensitivity of off-response in human VECP during selective chromatic adaptation (author's transl)]. *Albrecht Von Graefes Archives of clinical and Experimental Ophthalmoogyl, 206*(2), 121-133.

Jasper, H. H. (1957). Report on the committee on methods of clinical eaxmination in electroencephalography. *Electroencephalography and Clinical Neurophysiology (Supp)l, 10*, 370-375.

Johnson, E. N., Hawken, M. J., & Shapley, R. (2001). The spatial transformation of color in the primary visual cortex of the macaque monkey. *Nature Neuroscience, 4*(4), 409-416.

Jusuf, P. R., & Harris, W. A. (2009). Ptf1a is expressed transiently in all types of amacrine cells in the embryonic zebrafish retina. *Neural Development, 4*, 34.

Kaiser, K. P., & Boynton, R. M. (1996). *Colour Vision* (2nd Edition ed.). Washington D.C.: Optical Society of America.

Kaplan, E., Lee, B.B. & Shapley, R.M. (1990). New views of primate retinal function. In N. C. Osborne, J. (Ed.), *Progress in Retinal Eye Research* (pp. 273-336). Oxford: Pergamon press.

Kaplan, E., & Shapley, R. M. (1982). X and Y cells in the lateral geniculate nucleus of macaque monkeys. *Journal of Physiology, 330*, 125-143.

Karwoski, C. J., Newman, E. A., Shimazaki, H., & Proenza, L. M. (1985). Light-evoked increases in extracellular K+ in the plexiform layers of amphibian retinas. *Journal of General Physiology, 86*(2), 189-213.

Karwoski, C. J., & Xu, X. (1999). Current source-density analysis of light-evoked field potentials in rabbit retina. *Visual Neuroscience, 16*(2), 369-377.

Kellner, U., Sadowski, B., Zrenner, E., & Foerster, M. H. (1995). Selective cone dystrophy with protan genotype. *Investigative Ophthalmology and Visual Science, 36*(12), 2381-2387.

Kelly, D. H. (1974). Spatio-Temporal Frequency Characteristics of Color-Vision Mechanisms. *Journal of Optical Society of America A: Optics, Image Science and Vision, 64*(7), 983-990.

Kelly, D. H. (1983). Spatiotemporal Variation of Chromatic and Achromatic Contrast Thresholds. *Journal of Optical Society of America A: Optics, Image Science and Vision, 73*(6), 742-750

Kiper, D. C., Fenstemaker, S. B., & Gegenfurtner, K. R. (1997). Chromatic properties of neurons in macaque area V2. *Visual Neuroscience, 14*(6), 1061-1072.

Klug, K., Herr, S., Ngo, I. T., Sterling, P., & Schein, S. (2003). Macaque retina contains an S-cone OFF midget pathway. *Journal of Neuroscience, 23*(30), 9881-9887.

Knau, H., Jagle, H., & SHarpe, L. T. (2000). L/M cone ratios as function of retinal eccentricity. *Color Research and Application, Supplementray*, 128-132.

Kolb, H., & Dekorver, L. (1991). Midget ganglion cells of the parafovea of the human retina: a study by electron microscopy and serial section reconstructions. *Journal of Comparative Neurology, 303*(4), 617-636.

Kolb, H., Fernandez, E., Schouten, J., Ahnelt, P., Linberg, K. A., & Fisher, S. K. (1994). Are There 3 Types of Horizontal Cell in the Human Retina. *Journal of Comparative Neurology, 343*(3), 370-386.

Kolb, H., Linberg, K. A., & Fisher, S. K. (1992). Neurons of the Human Retina - a Golgi-Study. *Journal of Comparative Neurology, 318*(2), 147-187.

Kolb, H., Nelson, R., & Mariani, A. (1981). Amacrine cells, bipolar cells and ganglion cells of the cat retina: a Golgi study. *Vision Research, 21*(7), 1081-1114.

Komatsu, H., Ideura, Y., Kaji, S., & Yamane, S. (1992). Color selectivity of neurons in the inferior temporal cortex of the awake macaque monkey. *Journal of Neuroscience, 12*(2), 408-424.

Korth, M., & Nguyen, N. X. (1997). The effect of stimulus size on human cortical potentials evoked by chromatic patterns. *Vision Research, 37*(5), 649-657.

Korth, M., Nguyen, N. X., Rix, R., & Sembritzki, O. (1993). Interactions of spectral, spatial, and temporal mechanisms in the human pattern visual evoked potential. *Vision Research, 33*(17), 2397-2411.

Kouyama, N., & Marshak, D. W. (1992). Bipolar cells specific for blue cones in the macaque retina. *Journal of Neuroscience, 12*(4), 1233-1252.

Krauskopf, J. (1973). Contributions of the primary chromatic mechanisms to the generation of visual evoked potentials. *Vision Research, 13*(12), 2289-2298.

Krauskopf, J. (2000). Relative number of long- and middle-wavelength-sensitive cones in the human fovea. *Journal of Optical Society of America A: Optics, Image Science and Vision, 17*(3), 510-516.

Krauskopf, J., & Srebro, R. (1965). Spectral sensitivity of color mechanisms: derivation from fluctuations of color appearance near threshold. *Science, 150*(702), 1477-1479.

Krauskopf, J., Williams, D. R., & Heeley, D. W. (1982). Cardinal Directions of Color Space. *Vision Research, 22*(9), 1123-1131.

Kremers, J. (2003). The assessment of L- and M-cone specific electroretinographical signals in the normal and abnormal human retina. *Progress in Retinal Eye Research, 22*(5), 579-605.

Kremers, J., & Link, B. (2008). Electroretinographic responses that may reflect activity of parvo- and magnocellular post-receptoral visual pathways. *Journal of Vision, 8*(15), 11 11-14.

Kremers, J., & Meierkord, S. (1999). Rod-cone-interactions in deuteranopic observers: models and dynamics. *Vision Research, 39*(20), 3372-3385.

Kremers, J., Rodrigues, A. R., Silveira, L. C., & da Silva Filho, M. (2009). Flicker ERGs representing chromaticity and luminance signals. *Investigative Ophthalmology and Visual Science*.

Kremers, J., & Scholl, H. P. (2001). Rod-/L-cone and rod-/M-cone interactions in electroretinograms at different temporal frequencies. *Visual Neuroscience, 18*(3), 339-351.

Kremers, J., Scholl, H. P., Knau, H., Berendschot, T. T., Usui, T., & Sharpe, L. T. (2000). L/M cone ratios in human trichromats assessed by psychophysics, electroretinography, and retinal densitometry. *Journal of Optical Society of America A: Optics, Image Science and Vision, 17*(3), 517-526.

Kremers, J., Stepien, M. W., Scholl, H. P., & Saito, C. (2003). Cone selective adaptation influences L- and M-cone driven signals in electroretinography and psychophysics. *Journal of Vision, 3*(2), 146-160.

Kremers, J., Usui, T., Scholl, H. P., & Sharpe, L. T. (1999). Cone signal contributions to electroretinograms [correction of electrograms] in dichromats and trichromats. *Investigative Ophthalmology and Visual Science, 40*(5), 920-930.

Krill, A. E., Deutman, A. F., & Fishman, M. (1973). The cone degenerations. *Documenta Ophthalmologica, 35*(1), 1-80.

Kruger, J. (1977). Stimulus dependent colour specificity of monkey lateral geniculate neurons. *Experimental Brain Researchearch, 30*(2-3), 297-311.

Kulikowski, J., J, Murray , I. J, and ., & Russel, M.H.A. (1991). Effect of stimulus size on chromatic and achromatic VEPs. In J. D. M. B.Drum, A. Serra. (Ed.), *Colour Vision Defeciencies* (Vol. X, pp. 51-56). Netherland: Kulwer academic publishers.

Kulikowski, J. J. (1991). *On the nature of visual evoked potentails, unit responses and psychophysics*. New York: Plenum.

Kulikowski, J. J., McKeefry, D. J., & Robson, A. G. (1997). Selective stimulation of colour mechanisms: an empirical perspective. *Spatial Vision, 10*(4), 379-402.

Kulikowski, J. J., Murray, I.J, and Parry, N.R. (1989). Electrophysiological correlates of chromatic opponent and achromatic stimulation in man. In Dorderecht (Ed.), *Colour Vision Deficiencies IX*. Netherlands: Kulwer academic publishers.

Kulikowski, J. J., & Parry, N. R. A. (1987). Human Occipital Potentials-Evoked by Achromatic or Chromatic Checkerboards and Gratings. *Journal of Physiology-London, 388*, P45-P45.

Kulikowski, J. J., Robson, A. G., & McKeefry, D. J. (1996). Specificity and selectivity of chromatic visual evoked potentials. *Vision Research, 36*(21), 3397-3401.

Kulikowski, J. J., Robson, A. G., & Murray, I. J. (2002). Scalp VEPs and intra-cortical responses to chromatic and achromatic stimuli in primates. *Documenta Ophthalmologica, 105*(2), 243-279.

Kulikowski, J. J., & Vidya Sagar, T. R. (1987a). Neuronal Responses and Field Potentials-Evoked by Gratings in the Macaque Striate Cortex. *Journal of Physiology-London, 392*, P56-P56.

Kulikowski, J. J., & Vidya Sagar, T. R. (1987b). Neuronal responses and field potentials evoked by gratings in the macaque striate cortex. *Journal of Physiology, 392*, 56.

Lee, B. B. (1999). Receptor inputs to primate ganglion cells. In K. R. Gegenfurtner & L. T. Sharpe (Eds.), *Color vision: from molecular genetics to perception* (pp. 203-218). Cambridge: Cambridge university press.

Lee, B. B. (2004). Paths to colour in the retina. *Clinical and Experimental Optometry, 87*(4-5), 239-248.

Lee, B. B. (2010). Visual Pathways and Psychophysical Channels in the Primate. *Journal of Physiology*.

Lee, B. B., Kremers, J., & Yeh, T. (1998). Receptive fields of primate retinal ganglion cells studied with a novel technique. *Visual Neuroscience, 15*(1), 161-175.

Lee, B. B., Martin, P. R., & Valberg, A. (1989). Sensitivity of macaque retinal ganglion cells to chromatic and luminance flicker. *Journal of Physiology, 414*, 223-243.

Lee, B. B., Martin, P. R., Valberg, A., & Kremers, J. (1993). Physiological mechanisms underlying psychophysical sensitivity to combined luminance and chromatic modulation. *Journal of Optical Society of America A, 10*(6), 1403-1412.

Lee, B. B., Smith, V.C., Pokorny,J., Kremers, J. (1996). Rod inputs to macaque ganglion cells and their temporal dynamics. *Investigative Ophthalmology and Visual Science (Suupl.), 36*, 689.

Lee, S. C., Telkes, I., & Grunert, U. (2005). S-cones do not contribute to the OFF-midget pathway in the retina of the marmoset, Callithrix jacchus. *European Journal of Neuroscience, 22*(2), 437-447.

Lei, B., & Perlman, I. (1999). The contributions of voltage- and time-dependent potassium conductances to the electroretinogram in rabbits. *Visual Neuroscience, 16*(4), 743-754.

Lennie, P., Haake, P. W., & Williams, D. R. (1991). The design of the chromatically opponent receptive fields. In M. S. Landy & J. A. Movshon (Eds.), *Computational models of visual processing* (pp. 71-82). Cambridge, USA: MIT press.

Leventhal, A. G., Rodieck, R. W., & Dreher, B. (1981). Retinal ganglion cell classes in the Old World monkey: morphology and central projections. *Science, 213*(4512), 1139-1142.

Linn, D. M., Solessio, E., Perlman, I., & Lasater, E. M. (1998). The role of potassium conductance in the generation of light responses in Muller cells of the turtle retina. *Visual Neuroscience, 15*(3), 449-458.

Livingstone, M., & Hubel, D. (1988). Segregation of form, color, movement, and depth: anatomy, physiology, and perception. *Science, 240*(4853), 740-749.

Livingstone, M. S., & Hubel, D. H. (1983). Specificity of cortico-cortical connections in monkey visual system. *Nature, 304*(5926), 531-534.

Livingstone, M. S., & Hubel, D. H. (1984a). Anatomy and physiology of a color system in the primate visual cortex. *Journal of Neuroscience, 4*(1), 309-356.

Livingstone, M. S., & Hubel, D. H. (1984b). Anatomy and physiology of a color system in the primate visual cortex. *Journal of Neuroscience, 4*(1), 309-356.

Livingstone, M. S., & Hubel, D. H. (1987). Psychophysical evidence for separate channels for the perception of form, color, movement, and depth. *Journal of Neuroscience, 7*(11), 3416-3468.

Lueck, C. J., Zeki, S., Friston, K. J., Deiber, M. P., Cope, P., Cunningham, V. J., Lammertsma, A. A., Kennard, C., & Frackowiak, R. S. (1989). The colour centre in the cerebral cortex of man. *Nature, 340*(6232), 386-389.

Lund, J. S. (1973). Organization of neurons in the visual cortex, area 17, of the monkey (Macaca mulatta). *Journal of Comparative Neurology, 147*(4), 455-496.

Lund, J. S., Wu, Q., Hadingham, P. T., & Levitt, J. B. (1995). Cells and circuits contributing to functional properties in area V1 of macaque monkey cerebral cortex: bases for neuroanatomically realistic models. *Journal of Anatomy, 187 (Pt 3)*, 563-581.

MacLeod, D. I., & Boynton, R. M. (1979). Chromaticity diagram showing cone excitation by stimuli of equal luminance. *Journal of Optical Society of America, 69*(8), 1183-1186.

Marc, R. E., & Sperling, H. G. (1977). Chromatic organization of primate cones. *Science, 196* (4288), 454-456.

Mariani, A. P. (1984). Bipolar Cells in Monkey Retina Selective for the Cones Likely to Be Blue-Sensitive, *Nature,* 308, 184-186.

Mariani, A. P. (1985). Multiaxonal Horizontal Cells in the Retina of the Tree Shrew, Tupaia-Glis. *Journal of Comparative Neurology, 233*(4), 553-563.

Marmor, M. F., Zrenner, E. (1999). Standard for clinical electroretinography (Updated 1999). *Documenta Ophthalmologica*. 97, 143-156.

Martin, P. R. (1998). Colour processing in the primate retina: recent progress. *Journal of Physiology, 513 (3)*, 631-638.

Martin, P. R., Grunert, U., Chan, T. L., & Bumsted, K. (2000). Spatial order in short-wavelength-sensitive cone photoreceptors: a comparative study of the primate retina. *Journal of Optical Society of America A: Optics, Image Science and Vision, 17*(3), 557-567.

Martin, P. R., Lee, B. B., White, A. J., Solomon, S. G., & Ruttiger, L. (2001). Chromatic sensitivity of ganglion cells in the peripheral primate retina. *Nature, 410*(6831), 933-936.

Martin, P. R., White, A. J., Goodchild, A. K., Wilder, H. D., & Sefton, A. E. (1997). Evidence that blue-on cells are part of the third geniculocortical pathway in primates. *European Journal of Neuroscience, 9*(7), 1536-1541.

Massof, R. W., Johnson, M. A., Sunness, J. S., Perry, C., & Finkelstein, D. (1986). Flicker electroretinogram in retinitis pigmentosa. *Documenta Ophthalmologica, 62*(3), 231-245.

Maunsell, J. H., Nealey, T. A., & DePriest, D. D. (1990). Magnocellular and parvocellular contributions to responses in the middle temporal visual area (MT) of the macaque monkey. *Journal of Neuroscience, 10*(10), 3323-3334.

McKeefry, D. J., Murray, I. J., & Parry, N. R. (2007). Perceived shifts in saturation and hue of chromatic stimuli in the near peripheral retina. *Journal of Optical Society of America A: Optics, Image Science and Vision, 24*(10), 3168-3179.

McKeefry, D. J., Parry, N. R., & Murray, I. J. (2003). Simple reaction times in color space: the influence of chromaticity, contrast, and cone opponency. *Investigative Ophthalmology and Visual Science, 44*(5), 2267-2276.

McKeefry, D. J., Russell, M. H. A., Murray, I. J., & Kulikowski, J. J. (1996). Amplitude and phase variations of harmonic components in human achromatic and chromatic visual evoked potentials. *Visual Neuroscience, 13*(4), 639-653.

McKeefry, D. J., & Zeki, S. (1997). The position and topography of the human colour centre as revealed by functional magnetic resonance imaging. *Brain, 120 (12)*, 2229-2242.

McLellan, J. S., & Eskew, R. T. (2000). ON and OFF S-cone pathways have different long-wave cone inputs. *Vision Research, 40*(18), 2449-2465.

Merigan, W. H. (2000). Cortical area V4 is critical for certain texture discriminations, but this effect is not dependent on attention. *Visual Neuroscience, 17*(6), 949-958.

Merigan, W. H., & Maunsell, J. H. (1993). How parallel are the primate visual pathways? *Anual Reviews of Neuroscience, 16*, 369-402.

Michael, C. R. (1985). Double and single opponent colour cells in layer 4Cb of the monkey striate cortex. *Investigative Ophthalmology and Visual Science (Suppl), 26*(8).

Miller, R. F., & Dowling, J. E. (1970). Intracellular responses of the Muller (glial) cells of mudpuppy retina: their relation to b-wave of the electroretinogram. *Journal of Neurophysiology, 33*(3), 323-341.

Milner, A. D., & Goodale, M. A. (1995). The visual brain in action. Oxford: Oxford University press.

Mills, S. L., & Sperling, H. G. (1990). Red/green opponency in the rhesus macaque ERG spectral sensitivity is reduced by bicuculline. *Visual Neuroscience, 5*(3), 217-221.

Miyahara, E., Pokorny, J., Smith, V. C., Baron, R., & Baron, E. (1998). Color vision in two observers with highly biased LWS/MWS cone ratios. *Vision Research, 38*(4), 601-612.

Mollon, J. D. (1989). "Tho' she kneel'd in that place where they grew..." The uses and origins of primate colour vision. *Journal of Experimental Biology, 146*, 21-38.

Mollon, J. D., & Bowmaker, J. K. (1992). The spatial arrangement of cones in the primate fovea. *Nature, 360*(6405), 677-679.

Moreland, J., D., Bhatt, P. (1984). Retinal distrubution of retinal pigment. *Documenta Ophthalmologica Progession Series, 39*, 127-132.

Moreland, J. D., & Cruz, A. (1959). Colour perception in the peripheral retina. *Optica Acta, 6*, 117-151.

Moreland, J. D., Robson, A. G., Soto-Leon, N., & Kulikowski, J. J. (1998). Macular pigment and the colour-specificity of visual evoked potentials. *Vision Research, 38*(21), 3241-3245.

Mullen, K. T., & Kingdom, F. A. (1996). Losses in peripheral colour sensitivity predicted from "hit and miss" post-receptoral cone connections. *Vision Research, 36*(13), 1995-2000.

Mullen, K. T., & Kingdom, F. A. (2002). Differential distributions of red-green and blue-yellow cone opponency across the visual field. *Visual Neuroscience, 19*(1), 109-118.

Mullen, K. T., Sakurai, M., & Chu, W. (2005). Does L/M cone opponency disappear in human periphery? *Perception, 34*(8), 951-959.

Murakami, M., & Kaneko, A. (1966). Subcomponents of P3 in cold-blooded vertebrate retinae. *Nature, 210*(5031), 103-104.

Murakami, M., & Pak, W. L. (1970). Intracellularly recorded early receptor potential of the vertebrate photoreceptors. *Vision Research, 10*(10), 965-975.

Murphy, K.M., Jones, D.G., Van Sluyters, R.C. (1995). Cytochrome –oxidase blobs in cat primary visual cortex. *Journal of Neuroscience,* 15(6),4196-4208.

Murray, I. J., Kremers, J., & Parry, N. R. (2008). L- and M-cone isolating ERGs: LED versus CRT stimulation. *Visual Neuroscience, 25*(3), 327-331.

Murray, I. J., Parry, N. R., & McKeefry, D. J. (2006). Cone opponency in the near peripheral retina. *Visual Neuroscience, 23*(3-4), 503-507.

Murray, I. J., Parry, N. R. A., Carden, D., & Kulikowski, J. J. (1986). Human Visual Evoked-Potentials to Chromatic and Achromatic Gratings. *Clinical Vision Sciences, 1*(3), 231-244.

Nathans, J., Thomas, D., & Hogness, D. S. (1986). Molecular genetics of human color vision: the genes encoding blue, green, and red pigments. *Science, 232*(4747), 193-202.

Neitz, J., Carroll, J., Yamauchi, Y., Neitz, M., & Williams, D. R. (2002). Color perception is mediated by a plastic neural mechanism that is adjustable in adults. *Neuron, 35*(4), 783-792.

Nelson, R., Famiglietti, E. V., Jr., & Kolb, H. (1978). Intracellular staining reveals different levels of stratification for on- and off-center ganglion cells in cat retina. *Journal of Neurophysiology, 41*(2), 472-483.

Nerger, J. L., & Cicerone, C. M. (1992). The ratio of L cones to M cones in the human parafoveal retina. *Vision Research, 32*(5), 879-888.

Nerger, J. L., Volbrecht, V. J., & Ayde, C. J. (1995). Unique hue judgments as a function of test size in the fovea and at 20-deg temporal eccentricity. *Journal of Optical Society of America A: Optics, Image Science and Vision, 12*(6), 1225-1232.

Newman, E. A. (1989). Potassium conductance block by barium in amphibian Muller cells. *Brain Research, 498*(2), 308-314.

Noell, W. K. (1954). The origin of the electroretinogram. *American Journal of Ophthalmology, 38*(1:2), 78-90.

Norton, T. T., & Casagrande, V. A. (1982). Laminar organization of receptive-field properties in lateral geniculate nucleus of bush baby (Galago crassicaudatus). *Journal of Neurophysiology, 47*(4), 715-741.

Oakley, B., 2nd. (1977). Potassium and the photoreceptor-dependent pigment epithelial hyperpolarization. *Journal of General Physiology, 70*(4), 405-425.

Odom, J. V., Bach, M., Barber, C., Brigell, M., Marmor, M. F., Tormene, A. P., Holder, G. E., & Vaegan. (2004). Visual evoked potentials standard (2004). *Documenta Ophthalmologica, 108*(2), 115-123.

Odom, J. V., Bach, M., Brigell, M., Holder, G. E., McCulloch, D. L., Tormene, A. P., & Vaegan. (2010). ISCEV standard for clinical visual evoked potentials (2009). *Documenta Ophthalmologica, 120*(1), 111-119.

Ogden, T. E. (1973). The oscillatory waves of the primate electroretinogram. *Vision Research, 13*(6), 1059-1074.

Okada, T., Matsuda, T., Kandori, H., Fukada, Y., Yoshizawa, T., & Shichida, Y. (1994). Circular dichroism of metaiodopsin II and its binding to transducin: a comparative study between meta II intermediates of iodopsin and rhodopsin. *Biochemistry, 33*(16), 4940-4946.

Otake, S., Gowdy, P. D., & Cicerone, C. M. (2000). The spatial arrangement of L and M cones in the peripheral human retina. *Vision Research, 40*(6), 677-693.

Packer, O. S., & Dacey, D. M. (2002). Receptive field structure of H1 horizontal cells in macaque monkey retina. *Journal of Vision, 2*(4), 272-292.

Packer, O.S.,& Williams,D.(2003). *Photoreceptor topography and visual sampling*. In: The science of colour. (Ed):Steven K.S. Optical Society of America, 71-85. Elseiver publications.

Parry, N. R., McKeefry, D. J., & Murray, I. J. (2006). Variant and invariant color perception in the near peripheral retina. *Journal of Optical Society of America A: Optics, Image Science and Vision, 23*(7), 1586-1597.

Parry, N. R. A., Kulikowski, J.J., Murray, J.J., Kranda, K and Ott, H. (1988). *Visual Evoked potentials and reaction times to chromatic and achromatic stimulation.* . New York.

Paulus, W. (1997). Source analysis of visual evoked potentials in realistic head model. *Electroencephalogrphy and neurophysiology, 103*, 20-21.

Paulus, W. M., Homberg, V., Cunningham, K., & Halliday, A. M. (1986). Colour and brightness coding in the central nervous system: theoretical aspects and visual evoked

potentials to homogeneous red and green stimuli. *Proceedings of the Royal Society B: Biological Scienes, 227*(1246), 53-66.

Paulus, W. M., Homberg, V., Cunningham, K., Halliday, A. M., & Rohde, N. (1984). Color and Brightness Components of Foveal Visual Evoked-Potentials in Man. *Electroencephalography and Clinical NeurophysiologySuppl, 58*(2), 107-119.

Pepperberg, D. R., Brown, P. K., Lurie, M., & Dowling, J. E. (1978). Visual pigment and photoreceptor sensitivity in the isolated skate retina. *Journal of General Physiology, 71*(4), 369-396.

Perry, V. H., Oehler, R., & Cowey, A. (1984). Retinal ganglion cells that project to the dorsal lateral geniculate nucleus in the macaque monkey. *Neuroscience, 12*(4), 1101-1123.

Pigarev, I. N., Nothdurft, H. C., & Kastner, S. (2002). Neurons with radial receptive fields in monkey area V4A: evidence of a subdivision of prelunate gyrus based on neuronal response properties. *Experimental Brain Researchearch, 145*(2), 199-206.

Pokorny, J., Smith, V.C. (1987). L-M cone ratios and the null point of the perceptual red/green opponent system. *Die Farbe, 34*, 53-57.

Pokorny, J., Smith, V.C., Wesner, M.F (Ed.). (1991). *Variability cone populations and implications*. New York: Plenum.

Porciatti, V., & Sartucci, F. (1999). Normative data for onset VEPs to red-green and blue-yellow chromatic contrast. *Clinical Neurophysiology, 110*(4), 772-781.

Previc, F. H. (1986). Visual evoked potentials to luminance and chromatic contrast in rhesus monkeys. *Vision Research, 26*(12), 1897-1907.

Purpura, K., Kaplan, E., & Shapley, R. M. (1988). Background light and the contrast gain of primate P and M retinal ganglion cells. *Proc Natl Acad Sci U S A, 85*(12), 4534-4537.

Purpura, K., Tranchina, D., Kaplan, E., & Shapley, R. M. (1990). Light adaptation in the primate retina: analysis of changes in gain and dynamics of monkey retinal ganglion cells. *Visual Neuroscience, 4*(1), 75-93.

Rabin, J., & Adams, A. J. (1992). Cortical potentials evoked by short wavelength patterned light. *Optometry and Vision Science, 69*(7), 522-531.

Rabin, J., Switkes, E., Crognale, M., Schneck, M. E., & Adams, A. J. (1994). Visual evoked potentials in three-dimensional color space: correlates of spatio-chromatic processing. *Vision Research, 34*(20), 2657-2671.

Regan, D. (1972). Evoked Potentials in Psychology, Sensory Physiology and Clinical Medicine. London.

Regan, D., & Beverley, K. I. (1973). Electrophysiological evidence for existence of neurons sensitive to direction of depth movement. *Nature, 246*(5434), 504-506.

Regan, D., & Spekreijse, H. (1974). Evoked potential indications of colour blindness. *Vision Research, 14*(1), 89-95.

Reichel, E., Bruce, A. M., Sandberg, M. A., & Berson, E. L. (1989). An electroretinographic and molecular genetic study of X-linked cone degeneration. *American Journal of Ophthalmology, 108*(5), 540-547.

Reichelt, W., & Pannicke, T. (1993). Voltage-dependent K+ currents in guinea pig Muller (glia) cells show different sensitivities to blockade by Ba2+. *Neurosci Lett, 155*(1), 15-18.

Reid, R. C., & Shapley, R. M. (1992). Spatial structure of cone inputs to receptive fields in primate lateral geniculate nucleus. *Nature, 356*(6371), 716-718.

Reid, R. C., & Shapley, R. M. (2002). Space and time maps of cone photoreceptor signals in macaque lateral geniculate nucleus. *Journal of Neuroscience, 22*(14), 6158-6175.

Ribeiro, M. J., & Castelo-Branco, M. (2010). Psychophysical channels and ERP population responses in human visual cortex: area summation across chromatic and achromatic pathways. *Vision Research, 50*(13), 1283-1291.

Ripps, H., Noble, K. G., Greenstein, V. C., Siegel, I. M., & Carr, R. E. (1987). Progressive cone dystrophy. *Ophthalmology, 94*(11), 1401-1409.

Robson, A., & Kulikowski, J., J. (1995). Verification of VEPs elicited by gratings containing tritanopic pairs of hues. *Journal of Physiology*(485), 22.

Robson, A. G., Holder, G. E., Moreland, J. D., & Kulikowski, J. J. (2006). Chromatic VEP assessment of human macular pigment: comparison with minimum motion and minimum flicker profiles. *Visual Neuroscience, 23*(2), 275-283.

Robson, A. G., & Kulikowski, J. J. (1996). Chromatic -specific visual evoked potentials and the spatial limitations of grating stimuli modulated along the tritanopic axis. *Perception, 25*, 106.

Robson, A. G., & Kulikowski, J. J. (1998). Objective specification of tritanopic confusion lines using visual evoked potentials. *Vision Research, 38*(21), 3499-3503.

Robson, A. G., & Parry, N. R. (2008). Measurement of macular pigment optical density and distribution using the steady-state visual evoked potential. *Visual Neuroscience, 25*(4), 575-583.

Robson, T. (1999). *Topics in computerized to visual stimulus generation* (Vol. Oxford University press). Oxford.

Rodieck, R. W., & Rushton, W. A. (1976). Isolation of rod and cone contributions to cat ganglion cells by a method of light exchange. *Journal of Physiology, 254*(3), 759-773.

Rodieck, R. W., & Watanabe, M. (1993). Survey of the morphology of macaque retinal ganglion cells that project to the pretectum, superior colliculus, and parvicellular laminae of the lateral geniculate nucleus. *Journal of Comparative Neurology, 338*(2), 289-303.

Roorda, A., & Williams, D. R. (1999). The arrangement of the three cone classes in the living human eye. *Nature, 397*(6719), 520-522.

Ruddock, K. H. (1963). Evidence for Macular Pigmentation from Colour Matching Data. *Vision Research, 61*, 417-429.

Rushton, W. A., & Baker, H. D. (1964). Red--grees sensitivity in normal vision. *Vision Research, 4*(1), 75-85.

Russell, M. H., Murray, I. J., Metcalfe, R. A., & Kulikowski, J. J. (1991). The visual defect in multiple sclerosis and optic neuritis. A combined psychophysical and electrophysiological investigation. *Brain, 114 (Pt 6)*, 2419-2435.

Sakurai, M., Ayama, M., & Kumagai, T. (2003). Color appearance in the entire visual field: color zone map based on the unique hue component. *Journal of Optical Society of America A: Optics, Image Science and Vision, 20*(11), 1997-2009.

Sankeralli, M. J., & Mullen, K. T. (1996). Estimation of L-, M- and S- cone weights of the post-receptoral detection mechanisms. *Journal of Optical Society of America, 13*(5), 906-915.

Sartucci, F., Murri, L., Orsini, C., & Porciatti, V. (2001). Equiluminant red-green and blue-yellow VEPs in multiple sclerosis. *Journal of Clinical Neurophysiology, 18*(6), 583-591.

Sartucci, F., & Porciatti, V. (2006). Visual-evoked potentials to onset of chromatic red-green and blue-yellow gratings in Parkinson's disease never treated with L-dopa. *Journal of Clinical Neurophysiology, 23*(5), 431-435.

Saul, A. B., & Humphrey, A. L. (1992). Evidence of input from lagged cells in the lateral geniculate nucleus to simple cells in cortical area 17 of the cat. *Journal of Neurophysiology, 68*(4), 1190-1208.

Sawusch, M., Pokorny, J., & Smith, V. C. (1987). Clinical electroretinography for short wavelength sensitive cones. *Investigative Ophthalmology and Visual Science, 28*(6), 966-974.

Schein, S. J., & Desimone, R. (1990). Spectral properties of V4 neurons in the macaque. *Journal of Neuroscience, 10*(10), 3369-3389.

Schiller, P. H., Logothetis, N. K., & Charles, E. R. (1990). Functions of the Color-Opponent and Broad-Band Channels of the Visual-System. *Nature, 343*(6253), 68-70.

Schiller, P. H., & Malpeli, J. G. (1978). Functional specificity of lateral geniculate nucleus laminae of the rhesus monkey. *Journal of Neurophysiology, 41*(3), 788-797.

Schnapf, J. L., Kraft, T. W., & Baylor, D. A. (1987). Spectral sensitivity of human cone photoreceptors. *Nature, 325*(6103), 439-441.

Schnapf, J. L., Nunn, B. J., Meister, M., & Baylor, D. A. (1990). Visual transduction in cones of the monkey Macaca fascicularis. *Journal of Physiology, 427*, 681-713.

Scholl, H. P., & Kremers, J. (2000). Large phase differences between L-cone- and M-cone-driven electroretinograms in retinitis pigmentosa. *Investigative Ophthalmology and Visual Science, 41*(10), 3225-3233.

Schroeder, C. E., Tenke, C. E., Givre, S. J., Arezzo, J. C., & Vaughan, H. G., Jr. (1991). Striate cortical contribution to the surface-recorded pattern-reversal VEP in the alert monkey. *Vision Research, 31*(7-8), 1143-1157.

Schwartz, S. H. (1996). Spectral sensitivity as revealed by isolated step onsets and step offsets. *Ophthalmic and Physiological Optics, 16*(1), 58-63.

Sclar, G. (1987). Expression of "retinal" contrast gain control by neurons of the cat's lateral geniculate nucleus. *Experimental Brain Researchearch, 66*(3), 589-596.

Sclar, G., Maunsell, J. H., & Lennie, P. (1990). Coding of image contrast in central visual pathways of the macaque monkey. *Vision Research, 30*(1), 1-10.

Seiple, W., Holopigian, K., Greenstein, V., & Hood, D. C. (1992). Temporal frequency dependent adaptation at the level of the outer retina in humans. *Vision Research, 32*(11), 2043-2048.

Sereno, M. I., Dale, A. M., Reppas, J. B., Kwong, K. K., Belliveau, J. W., Brady, T. J., Rosen, B. R., & Tootell, R. B. (1995). Borders of multiple visual areas in humans revealed by functional magnetic resonance imaging. *Science, 268*(5212), 889-893.

Shapiro, A. G. (2002). Cone-specific mediation of rod sensitivity in trichromatic observers. *Investigative Ophthalmology and Visual Science, 43*(3), 898-905.

Shapiro, A. G., Pokorny, J., & Smith, V. C. (1996). Cone-rod receptor spaces with illustrations that use CRT phosphor and light-emitting-diode spectra. *Journal of Optical Society of America A: Optics, Image Science and Vision, 13*(12), 2319-2328.

Shapley, R., & Hawken, M. (2002). Neural mechanisms for color perception in the primary visual cortex. *Current Opinion in Neurobiology, 12*(4), 426-432.

Shapley, R., Kaplan, E., & Soodak, R. (1981). Spatial summation and contrast sensitivity of X and Y cells in the lateral geniculate nucleus of the macaque. *Nature, 292*(5823), 543-545.

Shapley, R., & Perry, V. H. (1986). Cat and Monkey Retinal Ganglion-Cells and Their Visual Functional Roles. *Trends in Neuroscience, 9*(5), 229-235.

Shichida, Y., Imai, H., Imamoto, Y., Fukada, Y., & Yoshizawa, T. (1994). Is chicken green-sensitive cone visual pigment a rhodopsin-like pigment? A comparative study of the molecular properties between chicken green and rhodopsin. *Biochemistry, 33*(31), 9040-9044.

Shinomori, K., Spillmann, L., & Werner, J. S. (1999). S-cone signals to temporal OFF-channels: asymmetrical connections to postreceptoral chromatic mechanisms. *Vision Research, 39*(1), 39-49.

Shinomori, K., & Werner, J. S. (2008). The impulse response of S-cone pathways in detection of increments and decrements. *Visual Neuroscience, 25*(3), 341-347.

Shipley, T., Jones, R. W., & Fry, A. (1965). Evoked visual potentials and human color vision. *Science, 150*(700), 1162-1164.

Shipp, S., & Zeki, S. (1985). Segregation of Pathways Leading from Area V2 to Areas V4 and V5 of Macaque Monkey Visual-Cortex. *Nature, 315*(6017), 322-325.

Shipp, S., & Zeki, S. (2002). The functional organization of area V2, I: Specialization across stripes and layers. *Visual Neuroscience, 19*(2), 187-210.

Sieving, P. A., Murayama, K., & Naarendorp, F. (1994). Push-pull model of the primate photopic electroretinogram: a role for hyperpolarizing neurons in shaping the b-wave. *Visual Neuroscience, 11*(3), 519-532.

Sillman, A. J., Ito, H., & Tomita, T. (1969). Studies on the mass receptor potential of the isolated frog retina. II. On the basis of the ionic mechanism. *Vision Research, 9*(12), 1443-1451.

Sincich, L. C., & Horton, J. C. (2002). Divided by cytochrome oxidase: a map of the projections from V1 to V2 in macaques. *Science, 295*(5560), 1734-1737.

Sincich, L. C., & Horton, J. C. (2005). The circuitry of V1 and V2: integration of color, form, and motion. *Anual Reviews of Neuroscience, 28*, 303-326.

Slaughter, M. M., & Miller, R. F. (1981). 2-amino-4-phosphonobutyric acid: a new pharmacological tool for retina research. *Science, 211*(4478), 182-185.

Smith, E. L., 3rd, Harwerth, R. S., Crawford, M. L., & Duncan, G. C. (1989). Contribution of the retinal ON channels to scotopic and photopic spectral sensitivity. *Visual Neuroscience, 3*(3), 225-239.

Smith, V. C., Lee, B. B., Pokorny, J., Martin, P. R., & Valberg, A. (1992). Responses of macaque ganglion cells to the relative phase of heterochromatically modulated lights. *Journal of Physiology, 458*, 191-221.

Smithson, H. E., & Mollon, J. D. (2004). Is the S-opponent chromatic sub-system sluggish? *Vision Research, 44*(25), 2919-2929.

Solomon, S. G., & Lennie, P. (2005). Chromatic gain controls in visual cortical neurons. *Journal of Neuroscience, 25*(19), 4779-4792.

Solomon, S. G., & Lennie, P. (2007). The machinery of colour vision. *Nature Reviews Neuroscience, 8*(4), 276-286.

Souza, G. S., Gomes, B. D., Lacerda, E. M., Saito, C. A., da Silva Filho, M., & Silveira, L. C. (2008). Amplitude of the transient visual evoked potential (tVEP) as a function of achromatic and chromatic contrast: contribution of different visual pathways. *Visual Neuroscience, 25*(3), 317-325.

Spekreijse, H., Estevez, O., & Reits, D. (Eds.). (1977). *Visual evoked potentails and the physiological analysis of visual process in man.* Oxford: Claredon press.

Spekreijse, H., Estevez, O., Reits, D.,. (1977). Visual ecoked potentials and physiological analysis of visual process in man. In J. E. Desmedt (Ed.), *Visual Evoked Potentials in Man: New Developments* (pp. 16-89). Oxford: Clarendon Press.

Sperling, H. G., & Mills, S. L. (1991). Red-green interactions in the spectral sensitivity of primates as derived from ERG and behavioral data. *Visual Neuroscience, 7*(1-2), 75-86.

Speros, P., & Price, J. (1981). Oscillatory potentials. History, techniques and potential use in the evaluation of disturbances of retinal circulation. *Survey of Ophthalmology, 25*(4), 237-252.

Stafford, D. K., & Dacey, D. M. (1997). Physiology of the A1 amacrine: a spiking, axon-bearing interneuron of the macaque monkey retina. *Visual Neuroscience, 14*(3), 507-522.

Steinberg, R. H., Schmidt, R., & Brown, K. T. (1970). Intracellular responses to light from cat pigment epithelium: origin of the electroretinogram c-wave. *Nature, 227*(5259), 728-730.

Stepniewska, I., Collins, C. E., & Kaas, J. H. (2005). Reappraisal of DL/V4 boundaries based on connectivity patterns of dorsolateral visual cortex in macaques. *Cerebral Cortex, 15*(6), 809-822.

Stockman, A., MacLeod, D. I., & Johnson, N. E. (1993a). Spectral sensitivities of the human cones. *Journal of Optical Society of America A: Optics, Image Science and Vision, 10*(12), 2491-2521.

Stockman, A., MacLeod, D. I., & Vivien, J. A. (1993b). Isolation of the middle- and long-wavelength-sensitive cones in normal trichromats. *Journal of Optical Society of America A: Optics, Image Science and Vision, 10*(12), 2471-2490.

Stockman, A., & Plummer, D. J. (2005). Spectrally opponent inputs to the human luminance pathway: slow +L and -M cone inputs revealed by low to moderate long-wavelength adaptation. *Journal of Physiology, 566*(1), 77-91.

Stockman, A., Sharpe, L. T., Ruther, K., & Nordby, K. (1995). Two signals in the human rod visual system: a model based on electrophysiological data. *Visual Neuroscience, 12*(5), 951-970.

Stockman, A., Sharpe, L. T., Zrenner, E., & Nordby, K. (1991). Slow and fast pathways in the human rod visual system: electrophysiology and psychophysics. *Journal of Optical Society of America A, 8*(10), 1657-1665.

Stockton, R. A., & Slaughter, M. M. (1989). B-wave of the electroretinogram. A reflection of ON bipolar cell activity. *Journal of General Physiology, 93*(1), 101-122.

Suttle, C. M., & Harding, G. F. (1999). Morphology of transient VEPs to luminance and chromatic pattern onset and offset. *Vision Research, 39*(8), 1577-1584.

Swanson, W. H., Birch, D. G., & Anderson, J. L. (1993). S-cone function in patients with retinitis pigmentosa. *Investigative Ophthalmology and Visual Science, 34*(11), 3045-3055.

Switkes, E., Crognale, M., Rabin, J., Schneck, M. E., & Adams, A. J. (1996). Reply to "specificity and selectivity of chromatic visual evoked potentials". *Vision Research, 36*(21), 3403-3405.

Szikra, T., & Witkovsky, P. (2001). Contributions of AMPA- and kainate-sensitive receptors to the photopic electroretinogram of the Xenopus retina. *Visual Neuroscience, 18*(2), 187-196.

Tailby, C., Solomon, S. G., & Lennie, P. (2006). Multiple S-cone pathways in the macaque visual system. *COSYNE, 20*.

Tobimatsu, S., Tomoda, H., & Kato, M. (1995). Parvocellular and magnocellular contributions to visual evoked potentials in humans: stimulation with chromatic and achromatic gratings and apparent motion. *Journal of Neurological Science, 134*(1-2), 73-82.

Tomita, T. (1950). Studies on the intraretinal action potential I. Relation between the localization of micropipette in the retina and the shape of the intraretinal action potential. *Japaneese Journal of Physiology, 1*, 110-117.

Tootell, R. B., & Hadjikhani, N. (2001). Where is 'dorsal V4' in human visual cortex? Retinotopic, topographic and functional evidence. *Cerebral Cortex, 11*(4), 298-311.

Tootell, R. B., Silverman, M. S., De Valois, R. L., & Jacobs, G. H. (1983). Functional organization of the second cortical visual area in primates. *Science, 220*(4598), 737-739.

Tootell, R. B., Silverman, M. S., Hamilton, S. L., De Valois, R. L., & Switkes, E. (1988). Functional anatomy of macaque striate cortex. III. Color. *Journal of Neuroscience, 8*(5), 1569-1593.

Tootell, R. B. H., Nelissen, K., Vanduffel, W., & Orban, G. A. (2004). Search for color 'center(s)' in macaque visual cortex. *Cerebral Cortex, 14*(4), 353-363.

Ts'o, D. Y., & Gilbert, C. D. (1988). The organization of chromatic and spatial interactions in the primate striate cortex. *Journal of Neuroscience, 8*(5), 1712-1727.

Tsumoto, T., Creutzfeldt, O. D., & Legendy, C. R. (1978). Functional organization of the corticofugal system from visual cortex to lateral geniculate nucleus in the cat (with an appendix on geniculo-cortical mono-synaptic connections). *Experimental Brain Researchearch, 32*(3), 345-364.

Uchikawa, K., Uchikawa, H., & Kaiser, P. K. (1982). Equating colors for saturation and brightness: the relationship to luminance. *Journal of Optical Society of America, 72*(9), 1219-1224.

Ungerleider, L. G., & Mishkin, M. (1982). Two cortical visual systems. Analysis of visual behaviour (pp. 549-586). Cambridge, MA: MIT press.

Usui, T., Kremers, J., Sharpe, L. T., & Zrenner, E. (1998). Flicker cone electroretinogram in dichromats and trichromats. *Vision Research, 38*(21), 3391-3396.

Vakrou, C., Whitaker, D., McGraw, P. V., & McKeefry, D. (2005). Functional evidence for cone-specific connectivity in the human retina. *Journal of Physiology, 566*(Pt 1), 93-102.

Valberg, A., & Lee, B. B. (1992). Main Cell Systems in Primate Visual Pathways. *Current Opinion in Ophthalmology, 3*(6), 813-823.

Valberg, A., & Rudvin, I. (1997). Possible contributions of magnocellular- and parvocellular-pathway cells to transient VEPs. *Visual Neuroscience, 14*(1), 1-11.

Valeton, J. M., & van Norren, D. (1983). Light adaptation of primate cones: an analysis based on extracellular data. *Vision Research, 23*(12), 1539-1547.

Van Essen, D. C., Lewis, J. W., Drury, H. A., Hadjikhani, N., Tootell, R. B., Bakircioglu, M., & Miller, M. I. (2001). Mapping visual cortex in monkeys and humans using surface-based atlases. *Vision Research, 41*(10-11), 1359-1378.

Van Essen, D. C., & Zeki, S. M. (1978). Topographic Organization of Rhesus-Monkey Prestriate Cortex. *Journal of Physiology-London, 277*(Apr), 193-226.

van Schooneveld, M. J., Went, L. N., & Oosterhuis, J. A. (1991). Dominant cone dystrophy starting with blue cone involvement. *Br J Ophthalmol, 75*(6), 332-336.

Vassilev, A., Zlatkova, M., Manahilov, V., Krumov, A., & Schaumberger, M. (2000). Spatial summation of blue-on-yellow light increments and decrements in human vision. *Visual Research, 40*(8), 989-1000.

Vaughan, H. G., Jr., & Gross, C. G. (1969). Cortical responses to light in unanesthetized monkeys and their alteration by visual system lesions. *Experimental Brain Researchearch, 8*(1), 19-36.

Vimal, R. L., Pokorny, J., Smith, V. C., & Shevell, S. K. (1989). Foveal cone thresholds. *Vision Research, 29*(1), 61-78.

Viswanathan, S., Frishman, L. J., & Robson, J. G. (2000). The uniform field and pattern ERG in macaques with experimental glaucoma: removal of spiking activity. *Investigative Ophthalmology and Visual Science, 41*(9), 2797-2810.

Viswanathan, S., Frishman, L. J., & Robson, J. G. (2002). Inner-retinal contributions to the photopic sinusoidal flicker electroretinogram of macaques. Macaque photopic sinusoidal flicker ERG. *Documenta Ophthalmologica, 105*(2), 223-242.

Viswanathan, S., Frishman, L. J., Robson, J. G., Harwerth, R. S., & Smith, E. L., 3rd. (1999). The photopic negative response of the macaque electroretinogram: reduction by experimental glaucoma. *Investigative Ophthalmology and Visual Science, 40*(6), 1124-1136.

Wachtmeister, L., & Dowling, J. E. (1978). The oscillatory potentials of the mudpuppy retina. *Investigative Ophthalmology and Visual Science, 17*(12), 1176-1188.

Wade, A., Augath, M., Logothetis, N., & Wandell, B. (2008). fMRI measurements of color in macaque and human. *Journal of Vision, 8*(10), 1-19.

Wade, A. R. (2009). Long-range suppressive interactions between S-cone and luminance channels. *Vision Research, 49*(12), 1554-1562.

Wald, G. (1964). The Receptors of Human Color Vision. *Science, 145*, 1007-1016.

Walraven, P. L. (1974). A closer look at the tritanopic convergence point. *Vision Research, 14*(12), 1339-1343.

Walsh, V., Butler, S. R., Carden, D., & Kulikowski, J. J. (1992). The effects of V4 lesions on the visual abilities of macaques: shape discrimination. *Behavioural Brain Researchearch, 50*(1-2), 115-126.

Walsh, V., Carden, D., Butler, S. R., & Kulikowski, J. J. (1993). The effects of V4 lesions on the visual abilities of macaques: hue discrimination and colour constancy. *Behavioural Brain Researchearch, 53*(1-2), 51-62.

Wassle, H., & Boycott, B. B. (1991). Functional architecture of the mammalian retina. *Physiological Reviews, 71*(2), 447-480.

Wassle, H., Boycott, B. B., & Rohrenbeck, J. (1989). Horizontal Cells in the Monkey Retina: Cone connections and dendritic network. *European Journal of Neuroscience, 1*(5), 421-435.

Watanabe, M., & Rodieck, R. W. (1989). Parasol and midget ganglion cells of the primate retina. *Journal of Comparative Neurology, 289*(3), 434-454.

Weale, R. A. (1951). Hue-discrimination in para-central parts of the human retina measured at different luminance levels. *Journal of Physiology, 113*(1), 115-122.

Webster, M. A., & Wilson, J. A. (2000). Interactions between chromatic adaptation and contrast adaptation in color appearance. *Vision Research, 40*(28), 3801-3816.

Weiss, S., Kremers, J., & Maurer, J. (1998). Interaction between rod and cone signals in responses of lateral geniculate neurons in dichromatic marmosets (Callithrix jacchus). *Visual Neuroscience, 15*(5), 931-943.

Wesner, M. F., Pokorny, J., Shevell, S. K., & Smith, V. C. (1991). Foveal cone detection statistics in color-normals and dichromats. *Vision Research, 31*(6), 1021-1037.

White, A. J., Wilder, H. D., Goodchild, A. K., Sefton, A. J., & Martin, P. R. (1998). Segregation of receptive field properties in the lateral geniculate nucleus of a New-World monkey, the marmoset Callithrix jacchus. *Journal of Neurophysiology, 80*(4), 2063-2076.

White, A. J. R., Solomon, S. G., & Martin, P. R. (2001). Spatial properties of koniocellular cells in the lateral geniculate nucleus of the marmoset Callithrix jacchus. *Journal of Physiology-London, 533*(2), 519-535.

Whitmore, A. V., & Bowmaker, J. K. (1995). Differences in the temporal properties of human longwave- and middlewave-sensitive cones. *European Journal of Neuroscience, 7*(6), 1420-1423.

Wiesel, T. N., & Hubel, D. H. (1966). Spatial and chromatic interactions in the lateral geniculate body of the rhesus monkey. *Journal of Neurophysiology, 29*(6), 1115-1156.

Wildberger, H. (1985). Acquired disorders of contrast sensitivity and color vision in mild optic neuropathies. *Klin Monatsbl Augenheilkd, 186*(3), 194-199.

Williams, D. R., MacLeod, D. I., & Hayhoe, M. M. (1981). Punctate sensitivity of the blue-sensitive mechanism. *Vision Research, 21*(9), 1357-1375.

Williams, D. R., Roorda, A. (1999). The trichromatic cone mosiac in the human eye, From Genes to Perception In K. R. Gegenfutner, Sharpe, L.T. (Eds.), 113-122.

Witkovsky, P., Dudek, F. E., & Ripps, H. (1975). Slow PIII component of the carp electroretinogram. *Journal of General Physiology, 65*(2), 119-134.

Wong-Riley, M. (1979) Changes in the visual system of monocularly sutured or enucleated cats demonstrable with cytochrome oxidase histochemistry. *Brain Research.* 171, 11-28.

Wyszecki, G., & Stiles, W. S. (1982). *Color science; Concepts and methods, Quantitative Data and Formulae*. New York, 1982: Wiley series.

Xiao, Y., Casti, A., Xiao, J., & Kaplan, E. (2007). Hue maps in primate striate cortex. *Neuroimage, 35*(2), 771-786.

Xiao, Y. P., Wang, Y., & Felleman, D. J. (2003). A spatially organized representation of colour in macaque cortical area V2. *Nature, 421*(6922), 535-539.

Xu, X., & Karwoski, C. (1995). Current source density analysis of the electroretinographic d wave of frog retina. *Journal of Neurophysiology, 73*(6), 2459-2469.

Xu, X., & Karwoski, C. J. (1994). Current source density analysis of retinal field potentials. II. Pharmacological analysis of the b-wave and M-wave. *Journal of Neurophysiology, 72*(1), 96-105.

Yonemura, D., & Kawasaki, K. (1967). The early receptor potential in the human electroretinogram. *Jpn Journal of Physiology, 17*(3), 235-244.

Yonemura, D., & Kawasaki, K. (1979). New approaches to ophthalmic electrodiagnosis by retinal oscillatory potential, drug-induced responses from retinal pigment epithelium and cone potential. *Documenta Ophthalmologica, 48*(1), 163-222.

Zeki, S. (1983). Colour coding in the cerebral cortex: the reaction of cells in monkey visual cortex to wavelengths and colours. *Neuroscience, 9*(4), 741-765.

Zeki, S. (1990). A century of cerebral achromatopsia. *Brain, 113 (Pt 6)*, 1721-1777.

Zeki, S. (1996). Are areas TEO and PIT of monkey visual cortex wholly distinct from the fourth visual complex (V4 complex)? *Proceedings of the Royal Society of London Series B-Biological Sciences, 263*(1376), 1539-1544.

Zeki, S., & Bartels, A. (1999). The clinical and functional measurement of cortical (in)activity in the visual brain, with special reference to the two subdivisions (V4 and V4 alpha) of the human colour centre. *Philosophical Transactions of the Royal Society B: Biological Sciences, 354*(1387), 1371-1382.

Zeki, S., & Shipp, S. (1989). Modular Connections between Areas V2 and V4 of Macaque Monkey Visual Cortex. *European Journal of Neuroscience, 1*(5), 494-506.

Zeki, S. M. (1973). Colour coding in rhesus monkey prestriate cortex. *Brain Research, 53*(2), 422-427.

Zeki, S. M. (1977). Colour coding in the superior temporal sulcus of rhesus monkey visual cortex. *Proceedings of the Royal Society London B: Biological Sciences, 197*(1127), 195-223.

Zeki, S. M. (1978a). Functional specialisation in the visual cortex of the rhesus monkey. *Nature, 274*(5670), 423-428.

Zeki, S. M. (1978b). Uniformity and diversity of structure and function in rhesus monkey prestriate visual cortex. *Journal of Physiology, 277*, 273-290.

Zrenner, E. (1983). Neurophysiological aspects of colour vision in primates. Comparative studies on simian retinal ganglion cells and the human visual system: Berlin: Springer-Verlag.. *Studies of brain function*: (9), 178-209.

Zrenner, E., & Gouras, P. (1979). Blue-sensitive cones of the cat produce a rodlike electroretinogram. *Investigative Ophthalmology and Visual Science, 18*(10), 1076-1081.

PRESENTATONS AND PUBLICATIONS

AMERICAN ACADEMY OF OPTOMETRY, ANNUAL MEETING (2008)

CIRCULAR SPOT CHROMATIC VISUAL EVOKED POTENTIALS AS FUNCTION OF CHROMATIC AXES IN MBDKL COLOUR SPACE (TALK ABSTRACT)

N. K.Challa[1], D. McKeefry[1]

Purpose: To study the influence of chromatic axis on the generation of colour VEPs and to asses the contribution of L-M and S-(L+M) opponent mechanisms to the generation of such responses.

Methods: The VEP stimuli consisted of homogenous circular discs subtending 2^o was centred on the fovea. The mean luminance of the discs was 20cd/m^2 and was surrounded by a grey background of the same mean luminance. The hue of circular patch was modulated in onset-offset fashion with a square wave temporal profile. Both onset and offset periods were 500ms. Isoluminance ratio of the disc was found using Heterochromatic Flicker Photometry. Stimuli were modulated along sixteen chromatic axes in MBDKL colour space that included L+M, L-M, +S-(L+M) and –S-(L+M) cardinal axes and twelve non-cardinal chromatic axes. For each stimulus, VEPs were recorded for the three electrode positions OZ, POZ and PZ. Five subjects, age range 24 to 40 years, were used. All subjects had visual acuities of 6/6 or better and were found to be colour normal, using the Farnsworth- Munsell 100 Hue colour vision test.

Results: VEP morphological differences were clearly appreciated as function of chromatic axis. Four major components N1, P2, N2 and P3 were analysed. N1 and P2 amplitudes were larger along -L+M and +L-M axis and gradually reduced as we shifted chromatic axes towards +S-(L+M) and -S-(L+M) cardinal axes. Differences in morphology were found between +S-(L+M) and –S-(L+M) isolating axes suggesting of existence of S-ON and S-OFF channels. VEPs along both of these chromatic axes seem to be effected by relatively sparse number of S cones.

Conclusions: Small circular spot stimulus can be successfully used to record chromatic VEPs, though their amplitudes are small. Chromatic VEPs are different along +S-(L+M) and –S-(L+M) axes suggesting the possible existence of two more opponent channels, S-ON and S-OFF, in addition to +L-M and +M-L channels.

INTERNATION COLOUR VISION SOCIETY ANNUAL SYMPOSIUM, 2009

L- AND M-CONE INPUT TO HUMAN ERGS AS A FUNCTION OF RETINAL ECCENTRICITY (TALK ABSTRACT).

N. K.Challa[1], D. McKeefry[1], N.R.A. Parry[2], J. Kremers[3], I.J. Murray[4] & A. Thanasis[4].

[1]. Bradford School of Optometry and Vision science, University of Bradford, UK.

[2]. Visual Sciences Centre, Manchester Royal Eye Hospital, Oxford Rd, Manchester, UK.

[3]. Department of Ophthalmology, University Hospital Erlangen, Erlangen, Germany.

[4]. Faculty of Life Sciences, University of Manchester, Manchester, UK.

Purpose: Physiological studies have led to conflicting views regarding the nature of L- and M-cone input to ganglion cell receptive fields in the peripheral compared to the central retina. There is support for a random wiring hypothesis, whereby receptive field centres and surrounds in peripheral ganglion cells receive mixed cone inputs. But others favour a cone selective hypothesis, where centres and surrounds receive input from single cone types, as is the case in the central retina. We wished to investigate the underlying nature of L- and M-cone input to chromatic mechanisms in the central and peripheral retina. We recorded ERGs from human subjects at temporal rates of 12Hz and 30Hz which isolate the activity of cone-opponent and non-opponent post-receptoral mechanisms, respectively (Kremers and Link, 2008, Journal of Vision 8(15):11, 1–14).

Methods: ERGs were obtained from a series of flickering stimuli (either 30Hz or 12Hz) with one of the following configurations: (1) Circular stimuli of different angular subtense which increased in 10^0 steps up to 70° diameter. (2) Annuli with 70° outer diameter but gradually ablated from the centre in 10° steps. L- and M-cone isolating responses were obtained from five colour normal subjects using a DTL fibre electrode. Cone contrasts were equalized for each stimulus condition.

Results: Fourier analysis of the ERG signals was used to measure the magnitude of the first harmonic of the response. The ratio of the L- and M-cone responses was found to be at or close to unity at 12Hz for central as well as peripheral stimuli. In contrast, at 30Hz the L- and M-cone ratio was found to vary from 4:1 to 10:1, for different observers. In addition the L- and M-cone phase differences at 12Hz were close to 180^o compared to the smaller phase differences measured for the 30Hz responses.

Conclusions: These results suggest that for ERGs which reflect the activity of the L-M cone-opponent post-receptoral mechanism, a constant 1:1 input ratio exists between L- and M-cones as a function of retinal eccentricity. This result points to the maintenance of cone selective input in the peripheral human retina in chromatic vision.

JOURNAL ABSTRACT (JOURNAL OF VISION)

ERG SIGNALS DRIVEN BY CHROMATIC AND LUMINANCE PROCESSING:VARIATION AS A FUNCTION OF RETINAL ECCENTRICITY.

Declan Joseph McKeefry[1], Neil Parry[2,] Naveen Challa[3], Jan Kremers[4], Ian Murray[5] & Athanasios Panarogias[6].

In order to investigate the how L- and M-cone input to the chromatic and luminance mechanisms varies as a function of retinal eccentricity we recorded ERGs from human subjects at temporal rates of 12Hz and 30Hz using a range of circular stimuli of different angular subtense which increased in 100 steps up to 70-deg diameter. In addition, we also recorded responses from annuli with a 70-deg outer diameter but gradually ablated from the centre in 100 steps. L- and M-cone isolating (rod silent) responses were obtained from five colour normal subjects using a DTL fibre electrode. Cone contrasts were equalized for each stimulus condition.

Fourier analysis of the ERGs was used to measure the magnitude of the first harmonic of the response. For the 12Hz response the ratio of the L- and M-cone contribution to the ERG signal was found close to unity for all subjects. The group averaged data showed that the L:M ratio remained remarkably constant (close to 1:1) as a function of retinal eccentricity. For the 30Hz response the L- and M-cone ratio was found to vary between 4:1 and 10:1 across observers. Furthermore, in contrast to the 12Hz response, the L:M ratio for the 30Hz exhibited a large degree of variation with retinal eccentricity.

These differences in response properties as a function of retinal eccentricity provide further evidence to support the view that L- and M-cone isolating ERGs reflect the operation of different retinal processing pathways when elicited by either fast (30Hz) or slow (12Hz) temporal stimulation.

JOURNAL ARTICLE ABSTRACT (OPHTHALMIC AND PHYSIOLOGICAL OPTICS) 2010

L- AND M-CONE INPUT TO 12HZ AND 30HZ FLICKER ERGs ACROSS THE HUMAN RETINA (ARTICLE ABSTRACT).

N. K.Challa[1], D. McKeefry[1], N.R.A. Parry[2], J. Kremers[3], I.J. Murray[4] & A. Thanasis[4].

[1]. Department of Optometry and Vision science, University of Bradford, UK.

[2]. Visual Sciences Centre, Manchester Royal Eye Hospital, Oxford Rd, Manchester, UK.

[3]. Department of Ophthalmology, University Hospital Erlangen, Erlangen, Germany.

[4]. Faculty of Life Sciences, University of Manchester, Manchester, UK.

We recorded L- and M-cone isolating ERGs from human subjects using a silent substitution technique at temporal rates of 12 and 30Hz. These frequencies isolate the activity of cone-opponent and non-opponent post-receptoral mechanisms, respectively. ERG were obtained using sequence of stimuli with different spatial configurations compromising; 1) circular stimuli of different sizes which increased in 10° steps up to 70° diameter, or 2)annular stimuli with a 70° outer diameter but with different sized central ablations from 10°steps up to 60°. L- and M- cone isolating ERGs were obtained from five colour normal subjects using a DTL fibre electrode. Fourier analysis of the ERGs was performed and we measured the amplitude of the first harmonic of the response. For 12Hz ERGs the L:M cone response amplitude ratio ($L:M_{ERG}$) was close to unity and remained stable irrespective of the spatial configuration of the stimulus. The maintenance of this balanced ratio points to the existence of cone selective input across the human retina for the L-M cone opponent mechanism. For the 30Hz the $L:M_{ERG}$ ratio was greater than unity but varied depending upon which region of the retina being stimulated. This variation we consider to be a consequence of the global response properties of M-cone ERGs rather than representing a real variation in L:M cone ratios across the retina.

*For full paper see attached manuscript.